SIRT1 DIMINISHES ATHEROGENESIS BY SUPPRESSING NF-κB SIGNALING-MEDIATED PRO-INFLAMMATORY EVENTS

Dissertation

zur

Erlangung der naturwissenschaftlichen Doktorwürde

(Dr. sc. nat.)

vorgelegt der

Mathematisch-naturwissenschaftlichen Fakultät

der

Universität Zürich

von

Matthias Alexander Sokrates Stein

aus

Brasilien und Deutschland

Promotionskommitee

Prof. Dr. Burkhard Becher (Vorsitz)

PD Dr. Christian M. Matter

Prof. Dr. Marc Y. Donath

Prof. Dr. Walter Wahli

Zürich, 2011

La sapienza è figliola della sperienzia

Leonardo da Vinci

For Steffi and my family

Table of Contents

Table of Figures

Figures 1, 2, 4, 5, 6, 8, and 10 were produced using Servier Medical Art (www.servier.com).

1 Zusammenfassung

Ziel dieser Doktorarbeit war es, die Funktion von SIRT1 und Peroxisome proliferator-activated receptor γ (PPARγ) coactivator 1α (PGC-1α) in der Atherosklerose zu erforschen. Atherosklerose ist eine chronisch inflammatorische Erkrankung die aus einem komplexen Zusammenspiel der Gefässwand mit Makrophagen, T Zellen und oxidierten LDL (*Lipoprotein niederer Dichte*) entsteht. Die Ruptur eines atherosklerotischen Plaques kann zur Bildung eines Thrombus führen und das Gefäss ganz verschliessen, was im schlimmsten Fall zu einem Herzinfarkt oder Schlaganfall führen kann. SIRT1 und PGC-1α sind Enzyme die wichtige metabolische und anti-inflammatorische Eigenschaften besitzen. SIRT1 ist ein Sirtuin (Klasse III Histone-Deacetylase), welches in der Lebensverlängerung durch eine niedrige Kaloriendiät sowie in metabolischen Schaltkreisen in verschiedenen Organismen beteiligt ist. PGC-1α ist ein transkriptioneller Kofaktor der die mitochondriale Biogenese und ebenfalls metabolische Prozesse reguliert. Die Deacetylierung von PGC-1α durch SIRT1 führt zur Aktivierung dieses nicht DNA-bindenden Kofaktors.

Um die Rolle dieser Moleküle in der Atherosklerose zu untersuchen, haben wir *SIRT1*$^{+/-}$ oder *PGC-1α*$^{-/-}$ mit atherosklerotischen *ApoE*$^{-/-}$ Mäusen gekreuzt, um dann *ApoE*$^{-/-}$ *SIRT1*$^{+/+}$ mit *ApoE*$^{-/-}$ *SIRT1*$^{+/-}$ bzw. *ApoE*$^{-/-}$ *PGC-1α*$^{+/+}$ mit *ApoE*$^{-/-}$ *PGC-1α*$^{-/-}$ Mäusen zu vergleichen.

Wir haben herausgefunden, dass haploinsuffiziente *ApoE*$^{-/-}$ *SIRT1*$^{+/-}$ Mäuse mehr Atherosklerose als die *ApoE*$^{-/-}$ *SIRT1*$^{+/+}$ Mäuse haben. Desweiteren konnten wir zeigen, dass die Supprimierung des NF-κB Signalwegs durch SIRT1 die Endothelzellaktivierung reduziert, die *Lox-1* Expression und Schaumzellbildung der Makrophagen inhibiert, sowie die endotheliale Expression von Thromboplastin (Faktor III, tissue factor) supprimiert.

ApoE$^{-/-}$ *PGC-1α*$^{+/+}$ und *ApoE*$^{-/-}$ *PGC-1α*$^{-/-}$ Mäuse bilden in etwa gleich viel Atherosklerose. Allerdings sind die *ApoE*$^{-/-}$ *PGC-1α*$^{-/-}$ Mäuse leichter und haben einen deutlich geringeren epididymalen Fettanteil, weniger Triglyceride im Plasma und eine differentielle Expression von wichtigen pro- und anti-inflammatorischen Molekülen. Eine Balance dieser Effekte könnte dazu führen, dass wir keinen atherosklerotischen Unterschied in diesen Mäusen beobachten können.

Während *PGC-1α* sowohl pro- als auch anti-atherosklerotische Eigenschaften besitzt, zeigen unsere Ergebnisse, dass SIRT1 vor allem protektive anti-atherosklerotische sowie anti-thrombotische Eigenschaften aufweist. Daher stellt SIRT1 ein vielversprechendes Zielgen für pharmakologische Therapieansätze für Patienten mit kardiovaskulären Erkrankungen dar.

2 Summary

The aim of this PhD thesis was to investigate of the role of SIRT1 and Peroxisome proliferator-activated receptor γ (PPARγ) coactivator 1α (PGC-1α) in atherosclerosis. Atherosclerosis is a chronic inflammatory disease resulting from the interaction of the vessel wall with macrophages, T cells and oxidized low-density lipoproteins (oxLDL). Rupture of an atherosclerotic plaque may result in thrombus formation and complete vessel occlusion, the primary cause of myocardial infarction and stroke. SIRT1 and PGC-1α are enzymes with important functions in various metabolic and anti-inflammatory processes. SIRT1 is a class III histone deacetylase that mediates the effects of caloric restriction on lifespan and metabolic pathways in various organisms. PGC-1α is a transcription coactivator involved in mitochondrial biogenesis and metabolic processes; it is a target protein of SIRT1.

To study the role of these molecules in atherosclerosis, we crossed *SIRT1*$^{+/-}$ or *PGC-1α*$^{-/-}$ with atherosclerosis-prone *ApoE*$^{-/-}$ mice, and compared *ApoE*$^{-/-}$ *SIRT1*$^{+/+}$ with *ApoE*$^{-/-}$ *SIRT1*$^{+/-}$ mice as well as *ApoE*$^{-/-}$ *PGC-1α*$^{+/+}$ with *ApoE*$^{-/-}$ *PGC-1α*$^{-/-}$ mice, respectively.

We found that haploinsufficient *ApoE*$^{-/-}$ *SIRT1*$^{+/-}$ mice developed more atherosclerotic lesions than *ApoE*$^{-/-}$ *SIRT1*$^{+/+}$ mice. Using in vitro, ex vivo and in vivo approaches, we showed that the atheroprotective effects of SIRT1 are mediated via suppression of NF-κB signaling: SIRT1 prevents the expression of endothelial adhesion molecules and reduces the expression of the scavenger receptor *Lox-1* as well as macrophage foam cell formation. We further demonstrated that suppression of NF-κB signaling diminishes the expression of tissue factor (coagulation factor III) in human aortic endothelial cells.

ApoE$^{-/-}$ *PGC-1α*$^{+/+}$ and *ApoE*$^{-/-}$ *PGC-1α*$^{-/-}$ mice did not differ in the amount of their atherosclerotic lesions. *ApoE*$^{-/-}$ *PGC-1α*$^{-/-}$ mice had markedly reduced body and epididymal white adipose tissue (WAT) weight, less plasma triglycerides, and differential expression of various pro and anti-atherogenic factors. A balance of these anti- and pro-atherogenic factors may explain the unchanged atherosclerotic phenotype of *ApoE*$^{-/-}$ *PGC-1α*$^{-/-}$ mice.

Taken together, our data reveal that the role of PGC-1α in atherogenesis remains to be clarified. On the other hand, SIRT1 has both anti-atherogenic and anti-thrombotic functions. Our findings suggest that SIRT1 activation may be a promising therapeutic approach to impede atherosclerosis.

3 Abbreviations

$^{12}/_{15}$-LO	$^{12}/_{15}$-Lipooxygenase
ACAT	Acyl CoA:cholesterol acyltransferase
acLDL	Acetylated LDL
ADP	Adenosine diphosphate
AMP	Adenosine monophosphate
ApoE	Apolipoprotein E
ATP	Adenosine triphosphate
ATVD	Atherothrombotic vascular disease
BM	Bone marrow
BMT	Bone marrow transplantation
BrdU	Bromodeoxyuridine
CVD	Cardiovascular disease
DAPI	4'-6-Diamidino-2-phenylindole
DiI	1,1',di-octadecyl-3,3,3'3'-tetramethylindocarbocyanine perchlorate
DiO	3,3'-dioladecyloxacarbocyanine perchlorate
DOI	Digital object identifier
E-Sel	E-Selectin
EC	Endothelial cell
eNOS	Endothelial nitric oxide synthase
FOXO	Forkhead box O (e.g., FOXO1, FOXO3, FOXO4)
GR	Glucagon receptor (also called Gcgr)
HAEC	Human aortic endothelial cell
HAT	Histone acetyltransferase
HDL	High density lipoprotein
HSL	Hormone sensitive lipase
ICAM-1	Intercellular adhesion molecule 1
IDL	Intermediate density lipoprotein
iNOS	Inducible nitric oxide synthase
LDL	Low density lipoprotein
LDL-R	LDL-Receptor

Lox-1	Lectin-like oxidized LDL receptor 1 (also called Olr1)
LPS	Lipopolysaccharide
LXRα/β	Liver x receptor
MCP-1	Monocyte chemoattractant protein 1 (also called chemokine (C-C motif) ligand 2 or Ccl2)
MPO	Myeloperoxidase
NAD	Nicotinamide adenine dinucleotide
NAM	Nicotinamide
NF-κB	Nuclear factor kappa B
NO	Nitric oxide
OAADPr	O-acetyl-ADP-ribose
ORO	Oil red O
oxLDL	Oxidized LDL
PC	Phosphatidyl choline
PGC-1α	PPARγ coactivator 1α
PLA_2	Phospholipase A_2
PLC	Phospholipase C
PPAR	Peroxisome proliferator-activated receptor (e.g., PPARα, PPARβ/δ, PPARγ)
PMID	PubMed unique identifier
ROS	Reactive oxygen species
siRNA	Small interfering RNA
SIRT1	Sirtuin 1 (silent mating type information regulation 2, homolog) 1
SMase	Sphingomyelinase
SR-A	Scavenger receptor A
SR-B	Scavenger receptor B
SR-PSOX/ CXCL16	Scavenger receptor for phosphatidylserine and oxidized lipoprotein/CXC chemokine ligand 16
TF	Tissue factor (also called coagulation factor III or Fe)
TNF-α	Tumor necrosis factor alpha
VCAM-1	Vascular cell adhesion molecule 1
VSMC	Vascular smooth muscle cell
vWF	Von Willebrand factor
WAT	White adipose tissue
WT	Wild-type

4 Introduction

4.1 Atherosclerosis

The exact date of the first description of the process of atherosclerosis is unknown. Early in the 20th century, Nikolai Anitschkow demonstrated that a cholesterol-rich diet leads to the accumulation of cholesterol in the arterial wall of rabbits, and consequently to the development of atherosclerotic plaques (Anitschkow and Chalatow, 1912). This was the first link between cholesterol feeding and atherosclerosis. Today it is well recognized that cholesterol promotes atherosclerosis and cardiovascular diseases (CVD) (Steinberg, 1989).

Atherosclerosis is the major cause of myocardial infarction and stroke, the two leading causes of mortality in the Western world (Hansson, 2005). Atherogenesis, the developmental process of atheromatous plaque formation, is a chronic inflammatory disease that results from interaction between modified low-density lipoproteins (LDL), activated endothelial cells (EC), monocyte-derived macrophages, T cells, and the vessel wall (Hansson, 2005) (Figure 1). The main steps in atherogenesis will be explained in more detail, focusing on the molecular aspects of the disease.

Figure 1 Model of atherogenesis

(see next page) Upon activation, endothelial cells (EC) express adhesion molecules (e.g., ICAM-1, blue, and VCAM-1, red) upon activation. Blood monocytes bind to these adhesion molecules, transmigrate from the arterial lumen (blood) into the arterial intima, and differentiate into macrophages. Increased uptake of modified LDL (mainly oxLDL) via scavenger receptors or decreased cholesterol efflux accelerates the accumulation of intracellular free cholesterol and cholesteryl ester-loaded lipid droplets that promote foam cell formation. Macrophages also interact and present antigens to T helper cells (Th cell). Macrophage foam cells eventually die and fall apart, thereby forming a necrotic core. Advanced, vulnerable plaques can rupture and contribute to the formation of an arterial thrombus, which may lead to myocardial infarction or stroke.

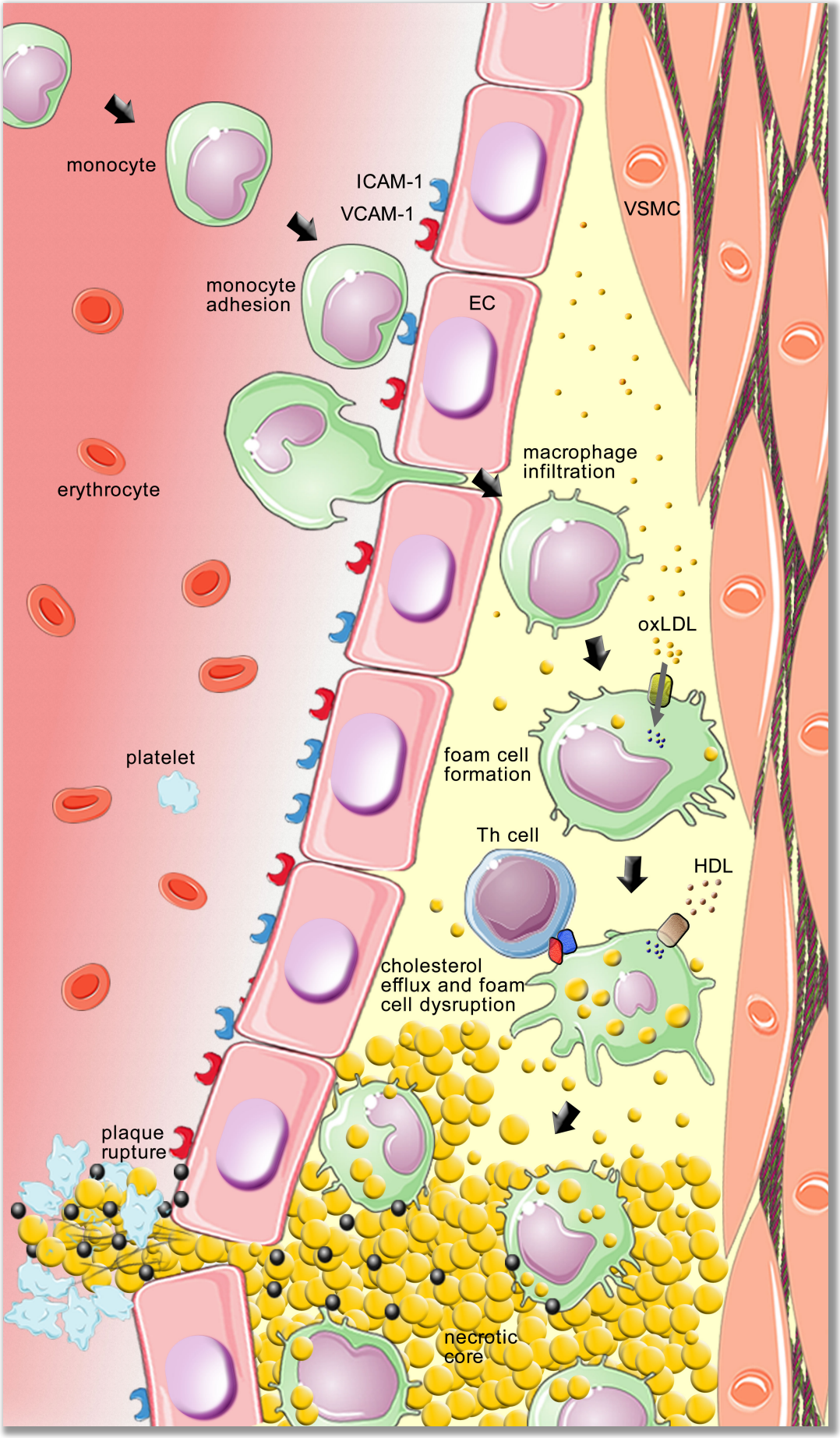
monocyte
ICAM-1
VCAM-1
VSMC
monocyte adhesion
EC
erythrocyte
macrophage infiltration
oxLDL
platelet
foam cell formation
Th cell
HDL
cholesterol efflux and foam cell dysruption
plaque rupture
necrotic core

Atherogenesis starts during embryonic development

Atherosclerosis it is a long-term disease that starts early in human development. Studies on premature human fetuses revealed that the formation of fatty streaks, small sub-endothelial deposits of monocyte-derived macrophages, may already start during embryonic development (Napoli et al., 1997). Although the placenta is impermeable to native LDL particles and children of hypercholesterolemic mothers generally have normal cholesterol levels, a correlation between maternal and fetal plasma cholesterol suggests that during early stages of pregnancy, maternal hypercholesterolemia may promote lesion formation in the fetus (Napoli et al., 1997; Palinski and Napoli, 2002).

LDL modifications – a key trigger of atherosclerosis

Lipoproteins are the cholesterol carriers in the blood stream. An LDL particle is mainly composed of ~ 700 phospholipids, ~ 600 free cholesterols, ~ 1600 cholesteryl esters, ~ 185 triglycerides, and one large apoB-100 protein (Esterbauer et al., 1992). LDL particles become atherogenic especially after undergoing covalent modifications that affect their functionality and receptor-binding specificity. These modifications are introduced by different proteolytic and lipolytic enzymes and oxidants. Chymase, tryptase, plasmin, kallikrein, thrombin and other types of proteases and matrix metalloproteinases are capable of cleaving apoB-100. Lypases, such as phospholipase A_2 (PLA_2), phospholipase C (PLC), sphingomyelinase (SMase), or carboxyl ester lipase, catalyze the hydrolysis of fatty acid esters, phospholipids, sphingomyelins, and lysophospholipids, respectively. Enzymes that oxidize LDL include $^{12}/_{15}$-lipooxygenase ($^{12}/_{15}$-LO), myeloperoxidase (MPO), and heme-oxygensase I (Oorni et al., 2000). Protein modifications can generate neoepitopes (e.g. 'oxidation-specific' epitopes) that are recognized by 'ox-LDL' antibodies in vitro and by macrophage scavenger receptors in vivo (Horkko et al., 1996; Palinski et al., 1996).

The most studied LDL modification is oxidation. LDL can be oxidized nonenzymatically and enzymatically. Nonenzymatic oxidations can be performed in vitro using copper ions (Cu^{2+}), which oxidize a large amount of polyunsaturated fatty acids (PUFA), increase the hydrate density of the particle and drastically alter the apoB-100 protein. These oxidative changes can be blocked with antioxidants, such as vitamin E (α-tocopherol) or probucol (Esterbauer et al., 1992; Henriksen et al., 1981; Olsson and Yuan, 1996; Steinbrecher et al., 1984). Enzymatic modifications of LDL can be achieved by incubating LDL with endothelial cells (EC), vascular smooth muscle cells (VSMC), monocytes, macrophages, fibroblasts or neutrophils.

The enzymatic function comes from $^{12}/_{15}$-LO, inducible nitric oxide synthase (iNOS), MPO, NAPDH oxidase, and other peroxidases (Steinberg, 2009).

Endothelial dysfunction – an early manifestation of atherosclerosis

Under physiological conditions the neurotransmitter acetylcholine binds to specific G protein coupled receptors on endothelial cells and the downstream signaling pathway leads to phosphorylation and activation of the endothelial nitric oxide synthase (eNOS). eNOS uses L-arginine as substrate to generate citrulline and nitric oxide (NO). NO diffuses to adjacent vascular smooth muscle cells (VSMCs) and activates an enzymatic pathway that leads to the relaxation of smooth muscle cells and, consequently, to vessel dilation (Murad, 2006). NO exerts additional protective effects such as prevention of monocyte adhesion to the endothelial layer, reduction of smooth muscle cell proliferation, and inhibition of platelet activation and aggregation (Forstermann, 2010).

Loss of proper endothelial function leads to chronic endothelial dysfunction, which is an indicator of CVD and an early step in atherogenesis (Kawashima and Yokoyama, 2004). Excessive production of reactive oxygen species (ROS) and oxidant stress, which are often observed in patients with hypertension, hypercholesterolemia or diabetes, impairs NO production and chemically inactivates NO to form toxic peroxynitrite ($ONOO^-$) (Forstermann, 2010). Peroxynitrite may 'uncouple' eNOS, which means that the oxygen reduction is uncoupled from the NO synthesis, thereby yielding a dysfunctional superoxide-generating enzyme that enhances vascular oxidative stress (Laursen et al., 2001). These and several other consequences of impaired NO synthesis affect endothelial function and induce a sustained endothelial inflammatory activation that contributes to the development of atherosclerosis (Deanfield et al., 2007; Kawashima and Yokoyama, 2004; Mueller et al., 2005; Stokes et al., 2001).

Endothelial activation and inflammatory cell recruitment

Cytokines (e.g. interleukins and TNF-α) and constituents of modified lipoproteins (e.g. lysophosphatidyl choline) lead to increased oxidative stress in endothelial cells, which in turn activates the NF-κB signaling pathway. Activated NF-κB migrates into the nucleus and induces the expression of numerous genes, including many pro-inflammatory genes such as P-Selectin, ICAM-1, and VCAM-1 (Collins et al., 1995; Gareus et al., 2008). These endothelial cells are considered 'activated'. In contrast, under physiological conditions aortic endothelial cells do not express these adhesion molecules, except for low constitutive levels of ICAM-1

(Wood et al., 1993). Secretion and presentation of these molecules attract and activate blood monocytes, which then transmigrate into the arterial intima. This transmigration of monocytes is stimulated by chemokines, such as monocyte chemoattractant protein-1 (MCP-1), MCP-4, regulated on activation normal T cell expressed and secreted (RANTES), and IL-8, which bind to G protein coupled-receptors and are expressed by various vascular cells (Zernecke et al., 2008). Adhesion of mononuclear phagocytes to activated endothelial cells starts early in atherogenesis (Faggiotto et al., 1984; Poole and Florey, 1958), suggesting that endothelial activation is an early inflammatory step of the disease.

Cholesterol uptake and macrophage foam cell formation

Infiltration of monocyte-derived macrophages into the subendothelial space is a key step in atherogenesis. These invading macrophages release and respond to inflammatory mediators and interact with cytotoxic (Tcyt) and helper (Th) T cells. While in vitro incubation of monocytes or macrophages with native LDL does not lead to cholesterol accumulation, incubation with acetylated LDL (acLDL) leads to a quick accumulation of cholesterol and foam cell formation (Goldstein et al., 1979). The reason is that the LDL receptor is downregulated when cholesterol concentrations increase in the cell (receptor-down regulation), whereas the receptor that recognizes acLDL, scavenger receptor A (SR-A), is not downregulated. The same concept holds true for other scavenger receptors. Instead of being downregulated at increasing intracellular cholesterol concentrations, some of them are even upregulated, thereby providing a fast and uni-directional accumulation of cholesterol from modified lipoproteins, such as acLDL and oxLDL (Steinberg, 2002).

Table 1 Classes of scavenger receptors

Class	Scavenger receptor
A	SR-AI, SR-AII, SR-AIII, MARCO, SRCL
B	SR-BI, CD36
E	Lox-1
F	SREC-I, SREC-II
G	SR-PSOX/CXCL16

Macrophage scavenger receptors (SRs) are classified into SR families based on their structural similarity (Table 1). The most prominent SRs that are expressed in atherosclerotic lesions include the scavenger receptor types AI and AII (Kodama et al., 1990; Rohrer et al.,

1990), CD36 (Endemann et al., 1993), lectin-like oxidized LDL receptor-1 (Lox-1) (Sawamura et al., 1997) and scavenger receptor for phosphatidylserine and oxidized lipoprotein/CXC chemokine ligand 16 [(SR-PSOX)/CXCL16] (Matloubian et al., 2000; Shimaoka et al., 2000).

Modified LDL particles are bound and ingested by scavenger receptors, and then delivered to lysosomes, where cholesteryl esters are enzymatically hydrolyzed to free cholesterol and fatty acids (Figure 2). Acyl CoA:cholesterol acyltransferase (ACAT; also called sterol O-acyltransferase or SOAT) catalyzes the formation of cholesteryl ester from free cholesterol, which accumulates in lipid droplets that lead to the foamy appearance of the cells. The hormone sensitive lipase (HSL; also known as neutral cholesterol hydrolase or NCEH) is a neutral lipase that reverses this esterification by mediating cholesterol ester hydrolysis, yielding free cholesterol (Li and Glass, 2002) (Figure 3).

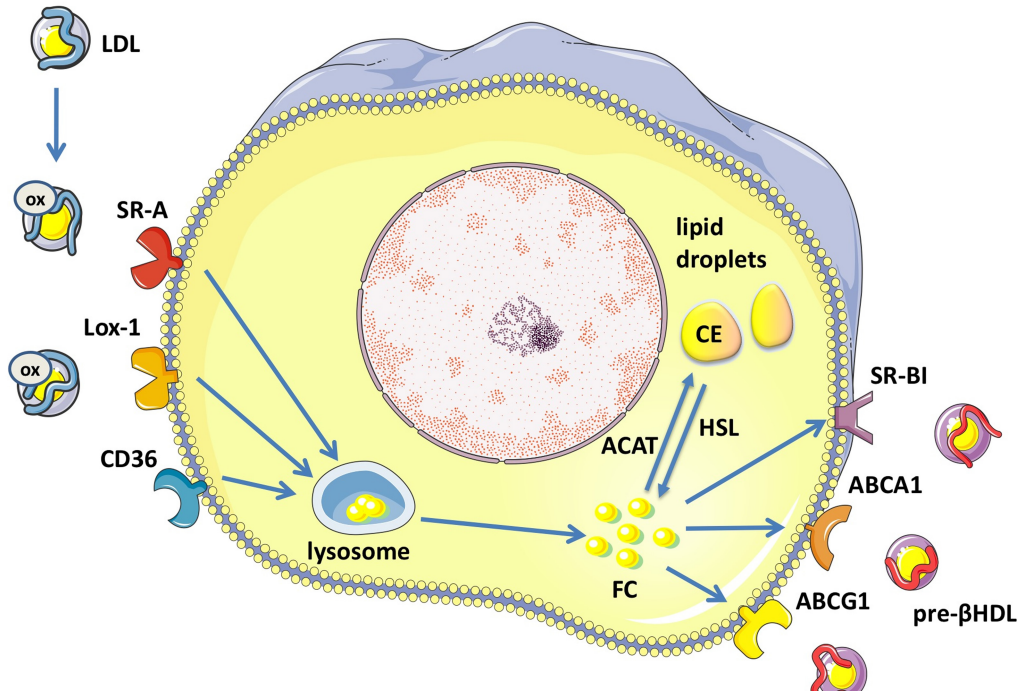

Figure 2 Cholesterol influx and efflux

Uncontrolled binding and uptake of modified LDL particles into macrophages is mediated by scavenger receptors, such as SR-A, Lox-1, and CD36. The lipoprotein particles are digested in lysosomes, and the resulting free cholesterol particles are released into the cytoplasm. Excess free cholesterol in the cytoplasm is esterified by ACAT to cholesteryl esters, which then accumulate in lipid droplets. HSL hydrolyzes cholesteryl esters back to free cholesterol. Additionally, free cholesterol can be used for reverse cholesterol transport, a process that is supported by ABC transporters, such as ABCA1 and ABCG1, and the scavenger receptor SR-BI.

The physiological role of scavenger receptors is the recognition and clearance of pathogens and apoptotic cells. However, many scavenger receptors have pleiotropic functions. For example, CD36 is involved in uptake and internalization of oxidized phospholipids and lipoproteins as well as apoptotic cells and pathogens in phagocytes, it binds to and supports the transport of long-chain fatty acids in adipose tissue and muscle, and in sensory cells it is involved in pheromone signaling in insect and fatty food preference in rodents (Silverstein and Febbraio, 2009).

An important and unresolved question is: Why do these receptors take up cholesterol in an uncontrolled manner? A perspicuous answer may be that modifications in lipoprotein contents resemble pathogen-associated molecular patterns (PAMPs) that are normally recognized by these pathogen recognition receptors (PRRs) in innate immunity. For example, phosphatidyl choline (PC) moieties of oxLDL mimic the PCs found on the surface of many pathogens, and one PPR for this molecular pattern is the scavenger receptor CD36 (Horkko et al., 1999; Horkko et al., 1996).

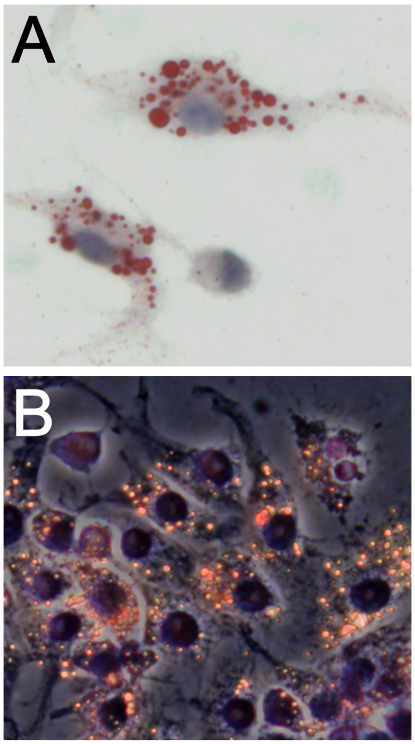

Figure 3 Macrophage foam cell

Treatment of macrophages with oxLDL leads to intracellular cholesterol accumulation and gives the cells their foamy appearance. (A) Brightfield image of peritoneal macrophages that were treated with oxLDL and stained with Oil Red O (ORO). The lysochrome diazo dye ORO stains neutral triglycerides, lipids, and lipoproteins. Lipid droplets are stained red. (B) Phase contrast image of RAW 264.7 macrophages upon treatment with DiI-labeled oxLDL. DiI is a carbocyanine, fluorescent lipophilic dye, with its emission in the yellow/red spectrum. Magnifications, x400. Nuclei are stained with DAPI, light blue to violet.

Reverse cholesterol transport

Mammalian cells are unable to degrade the sterol ring of cholesterol, and most excess sterols can only be eliminated from the body by biliary excretion. Therefore, macrophages and other

cell types must export cholesterol to extracellular acceptors, mainly HDLs, for transport to the liver. This reverse cholesterol transport involves many enzymes and receptors, such as liver X receptors (LXRs) and their binding partners retinoid X receptor (RXRs), peroxisome-proliferator activated receptors (PPARs), the ABC transporters ABCA1 and ABCG1 as well as the scavenger receptor SR-BI. An dysfunctional reverse cholesterol transport may lead to excessive accumulation of cholesterol in the cell and therefore stimulate foam cell formation and disease progression (Li and Glass, 2002).

Adaptive immunity in atherosclerosis

The adaptive immunity is composed of the lymphatic B and T cells. While B cells are only marginally detectable in atherosclerotic plaques, T cells are quite abundant (up to 20% of plaque cells) and play an important role in atheromatous plaque formation. T cells can be subdivided into cytotoxic ($CD8^+$ T cells, Tcyt) and helper T cells ($CD4^+$ T cells, Th), and the helper T cells can be further subclassified as Th1, Th2, Treg (regulatory T cells), and Th17 cells, depending on the cytokines that these cells secrete after activation.

LDL-R-/- RAG1-/- or ApoE-/- DNA-PK-/- mice have no lymphocytes and develop less atherosclerosis than immunocompetent control mice (Song et al., 2001; Zhou et al., 2000). Th1-slanted ApoE-/- C57BL/6 mice develop more atherosclerosis compared with ApoE-/- BALB/c mice, which display predominantly Th2 responses by CD4+ T cells, supporting a proatherogenic role for Th1 response (Schulte et al., 2008). In addition, atherosclerotic plaques generally display high IFN-γ (Th1 marker) and low IL-4 (Th2 marker) levels, suggesting that Th1 cells are the primary T cell subtype found in plaques. Furthermore, expression of the CD45 RO isoform and secretion of IFN-γ suggest that most plaque T cells are activated (Packard et al., 2009). Tregs play a crucial role in the maintenance of tolerance to self-antigens and the regulation of adaptive immunity. Tregs have an anti-atherogenic function by suppressing the activation of other T cells in secondary lymphoid organs or directly in the plaques (Packard et al., 2009).

The role of B cells in atherosclerosis is less clear. While some groups reported that B cells have an overall protective function in atherosclerosis (Caligiuri et al., 2002; Major et al., 2002), a recent study demonstrates that depletion of mature B cells using CD20 antibodies decreases atherosclerosis (Ait-Oufella et al., 2010).

Plaque vulnerability

Human atherosclerotic plaques can be divided into three distinct components: (1) The atheroma, which is closest to the arterial lumen and has a nodular structure consisting mainly of macrophage foam cells, (2) the underlying areas of cholesterol crystals, and (3) calcification at the outer base of advanced lesions. The development of human atherosclerosis, linking the lipoprotein/cholesterol disorder and the inflammatory processes, continues for years and decades. Besides contributing to plaque destabilization when falling apart in a necrotic fashion, macrophage foam cells secrete extracellular matrix proteases (ECM) and collagenases that digest the ECM and collagen fibrils that are enriched in fibrous caps, respectively. Vascular smooth muscle cells also secrete these proteolytic enzymes, thereby enhancing this destabilizing process. Atheromatous plaques that are susceptible to arterial wall breakdown are described as vulnerable plaques and characterized by thin fibrous caps, large necrotic areas, and increased number inflammatory cells and molecules (Tabas, 2010).

Atherothrombosis

Atherothrombotic vascular disease (ATVD) is the primary cause of myocardial infarction and stroke, which are the main causes of morbidity and mortality in developed countries.

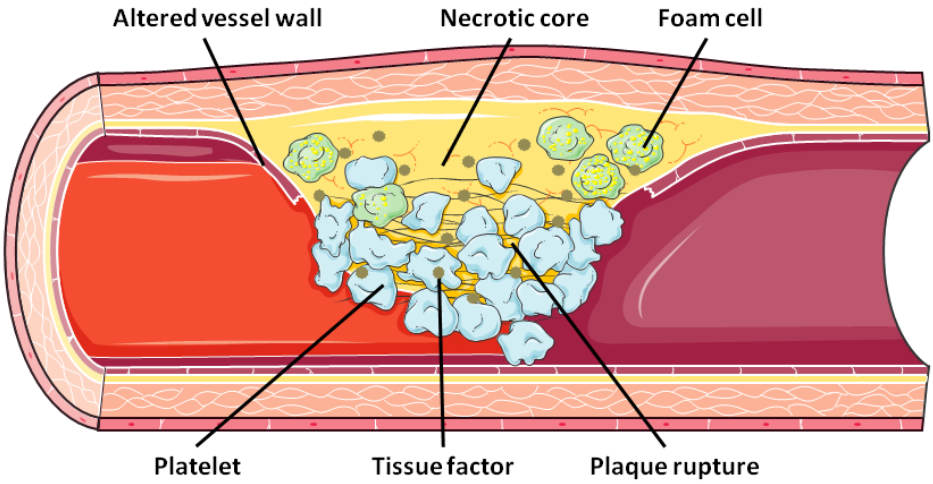

Figure 4 Arterial thrombosis

The primary trigger of arterial thrombosis is rupture of an atherosclerotic plaque. The disruption of the endothelium releases the thrombogenic plaque content, including tissue factor, into the lumen of the blood vessel. Platelets will be recruited and aggregate at the forming thrombus.

The main trigger of thrombosis is the rupture of a vulnerable atherosclerotic plaque. Once an atherosclerotic plaque ruptures, thrombogenic material attracts platelets to the site of injury, thereby inducing platelet aggregation and an increase of the nascent thrombus. Tissue factor (coagulation factor III) is abundantly expressed by various cells in atherosclerotic plaques and released into the blood during rupture, thereby activating the coagulation cascade that will activate platelets. Activated platelets then release the contents of granules, which further promote platelet recruitment, adhesion, aggregation and activation (Figure 4) (Mackman, 2008).

Mouse models of atherosclerosis

Normal wild-type mice do not develop atherosclerosis when kept under normal diet. The reason is that wild-type mice have extremely low levels of remnant lipoproteins (chylomicrons and IDL remnants). When kept under a high-cholesterol, high-fat diet the development of atherosclerosis is strain dependent, e.g. C3H is an atherosclerosis-resistant strain, while C57BL/6 is an atherosclerosis-susceptible strain (Paigen et al., 1987). The two most abundantly used mouse models to study atherogenesis are apolipoprotein E (*ApoE*) and LDL-Receptor (*LDL-R*) knockout mice (Ishibashi et al., 1993; Plump et al., 1992; Zhang et al., 1992). *ApoE*$^{-/-}$ mice lack apolipoprotein E, which normally clears remnant lipoproteins from the bloodstream through binding to the LDL-Receptor (that is lacking in *LDL-R*$^{-/-}$ mice) or the LDL receptor-related protein (LRP) in hepatocytes. Absence of these molecules leads to accumulation of remnant lipoproteins in the blood and thereby to the development of atherosclerosis (Breslow, 1996).

4.2 Sirtuins and Nε-lysine deacetylation

Acetylation of the Nε-lysine residue is a reversible, posttranslational protein modification. Histone acetyltransferases (HATs) transfer the acetyl moiety from acetyl coenzyme A to the ε-$NH3^+$ groups of internal lysine residues. Addition of this acetyl group neutralizes the positive charge and thereby increases hydrophobicity. In addition this modification is able to influence the interaction with other proteins as well as other posttranslational modifications, such as methylation, ubiquitination and sumoylation. Histone deacetylases (HDACs) promote the reversible reaction, the deacetylation of the acetyl-Nε-lysine residue and thereby re-establish the positive charge of the protein (Kuo and Allis, 1998). Nε-lysine acetylation and deacetylation was initially observed in histone proteins, but later on other non-histone proteins were also shown to undergo this posttranslational protein modification.

HDACs are classified into 4 families: Classes I, II, III, and IV. Class III HDACs are also called sirtuins. The mammalian sirtuin family consists of 7 HDACs that share a conserved catalytic core domain and are expressed ubiquitously (Michan and Sinclair, 2007). Except SIRT4, all sirtuins exhibit a nicotinamide adenine dinucleotide (NAD^+)-dependent deacetylase activity. At least SIRT4, SIRT6 and SIRT7 show an (additional) enzymatic ADP-ribosyltransferase activity and can transfer the ADP-ribosyl moiety of NAD^+ to a target protein (Houtkooper et al., 2010; Lavu et al., 2008). Sirtuins reverse Nε-lysine acetylations of their target proteins by hydrolyzing one NAD^+ and releasing nicotinamide (NAM), a unique byproduct called O-acetyl-ADP-ribose (OAADPr), and the deacetylated substrate (Figure 5) (Avalos et al., 2005; Denu, 2005; Tanner et al., 2000). Recent studies suggest that OAADPr may have biological functions on its own (Taylor et al., 2008).

SIRT1, SIRT6 and SIRT7 are nuclear deacetylases, with SIRT7 localizing mainly to nucleoli. SIRT3, SIRT4, and SIRT5 are localized mainly in mitochondria, whereas SIRT2 is detected primarily in the cytoplasm. Nevertheless, SIRT1 and SIRT3 have also been detected in the cytoplasm, and some studies suggest that SIRT2 can also be found in the nucleus (Finkel et al., 2009; Haigis and Guarente, 2006; Michan and Sinclair, 2007; Taylor et al., 2008).

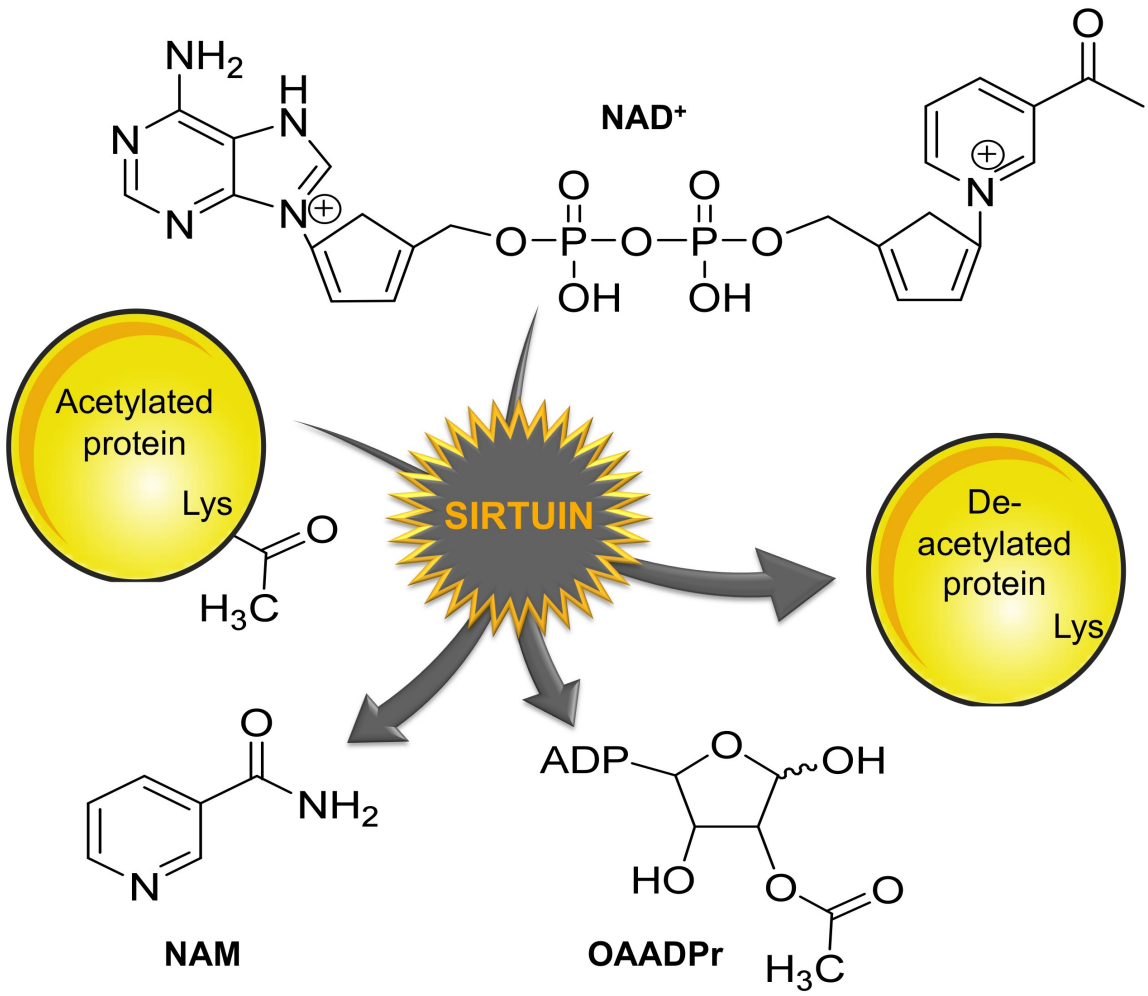

Figure 5 Nε-lysine deacetylation by sirtuins

Sirtuins deacetylate specific acetylated Nε-lysine residues of their target proteins in a reaction that consumes NAD^+, and yields the deacetylated protein, NAM, and OAADPr.

4.3 SIRT1

Sir2, the yeast homolog of SIRT1, was discovered as a factor necessary for the transcriptional silencing of the silent mating-type loci and telomeric areas in yeast by inducing DNA heterochromatization (Gottlieb and Esposito, 1989; Maillet et al., 1996; Rine and Herskowitz, 1987). Homologues are also found in *Escherichia coli*, *Salmonella typhimurium*, *Caenorhabditis elegans*, *Drosophila melanogaster*, *Mus musculus*, *Macaca mulatta*, humans, and many other species, showing that the Sir2 family is conserved from bacteria to humans (Blander and Guarente, 2004; Brachmann et al., 1995; Frye, 1999; Tsang and Escalante-Semerena, 1998).

The finding that extra copies of *Sir2* prolong the life span of yeast, while *Sir2* deficiency caused the opposite (Kaeberlein et al., 1999), drew the attention of many scientists to the

Sir2/sirtuin field. Shortly afterwards, it was shown that Sir2 is an NAD^+-dependent histone deacetylase and that both Sir2 and NAD^+ are required for calorie restriction-mediated life span extension in yeast (Imai et al., 2000; Lin et al., 2000; Lin et al., 2004b; Lin et al., 2002). These findings placed Sir2 into a central position linking the metabolic state of a cell with the transcriptional control of gene expression.

Sir2 homologues and Sir2 activators also regulate life span in *Caenorhabditis elegans* and *Drosophila melanogaster* (Rogina and Helfand, 2004; Tissenbaum and Guarente, 2001; Wood et al., 2004), and it was recently demonstrated that moderate caloric restriction lowers the incidence of aging-related deaths in rhesus monkeys (Colman et al., 2009). Nevertheless, if sirtuins are directly involved in calorie restriction-mediated lifespan extension remains unclear (Baur et al., 2010; Fontana et al., 2010; Kaeberlein, 2010; Kaeberlein and Powers, 2007). What seems clear, on the other hand, is the central role of SIRT1 as a metabolic regulator. The function of many important metabolic proteins is regulated by SIRT1, including peroxisome proliferator-activated receptor γ (PPARγ), PPARγ coactivator 1α (PGC-1α), nuclear factor-κB (NF-κB), Liver X receptor α (LXRα or Nr1h3), and endothelial nitric oxide synthase (eNOS) (Lagouge et al., 2006; Li et al., 2007; Mattagajasingh et al., 2007; Picard et al., 2004; Rodgers et al., 2005; Yeung et al., 2004). Interestingly, some of these molecules have also been shown to play a direct or indirect role in atherogenesis (Kim et al., 2007b; Knowles et al., 2000; Thurberg and Collins, 1998; Tontonoz and Spiegelman, 2008).

Several studies propose that SIRT1 could exert a protective role in the cardiovascular system: In rat aortic rings prepared ex vivo SIRT1 improves endothelial dysfunction by activating eNOS (Mattagajasingh et al., 2007), suggesting that SIRT1 may prevent an early atherogenic event. SIRT1 regulates angiogenesis and ischemia-induced neovascularization in zebrafish and mice via deacetylation of the anti-angiogenic transcription factor Foxo1 (Potente et al., 2007). Cholesterol efflux, an event that is important in later stages of atherogenesis, may also be influenced by SIRT1. It was demonstrated that SIRT1 regulates the transcriptional activity of LXRα via direct deacetylation in in vitro and ex vivo experiments using macrophages (Li et al., 2007).

Given the multiple targets of SIRT1, it is likely that other targets apart from eNOS, Foxo1, and LXR and the involved mechanisms are regulated by SIRT1 in atherogenesis. In particular, the role of SIRT1 in monocyte adhesion, macrophage infiltration as well as lipid uptake and foam cell formation has not yet been investigated. During the course of this PhD thesis some studies from other groups as well as the results of our studies demonstrated that SIRT1 is

indeed involved in different processes in atherogenesis. The consensus and discrepancy between these studies will be discussed.

4.4 PGC-1α

One of the best-characterized deacetylation targets of SIRT1 is PGC-1α (Rodgers et al., 2005). PGC-1α is an important cofactor in the transcriptional regulation of genes encoding metabolic enzymes and mitochondrial proteins (Lin et al., 2005). PGC-1α was the first described member of the small PGC-1 family of coactivators (Puigserver et al., 1998). Other members of this protein family are PGC-1β and PGC-related coactivator (PRC). NAD^+-dependent deacetylation by SIRT1 activates PGC-1α, which in turn modulates the expression of many genes, including genes with a crucial role in glucose homeostasis, oxidative phosphorylation and mitochondrial biogenesis (Lagouge et al., 2006; Rodgers et al., 2005).

A well characterized metabolic signaling cascade involves the 5'-AMP-activated protein kinase (AMPK), changes in intracellular NAD^+ levels, SIRT1, and PGC-1α (Canto and Auwerx, 2009). Cells that are subjected to metabolic stress that interferes with ATP synthesis, develop an increased ADP:ATP ratio. The adenylate kinase, which catalyzes the interconversion of adenine nucleotides, further amplifies this effect by increasing the ratio of AMP:ATP. Enhanced intracellular levels of AMP then activate the AMPK, which blocks anabolic processes requiring energy and favors catabolic processes generating ATP (Hardie, 2007). A result of this AMPK-mediated metabolic adaptation is an increase in the NAD^+:NADH ratio (Canto et al., 2009). Increased levels of NAD^+ will then activate SIRT1, which in turn deacetylates and activates PGC-1α and other important transcriptional regulators that help the cell to adapt to the metabolic stress (Canto et al., 2010). Therefore, it could well be that atheroprotective effects of SIRT1 (or AMPK) might act via PGC-1α activation.

However, PGC-1α may also affect atherogenesis independently of SIRT1. PGC-1α interacts with many different transcription factors, some of which play important roles in metabolic processes, such as PPARα, PPARβ/δ, PPARγ, LXRα/β, GR, and Foxo1 (Kressler et al., 2002; Oberkofler et al., 2003; Puigserver et al., 2003; Puigserver and Spiegelman, 2003; Vega et al., 2000; Wang et al., 2003; Yoon et al., 2001). Overexpression of PGC-1α in human aortic endothelial cells (HAECs) and human aortic smooth muscle cells (HASMCs) prevents TNF-α-induced ROS production, mitochondrial NAD(P)H oxidase activity, and the expression of the pro-inflammatory molecules MCP-1 and VCAM-1 (Kim et al., 2007b). Furthermore, two

genetic correlation studies strengthen the possible correlation between PGC-1α and atherogenesis: Xie et al. reported a correlation between the G482S and +2962A/G polymorphisms of the PGC-1α gene and severe hypertension (Xie et al., 2007), and Zhang et al. showed a correlation between PGC-1α G482S polymorphism and the prevalence of coronary artery disease (Zhang et al., 2008b).

4.4 Hypotheses and specific aims

Based on the published observations described above, we hypothesized that both SIRT1 and PGC-1α are atheroprotective proteins (Figure 6):

- **SIRT1** protects against atherosclerosis by activating atheroprotective molecules, such as eNOS, hence improving endothelial function, and/or by inhibiting pro-atherogenic proteins and pathways, such as NF-κB signaling, thus preventing endothelial inflammation.
- **PGC-1α** prevents atherosclerosis by mediating SIRT1-dependent effects or SIRT1-independent effects, such as suppression of endothelial adhesion molecule expression.

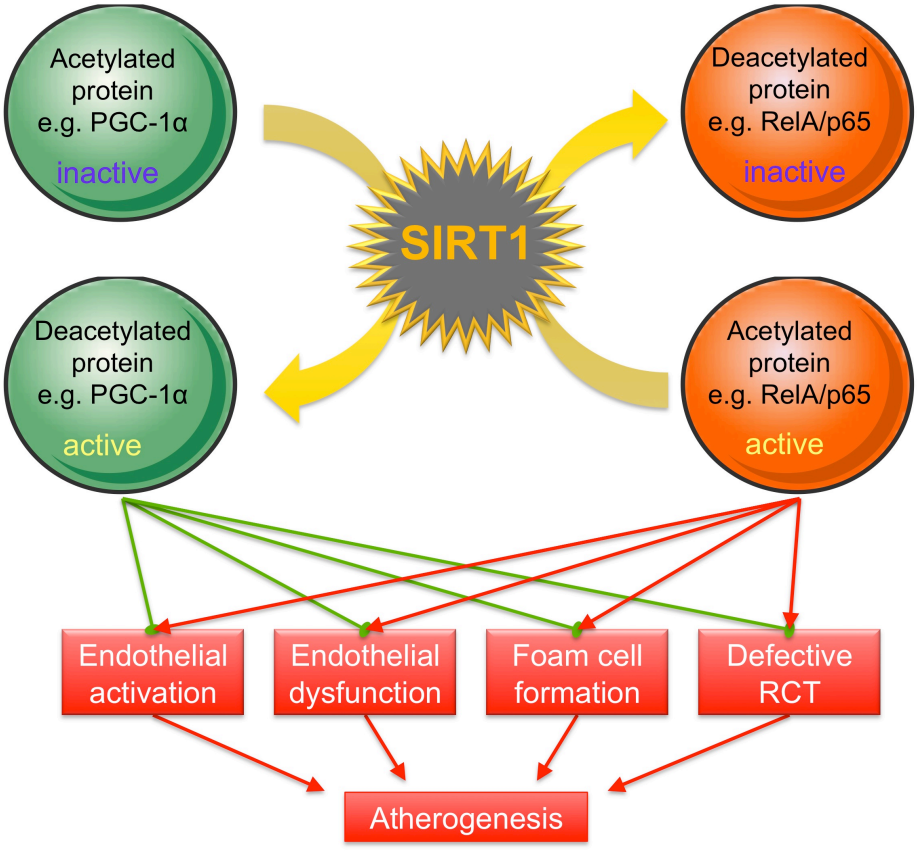

Figure 6 PhD hypotheses

Activation or overexpression of SIRT1 leads to deacetylation of various target proteins. We hypothesized that SIRT1-dependent deacetylation activates anti-atherogenic targets (e.g., PGC-1α and eNOS) and deactivates pro-atherogenic protein and pathways (e.g., NF-κB).

Specific aims

Based on these hypotheses, we formulated following research aims:

Aim 1 – Characterize the role of SIRT1 in atherogenesis: Comparison of 20-week-old male *ApoE*$^{-/-}$ *SIRT1*$^{+/+}$ and *ApoE*$^{-/-}$ *SIRT1*$^{+/-}$ mice kept on a high-cholesterol diet for 12 weeks.

Aim 2 – Determine the role of SIRT1 in arterial thrombosis: Analyze the expression of tissue factor upon genetic and pharmacological SIRT1 modulation in vitro in HAECs and in pharmacological approaches in C57BL/6 mice in vivo.

Aim 3 – Asses the role of PGC-1α in atherogenesis: Comparison of 20-week-old male *ApoE*$^{-/-}$ *PGC-1α*$^{+/+}$ and *ApoE*$^{-/-}$ *PGC-1α*$^{-/-}$ mice kept on a high-cholesterol diet for 12 weeks.

General approach to study atherosclerosis in mice (Figure 7):

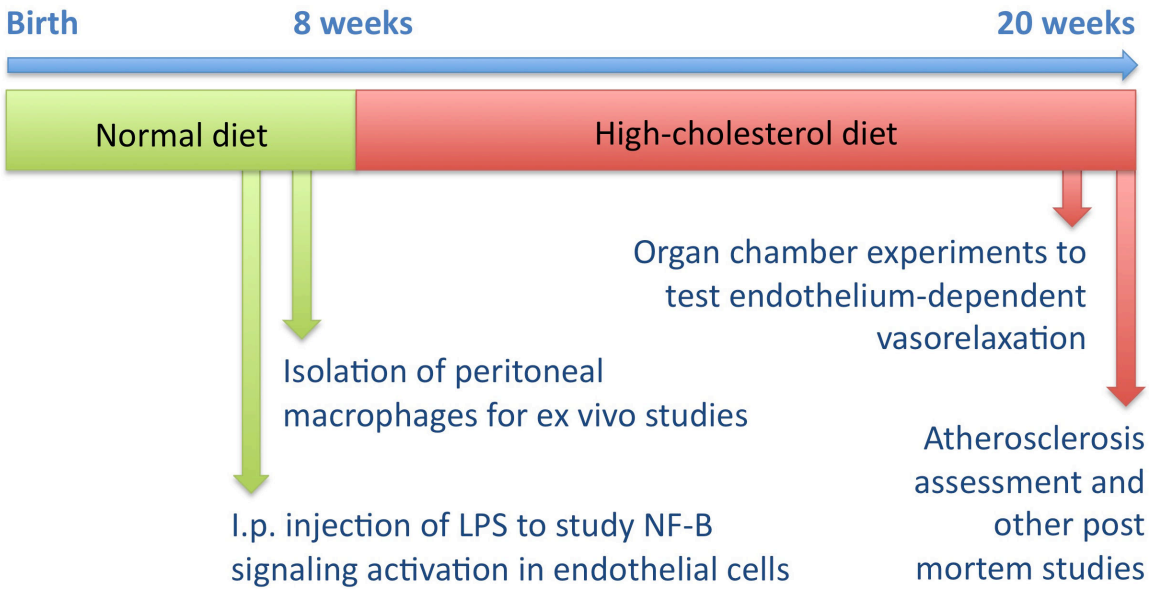

Figure 7 Time point for the most important in vivo and ex vivo experiments

6 to 8-week-old male mice fed a normal diet were used for LPS injection assays to study the effect of acute NF-κB signaling activation or to isolate thioglycolate-elicited peritoneal macrophages for ex vivo assays. Endothelium-dependent vascular function and atherosclerosis were studied in 20-week-old male mice that were fed a 1.25% high-cholesterol diet for 12 weeks. Besides quantifying plaques in the thoraco-abdominal aortae en face, advanced plaque parameters and inflammatory burden were assessed in cross sections of plaques from the aortic sinus and/or aortic arch.

5 Results

Overview of research articles

5.1 SIRT1 decreases Lox-1-mediated foam cell formation in atherogenesis.

Stein, S., Lohmann, C., Schäfer, N., Hofmann, J., et al.
Eur Heart J. 2010 Apr 23. Epub ahead of print.

5.2 SIRT1 reduces endothelial activation without affecting vascular function in ApoE-/- mice.

Stein, S., Schafer, N., Breitenstein, A., Besler, C., et al.
Aging (Albany NY). 2010; 2(6):353-360.

5.3 Sirt1 inhibition induces in vivo arterial thrombosis and tissue factor expression in activated human endothelial cells.

Breitenstein, A., Stein, S., Holy, E.W., Camici, G.G., et al.
Cardiovasc Res. 2010 Nov 21. Epub ahead of print.

5.4 ApoE-/- PGC-1a-/- mice display reduced IL-18 levels and do not develop enhanced atherosclerosis.

Stein, S., Lohmann, C., Handschin, C., Stenfeldt, E., et al.
PLoS ONE. 2010; 5(10): e13539.

Contribution to other published projects within the PhD thesis period

Heart-infiltrating prominin-1+/CD133+ progenitor cells represent the cellular source of TGF-β-mediated cardiac fibrosis in experimental autoimmune myocarditis

Authors:	Gabriela Kania, Przemyslaw Blyszczuk, Sokrates Stein, Alan Valaperti, Davide Germano, Stephan Dirnhofer, Lukas Hunziker, Christian Matter, Urs Eriksson
Journal:	Circ Res. 2009; 105(5):462-70.
DOI:	10.1161/CIRCRESAHA.109.196287
PMID:	19628793
Comment in:	Madeleine W. Cunningham Circ Res. 2009 Aug 28;105(5):403-5
Contribution:	Performance of Phospho-Smad2 and Smad2/3 Western blots on murine heart lysates.

Atherosclerotic Mice Exhibit Systemic Inflammation in Periadventitial and Visceral Adipose Tissue, Liver, and Pancreatic Islets

Authors:	Christine Lohmann, Nicola Schäfer, Tobias von Lukowicz, M. A. Sokrates Stein, Jan Boren, Sabine Rütti, Walter Wahli, Marc Y. Donath, Thomas F. Lüscher, Christian M. Matter
Journal:	Atherosclerosis. 2009; 207(2):360-7.
DOI:	10.1016/j.atherosclerosis.2009.05.004
PMID:	19481752
Contribution:	Performance and analyses of real-time PCRs of transcripts regulating lipid metabolism.

Editorial - A dual role of CD4+ T cells in adipose tissue?

Authors:	Christian M. Matter & M. A. Sokrates Stein
Journal:	Circ Res. 2009; 104(8):928-30
DOI:	10.1161/CIRCRESAHA.109.197004
PMID:	19390060
Comment on:	Ariane Sultan et al. Circ Res. 2009 Apr 24;104(8):961-8.
Contribution:	Writing the editorial

5.1 SIRT1 decreases Lox-1-mediated foam cell formation in atherogenesis

Authors:	Sokrates Stein, Christine Lohmann, Nicola Schäfer, Janin Hofmann, Lucia Rohrer, Christian Besler, Karin M. Rothgiesser, Burkhard Becher, Michael O. Hottiger, Jan Borén, Michael W. McBurney, Thomas F. Lüscher and Christian M. Matter
Journal:	European Heart Journal. 2010 Apr 23. Epub ahead of print.
DOI:	10.1093/eurheartj/ehq107
PMID:	20418343
Contribution:	Design and analyses of all experiments; performance of most experiments; writing the manuscript.

European Heart Journal Advance Access published April 23, 2010

European Heart Journal
doi:10.1093/eurheartj/ehq107

BASIC SCIENCE

SIRT1 decreases Lox-1-mediated foam cell formation in atherogenesis

Sokrates Stein[1,2], Christine Lohmann[1,2], Nicola Schäfer[1,2], Janin Hofmann[3], Lucia Rohrer[2,4], Christian Besler[1,2], Karin M. Rothgiesser[5], Burkhard Becher[2,3], Michael O. Hottiger[2,5], Jan Borén[6], Michael W. McBurney[7], Ulf Landmesser[1,2], Thomas F. Lüscher[1,2], and Christian M. Matter[1,2]*

[1]Cardiovascular Research, Institute of Physiology, Zurich University and Cardiology, Cardiovascular Center, University Hospital Zurich, Winterthurerstrasse 190, CH-8057 Zurich, Switzerland; [2]Zurich Center for Integrative Human Physiology (ZIHP), Zurich CH-8057, Switzerland; [3]Neuroimmunology Unit, Inst. Experimental Immunology, Zurich CH-8057, Switzerland; [4]Institute for Clinical Chemistry, Zurich CH-8057, Switzerland; [5]Institute of Veterinary Biochemistry and Molecular Biology, University of Zurich and University Hospital Zurich, Zurich CH-8057, Switzerland; [6]Sahlgrenska Center for Cardiovascular and Metabolic Research, University of Goteborg, Goteborg SE-41345, Sweden; and [7]Department of Medicine, Ottawa Health Research Institute, University of Ottawa, Ottawa, ON, Canada K1Y 4E9

Received 11 October 2009; revised 26 February 2010; accepted 12 March 2010

This paper was guest edited by Prof. Stefan Janssens, University Hospital Gasthuisberg, Leuven, Belgium

Aims Endothelial activation, macrophage infiltration, and foam cell formation are pivotal steps in atherogenesis. Our aim in this study was to analyse the role of SIRT1, a class III deacetylase with important metabolic functions, in plaque macrophages and atherogenesis.

Methods and results Using partial *SIRT1* deletion in atherosclerotic mice, we demonstrate that SIRT1 protects against atherosclerosis by reducing macrophage foam cell formation. Peritoneal macrophages from heterozygous *SIRT1* mice accumulate more oxidized low-density lipoprotein (oxLDL), thereby promoting foam cell formation. Bone marrow-restricted *SIRT1* deletion confirmed that SIRT1 function in macrophages is sufficient to decrease atherogenesis. Moreover, we show that SIRT1 reduces the uptake of oxLDL by diminishing the expression of *lectin-like oxLDL receptor-1* (*Lox-1*) via suppression of the NF-κB signalling pathway.

Conclusion Our findings demonstrate protective effects of SIRT1 in atherogenesis and suggest pharmacological SIRT1 activation as a novel anti-atherosclerotic strategy by reducing macrophage foam cell formation.

Keywords SIRT1 • Macrophage foam cell • Atherogenesis

Introduction

Atherosclerosis is a chronic inflammatory disease that results from interaction between oxidized low-density lipoprotein (oxLDL), activated endothelial cells, monocyte-derived macrophages, T cells, and the arterial wall. Activated endothelial cells express adhesion molecules, e.g. vascular cell adhesion molecule 1 (VCAM-1) and intercellular adhesion molecule-1 (ICAM-1), which attract and recruit blood monocytes to the vessel wall. These monocytes differentiate into macrophages and infiltrate to the sub-endothelial space where they release and respond to inflammatory mediators such as tumour necrosis factor-α (TNFα), VCAM-1, and interleukins (IL). Eventually, these inflammatory macrophages ingest oxLDL via scavenger receptors, such as scavenger receptor-A (SR-A), CD36 or lectin-like oxLDL receptor 1 (Lox-1), becoming foam cells, and thereby promoting plaque formation.[1]

Sir2 is an NAD-dependent class III deacetylase that was found to increase lifespan in yeast.[2] Its mammalian orthologue SIRT1 senses caloric restriction, improves insulin secretion in pancreatic beta

* Corresponding author. Tel: +41 44 635 6467, Fax: +41 44 635 6827, Email: christian.matter@access.uzh.ch

cells, and reduces accumulation of fatty acids in white adipose tissue (WAT).[3–5] Various targets of SIRT1 have been characterized, including PPARγ coactivator 1α (PGC-1α), nuclear factor κB (NF-κB), p53, FOXO transcription factors, and endothelial nitric oxide synthase (eNOS).[6–13] Interestingly, many of these targets that are critically involved in regulating metabolism have also been shown to play a role in atherogenesis.[14–18] However, little is known about the relevance of SIRT1 in the latter.

In atherogenesis, chronic endothelial dysfunction is a trigger of plaque formation,[19] and endothelial *SIRT1* overexpression has been shown to prevent atherosclerosis by improving vascular function.[20] Nevertheless, the relevance of SIRT1 on the cellular and molecular events governing atherogenesis is unknown. As multiple targets of SIRT1 may play a role in plaque formation, it is likely that eNOS is not the only mechanism by which SIRT1 prevents atherogenesis. In particular, the role of SIRT1 in monocyte adhesion, macrophage infiltration, lipid uptake, and foam cell formation remains to be determined.

To investigate the role of SIRT1 in these cellular and molecular processes, we compared hypercholesterolaemic *ApoE*$^{-/-}$ *SIRT1*$^{+/+}$ with *ApoE*$^{-/-}$ *SIRT1*$^{+/-}$ mice. These mice have an *SIRT1* haploinsufficiency, but do not display the autoimmune and dysmorphic phenotype of *SIRT1*$^{-/-}$ mice.[21,22]

Methods

Animals

SIRT1 knockout mice on a 129 background[22] were crossed into *ApoE*$^{-/-}$ C57BL/6 mice[23] to generate *ApoE*$^{-/-}$ *SIRT1*$^{+/-}$ mice and *ApoE*$^{-/-}$ *SIRT1*$^{+/+}$ littermates. Of those, male mice were fed a high-cholesterol diet (1.25% total cholesterol, Research Diets) for 12 weeks starting at the age of 8 weeks. Because the few *ApoE*$^{-/-}$ *SIRT1*$^{-/-}$ mice showed a similar dysmorphic phenotype as *SIRT1*$^{-/-}$ mice,[21,22] we did not use them in this study. All animal procedures were approved by the local animal committee and performed in accordance with our institutional guidelines.

Bone marrow transplantation

Bone marrow donor mice were *ApoE*$^{-/-}$ *SIRT1*$^{+/-}$ ($n = 3$; pooled) and *ApoE*$^{-/-}$ *SIRT1*$^{+/+}$ ($n = 3$; pooled) mice, and recipients pure *ApoE*$^{-/-}$ mice (from Jackson Laboratories). Donor mice were split—dose-irradiated under SPF conditions in filter cages with a total irradiation of 1100 rad.[24] Recipient mice were injected intravenously with 10^6 bone marrow cells (*ApoE*$^{-/-}$ *SIRT1*$^{+/-}$ → 7 *ApoE*$^{-/-}$ mice; *ApoE*$^{-/-}$ *SIRT1*$^{+/+}$ → 6 *ApoE*$^{-/-}$ mice). Transplanted mice recovered for 5 weeks and were then fed a high-cholesterol diet for 11 weeks.

Lipoprotein uptake

RAW 264.7 and thioglycolate-elicited peritoneal macrophages were starved for 48 h and then incubated with 10 μg/mL oxLDL for 2 h at 37°C/5% CO_2. After washing away unspecifically bound LDL, cells were fixed and stained with Oil red O (ORO). Experiments were done twice with six independent pools isolated from six mice of each genotype, ORO staining analysed using a light microscope and quantified using analySIS. Low-density lipoprotein uptake was quantified as the ratio of the percentage of the ORO-positive area divided by the percentage of the total cell area in at least 150 cells per genotype. For CD36 blocking studies, RAW 264.7 macrophages were first pre-stimulated for 5 h with 10 ng/mL murine TNFα, and then pre-incubated with 2 μg/mL mouse anti-CD36 (Cascade Bioscience) before adding 10 μg/mL oxLDL over night.

Cell culture

Murine RAW 264.7 cells (Mouse leukaemic monocyte macrophage cell line) were treated with 200 μM splitomicin (Sigma-Aldrich) to perform cholesterol efflux and oxLDL uptake studies. RAW 264.7 cells were stimulated for with 10 ng/mL murine TNFα for 5 h. *SIRT1*$^{-/-}$ mouse embryonic fibroblasts (MEF)[25] were kindly provided by Frederick W. Alt (Harvard University, Boston, MA, USA), and *RelA/p65*$^{-/-}$ MEF with reconstituted wt-RelA/p65 or non-acetylatable RelA/p65 were described previously.[26]

Plasmid and siRNA transfection

Transient transfection of pcDNA3.1::SIRT1 or siRNA into RAW 264.7 or MEF were done with lipofectamin 2000 or lipofectamin RNAi MAX (both Invitrogen). The oligos used for SIRT1-siRNA have been described previously.[5]

Immunohistochemistry and immunocytochemistry

Serial cryosections from the aortic sinus were stained with ORO, rat anti-CD68, rat anti-CD3 (Abcam), rat anti-CD31, rabbit anti-SIRT1 (Upstate/Millipore). Means were taken from $n = 6$ different mice evaluating six serial cryosections/tissue from each mouse. Thoraco-abdominal aortae were fixed and plaques stained with ORO. Collagen, fibrous cap thickness, and necrotic core size were analysed by Elastica van Gieson and Massons trichrome stainings. Cell death was assessed with the terminal deoxyribonucleotidyl transferase-mediated dUTP nick-end labelling kit (Roche).

RNA and protein analysis

Total RNA isolated from proximal aortae was extracted with TRIZOL (Invitrogen), reverse transcribed, and the cDNA quantified by SYBR green qPCR using specific primers. For protein analysis, aortic tissue lysates were blotted and incubated with rabbit anti-SIRT1 (Upstate/Millipore), rabbit anti-eNOS, rabbit anti-phospho-eNOS (Ser1177).

Cholesterol efflux

For cholesterol efflux experiments, RAW 264.7 cells were labelled with 2 μCi/mL [1,2-^{3}H]cholesterol (Perkin Elmer) for 24 h. Following the labelling period, cells were washed and allowed to equilibrate overnight in DMEM containing 0.2% BSA supplemented with cholesterol in the presence or absence of 0.1 mM splitomicin together with 0.3 mM 8-Br-cAMP or 22(R)-HC and 9-cisRA (Sigma). After 24 h stimulation, cells were washed and incubated for 6 h in DMEM containing 0.2% BSA in the presence or absence of 28 μg/mL lipid-free apoA-I. The radioactivity recovered in the culture medium and cell lysates was measured. The apoA-I-mediated cholesterol efflux was calculated as the percentage of total [1,2-^{3}H]cholesterol released into the medium after subtracting the values obtained in the absence of apoA-I. The cholesterol efflux assays were performed in duplicates with three pairs per treatment group.

Plasma lipids and cytokines

Total plasma cholesterol, triglycerides, and free fatty acids were analysed using TR13421, TR22421 (Thermo Electron, Inc.), and 994–75409 (Wako Chemicals). The lipid distribution in plasma lipoprotein fractions was assessed by fast-performance liquid chromatography gel filtration with a Superose 6 HR 10/30 column (Pharmacia).[27] Plasma values of VCAM-1 (MVC00) and ICAM-1 (MIC100; R&D) were

determined using ELISA, and TGF-β, IFNγ, IL-6, IL-10, and mKC using multiplex array systems (Becton, Dickinson and Company).

Flow cytometry

For blood and spleen FACS analyses, single cell suspensions were incubated with antibodies against CD4, CD8, B220, CD11c, CD11b, CD62L, CD44, and CD25 (BD Pharmingen) and then cells were analysed with a FACSCantoII (BD Pharmingen) and FACSDiva software. Post-acquisition analysis was done with FACSDiva (BD Pharmingen) or FlowJo7 software (Tree Star).

Statistical analysis

Data are presented as mean ± SEM. The en face ORO quantifications were analysed with a non-parametric Mann–Whitney *U*-test. Statistical significance of differences was calculated using an ANOVA with *post hoc* Tukey's test or Student unpaired *t*-test. Significance was accepted at the level of $P < 0.05$.

Results

SIRT1 protects against atherosclerosis

To address the role of SIRT1 in atherogenesis, we compared SIRT1 expression in aortic lysates obtained from atherosclerotic $ApoE^{-/-}$ and normal wild-type (WT) mice. Aortic SIRT1 protein expression was lower in $ApoE^{-/-}$ than in WT mice (see Supplementary material online, *Figure S1A*), suggesting a protective role of SIRT1 in atherogenesis. In order to establish a cause–effect relationship between SIRT1 expression and atherosclerosis, we applied genetic deletion of *SIRT1* in atherosclerotic mice. For this purpose, we compared 20-week-old male $ApoE^{-/-}$ $SIRT1^{+/+}$ and $ApoE^{-/-}$ $SIRT1^{+/-}$ mice that were kept on a high-cholesterol diet for 12 weeks (see Supplementary material online, *Figure S2A*). Of note, SIRT1 expression is only slightly reduced in WT mice treated with a high-cholesterol diet (see

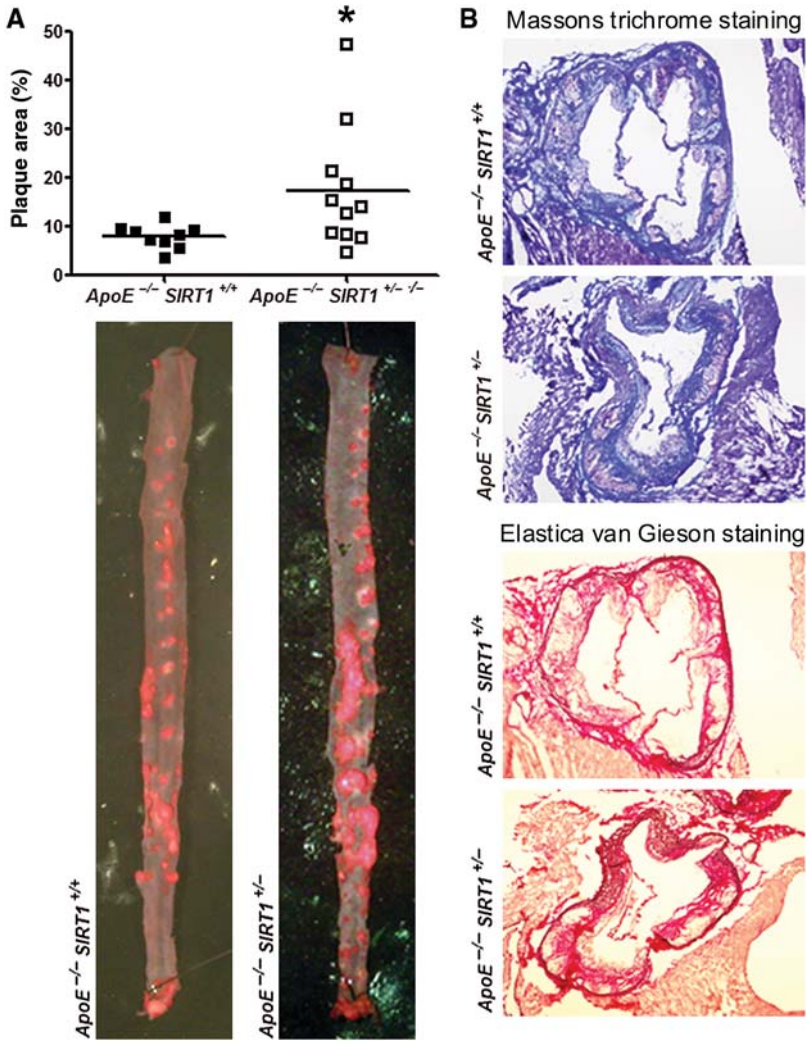

Figure 1 SIRT1 protects mice against atherosclerosis. (*A*) *En face* Oil red O (ORO) staining of thoraco-abdominal aortae and quantifications of plaque area. $n = 9$, $ApoE^{-/-}$ $SIRT1^{+/+}$(■); $n = 11$, $ApoE^{-/-}$ $SIRT1^{+/-}$(□). (*B*) Representative images for Massons trichrome and Elastica van Gieson stainings from animals with comparable plaque sizes. Magnification: X 40. *$P < 0.05$.

Supplementary material online, *Figure S1B*). To examine any SIRT1 compensation for the missing *SIRT1* allele, we assessed SIRT1 expression in aortic lysates of the two genotypes. Aortic SIRT1 protein in *ApoE*$^{-/-}$ *SIRT1*$^{+/-}$ mice amounted to about 60% of protein in *ApoE*$^{-/-}$ *SIRT1*$^{+/+}$ mice (see Supplementary material online, *Figure S1C*). Importantly, *en face* plaque quantifications in thoraco-abdominal aortae and in serial cross sections of aortic roots revealed fewer atherosclerotic plaques in *ApoE*$^{-/-}$ *SIRT1*$^{+/+}$ compared with *ApoE*$^{-/-}$ *SIRT1*$^{+/-}$ mice (*Figures 1A* and *2*). Massons trichrome and van Gieson stainings revealed that total collagen content, necrotic core size, and fibrous cap thickness did not differ between the two groups (*Figure 1B*, see Supplementary material online, *Figure S1D–F*). No difference was observed in the amount of apoptotic cells (see Supplementary material online, *Figure S1F*). These findings indicate that endogeneous SIRT1 protects against atherosclerosis.

Accumulation of plaque macrophages and T cells is reduced by SIRT1

Accumulation of macrophages and T cells in the subintimal space plays a central role in atherogenesis.[1] Our analyses revealed increased accumulation of macrophages and T cells in atherosclerotic plaques of *ApoE*$^{-/-}$ *SIRT1*$^{+/-}$ compared with *ApoE*$^{-/-}$ *SIRT1*$^{+/+}$ mice (*Figure 2*). SIRT1 staining in aortae of healthy WT mice or *ApoE*$^{-/-}$ mice under normal diet showed that SIRT1 is expressed in smooth muscle and endothelial cells (see Supplementary material online, *Figure S3A*). In diseased aortae from *ApoE*$^{-/-}$ mice under high-cholesterol diet, SIRT1 is also expressed in cells within the plaques (see Supplementary material online, *Figure S3A*). Double stainings revealed that SIRT1 is expressed in both plaque endothelial cells and macrophages in diseased *ApoE*$^{-/-}$ aortae (see Supplementary material online, *Figure S3B*).

SIRT1 in macrophages is sufficient to reduce foam cell formation and atherogenesis

We observed no difference neither in fasted nor fed plasma glucose or insulin levels, total body or epididymal fat weight (see Supplementary material online, *Figure S4*) and found no difference in total cholesterol and its subfractions between *ApoE*$^{-/-}$ *SIRT1*$^{+/+}$ and *ApoE*$^{-/-}$ *SIRT1*$^{+/-}$ mice (see Supplementary material online, *Figure S5* and *Table S1*). Further, plasma cytokine levels were similar in the two genotypes (see Supplementary material online, *Table S2*). Since inflammatory factors from WAT may enhance atherogenesis,[28,29] we examined the expression of several adipokines and adipose-derived hormones in epididymal WAT. Expression of *Adiponectin* (*Adipoq*), *Leptin*, *Visfatin* (*Nampt*), *Chemerin* (*Rarres2*), *Resistin* (*Retn*) were equivalent, whereas expression of *Plasminogen activator inhibitor 1* (*PAI-1* or *Serpine1*) was slightly, but not significantly elevated in A*poE*$^{-/-}$ *SIRT1*$^{+/-}$ compared with *ApoE*$^{-/-}$ *SIRT1*$^{+/+}$ epididymal WAT (see

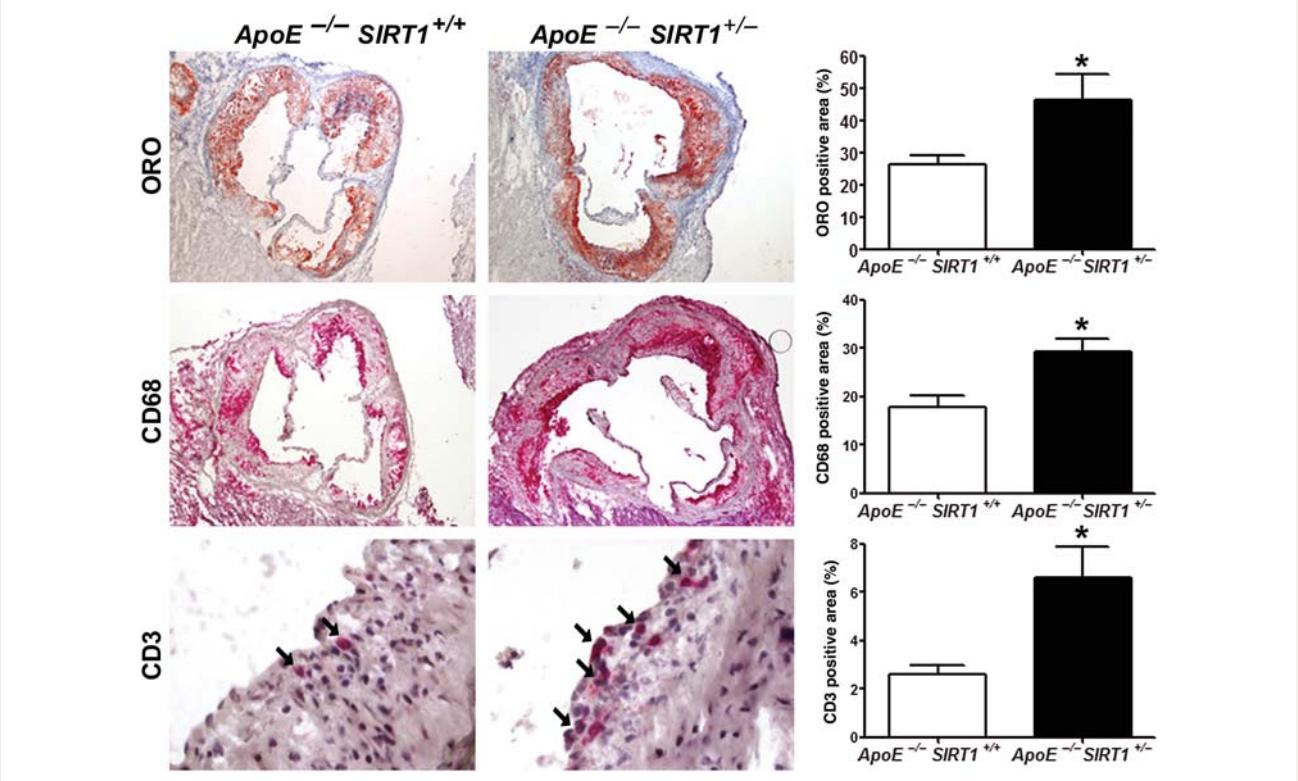

Figure 2 *SIRT1* deletion increases macrophage and T-cell accumulation in plaques. Immunohistochemistry with quantifications of Oil red O (ORO), CD68, and CD3 (arrows) on plaques from aortic sinus. Magnifications: Oil red O, CD68: ×40; CD3: ×400. $n = 6$ per genotype. *$P < 0.05$.

Supplementary material online, *Figure S6*). These data do not exclude a contribution of systemic inflammatory factors such as WAT, but suggest that the damaging effects of partial *SIRT1* deficiency are mainly mediated via inflammatory cells localized in plaques.

Therefore, we focused on the role of SIRT1 in macrophages. Foam cell formation is a crucial step in atherogenesis.[1] We observed no difference in basal LDL uptake in peritoneal-elicited macrophages from $ApoE^{-/-}$ $SIRT1^{+/-}$ compared with $ApoE^{-/-}$ $SIRT1^{+/+}$ mice, but found enhanced uptake upon stimulation with oxLDL (*Figure 3A*). Pharmacological inhibition of SIRT1 with splitomicin in RAW 264.7 macrophages showed a trend towards increasing oxLDL uptake (see Supplementary material online, *Figure S7*). Consistently, siRNA-induced SIRT1 knockdown increased uptake of oxLDL in RAW 264.7 macrophages compared with control cells (*Figure 3B* and *C*). To study a potential role of CD36 in oxLDL uptake, we blocked CD36-mediated oxLDL uptake using an anti-CD36 antibody in scrambled or SIRT1-siRNA-treated macrophages. Neutralization of CD36 decreased uptake of oxLDL by ~50% compared with non-neutralized cells (*Figure 3C*). A higher elevation of oxLDL uptake was observed in SIRT1-siRNA-treated macrophages with additional CD36 neutralization, but did not reach significance difference compared with any other group (*Figure 3C*). These

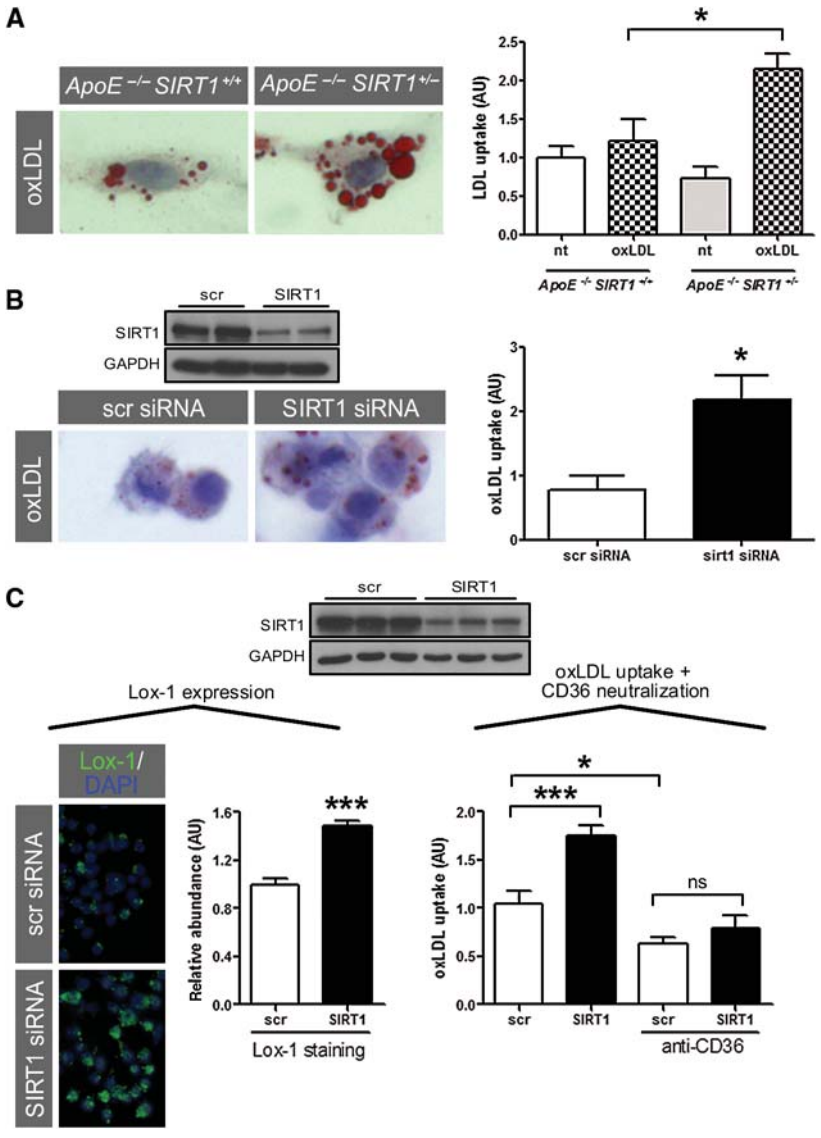

Figure 3 SIRT1 reduces foam cell formation. (*A*) Increased uptake of oxLDL in peritoneal thioglycolate-elicited macrophages from $ApoE^{-/-}$ $SIRT1^{+/-}$ compared with $ApoE^{-/-}$ $SIRT1^{+/+}$ mice. oxLDL uptake is given as the ratio of the percentage of ORO-positive area divided by the percentage of total cell area in at least 150 cells per genotype. (*B*) siRNA-induced SIRT1 knockdown increases uptake of oxLDL in RAW 264.7 macrophages compared with scr-siRNA-treated cells. (*C*) siRNA-mediated SIRT1 silencing in 5 h TNFα-pretreated RAW 264.7 macrophages: left panel, expression of Lox-1; right panel, uptake of oxLDL in neutralizing anti-CD36 antibody-treated cells. $*P < 0.05$. $***P < 0.001$. Magnifications: ×400.

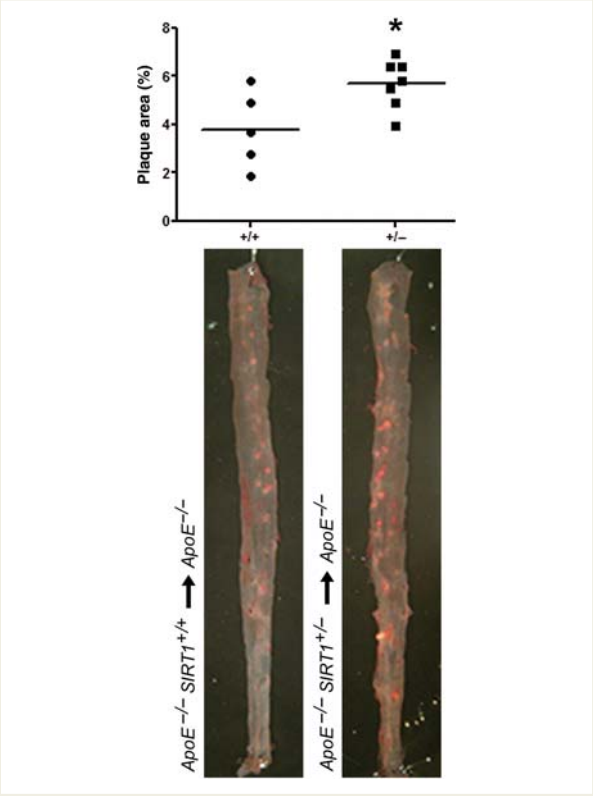

Figure 4 SIRT1 function in macrophages is sufficient to decrease atherogenesis. Chimeric $ApoE^{-/-}$ mice that received $ApoE^{-/-}$ $SIRT1^{+/-}$ ($n = 7$) bone marrow cells develop more atherosclerosis than those which received $ApoE^{-/-}$ $SIRT1^{+/+}$ ($n = 5$) bone marrow cells. *$P < 0.05$.

data suggest that SIRT1 exerts CD36-dependent and -independent effects in oxLDL uptake.

To examine whether an SIRT1-dependent mechanism in macrophages accounts for decreased atherosclerosis *in vivo*, we performed bone marrow transplantation experiments. Bone marrow from $ApoE^{-/-}$ $SIRT1^{+/-}$ or $ApoE^{-/-}$ $SIRT1^{+/+}$ mice was transplanted into irradiated 6-week-old $ApoE^{-/-}$ mice (see Supplementary material online, *Figure S2B*), respectively. Flow cytometry analyses of blood and spleen samples from transplanted mice revealed an increased number of blood monocytes of $ApoE^{-/-}$ recipient mice receiving $ApoE^{-/-}$ $SIRT1^{+/-}$ bone marrow cells, but no proportional difference in T-cell subtypes, $MHCII^{+}$ cells, B cells or macrophages (see Supplementary material online, *Figure S8*). Chimeric $ApoE^{-/-}$ recipient mice receiving $ApoE^{-/-}$ $SIRT1^{+/-}$ bone marrow showed more atherosclerotic lesions compared with mice transplanted with $ApoE^{-/-}$ $SIRT1^{+/+}$ bone marrow (*Figure 4*). These findings support the notion that SIRT1 function in macrophages is sufficient to decrease atherogenesis.

Deacetylation of RelA/p65 by SIRT1 diminishes Lox-1 expression

Active uptake of modified cholesterol in macrophages is mainly regulated by SR-A, SR-B, CD36, and Lox-1,[30] whereas cholesterol efflux is driven by ATP-binding cassette transporters.[31] Expression of CD36, SR-A, and SR-B was not altered (see Supplementary material online, *Figure S9*), whereas *Lox-1* expression was higher in $ApoE^{-/-}$ $SIRT1^{+/-}$ aortic lysates (*Figure 5A*). Because expression of Lox-1 in SIRT1-siRNA-treated macrophages was increased (*Figure 3C*), we planned to study the SIRT1–Lox-1 pathway more in detail. Deletion of *Lox-1* has been shown to reduce atherosclerosis in mice.[32] Since *Lox-1* is an NF-κB target[33] and SIRT1 deacetylates RelA/p65 in murine macrophages,[34] we compared *Lox-1* RNA levels in TNFα-stimulated RAW 264.7 cells pretreated with splitomicin. We observed an increase in *Lox-1* expression in splitomicin-treated macrophages compared with untreated control cells (*Figure 5B*). These data suggest that SIRT1 suppresses NF-κB signalling in macrophages, thereby reducing *Lox-1* expression and oxLDL uptake.

To get more insight into the molecular events underlying SIRT1-dependent NF-κB deacetylation in murine cells, we analysed SIRT1 expression in different MEF cell lines. Ectopic expression of SIRT1 in $SIRT1^{-/-}$ MEF reduced *Lox-1* expression upon TNFα treatment (*Figure 5C*). In $RelA/p65^{-/-}$ MEF with reconstituted wt-RelA/p65 expression,[26] siRNA-induced SIRT1 knockdown enhanced *Lox-1* expression upon TNFα stimulation. In contrast, SIRT1-siRNA had no effect on *Lox-1* expression in TNFα-stimulated $RelA/p65^{-/-}$ MEF with reconstituted non-acetylatable K310R-mutant-RelA/p65[26] (*Figure 5D*). These data show that SIRT1-dependent deacetylation of RelA/p65 at K310 is sufficient to reduce *Lox-1* gene expression.

Several reports show a link between Lox-1 and matrix metalloproteinases (MMPs) that are expressed and secreted by human endothelial cells, including the collagenase MMP1, stromelysin-1 (MMP3), the membrane type 1 MMP (MT1-MMP or MMP14), and the tissue inhibitor of metalloproteinase 3 (TIMP3).[35–38] To investigate if metalloproteinase expression is affected by SIRT1, we quantified aortic expression of *MMP13*, *MMP3*, *MMP8*, *MMP9*, *MMP14*, and *TIMP3*. No significant change in the expression of these MMPs was observed in $ApoE^{-/-}$ $SIRT1^{+/-}$ compared with $ApoE^{-/-}$ $SIRT1^{+/+}$ aortae (see Supplementary material online, *Figure S10*), indicating that the phenotype of $ApoE^{-/-}$ $SIRT1^{+/-}$ mice is not related to SIRT1–Lox-1-mediated expression of MMPs.

Atheroprotective effects of SIRT1 do not affect cholesterol efflux

When examining cholesterol efflux, we found that expression of *ABCA1* was not altered in aortic lysates from $ApoE^{-/-}$ $SIRT1^{+/-}$ compared with $ApoE^{-/-}$ $SIRT1^{+/+}$ mice (see Supplementary material online, *Figure S11A*). Similarly, expression levels of *ABCA1* and *ABCG1* were not different in peritoneal macrophages from $ApoE^{-/-}$ $SIRT1^{+/+}$ and $ApoE^{-/-}$ $SIRT1^{+/-}$ mice (see Supplementary material online, *Figure S11B*). Cholesterol efflux assays in RAW 264.7 macrophages treated with splitomicin revealed no ApoA-I-dependent changes (see Supplementary material online, *Figure S11C*). Furthermore, we detected no difference in aortic expression of the ABCA1 regulators LXRα, PPARγ, or its coactivator PGC-1α (PPARγ coactivator 1α) (see Supplementary material online, *Figure S11D–F*). These data suggest that aortic cholesterol efflux is not affected by SIRT1 in atherosclerotic mice.

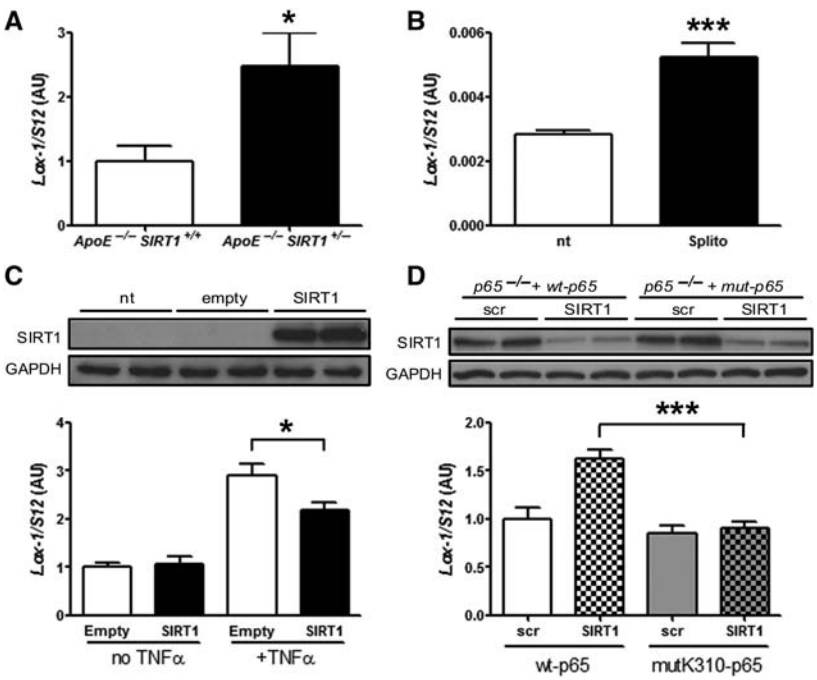

Figure 5 Deacetylation of RelA/p65 by SIRT1 diminishes Lox-1 expression. (*A*) Aortic *Lox-1* expression is increased in *ApoE*$^{-/-}$ *SIRT1*$^{+/-}$ compared with *ApoE*$^{-/-}$ *SIRT1*$^{+/+}$ mice. (*B*) *Lox-1* expression is higher in 5 h TNFα-stimulated RAW 264.7 macrophages pretreated with 200 μM splitomicin (Splito) compared with untreated cells (nt). (*C*) Ectopic *SIRT1* expression in *SIRT1*$^{-/-}$ MEF reduces *Lox-1* expression. (*D*) In *RelA/p65*$^{-/-}$ MEF with reconstituted wt-RelA/p65, siRNA-mediated SIRT1 knockdown enhances *Lox-1* expression upon 5 h TNFα stimulation, whereas no effect is observed in *RelA/p65*$^{-/-}$ MEF with a reconstituted mutated, non-acetylatable K310-RelA/p65. *$P < 0.05$; ***$P < 0.001$.

Discussion

Recently, SIRT1 has been shown to decrease atherosclerosis by improving endothelium-dependent vascular function in *ApoE*$^{-/-}$ mice with an endothelial SIRT1 overexpression that were kept on a high-fat diet.[20] Our study shows that endogenous SIRT1 prevents macrophage foam cell formation in atherogenesis independently of systemic lipid levels. We demonstrate that loss of a single *SIRT1* allele in *ApoE*$^{-/-}$ *SIRT1*$^{+/-}$ mice is sufficient to increase plaque formation.

Macrophage-derived foam cell formation is enhanced upon a relative increase in cholesterol uptake or by a defective cholesterol efflux, respectively.[39] Our *in vitro* foam cell assay reveals that SIRT1 activation diminishes oxLDL uptake in peritoneal macrophages. Among the receptors that may account for this increased LDL uptake by macrophages, we identified Lox-1 to be critically involved: SIRT1 inhibits TNFα-induced expression of *Lox-1* in macrophages. In fact, the *Lox-1* promoter contains NF-κB binding sites and is expressed upon TNFα stimulation.[33] Using *RelA/p65*$^{-/-}$ MEF, we could further show that the deacetylation of RelA/p65 by SIRT1 suppresses *Lox-1* expression. We acknowledge that the final proof of a Lox-1-mediated effect on foam cell formation would require additional evidence from genetic loss-of-function or neutralizing antibody experiments. These questions need to be addressed in future studies.

To test whether an SIRT1-dependent mechanism in bone marrow-derived cells accounts for the increase in atherosclerosis *in vivo*, we performed bone marrow transplantation experiments. Chimeric *ApoE*$^{-/-}$ mice receiving *ApoE*$^{-/-}$ *SIRT1*$^{+/-}$ bone marrow showed increased atherosclerotic plaques compared with mice receiving *ApoE*$^{-/-}$ *SIRT1*$^{+/+}$ bone marrow. These findings demonstrate that partial *SIRT1* deletion in bone marrow-derived macrophages is sufficient to enhance atherogenesis.

The role of NF-κB in plaque macrophages and lipoprotein uptake in atherogenesis is controversial. Disruption of NF-κB signalling by partial *IKK2* deletion in macrophages increased atherosclerosis.[40] Conversely, studies using macrophage-specific *p50* deletion or a dominant-negative *IκBα* mutant to disrupt NF-κB signalling, resulted in smaller atherosclerotic lesions and diminished uptake of lipoproteins.[41,42] Since NF-κB and its transcriptional activity are tightly regulated,[43,44] pharmacological modulation of an upstream regulator of NF-κB seems more promising in preventing atherogenesis than direct NF-κB modulation.[45] Our study shows that SIRT1 might be an attractive modulator, since its interference with the NF-κB signalling pathway exerts beneficial effects on plaque formation.

Several reports suggest that other SIRT1 targets may also contribute to atherogenesis. For instance, PPARγ, a key transcription factor in adipocyte differentiation, plays a pivotal role in macrophages and modulates the extent of atherosclerosis.[14] Both PPARγ and its target LXR are regulated by SIRT1 in adipocytes and macrophages.[5,46] Interestingly, Li *et al.*[46] showed reduced cholesterol efflux in primary macrophages from *SIRT1*$^{-/-}$ compared with *SIRT1*$^{+/+}$ mice. We could neither observe a difference

in the aortic expression of ABCA1, ABCG1, PPARγ, or LXRα nor an ApoA-I-dependent decrease in cholesterol efflux upon splitomicin treatment in RAW 264.7 macrophages. Possibly, the effect of a single missing *SIRT1* allele is not sufficient to affect cholesterol efflux in atherosclerotic mice.

Taken together, our results reveal a novel mechanism by which SIRT1 prevents atherogenesis: SIRT1 suppresses NF-signalling by deacetylating RelA/p65, thereby reducing *Lox-1* expression and diminishing uptake of oxLDL and foam cell formation. Given the availability of specific SIRT1-activating drugs that are being tested in clinical trials in patients with type 2 diabetes, pharmacological activation of SIRT1 may also become an attractive anti-atherogenic strategy by preventing macrophage foam cell formation.[47]

Supplementary material

Supplementary material is available at *European Heart Journal* online.

Acknowledgements

We thank Elin Stenfeldt (University of Gothenburg), Sabine Rütti, and Chad E. Brokopp (University Hospital Zurich) for technical assistance and the Center for Microscopy and Image Analysis at the University of Zurich for using their facilities.

Funding

This work was funded by grants from the Swiss National Science Foundation [grant numbers 31-114094/1 to C.M.M. and 3100-068118 to T.F.L.] and the University Research Priority Program 'Integrative Human Physiology' at the University of Zurich. Further support was provided by unrestricted grants from the MERCATOR Foundation Switzerland and a strategic alliance with Pfizer, Inc., New York. Funding to pay the Open Access publication charges for this article was provided by the Swiss National Science Foundation.

Conflict of interest: none declared.

References

1. Libby P. Inflammation in atherosclerosis. *Nature* 2002;**420**:868–874.
2. Kaeberlein M, McVey M, Guarente L. The SIR2/3/4 complex and SIR2 alone promote longevity in *Saccharomyces cerevisiae* by two different mechanisms. *Genes Dev* 1999;**13**:2570–2580.
3. Chen D, Steele AD, Lindquist S, Guarente L. Increase in activity during calorie restriction requires Sirt1. *Science* 2005;**310**:1641.
4. Bordone L, Motta MC, Picard F, Robinson A, Jhala US, Apfeld J, McDonagh T, Lemieux M, McBurney M, Szilvasi A, Easlon EJ, Lin SJ, Guarente L. Sirt1 regulates insulin secretion by repressing UCP2 in pancreatic beta cells. *PLoS Biol* 2006;**4**:e31.
5. Picard F, Kurtev M, Chung N, Topark-Ngarm A, Senawong T, Machado De Oliveira R, Leid M, McBurney MW, Guarente L. Sirt1 promotes fat mobilization in white adipocytes by repressing PPAR-gamma. *Nature* 2004;**429**:771–776.
6. Vaziri H, Dessain SK, Ng Eaton E, Imai SI, Frye RA, Pandita TK, Guarente L, Weinberg RA. hSIR2(SIRT1) functions as an NAD-dependent p53 deacetylase. *Cell* 2001;**107**:149–159.
7. Brunet A, Sweeney LB, Sturgill JF, Chua KF, Greer PL, Lin Y, Tran H, Ross SE, Mostoslavsky R, Cohen HY, Hu LS, Cheng HL, Jedrychowski MP, Gygi SP, Sinclair DA, Alt FW, Greenberg ME. Stress-dependent regulation of FOXO transcription factors by the SIRT1 deacetylase. *Science* 2004;**303**:2011–2015.
8. Motta MC, Divecha N, Lemieux M, Kamel C, Chen D, Gu W, Bultsma Y, McBurney M, Guarente L. Mammalian SIRT1 represses forkhead transcription factors. *Cell* 2004;**116**:551–563.
9. Mattagajasingh I, Kim CS, Naqvi A, Yamamori T, Hoffman TA, Jung SB, DeRicco J, Kasuno K, Irani K. SIRT1 promotes endothelium-dependent vascular relaxation by activating endothelial nitric oxide synthase. *Proc Natl Acad Sci USA* 2007;**104**:14855–14860.
10. Lagouge M, Argmann C, Gerhart-Hines Z, Meziane H, Lerin C, Daussin F, Messadeq N, Milne J, Lambert P, Elliott P, Geny B, Laakso M, Puigserver P, Auwerx J. Resveratrol improves mitochondrial function and protects against metabolic disease by activating SIRT1 and PGC-1alpha. *Cell* 2006;**127**:1109–1122.
11. Rodgers JT, Lerin C, Haas W, Gygi SP, Spiegelman BM, Puigserver P. Nutrient control of glucose homeostasis through a complex of PGC-1alpha and SIRT1. *Nature* 2005;**434**:113–118.
12. Yeung F, Hoberg JE, Ramsey CS, Keller MD, Jones DR, Frye RA, Mayo MW. Modulation of NF-kappaB-dependent transcription and cell survival by the SIRT1 deacetylase. *EMBO J* 2004;**23**:2369–2380.
13. Luo J, Nikolaev AY, Imai S, Chen D, Su F, Shiloh A, Guarente L, Gu W. Negative control of p53 by Sir2alpha promotes cell survival under stress. *Cell* 2001;**107**:137–148.
14. Tontonoz P, Spiegelman BM. Fat and beyond: the diverse biology of PPARgamma. *Annu Rev Biochem* 2008;**77**:289–312.
15. Kim HJ, Park KG, Yoo EK, Kim YH, Kim YN, Kim HS, Kim HT, Park JY, Lee KU, Jang WG, Kim JG, Kim BW, Lee IK. Effects of PGC-1alpha on TNF-alpha-induced MCP-1 and VCAM-1 expression and NF-kappaB activation in human aortic smooth muscle and endothelial cells. *Antioxid Redox Signal* 2007;**9**:301–307.
16. Brand K, Page S, Rogler G, Bartsch A, Brandl R, Knuechel R, Page M, Kaltschmidt C, Baeuerle PA, Neumeier D. Activated transcription factor nuclear factor-kappa B is present in the atherosclerotic lesion. *J Clin Invest* 1996;**97**:1715–1722.
17. Knowles JW, Reddick RL, Jennette JC, Shesely EG, Smithies O, Maeda N. Enhanced atherosclerosis and kidney dysfunction in eNOS(−/−)Apoe(−/−) mice are ameliorated by enalapril treatment. *J Clin Invest* 2000;**105**:451–458.
18. Guevara NV, Kim HS, Antonova EI, Chan L. The absence of p53 accelerates atherosclerosis by increasing cell proliferation *in vivo*. *Nat Med* 1999;**5**:335–339.
19. Kawashima S, Yokoyama M. Dysfunction of endothelial nitric oxide synthase and atherosclerosis. *Arterioscler Thromb Vasc Biol* 2004;**24**:998–1005.
20. Zhang QJ, Wang Z, Chen HZ, Zhou S, Zheng W, Liu G, Wei YS, Cai H, Liu DP, Liang CC. Endothelium-specific overexpression of class III deacetylase SIRT1 decreases atherosclerosis in apolipoprotein E-deficient mice. *Cardiovasc Res* 2008;**80**:191–199.
21. Sequeira J, Boily G, Bazinet S, Saliba S, He X, Jardine K, Kennedy C, Staines W, Rousseaux C, Mueller R, McBurney MW. Sirt1-null mice develop an autoimmune-like condition. *Exp Cell Res* 2008;**314**:3069–3074.
22. McBurney MW, Yang X, Jardine K, Hixon M, Boekelheide K, Webb JR, Lansdorp PM, Lemieux M. The mammalian SIR2alpha protein has a role in embryogenesis and gametogenesis. *Mol Cell Biol* 2003;**23**:38–54.
23. Plump AS, Smith JD, Hayek T, Aalto-Setala K, Walsh A, Verstuyft JG, Rubin EM, Breslow JL. Severe hypercholesterolemia and atherosclerosis in apolipoprotein E-deficient mice created by homologous recombination in ES cells. *Cell* 1992;**71**:343–353.
24. Becher B, Durell BG, Miga AV, Hickey WF, Noelle RJ. The clinical course of experimental autoimmune encephalomyelitis and inflammation is controlled by the expression of CD40 within the central nervous system. *J Exp Med* 2001;**193**:967–974.
25. Chua KF, Mostoslavsky R, Lombard DB, Pang WW, Saito S, Franco S, Kaushal D, Cheng HL, Fischer MR, Stokes N, Murphy MM, Appella E, Alt FW. Mammalian SIRT1 limits replicative life span in response to chronic genotoxic stress. *Cell Metab* 2005;**2**:67–76.
26. Buerki C, Rothgiesser KM, Valovka T, Owen HR, Rehrauer H, Fey M, Lane WS, Hottiger MO. Functional relevance of novel p300-mediated lysine 314 and 315 acetylation of RelA/p65. *Nucleic Acids Res* 2008;**36**:1665–1680.
27. Purcell-Huynh DA, Farese RV Jr, Johnson DF, Flynn LM, Pierotti V, Newland DL, Linton MF, Sanan DA, Young SG. Transgenic mice expressing high levels of human apolipoprotein B develop severe atherosclerotic lesions in response to a high-fat diet. *J Clin Invest* 1995;**95**:2246–2257.
28. Trayhurn P, Wood IS. Adipokines: inflammation and the pleiotropic role of white adipose tissue. *Br J Nutr* 2004;**92**:347–355.
29. Lyon CJ, Law RE, Hsueh WA. Minireview: adiposity, inflammation, and atherogenesis. *Endocrinology* 2003;**144**:2195–2200.
30. Moore KJ, Freeman MW. Scavenger receptors in atherosclerosis: beyond lipid uptake. *Arterioscler Thromb Vasc Biol* 2006;**26**:1702–1711.
31. Tiwari RL, Singh V, Barthwal MK. Macrophages: an elusive yet emerging therapeutic target of atherosclerosis. *Med Res Rev* 2008;**28**:483–544.
32. Mehta JL, Sanada N, Hu CP, Chen J, Dandapat A, Sugawara F, Satoh H, Inoue K, Kawase Y, Jishage K, Suzuki H, Takeya M, Schnackenberg L, Beger R, Hermonat PL, Thomas M, Sawamura T. Deletion of LOX-1 reduces atherogenesis in LDLR knockout mice fed high cholesterol diet. *Circ Res* 2007;**100**:1634–1642.
33. Nagase M, Abe J, Takahashi K, Ando J, Hirose S, Fujita T. Genomic organization and regulation of expression of the lectin-like oxidized low-density lipoprotein receptor (LOX-1) gene. *J Biol Chem* 1998;**273**:33702–33707.

34. Shen Z, Ajmo JM, Rogers CQ, Liang X, Le L, Murr MM, Peng Y, You M. Role of SIRT1 in regulation of LPS- or two ethanol metabolites-induced TNF{alpha} production in cultured macrophage cell lines. *Am J Physiol Gastrointest Liver Physiol* 2009;**296**:G1047–1053.
35. Sugimoto K, Ishibashi T, Sawamura T, Inoue N, Kamioka M, Uekita H, Ohkawara H, Sakamoto T, Sakamoto N, Okamoto Y, Takuwa Y, Kakino A, Fujita Y, Tanaka T, Teramoto T, Maruyama Y, Takeishi Y. LOX-1-MT1-MMP axis is crucial for RhoA and Rac1 activation induced by oxidized low-density lipoprotein in endothelial cells. *Cardiovasc Res* 2009;**84**:127–136.
36. Kakinuma T, Yasuda T, Nakagawa T, Hiramitsu T, Akiyoshi M, Akagi M, Sawamura T, Nakamura T. Lectin-like oxidized low-density lipoprotein receptor 1 mediates matrix metalloproteinase 3 synthesis enhanced by oxidized low-density lipoprotein in rheumatoid arthritis cartilage. *Arthritis Rheum* 2004;**50**:3495–3503.
37. Li D, Liu L, Chen H, Sawamura T, Ranganathan S, Mehta JL. LOX-1 mediates oxidized low-density lipoprotein-induced expression of matrix metalloproteinases in human coronary artery endothelial cells. *Circulation* 2003;**107**:612–617.
38. Li D, Williams V, Liu L, Chen H, Sawamura T, Antakli T, Mehta JL. LOX-1 inhibition in myocardial ischemia-reperfusion injury: modulation of MMP-1 and inflammation. *Am J Physiol Heart Circ Physiol* 2002;**283**:H1795–H1801.
39. Li AC, Glass CK. The macrophage foam cell as a target for therapeutic intervention. *Nat Med* 2002;**8**:1235–1242.
40. Kanters E, Pasparakis M, Gijbels MJ, Vergouwe MN, Partouns-Hendriks I, Fijneman RJ, Clausen BE, Forster I, Kockx MM, Rajewsky K, Kraal G, Hofker MH, de Winther MP. Inhibition of NF-kappaB activation in macrophages increases atherosclerosis in LDL receptor-deficient mice. *J Clin Invest* 2003;**112**:1176–1185.
41. Ferreira V, van Dijk KW, Groen AK, Vos RM, van der Kaa J, Gijbels MJ, Havekes LM, Pannekoek H. Macrophage-specific inhibition of NF-kappaB activation reduces foam-cell formation. *Atherosclerosis* 2007;**192**:283–290.
42. Kanters E, Gijbels MJ, van der Made I, Vergouwe MN, Heeringa P, Kraal G, Hofker MH, de Winther MP. Hematopoietic NF-kappaB1 deficiency results in small atherosclerotic lesions with an inflammatory phenotype. *Blood* 2004;**103**:934–940.
43. Cheong R, Hoffmann A, Levchenko A. Understanding NF-kappaB signaling via mathematical modeling. *Mol Syst Biol* 2008;**4**:192.
44. Gilmore TD. Introduction to NF-kappaB: players, pathways, perspectives. *Oncogene* 2006;**25**:6680–6684.
45. Ahn KS, Sethi G, Aggarwal BB. Nuclear factor-kappa B: from clone to clinic. *Curr Mol Med* 2007;**7**:619–637.
46. Li X, Zhang S, Blander G, Tse JG, Krieger M, Guarente L. SIRT1 deacetylates and positively regulates the nuclear receptor LXR. *Mol Cell* 2007;**28**:91–106.
47. Milne JC, Lambert PD, Schenk S, Carney DP, Smith JJ, Gagne DJ, Jin L, Boss O, Perni RB, Vu CB, Bemis JE, Xie R, Disch JS, Ng PY, Nunes JJ, Lynch AV, Yang H, Galonek H, Israelian K, Choy W, Iffland A, Lavu S, Medvedik O, Sinclair DA, Olefsky JM, Jirousek MR, Elliott PJ, Westphal CH. Small molecule activators of SIRT1 as therapeutics for the treatment of type 2 diabetes. *Nature* 2007;**450**:712–716.

Supplemental Data for

SIRT1 decreases Lox-1-mediated foam cell formation in atherogenesis

Sokrates Stein[1,2], Christine Lohmann[1,2], Nicola Schäfer[1,2], Janin Hofmann[3], Lucia Rohrer[2,4], Christian Besler[1,2], Karin M. Rothgiesser[5], Burkhard Becher[2,3], Michael O. Hottiger[2,5], Jan Borén[6], Michael W. McBurney[7], Ulf Landmesser[1,2], Thomas F. Lüscher[1,2] and Christian M. Matter [1,2*]

[1]Cardiovascular Research, Institute of Physiology; [2]Zurich Center for Integrative Human Physiology (ZIHP); [3]Neuroimmunology Unit, Inst. Experimental Immunology; [4]Institute for Clinical Chemistry; [5]Institute of Veterinary Biochemistry and Molecular Biology, University of Zurich and University Hospital Zurich, CH-8057 Zurich, Switzerland. [6]Sahlgrenska Center for Cardiovascular and Metabolic Research, University of Goteborg, SE-41345 Goteborg, Sweden. [7]Ottawa Health Research Institute, Department of Medicine, University of Ottawa, ON K1Y 4E9 Ottawa, Canada.

[*]**Corresponding author:** Christian M. Matter. e-mail: cmatter@physiol.uzh.ch.

SUPPLEMENTARY FIGURES

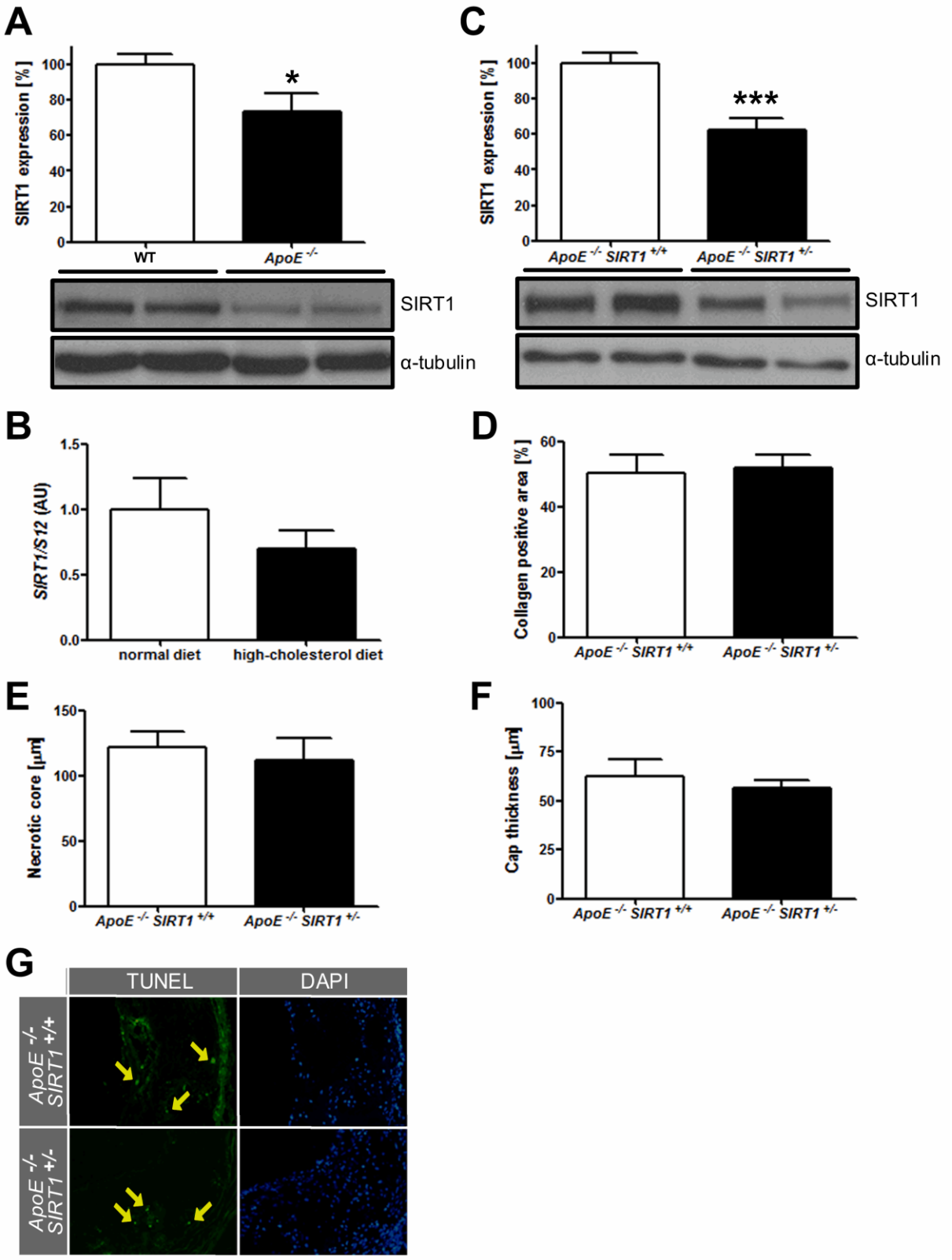

Supplemental Figure 1. Correlation between SIRT1 and atherogenesis. (A) Protein expression of SIRT1 and α-tubulin in *ApoE-/-* and WT aortic lysates. n=6 per genotype. (B)

SIRT1 mRNA levels in aortic tissue of wild-type mice treated a normal or high-cholesterol diet. n=4 per treatment group. (C) *ApoE*$^{-/-}$ *SIRT1*$^{+/-}$ mice express approximately 60% of *ApoE*$^{-/-}$ *SIRT1*$^{+/+}$ protein levels in aortic lysates. n=9 per genotype. (D-F) Quantification of collagen content (D), necrotic core size (E), and cap thickness in plaques from aortic sinus. n=8 per genotype. (F) TUNEL staining revealed no difference in amount of apoptotic cells. n=6 per genotype.

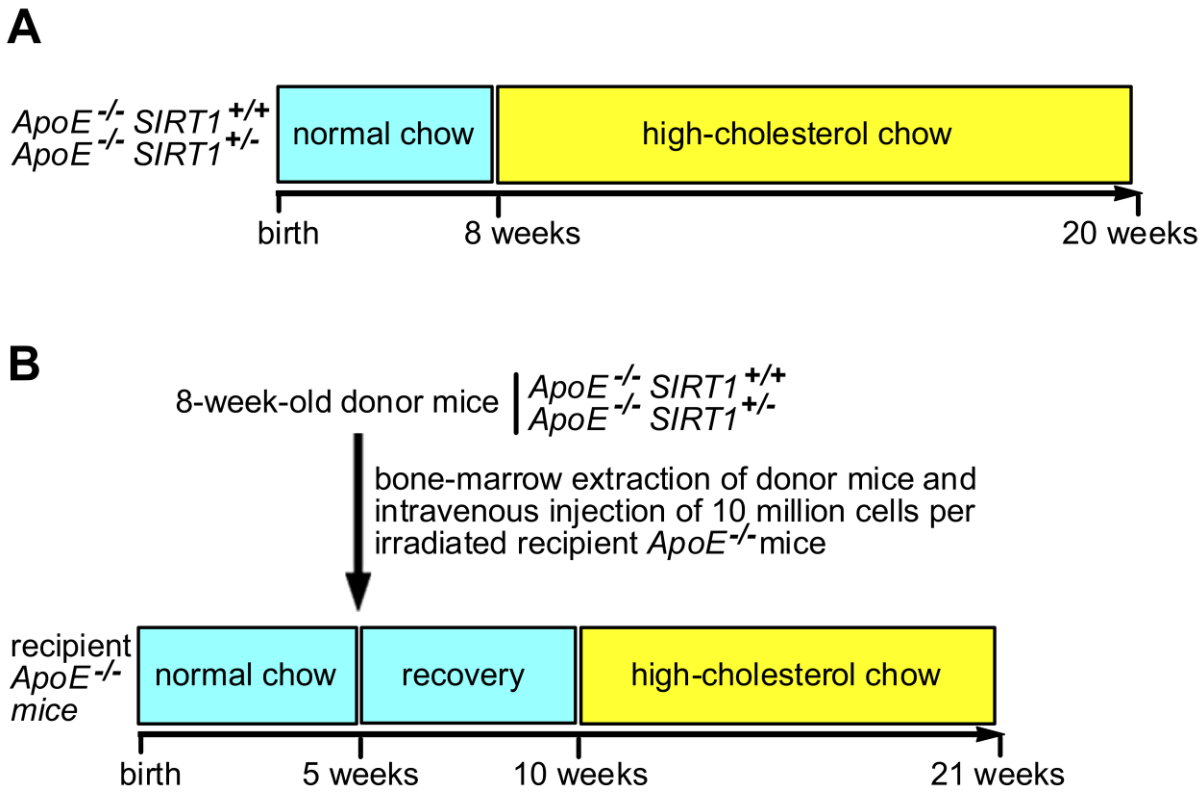

Supplemental Figure 2. Diet schemes. **(A)** 8 weeks after birth, *ApoE*$^{-/-}$ *SIRT1*$^{+/+}$ and *ApoE*$^{-/-}$ *SIRT1*$^{+/-}$ mice were kept on a high-cholesterol diet for 12 weeks. 20-week-old male animals were euthanized for tissue harvesting. **(B)** Bone-marrow from 8-week-old donor mice (*ApoE*$^{-/-}$ *SIRT1*$^{+/-}$ and *ApoE*$^{-/-}$ *SIRT1*$^{+/+}$) was extracted, and 10^6 bone-marrow cells were injected intravenous into irradiated recipient *ApoE*$^{-/-}$ mice. Transplanted mice were allowed to recover for 5 weeks, and were then fed a high-cholesterol diet for 11 weeks prior to tissue harvesting.

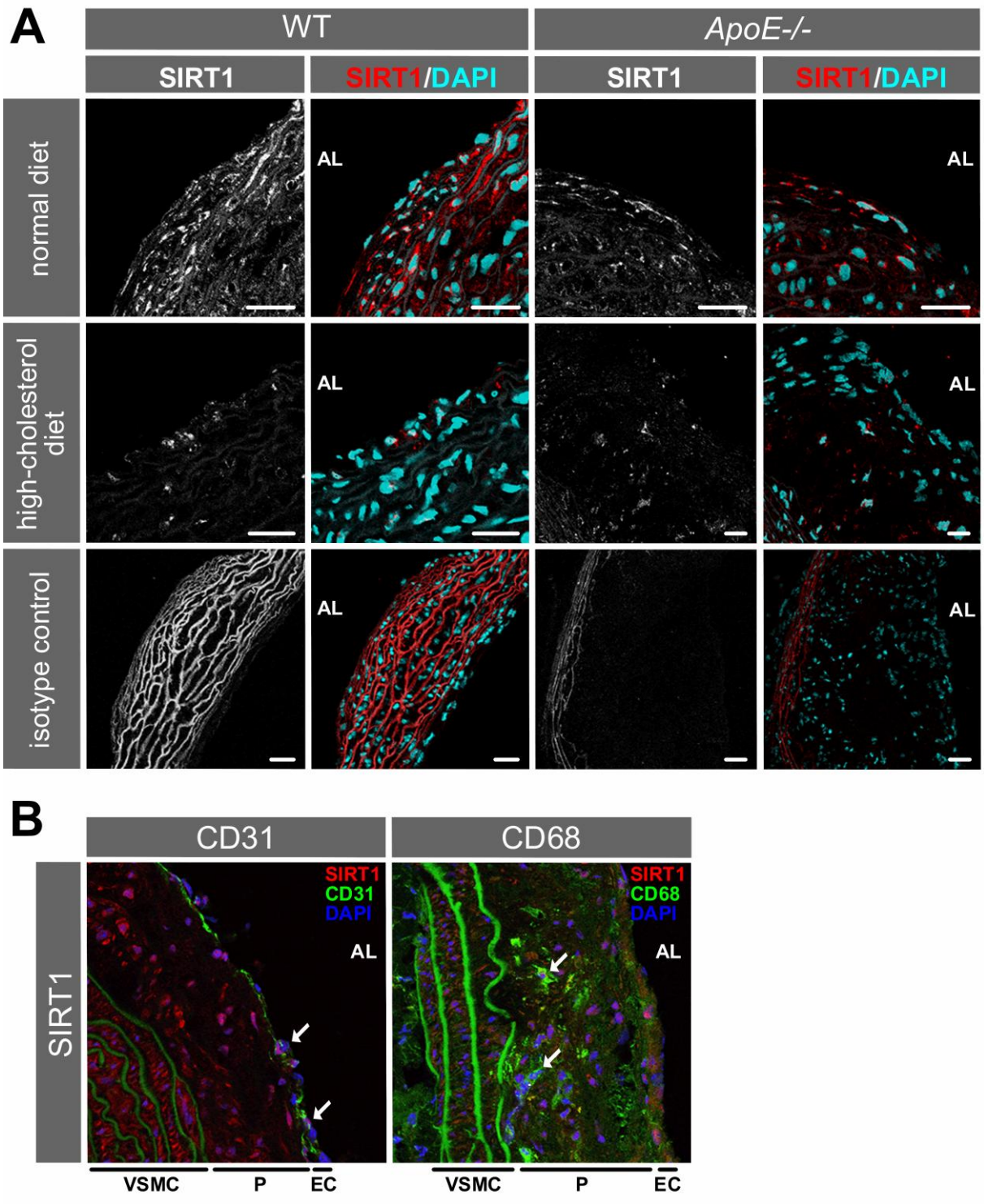

Supplemental Figure 3. SIRT1 staining in aortic plaque of wild-type (healthy) and ApoE-/- (diseased) mice. (**A**) Aortic expression of SIRT1 in wild-type and *ApoE*$^{-/-}$ mice fed a normal or high-cholesterol (HC) diet. Large plaques are only observed in *ApoE*$^{-/-}$ mice fed a HC diet. Isotype controls were exposed longer and show only unspecific staining of the connective tissue. Bar = 25 µm. AL: Arterial lumen. (**B**) SIRT1 colocalizes with endothelial cells (CD31;

arrows), and with macrophages (CD68; arrows) in atherosclerotic plaques. EC: endothelial cell layer; P: Plaque; VSMC: Vascular smooth muscle cells; AL: Arterial lumen.

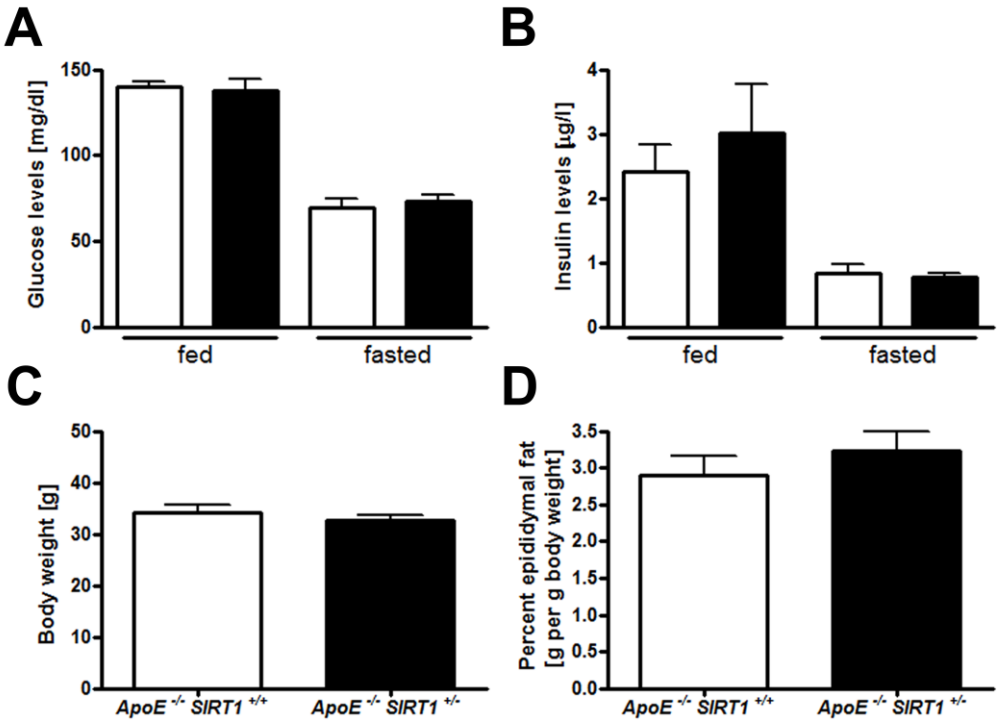

Supplemental Figure 4. No difference between *ApoE*$^{-/-}$ *SIRT1*$^{+/+}$ (white columns) and *ApoE*$^{-/-}$ *SIRT1*$^{+/-}$ (black columns) mice regarding glucose plasma levels, body weight, and weight of epididymal fat pad. (**A**) Plasma glucose levels in fed and fasted animals. (**B**) Plasma insulin levels in fed and fasted animals. (**C**) Total body weight of mice prior to harvesting. (**D**) Percent epididymal fat, given as the percentage of the epididymal fat per total body weight. n≥10 per genotype.

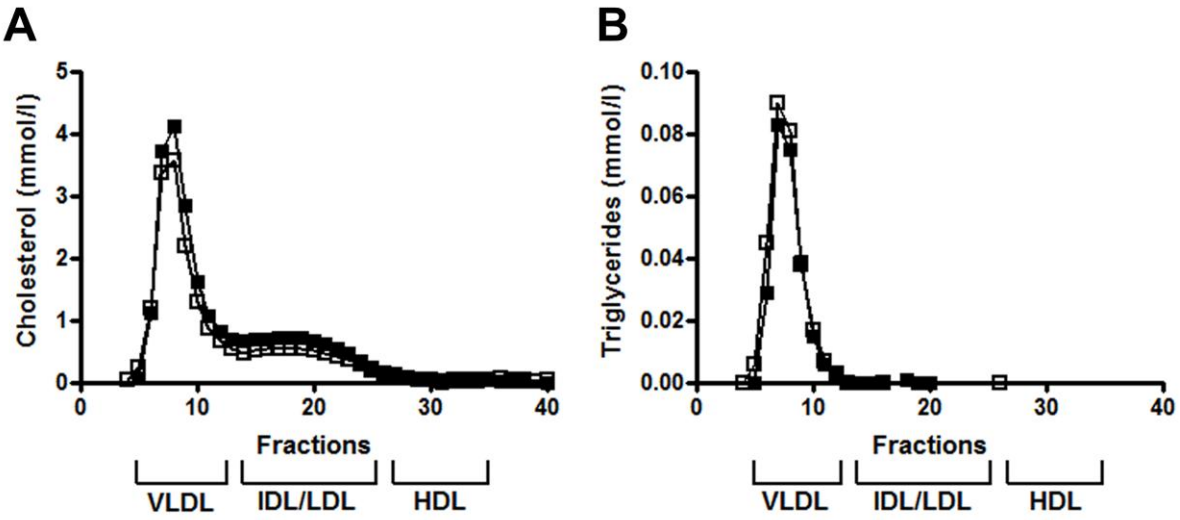

Supplemental Figure 5. No alterations of plasma lipid distribution in *ApoE*$^{-/-}$ *SIRT1*$^{+/+}$ & *ApoE*$^{-/-}$ *SIRT1*$^{+/-}$ mice. (**A, B**) Distribution of cholesterol and triglycerides in the plasma of *ApoE*$^{-/-}$ *SIRT1*$^{+/+}$ mice (■, n = 10 (pooled)) or *ApoE*$^{-/-}$ *SIRT1*$^{+/-}$ mice (□, n = 15 (pooled)). No differences in the distribution of cholesterol or triglycerides are observed between *ApoE*$^{-/-}$ *SIRT1*$^{+/+}$ & *ApoE*$^{-/-}$ *SIRT1*$^{+/-}$ mice. VLDL, very low-density lipoprotein; IDL, intermediate-density lipoprotein; LDL, low-density lipoprotein; HDL, high-density lipoprotein.

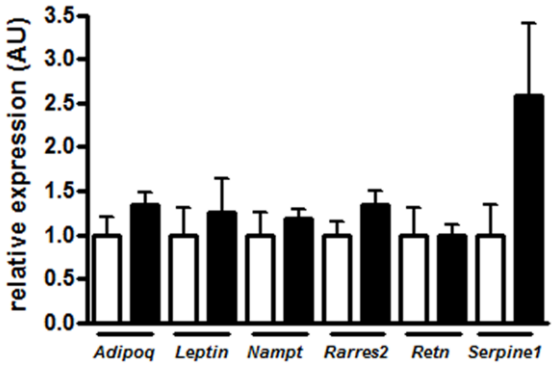

Supplemental Figure 6. Epididymal white adipose tissue expression of Adiponectin (Adipoq), Leptin, Visfatin (Nampt), Chemerin (Rarres2), Resistin (Retn) and Plasminogen activator inhibitor 1 (PAI-1 or Serpine1) in ApoE$^{-/-}$ SIRT1$^{+/+}$ (white columns) and ApoE$^{-/-}$ SIRT1$^{+/-}$ (black columns) mice. n=6 per genotype.

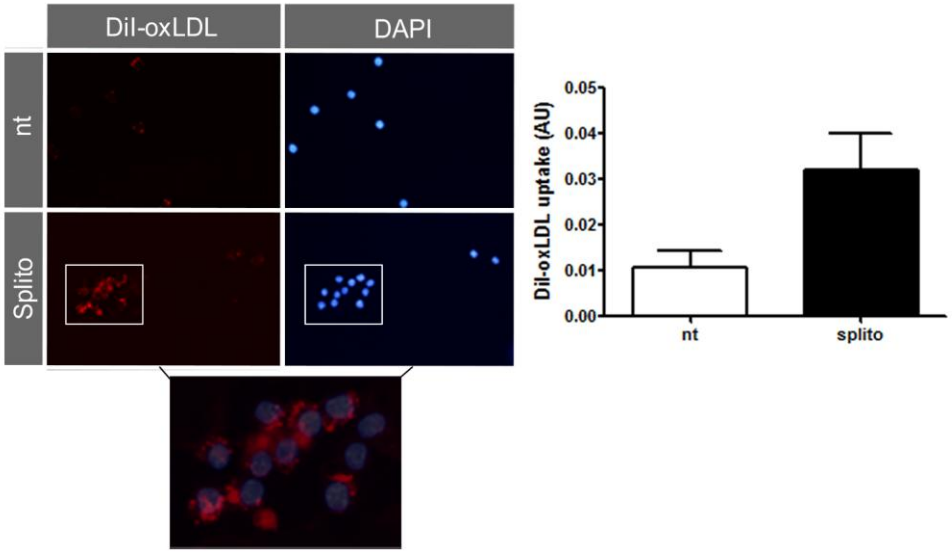

Supplemental Figure 7. SIRT1 inhibition with splitomicin (splito) shows a trend towards increased accumulation of oxLDL in RAW 264.7 cells compared to non-treated cells.

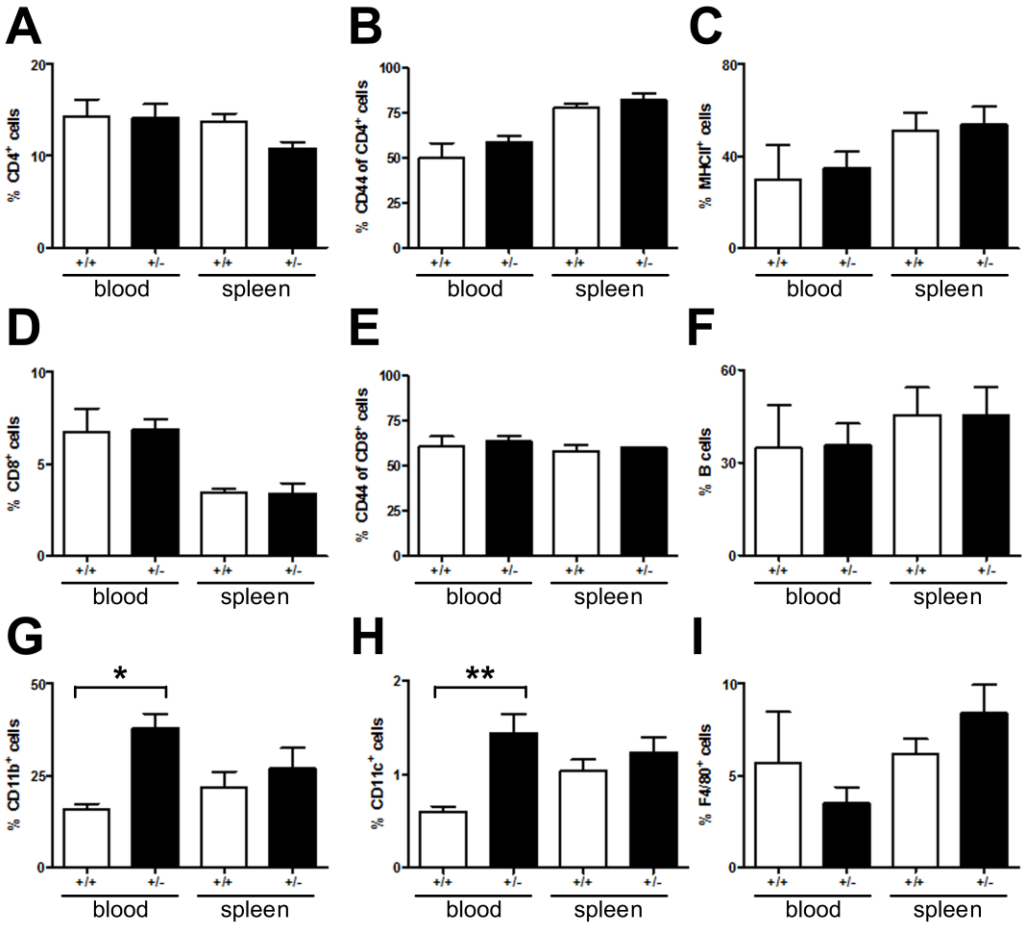

Supplemental Figure 8. Blood and spleen analysis of bone-marrow transplanted mice. Percental FACS analyses of **(A)** $CD4^+$ cells, **(B)** $CD44^+$ population of $CD4^+$ cells, **(C)** $MHCII^+$ cells, **(D)** $CD8^+$ cells, **(E)** $CD44^+$ population of $CD8^+$ cells, **(F)** B cells, **(G)** $CD11b^+$ cells, **(H)** $CD11c^+$ cells, **(I)** $F4/80^+$ cells. n=3/transplanted genotype. *p<0.05; **p< 0.01**.**

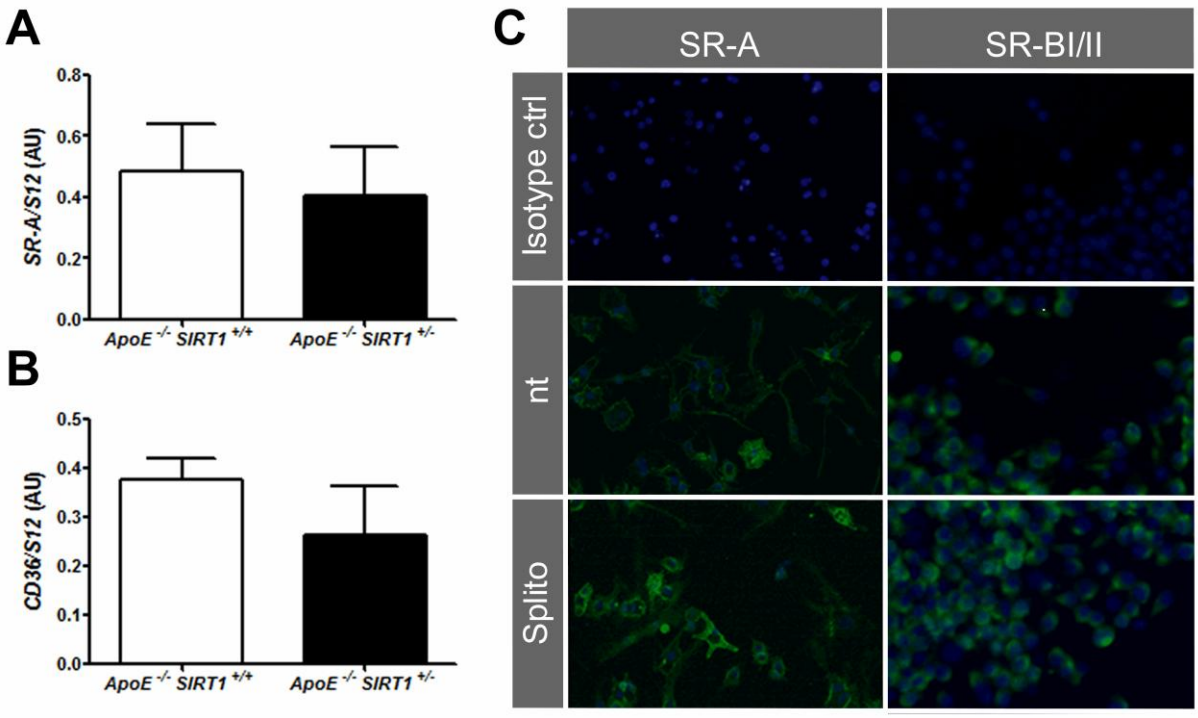

Supplemental Figure 9. SIRT1 does not affect the expression of SR-A, CD36, or SR-B. Aortic RNA levels of *SR-A* (**A**) and *CD36* (**B**). **(C)** SR-A and SR-B immunofluorescence in RAW 264.7 macrophages reveals no difference upon splitomicin (Splito) treatment compared with non-treated cells (nt).

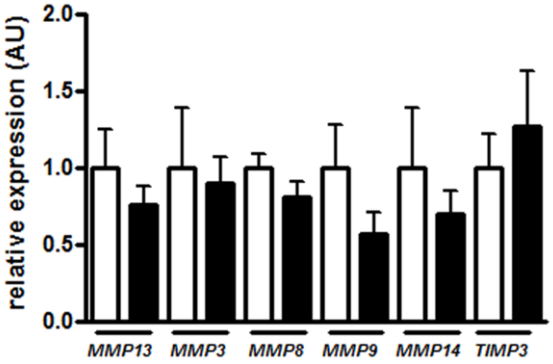

Supplemental Figure 10. Aortic expression of *MMP13*, *MMP3*, *MMP8*, *MMP9*, *MMP14*, and *TIMP3* in *ApoE*$^{-/-}$ *SIRT1*$^{+/+}$ (white columns) and *ApoE*$^{-/-}$ *SIRT1*$^{+/-}$ (black columns) mice. n=10 per genotype.

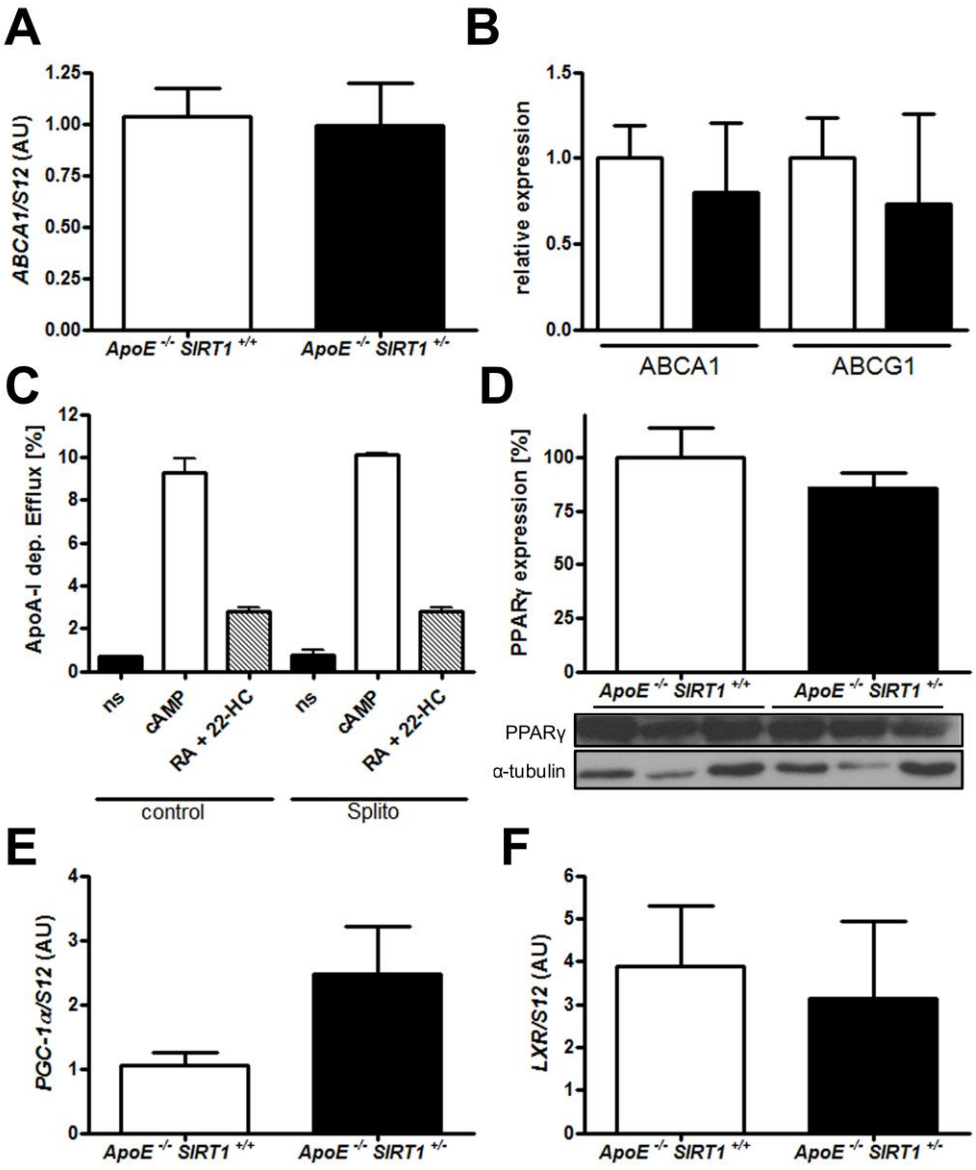

Supplemental Figure 11. SIRT1 does not affect cholesterol efflux in macrophages. (**A**) Aortic RNA levels of *ABCA1*. n=6 per genotype. **(B)** Expression of ABCA1 and ABCG1 in *ApoE*$^{-/-}$ *SIRT1*$^{+/+}$ (white columns) and *ApoE*$^{-/-}$ *SIRT1*$^{+/-}$ (black columns) peritoneal macrophages. n=4 per genotype. (**C**) ApoA-1-dependent cholesterol efflux in RAW 264.7 macrophages is not affected by 100 μM splitomicin (Splito) compared with untreated control groups (nt). 9 *cis*-retinoic acid (RA) + 22-hydroxycholesterol (22-HC)-stimulation is done to analyze LXR/RXR-dependent efflux, cAMP-stimulation to study LXR/RXR-independent efflux. n=3 per treatment group. **(D)** Aortic expression of PPARγ. n=6 per genotype. **(E, F)** Aortic RNA levels of PGC-1α (E, n=10 per genotype) and LXRα (F, n=6 per genotype).

SUPPLEMENTARY TABLES

Supplemental Table 1: Plasma lipid profiles of *ApoE*$^{-/-}$ *SIRT1*$^{+/+}$ and *ApoE*$^{-/-}$ *SIRT1*$^{+/-}$.

	***ApoE*$^{-/-}$ *SIRT1*$^{+/+}$ (n=10)**	***ApoE*$^{-/-}$ *SIRT1*$^{+/-}$ (n=14)**
Total cholesterol (mmol/l)	45.54 ± 6.15	39.72 ± 2.56
Triglycerides (mmol/l)	2.12 ± 0.24	2.03 ± 0.18
Free fatty acids (mmol/l)	0.99 ± 0.13	0.93 ± 0.09

mean ± SEM.

Supplemental Table 2: Plasma cytokine values of *ApoE*$^{-/-}$ *SIRT1*$^{+/+}$ and *ApoE*$^{-/-}$ *SIRT1*$^{+/-}$.

	***ApoE*$^{-/-}$ *SIRT1*$^{+/+}$ (n=10)**	***ApoE*$^{-/-}$ *SIRT1*$^{+/-}$ (n=15)**
VCAM-1 (ng/ml)	1146 ± 59.7	1266 ± 62.8
ICAM-1 (ng/ml)	843 ± 51.4	813 ± 31.1
TGF-β	6431 ± 644.5	6167 ± 332.7
IFN-γ (pg/ml)	7.27 ± 3.67	16.15 ± 8.26
IL-6 (pg/ml)	65.36 ± 21.17	127.54 ± 57.67
IL-10 (pg/ml)	86.40 ± 40.27	189.30 ± 85.90
mKC	110.44 ± 22.01	138.81 ± 15.64

mean ± SEM.

5.2 SIRT1 reduces endothelial activation without affecting vascular function in ApoE-/- mice

Authors:	Sokrates Stein, Nicola Schäfer, Alexander Breitenstein, Christian Besler, Stephan Winnik, Christine Lohmann, Kathrin Heinrich, Chad E. Brokopp, Christoph Handschin, Ulf Landmesser, Felix C. Tanner, Thomas F. Lüscher, and Christian M. Matter
Journal:	Aging (Albany NY). 2010; 2(6):353-360.
DOI:	v2/n6/full/100162.html [pii]
PMID:	20606253
Comment in:	Zhihong Yang and Xiu-Fen Ming Aging (Albany NY). 2010 June;2(6). Epub ahead of print
Contribution:	Design and analyses of all experiments; performance of most experiments; writing the manuscript.

Research Paper

SIRT1 reduces endothelial activation without affecting vascular function in ApoE-/- mice

Sokrates Stein[1], Nicola Schäfer[1], Alexander Breitenstein[1], Christian Besler[1], Stephan Winnik[1], Christine Lohmann[1], Kathrin Heinrich[1], Chad E. Brokopp[1], Christoph Handschin[2], Ulf Landmesser[1], Felix C. Tanner[1], Thomas F. Lüscher[1], and Christian M. Matter[1]

[1] Cardiovascular Research, Institute of Physiology, Zurich Center for Integrative Human Physiology (ZIHP), University of Zurich, and Cardiovascular Center, Cardiology, University Hospital Zurich, CH-8057 Zurich, Switzerland

[2] Biozentrum, University of Basel, CH-4056 Basel, Switzerland

Key words: *SIRT1, atherosclerosis, endothelium, inflammation*
Received: *06/23/10; accepted: 06/26/10; published on line: 06/28/10*
Correspondence: *sokrates@access.uzh.ch; christian.matter@access.uzh.ch*

Abstract: Excessive production of reactive oxygen species (ROS) contributes to progression of atherosclerosis, at least in part by causing endothelial dysfunction and inflammatory activation. The class III histone deacetylase SIRT1 has been implicated in extension of lifespan. In the vasculature, *SIRT1* gain-of-function using *SIRT1* overexpression or activation has been shown to improve endothelial function in mice and rats via stimulation of endothelial nitric oxide (NO) synthase (eNOS). However, the effects of *SIRT1* loss-of-function on the endothelium in atherosclerosis remain to be characterized. Thus, we have investigated the endothelial effects of decreased endogenous *SIRT1* in hypercholesterolemic *ApoE*$^{-/-}$ mice. We observed no difference in endothelial relaxation and eNOS (Ser^{1177}) phosphorylation between 20-week old male atherosclerotic *ApoE*$^{-/-}$ *SIRT1*$^{+/-}$ and *ApoE*$^{-/-}$ *SIRT1*$^{+/+}$ mice. However, SIRT1 prevented endothelial superoxide production, inhibited NF-κB signaling, and diminished expression of adhesion molecules. Treatment of young hypercholesterolemic *ApoE*$^{-/-}$ *SIRT1*$^{+/-}$ mice with lipopolysaccharide to boost NF-κB signaling led to a more pronounced endothelial expression of ICAM-1 and VCAM-1 as compared to *ApoE*$^{-/-}$ *SIRT1*$^{+/+}$ mice. In conclusion, endogenous SIRT1 diminishes endothelial activation in *ApoE*$^{-/-}$ mice, but does not affect endothelium-dependent vasodilatation.

INTRODUCTION

Inflammation plays a key role in the development and progression of atherosclerosis. In early stages of the disease, endothelial cells get activated by circulating proinflammatory molecules such as cytokines (e.g. TNFα) or modified lipoproteins (e.g. oxidized LDL). Once activated, these cells express chemokines, cytokines, and adhesion molecules, which attract and recruit inflammatory cells such as macrophages and T cells [1, 2]. Hypertension, hypercholesterolemia, diabetes, and aging, which may all be associated with an excessive production of reactive oxygen species (ROS) and oxidant stress, may contribute to atherosclerosis by affecting endothelial function and inducing sustained endothelial activation [2-5].

The NAD-dependent class III histone deacetylase Sir2 was found to increase lifespan in yeast [6]. Its mammalian orthologue SIRT1 senses caloric restriction, improves insulin secretion in pancreatic beta cells, and reduces accumulation of fatty acids in white adipose tissue [7-9]. Various other SIRT1 targets have been identified and characterized in recent years, including PGC-1α, NF-κB and LXR [10-13]. NF-κB is of special interest in endothelial cells, since it drives the expression of important adhesion molecules, such as vascular cell

adhesion molecule-1 (VCAM-1) and intercellular adhesion molecule-1 (ICAM-1), which recruit blood monocytes to atherosclerotic lesions [14-16].

Endogenous SIRT1 has been shown to decrease macrophage foam cell formation and atherogenesis in hypercholesterolemic *ApoE*$^{-/-}$ *SIRT1*$^{+/-}$ mice [17]. In non-atherosclerotic aortae of rats, dominant-negative SIRT1 transfection impairs endothelial function via eNOS inhibition *ex vivo* [18], and endothelial overexpression of human SIRT1 diminishes atherogenesis in *ApoE*$^{-/-}$ mice and improves vascular function [19]. In addition, activation of SIRT1 prevents hyperglycemia-induced vascular cell senescence in mice with diabetes, thereby protecting from vascular dysfunction [20]. Nevertheless, the impact of a *SIRT1* haploinsufficiency on endothelium-dependent vasomotion and endothelial cell activation in atherosclerotic mice remains to be determined.

In the present study, we therefore investigated the effects of a single SIRT1 allele on aortic relaxation and endothelial activation in 20-week-old atherosclerotic *ApoE*$^{-/-}$ *SIRT1*$^{+/+}$ and *ApoE*$^{-/-}$ *SIRT1*$^{+/-}$ mice.

RESULTS

Endogenous SIRT1 does not alter endothelial function in *ApoE*$^{-/-}$ mice

Overexpression of human SIRT1 in mouse endothelial cells has been shown to diminish atherogenesis in *ApoE*$^{-/-}$ mice. [19] However, the underlying mechanisms remain to be further characterized. To investigate the effect of endogenous *SIRT1* on endothelium-dependent vasodilatation and endothelial inflammatory activation, we assessed endothelium-dependent function and inflammatory pathways in aortic rings from 20-week-old atherosclerotic *ApoE*$^{-/-}$ *SIRT1*$^{+/+}$ or *ApoE*$^{-/-}$ *SIRT1*$^{+/-}$ mice. Interestingly, the acetylcholine-mediated relaxation of aortic rings after precontraction with norepinephrine did not differ between *ApoE*$^{-/-}$ *SIRT1*$^{+/+}$ and the haploinsufficient *ApoE*$^{-/-}$ *SIRT1*$^{+/-}$ mice (Figure 1A). Vasoconstriction with norepinephrine and endothelium-independent vasodilatation with sodium nitroprusside were normal (Figure 1B, C). eNOS-derived NO plays an important role in vascular relaxation, and eNOS activity is mainly regulated by Akt-dependent Ser^{1177} phosphorylation [21]. We observ-

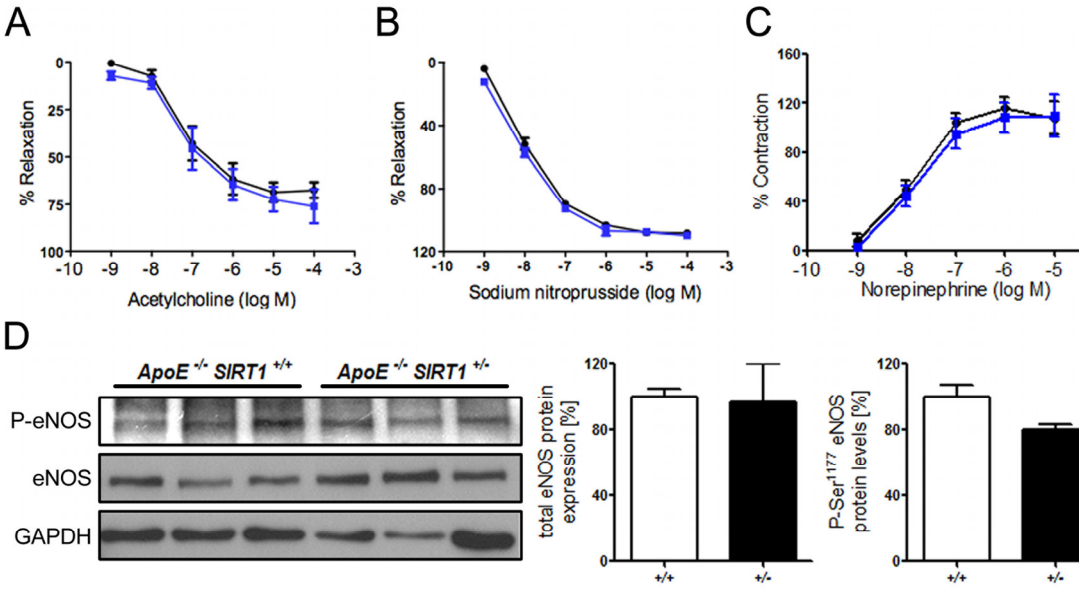

Figure 1. *ApoE*$^{-/-}$ *SIRT1*$^{+/-}$ mice do not exhibit endothelial dysfunction. (**A**) No difference in relaxation of aortic rings preconstricted with norepinephrine to the vasodilator acetylcholine. % Relaxation = % of precontraction to norepinephrine. (**B**) Relaxation of aortic rings at increasing sodium nitroprusside concentrations after norepinephrine precontraction. % Relaxation = % of precontraction to norepinephrine. (**C**) Contraction of aortic rings at increasing norepinephrine concentrations. % Contraction = % of contraction to 80 mM KCl. *ApoE*$^{-/-}$ *SIRT1*$^{+/-}$ (blue line) and *ApoE*$^{-/-}$ *SIRT1*$^{+/+}$ (black line). (**D**) Aortic protein levels of total eNOS and phospho-eNOS (Ser1177). *ApoE*$^{-/-}$ *SIRT1*$^{+/-}$ (+/- and black columns) and *ApoE*$^{-/-}$ *SIRT1*$^{+/+}$ (+/+ and white columns). n=6 per genotype

ed no difference in the Ser^{1177} phosphorylation status (Figure 1D). Our data indicate that endogenous SIRT1 in atherosclerotic *ApoE*$^{-/-}$ mice does not affect endothelial function.

Silencing of SIRT1 enhances production of endothelial superoxide

Common risk factors predisposing to atherosclerosis, such as hypercholesterolemia or aging, are associated with oxidant stress at least in part due to an increased production of ROS [22]. We measured ROS production in human aortic endothelial cells (HAECs) treated with either scrambled- or SIRT1-siRNA. SIRT1 silencing elevated endothelial ROS levels upon TNFα stimulation, whereas under basal conditions there was no effect of SIRT1 silencing was observed (Figure 2).

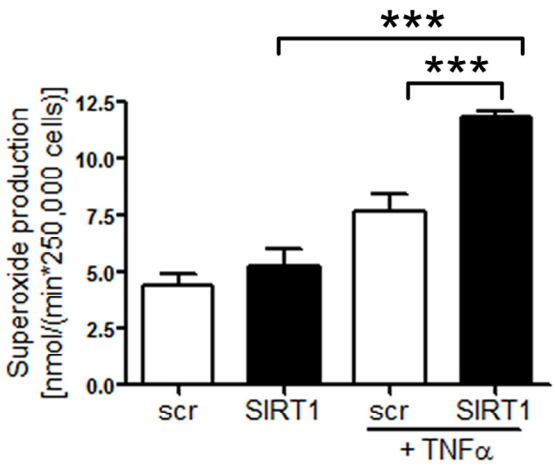

Figure 2. Superoxide production is increased in HAECs after SIRT1-siRNA compared with scrambled-siRNA-treatment 1 h after TNFα stimulation. n=2. ***p<0.001.

Enhanced expression of adhesion molecules in *ApoE*$^{-/-}$ *SIRT1*$^{+/-}$ plaques

Accumulating evidence suggests that chronic production of ROS may favor atherogenesis by inducing sustained endothelial inflammatory activation [2, 5]. Expression of endothelial adhesion molecules play an important role in atherogenesis by promoting monocyte-derived macrophage recruitment and accumulation in the arterial intima [16]. Interestingly, expression of ICAM-1 and VCAM-1 was increased in atherosclerotic plaques of *ApoE*$^{-/-}$ *SIRT1*$^{+/-}$ compared with *ApoE*$^{-/-}$ *SIRT1*$^{+/+}$ mice (Figure 3). These findings show that SIRT1 prevents adhesion molecule expression, an important step in endothelial cell activation.

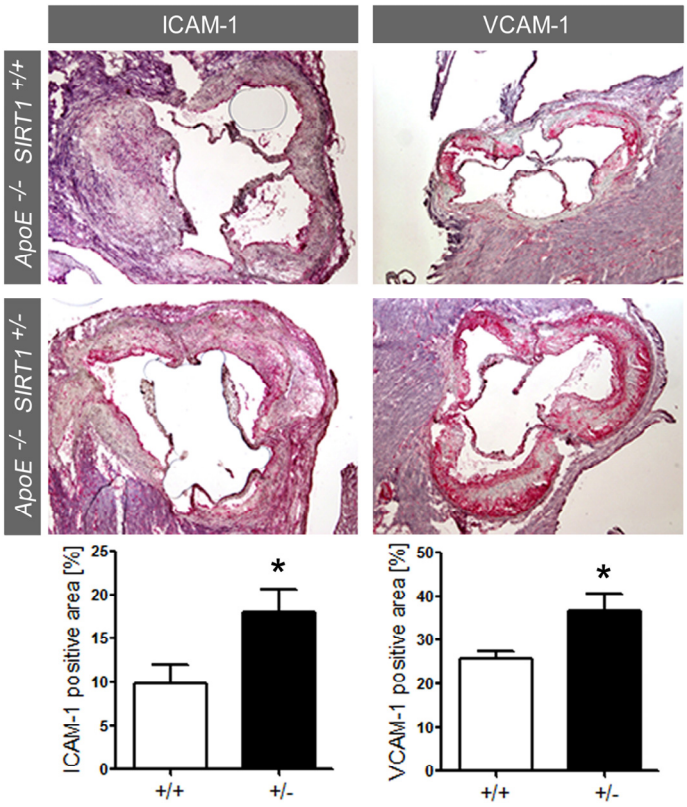

Figure 3. *SIRT1* deletion increases adhesion molecule expression. ICAM-1 and VCAM-1 staining and quantification in plaques from aortic sinus. Magnifications: X40. *ApoE*$^{-/-}$ *SIRT1*$^{+/+}$ (+/+, n=6, white columns) and *ApoE*$^{-/-}$ *SIRT1*$^{+/-}$ (+/-, n=6, black columns). *p<0.05.

SIRT1 regulates the expression of endothelial adhesion molecules via suppression of NF-κB signaling *in vitro*

NF-κB plays a central role in inflammatory processes and its signaling pathway is inhibited by SIRT1 via deacetylation [12, 23]. NF-κB induces expression of adhesion molecules and inflammatory cytokines, and endothelial-specific inhibition of the NF-κB pathway protects mice from atherosclerosis [24]. SIRT1 has been shown to deacetylate the lysine residue K310 of RelA/p65 in human epithelial lung cells [12]. To test whether RelA/p65 signaling is suppressed by SIRT1 in HAECs, we quantified DNA-bound RelA/p65 in TNFα-stimulated and unstimulated cells pretreated with the SIRT1 inhibitor splitomicin [25]. Binding of RelA/p65 to naked DNA was enhanced upon treatment with the SIRT1 inhibitor splitomicin after TNFα stimulation (Figure 4A). To evaluate, if SIRT1 is also deacetylating K310 of RelA/p65 in HAECs, as previously reported

for HEK 293T cells [12], we stimulated SIRT1- or scrambled-siRNA-treated HAECs with TNFα and performed p65 immunoprecipitations. K310-p65 was increased in SIRT1-siRNA-treated HAECs (Figure 4B). To further test if suppression of NF-κB signaling also affects the expression of adhesion molecules, we analyzed the expression of VCAM-1, a known NF-κB signaling target, in more detail. SIRT1-siRNA treatment enhanced expression of VCAM-1 in HAECs upon TNFα stimulation (Figure 4C).

SIRT1 regulates the expression of inflammatory endothelial molecules *in vivo*

Since SIRT1 suppresses NF-κB signaling in HAECs, we investigated whether the same concept holds true in mouse aortae. Binding of RelA/p65 to naked DNA was higher in nuclear extracts of *ApoE*$^{-/-}$ *SIRT1*$^{+/-}$ than *ApoE*$^{-/-}$ *SIRT1*$^{+/+}$ mice (Figure 5A). Importantly, aortic expression of other inflammatory molecules, namely *IL-1β*, *TNFα*, and *P-Selectin* (*P-Sel*), was also enhanced in *ApoE*$^{-/-}$ *SIRT1*$^{+/-}$ compared to *ApoE*$^{-/-}$ *SIRT1*$^{+/+}$ mice (Figure 5B). The expression of these inflammatory genes is regulated by NF-κB. Lipopolysaccharides (LPS) induce strong activation of NF-κB signaling and the expression of target genes [26]. To address the *in vivo* relevance of the NF-κB suppression by SIRT1, we examined the expression of two known NF-κB-dependent genes, ICAM-1 and VCAM-1, in aortae from young 8-week-old *ApoE*$^{-/-}$ *SIRT1*$^{+/-}$ and *ApoE*$^{-/-}$ *SIRT1*$^{+/+}$ mice without atherosclerosis in descending thoracic aortae 3 hours after intraperitoneal injection of LPS. LPS induced an upregulation of both ICAM-1 and VCAM-1 in intimal endothelial cells of aortae from *ApoE*$^{-/-}$ *SIRT1*$^{+/-}$ compared with *ApoE*$^{-/-}$ *SIRT1*$^{+/+}$ mice (Figure 5C, D). These findings indicate that endogenous SIRT1 is sufficient to prevent adhesion molecule expression in both human and mouse activated endothelial cells.

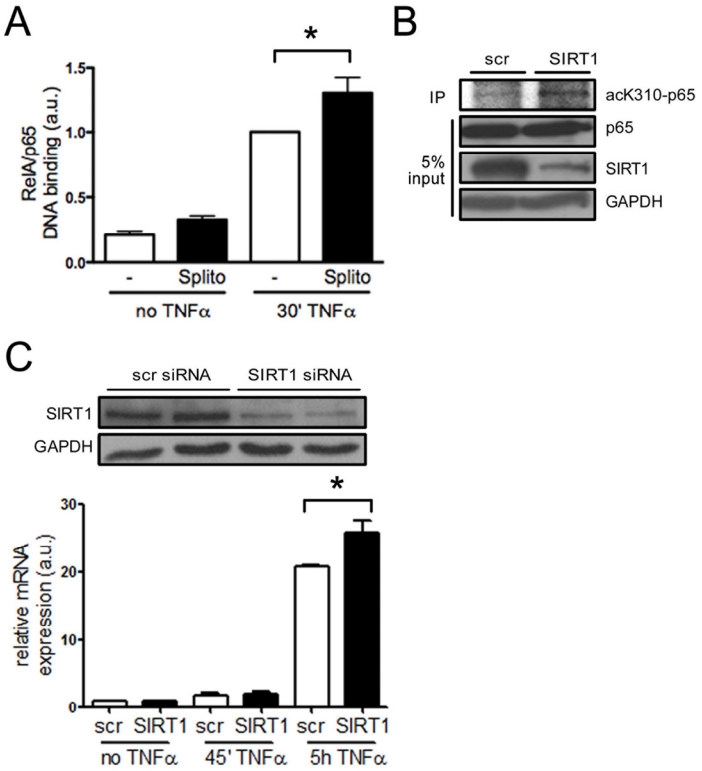

Figure 4. SIRT1 suppresses NF-κB signaling in HAECs. (A) RelA/p65 DNA binding is higher in HAEC pretreated with splitomicin (Splito) compared with the untreated group (-), 30 min after TNFα-stimulation. n=5. **(B)** RelA/p65 immunoprecipitation in HAECs reveals more acetyl-K310-RelA/p65 upon SIRT1-siRNA treatment 20 min after TNFα-stimulation compared to scrambled siRNA-treated cells. n=2. **(C)** Western blot showing SIRT1 silencing using siRNA (top), and VCAM-1 mRNA expression 5 h after TNFα stimulation in SIRT1-siRNA treated HAECs (graph). n=4. *p<0.05.

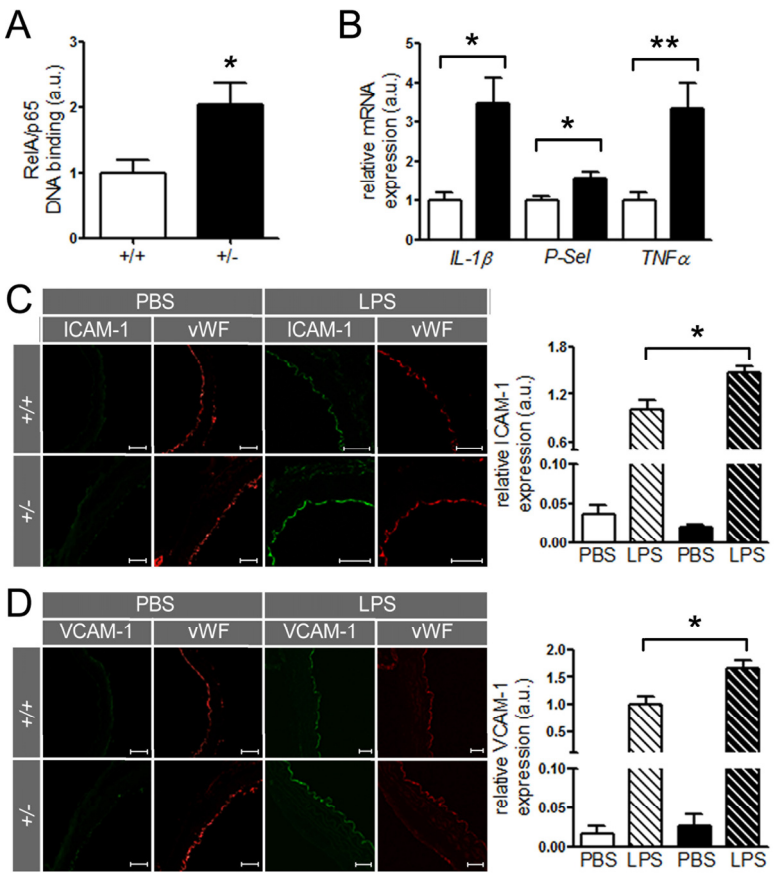

Figure 5. SIRT1 prevents expression of endothelial adhesion molecules. **(A)** RelA/p65 DNA-binding in aortic nuclear extracts from *ApoE*$^{-/-}$ *SIRT1*$^{+/-}$ (+/-, n=8, black column) is elevated in *ApoE*$^{-/-}$ *SIRT1*$^{+/+}$ (+/+, n=6, white column) mice. **(B)** Expression levels of *IL-1β*, *P-Selectin*, and *TNFα* in aortic lysates of *ApoE*$^{-/-}$ *SIRT1*$^{+/+}$ (white columns) and *ApoE*$^{-/-}$ *SIRT1*$^{+/-}$ (black columns) mice. n=8 per genotype. Enhanced expression of ICAM-1 **(C)** and VCAM-1 **(D)** is observed in non-atherosclerotic *ApoE*$^{-/-}$ *SIRT1*$^{+/-}$ (+/- and black columns) compared with *ApoE*$^{-/-}$ *SIRT1*$^{+/+}$ (+/+ and white columns) aortae 3 h post intra-peritoneal LPS (striped columns) injection. n=6 per genotype. Scale: 50 µm. *p<0.05; **p< 0.01.

DISCUSSION

Enhanced atherogenesis in *ApoE*$^{-/-}$ *SIRT1*$^{+/-}$ mice is causally linked to increased expression of adhesion molecules in aortae. Indeed, we provide *in vitro* and *in vivo* evidence that underlines this concept by demonstrating that *ApoE*$^{-/-}$ *SIRT1*$^{+/-}$ mice exhibit increased endothelial expression of ICAM-1 and VCAM-1 upon LPS injection. Importantly, upregulation of these adhesion molecules promotes recruitment of monocytes and T cells to luminal endothelial cells [27]. In concert with increased levels of IL-1β, TNFα, and P-Sel in the activated arterial wall, these molecular events are sufficient to recruit circulating leukocytes to atherosclerotic lesions, especially monocyte-derived macrophages and T cells.

At the molecular level, the inhibitory effects of SIRT1 on adhesion molecule expression may be mediated via RelA/p65 signaling**.** Our data show that SIRT1 suppresses binding of RelA/p65 to naked DNA, therefore interfering with a crucial step in the transcriptional activation of NF-κB. These findings are in line with previous reports showing that SIRT1 deacetylases RelA/p65 at the lysine residue K310 in human epithelial lung cells [12]. In agreement with these reports, we demonstrate that this mechanism of RelA/p65 signaling suppression is present in HAECs.

Surprisingly, we observe no endothelial dysfunction in *ApoE*$^{-/-}$ *SIRT1*$^{+/-}$ mice. In contrast, Pearson et al. showed improved endothelial function in mice kept on a diet with a very high resveratrol content (2400 mg/kg/food) that could be mediated by SIRT1 activation [28]. However, such effects may also be related to activation of AMPK by resveratrol or via other targets of this compound [29, 30]. Furthermore, adenovirus-mediated inhibition of endothelial SIRT1 diminishes endothelium-dependent vasodilatation in rat aortic rings and decreases bioavailable NO levels [18]. Others reported improved relaxation in *ApoE*$^{-/-}$ mice with endothelial *SIRT1* overexpression that were kept on a high-fat diet [19]. However, in this study WT aortic rings showed also marked endothelial dysfunction by relaxing only up to 50%, thereby casting doubts on the endothelial integrity of the preparations [19]. In contrast, we observed no change in endothelial function or aortic eNOS activity between hyper-cholesterolemic *ApoE*$^{-/-}$ *SIRT1*$^{+/-}$ and *ApoE*$^{-/-}$ *SIRT1*$^{+/+}$ mice, suggesting that the endothelial-protective effects of SIRT1 include factors other than eNOS-dependent NO production. Indeed, we detected a profound increase in ROS-production after silencing of SIRT1 in TNFalpha-stimulated endothelial cells, indicating that endogenous SIRT1 inhibits agonist-induced ROS production in endothelial cells. Of note, an excessive production of ROS has been implicated in endothelial inflammatory activation and the pathogenesis of atherosclerosis [31]. Therefore, inhibition of excessive endothelial ROS production likely represents an important endothelial-protective action of endogenous SIRT1.

Taken together, our results show that SIRT1 does not influence endothelium-dependent vascular function in *ApoE*$^{-/-}$ mice, but it prevents superoxide production in endothelial cells and reduces the expression of inflammatory adhesion molecules by suppressing NF-κB signaling. Although the specificity of available SIRT1 activators has been questioned recently [32], it is likely that SIRT1 activators may prevent atherosclerosis and other inflammatory diseases by hindering pro-oxidative and inflammatory processes.

MATERIALS AND METHODS

Animals. *ApoE*$^{-/-}$ *SIRT1*$^{+/-}$ and *ApoE*$^{-/-}$ *SIRT1*$^{+/+}$ mice were described previously [17]. Male mice were fed a high-cholesterol diet (1.25% total cholesterol, Research Diets) for 12 weeks starting at the age of 8 weeks. All animal procedures were approved by the local animal committee and performed in accordance with our institutional guidelines.

Cell culture. Human aortic endothelial cells (HAEC, Cambrex Bio Science) were treated with 100 μM splitomicin (Sigma-Aldrich) to perform analysis of NF-κB binding to DNA. HAEC were stimulated for 30 minutes with 10 ng/ml human TNFα (R&D Systems).

siRNA transfection. Transient transfection siRNA into HAEC were done with lipofectamin lipofectamin RNAi MAX (Invitrogen). The oligos used for SIRT1-siRNA have been described previously [9].

Immunohistochemistry and immunofluorescence. Serial cryosections from the aortic sinus were stained with rabbit anti-von Willebrand Factor (Dako), rat anti-CD31, rat anti-VCAM-1 (BD Biosciences), rat anti-ICAM-1 (Serotec). Fluorescence was analyzed on a Leica TCS SP2 confocal microscope and means were taken from n=6 different mice evaluating 6 serial cryosections/tissue from each mouse.

RNA and protein analysis. Total RNA isolated from proximal aortae and HAEC was extracted with TRIZOL (Invitrogen), reverse transcribed, and the cDNA quantified by SYBR green qPCR using specific primers. For protein analysis, aortic tissue lysates were blotted and incubated with rabbit anti-SIRT1, rabbit anti-eNOS (Santa Cruz Biotechnology), and rabbit anti-Phospho-eNOS (Ser^{1177}) (Cell Signaling Technology).

Endothelial function. Aortic rings (2–3 mm long) were connected to an isometric force transducer (MultiMyograph), suspended in a 95% O_2/5% CO_2 aerated organ chamber filled with KREBS buffer (118 mM NaCl, 4.7 mM KCl, 1.2 mM $MgCl_2$, 1.2 mM NaH_2PO_4, 1.2 mM Na_2SO_4, 2.5 mM $CaCl_2$, 25 mM $NaHCO_3$, 10 mM glucose, pH to 7.4). Concentration-dependent contractions were established by using norepinephrine (10^{-9} to 10^{-4} mol/liter; Sigma–Aldrich). Concentration–response curves were obtained in a cumulative fashion. 8 rings cut from the same artery were studied in parallel. Responses to acetylcholine (10^{-9} to 10^{-6} mol/liter; Sigma–Aldrich) were obtained during submaximal contraction to norepinephrine. The NO donor sodium nitroprusside (10^{-10} to 10^{-5} mol/liter; Sigma–Aldrich) was added to test endothelium-independent relaxations.

LPS assay. 6 8-week-old *ApoE*$^{-/-}$ *SIRT1*$^{+/-}$ and *ApoE*$^{-/-}$ *SIRT1*$^{+/+}$ mice kept on standard diet were used for this assay. At this age and under normal diet, *ApoE*$^{-/-}$ mice do not exhibit plaques in their thoraco-abdominal aortae. Mice were injected i.p. with 100 μg of LPS (Sigma) in PBS, sacrificed 3 hours post injection and thoraco-abdominal aortae embedded in OCT. Cryosections (5 μm) were cut and stained for ICAM-1

or VCAM-1. Relative expression is given as the ratio of ICAM-1 or VCAM-1 staining area to von Willebrand Factor (vWF) staining area, respectively. Quantification of fluorescence was done with analySIS (Olympus) on microscopic images using identical exposure settings.

Quantification of DNA-bound RelA/p65. HAEC were pretreated with splitomicin for one hour and stimulated with 10 ng/ml TNFα for 30 minutes. Nuclear extracts of aortic tissue samples were obtained with the Nuclear Extract kit (ActiveMotif) using a Dounce pestle, and a RelA/p65 transcription factor assay was performed using the TransAM kit (ActiveMotif) according to the manufacturer's instructions.

Immunoprecipitation. HAEC were treated with 50 μM SIRT1 or scrambled siRNA over night, followed by 10 ng/ml TNFα stimulation for 20 minutes. Cells were then harvested and protein extracted in lysis buffer (20 mM HEPES, pH 7.5, 80 mM NaCl, 2.5 mM MgCl2, 1 mM EDTA, 100 μM Splitomicin, 0.5% NP-40, 1 mM PMFS (phenylmethylsulfonyl fluoride), 10 μg/ml aprotinin, and 10 μg/ml leupeptin). 1 mg whole-cell lysates were immunoprecipitated with rabbit anti-p65 (Santa Cruz) using Protein G agarose (Millipore). Immuno-precipitated samples were immunoblotted with rabbit anti-acK310-p65 (Abcam), and the total lysates (5% input) with rabbit anti-SIRT1 and rabbit anti-p65.

Detection of endothelial cell superoxide production by electron spin resonance spectroscopy. The effect of SIRT1 on endothelial cell superoxide production was assessed in unstimulated and TNFα-stimulated (10 ng/ml) HAEC by ESR spectroscopy using the spin probe 1-hydroxy-3-methoxycarbonyl-2,2,5,5-tetra-methylpyrrolidine (CMH; Noxygen). HAEC were incubated with 50 nM scrambled or SIRT1-siRNA with or without TNFα for one hour and resuspended in Krebs-Hepes buffer (pH 7.4; Noxygen) containing diethyldithiocarbamic acid sodium salt (5 μM, Noxygen) and deferoxamine methanesulfonate salt (25 μM, Noxygen). ESR spectra were recorded after addition of CMH (final concentration 200 μM) under stable temperature conditions using a Bruker e-scan spectrometer (Bruker Biospin). The ESR instrumental settings were as follows: center field, 3495 G; field sweep width, 10.000 G; microwave frequency, 9.75 GHz; microwave power, 19.91 mW; magnetic field modulation frequency, 86.00 kHz; modulation amplitude, 2.60 G; conversion time, 10.24 msec; detector time constant, 328 msec; nuber of x-scans, 10.

Statistical analyses. Data are presented as mean ± SEM. Statistical significance of differences was calculated using an ANOVA with post hoc Tukey's test or Student's unpaired t test. Significance was accepted at $p<0.05$.

ACKNOWLEDGEMENTS

We thank the Center for Microscopy and Image Analysis at the University of Zurich for making their facilities available.

SOURCES AND FUNDING

This work was funded by grants from the Swiss National Science Foundation (#31-114094/1, #310030_130626/1, and #3100-068118) and the University Research Priority Program "Integrative Human Physiology" at the University of Zurich.

CONFLICT OF INTERESTS STATEMENT

The authors of this manuscript have no conflict of interests to declare.

REFERENCES

1. Hansson GK. Inflammation, atherosclerosis, and coronary artery disease. N Engl J Med. 2005;352:1685-1695.

2. Deanfield JE, Halcox JP, Rabelink TJ. Endothelial function and dysfunction: Testing and clinical relevance. Circulation. 2007;115:1285-1295.

3. Mueller CF, Laude K, McNally JS, Harrison DG. Atvb in focus: Redox mechanisms in blood vessels. Arterioscler Thromb Vasc Biol. 2005;25:274-278.

4. Kawashima S, Yokoyama M. Dysfunction of endothelial nitric oxide synthase and atherosclerosis. Arterioscler Thromb Vasc Biol. 2004;24:998-1005.

5. Stokes KY, Clanton EC, Russell JM, Ross CR, Granger DN. Nad(p)h oxidase-derived superoxide mediates hypercholestero-lemia-induced leukocyte-endothelial cell adhesion. Circ Res. 2001;88:499-505.

6. Kaeberlein M, McVey M, Guarente L. The sir2/3/4 complex and sir2 alone promote longevity in saccharomyces cerevisiae by two different mechanisms. Genes Dev. 1999;13:2570-2580.

7. Chen D, Steele AD, Lindquist S, Guarente L. Increase in activity during calorie restriction requires sirt1. Science. 2005;310:1641.

8. Bordone L, Motta MC, Picard F, Robinson A, Jhala US, Apfeld J, McDonagh T, Lemieux M, McBurney M, Szilvasi A, Easlon EJ, Lin SJ, Guarente L. Sirt1 regulates insulin secretion by repressing ucp2 in pancreatic beta cells. PLoS Biol. 2006;4:e31.

9. Picard F, Kurtev M, Chung N, Topark-Ngarm A, Senawong T, Machado De Oliveira R, Leid M, McBurney MW, Guarente L. Sirt1 promotes fat mobilization in white adipocytes by repressing ppar-gamma. Nature. 2004;429:771-776.

10. Lagouge M, Argmann C, Gerhart-Hines Z, Meziane H, Lerin C, Daussin F, Messadeq N, Milne J, Lambert P, Elliott P, Geny B, Laakso M, Puigserver P, Auwerx J. Resveratrol improves mitochondrial function and protects against metabolic disease by activating sirt1 and pgc-1alpha. Cell. 2006;127:1109-1122.

11. Rodgers JT, Lerin C, Haas W, Gygi SP, Spiegelman BM, Puigserver P. Nutrient control of glucose homeostasis through a complex of pgc-1alpha and sirt1. Nature. 2005;434:113-118.
12. Yeung F, Hoberg JE, Ramsey CS, Keller MD, Jones DR, Frye RA, Mayo MW. Modulation of nf-kappab-dependent transcription and cell survival by the sirt1 deacetylase. Embo J. 2004;23:2369-2380.
13. Li X, Zhang S, Blander G, Tse JG, Krieger M, Guarente L. Sirt1 deacetylates and positively regulates the nuclear receptor lxr. Mol Cell. 2007;28:91-106.
14. Kim I, Moon SO, Kim SH, Kim HJ, Koh YS, Koh GY. Vascular endothelial growth factor expression of intercellular adhesion molecule 1 (icam-1), vascular cell adhesion molecule 1 (vcam-1), and e-selectin through nuclear factor-kappa b activation in endothelial cells. J Biol Chem. 2001;276:7614-7620.
15. O'Brien KD, McDonald TO, Chait A, Allen MD, Alpers CE. Neovascular expression of e-selectin, intercellular adhesion molecule-1, and vascular cell adhesion molecule-1 in human atherosclerosis and their relation to intimal leukocyte content. Circulation. 1996;93:672-682.
16. Libby P. Inflammation in atherosclerosis. Nature. 2002;420:868-874.
17. Stein S, Lohmann C, Schäfer N, Hofmann J, Rohrer L, Besler C, Rothgiesser KM, Becher B, Hottiger MO, Borén J, McBurney MW, Landmesser U, Lüscher TF, Matter CM. Sirt1 decreases lox-1-mediated foam cell formation in atherogenesis. Eur Heart J. 2010; Apr:23. [Epub ahead of print], doi: 10.1093/eurheartj/ehq107.
18. Mattagajasingh I, Kim CS, Naqvi A, Yamamori T, Hoffman TA, Jung SB, DeRicco J, Kasuno K, Irani K. Sirt1 promotes endothelium-dependent vascular relaxation by activating endothelial nitric oxide synthase. Proc Natl Acad Sci U S A. 2007;104:14855-14860.
19. Zhang QJ, Wang Z, Chen HZ, Zhou S, Zheng W, Liu G, Wei YS, Cai H, Liu DP, Liang CC. Endothelium-specific overexpression of class iii deacetylase sirt1 decreases atherosclerosis in apolipoprotein e-deficient mice. Cardiovasc Res. 2008;80:191-199.
20. Orimo M, Minamino T, Miyauchi H, Tateno K, Okada S, Moriya J, Komuro I. Protective role of sirt1 in diabetic vascular dysfunction. Arterioscler Thromb Vasc Biol. 2009;29:889-894.
21. Dimmeler S, Fleming I, Fisslthaler B, Hermann C, Busse R, Zeiher AM. Activation of nitric oxide synthase in endothelial cells by akt-dependent phosphorylation. Nature. 1999;399:601-605.
22. Cai H, Harrison DG. Endothelial dysfunction in cardiovascular diseases: The role of oxidant stress. Circ Res. 2000;87:840-844.
23. Nichols TC, Fischer TH, Deliargyris EN, Baldwin AS, Jr. Role of nuclear factor-kappa b (nf-kappa b) in inflammation, periodontitis, and atherogenesis. Ann Periodontol. 2001;6:20-29.
24. Gareus R, Kotsaki E, Xanthoulea S, van der Made I, Gijbels MJ, Kardakaris R, Polykratis A, Kollias G, de Winther MP, Pasparakis M. Endothelial cell-specific nf-kappab inhibition protects mice from atherosclerosis. Cell Metab. 2008;8:372-383.
25. Bedalov A, Gatbonton T, Irvine WP, Gottschling DE, Simon JA. Identification of a small molecule inhibitor of sir2p. Proc Natl Acad Sci U S A. 2001;98:15113-15118.
26. Muller JM, Ziegler-Heitbrock HW, Baeuerle PA. Nuclear factor kappa b, a mediator of lipopolysaccharide effects. Immunobiology. 1993;187:233-256.
27. Hansson GK, Libby P. The immune response in atherosclerosis: A double-edged sword. Nat Rev Immunol. 2006;6:508-519.
28. Pearson KJ, Baur JA, Lewis KN, Peshkin L, Price NL, Labinskyy N, Swindell WR, Kamara D, Minor RK, Perez E, Jamieson HA, Zhang Y, et al.. Resveratrol delays age-related deterioration and mimics transcriptional aspects of dietary restriction without extending life span. Cell Metab. 2008;8:157-168.
29. Pirola L, Frojdo S. Resveratrol: One molecule, many targets. IUBMB Life. 2008;60:323-332.
30. Baur JA, Pearson KJ, Price NL, Jamieson HA, Lerin C, Kalra A, Prabhu VV, Allard JS, Lopez-Lluch G, Lewis K, Pistell PJ, Poosala S, et al. Resveratrol improves health and survival of mice on a high-calorie diet. Nature. 2006;444:337-342.
31. Alom-Ruiz SP, Anilkumar N, Shah AM. Reactive oxygen species and endothelial activation. Antioxid Redox Signal. 2008;10:1089-1100.
32. Pacholec M, Bleasdale JE, Chrunyk B, Cunningham D, Flynn D, Garofalo RS, Griffith D, Griffor M, Loulakis P, Pabst B, Qiu X, Stockman B, et al. Srt1720, srt2183, srt1460, and resveratrol are not direct activators of sirt1. *J Biol Chem.* 2010;285:8340-8351.

5.3 Sirt1 inhibition induces in vivo arterial thrombosis and tissue factor expression in activated human endothelial cells

Authors:	Alexander Breitenstein*, Sokrates Stein*, Erik W. Holy, Giovanni G. Camici, Christine Lohmann, Alexander Akhmedov, Remo Spescha, Peter J. Elliott, Christoph H. Westphal, Christian M. Matter, Thomas F. Lüscher, Felix C. Tanner
Journal:	Cardiovasc Res. 2010 Nov 21. Epub ahead of print.
DOI:	10.1093/cvr/cvq339
PMID:	20978007
Contribution:	*equal contribution; Design and performance of all experiments with SIRT1-/- MEF, p65-/- MEF, siRNA-mediated SIRT1-silencing in MEFs and HAECs, RelA/p65 immunoprecipitation, and RelA/p65 nuclear/cytoplasmic translocation.

Cardiovascular Research Advance Access published November 21, 2010

Cardiovascular Research
doi:10.1093/cvr/cvq339

Sirt1 inhibition promotes *in vivo* arterial thrombosis and tissue factor expression in stimulated cells

Alexander Breitenstein[1,2,3†], Sokrates Stein[1,2†], Erik W. Holy[1,2,3], Giovanni G. Camici[1,2], Christine Lohmann[1,2], Alexander Akhmedov[1,2], Remo Spescha[1,2], Peter J. Elliott[4], Christoph H. Westphal[4], Christian M. Matter[1,2,3], Thomas F. Lüscher[1,2,3], and Felix C. Tanner[1,2,3*]

[1]Cardiovascular Research, Physiology Institute, University of Zurich, 8057 Zurich, Switzerland; [2]Center for Integrative Human Physiology (ZHIP), University of Zurich, Zurich, Switzerland; [3]Cardiology, Cardiovascular Center, University Hospital Zurich, Rämistrasse 100, 8091 Zurich, Switzerland; and [4]Sirtris, a GSK company, 200 Technology Square, Cambridge, MA 02139, USA

Received 17 March 2010; revised 7 October 2010; accepted 21 October 2010

Time for primary review: 32 days

Aims The mammalian silent information regulator-two 1 (Sirt1) blunts the noxious effects of cardiovascular risk factors such as type 2 diabetes mellitus and obesity. Nevertheless, the role of Sirt1 in regulating the expression of tissue factor (TF), the key trigger of coagulation, and arterial thrombus formation remains unknown.

Methods and results Human as well as mouse cell lines were used for *in vitro* experiments, and C57Bl/6 mice for *in vivo* procedures. Sirt1 inhibition by splitomicin or sirtinol enhanced cytokine-induced endothelial TF protein expression as well as surface activity, while TF pathway inhibitor protein expression did not change. Sirt1 inhibition further enhanced TF mRNA expression, TF promoter activity, and nuclear translocation as well as DNA binding of the p65 subunit of nuclear factor-kappa B (NFκB/p65). Sirt1 siRNA enhanced TF protein and mRNA expression, and this effect was reduced in *NFκB/p65*$^{-/-}$ mouse embryonic fibroblasts reconstituted with non-acetylatable Lys^{310}-mutant NFκB/p65. Activation of the mitogen-activated protein kinases p38, c-Jun NH_2-terminal kinase, and p44/42 (ERK) remained unaffected. *In vivo*, mice treated with the Sirt1 inhibitor splitomicin exhibited enhanced TF activity in the arterial vessel wall and accelerated carotid artery thrombus formation in a photochemical injury model.

Conclusion We provide pharmacological and genetic evidence that Sirt1 inhibition enhances TF expression and activity by increasing NFκB/p65 activation in human endothelial cells. Furthermore, Sirt1 inhibition induces arterial thrombus formation *in vivo*. Hence, modulation of Sirt1 may offer novel therapeutic options for targeting thrombosis.

Keywords Tissue factor • Sirt1 • Thrombosis • NFκB

1. Introduction

Cardiovascular diseases represent a major health burden. Acute vascular events such as myocardial infarction and ischaemic stroke account for the majority of deaths in Western countries.[1] Formation of an arterial thrombus is the central event in such acute vascular syndromes. Tissue factor (TF) is the key trigger of the coagulation cascade and thereby crucially involved in arterial thrombosis.[2–4] Its impact on thrombus formation may be enhanced in atherosclerosis since TF expression is induced in the inflammatory environment of atherosclerotic plaques.[5] In line with this notion, clinical studies demonstrate higher TF levels in the culprit lesion of patients with acute coronary syndromes.[6] Numerous inflammatory mediators such as tumour necrosis factor alpha (TNF-α[7]) or histamine,[8] but also pro-thrombotic mediators like thrombin,[9] induce endothelial TF expression by activating the MAP kinases p38, ERK, and c-Jun NH_2-terminal kinase (JNK), and consequently transcription factors such as nuclear factor-kappa B (NFκB).[2]

Silent information regulator-two (Sir2) is an NAD^+-dependent class III histone deacetylase.[10] The mammalian sirtuins are evolutionarily conserved homologues of the yeast Sir2,[11] and silent information regulator-two 1 (Sirt1) is the closest orthologue.[12] In addition to maintaining chromatin structure,[10] Sirt1 has been shown to regulate transcription factors such as forkhead box class O (FOXO),[13]

† These authors contributed equally to this work.

* Corresponding author. Tel: +41 44 255 11 11; fax: +41 44 635 68 27, Email: felix.tanner@access.uzh.ch

p53,[14] peroxisome proliferator-activated receptor-γ,[15] endothelial nitric oxide synthase (eNOS),[16] and p65 subunit of nuclear factor-kappa B (NFκB/p65).[17] Hence, Sirt1 is critically involved in cellular responses to stress,[18] senescence,[19] and mitochondrial function.[20] Furthermore, endothelial overexpression of Sirt1 diminishes plaque formation in a mouse model of atherosclerosis,[21] and pharmacological activation of Sirt1 improves glucose homeostasis in mice and humans.[22] Based on these findings, Sirt1 modulators are under investigation in clinical trials for the treatment of patients with cardiovascular risk factors.

Since downstream targets of Sirt1 such as NFκB are involved in the regulation of TF expression, this study was designed to investigate the effect of Sirt1 on TF expression and arterial thrombus formation.

2. Methods

2.1 Cell culture

Human aortic endothelial cells (HAECs; Clonetics, Allschwil, Switzerland) were cultured as described.[23] Briefly, adhering HAECs were grown to confluence and rendered quiescent for 24 h in medium containing 0.5% FCS before stimulation. *Sirt1*$^{-/-}$ mouse embryonic fibroblasts (MEFs) were kindly provided by David Sinclair (Harvard Medical School, Boston, MA, USA) and were grown to confluence in Dulbecco's modified Eagle's medium supplemented with 10% FCS. Similarly, *NFκB/p65*$^{-/-}$ MEFs with reconstituted wild-type NFκB/p65 or non-acetylatable Lys^{310}-mutant NFκB/p65 were used as described previously.[24] Cells were pre-treated with splitomicin (Sigma, Buchs, Switzerland), sirtinol (Calbiochem, Lucerne, Switzerland), or resveratrol (Sigma) for 1 h before stimulation with 5 or 10 ng/mL TNF-α (R&D Systems, Minneapolis, MN, USA), 1 U/mL thrombin (R&D Systems), or 10^{-5} mol/L histamine (Sigma), respectively. Transient transfection with pcDNA3.1-SIRT1 or Sirt1 siRNA (Sirt1 siRNA oligonucleotide sequence: 5′-GATGAAGTTGACCTCCTCA-3′) was performed using Lipofectamine Reagent (Invitrogen, Basel, Switzerland) or Lipofectamine RNAi MAX (Invitrogen), respectively, as described previously.[15,25] Cytotoxicity was assessed by a colorimetric assay to detect lactate dehydrogenase (LDH; Roche, Basel, Switzerland).

2.2 Western blot analysis

Protein expression was determined as described.[8] Antibodies against human TF, tissue factor pathway inhibitor (TFPI; both from American Diagnostica, Stamford, CT, USA), and Sirt1 (Santa Cruz Biotechnology, Santa Cruz, CA, USA) were used at 1:2000 dilution. Antibodies against phosphorylated p38 mitogen-activated protein (MAP) kinase (p38), p44/42 MAP kinase (ERK), and JNK (all from Cell Signaling, Danvers, MA, USA) were used at 1:1000, 1:5000, and 1:1000 dilution, respectively. Antibodies against total p38, ERK, and JNK (all from Cell Signaling) were diluted to 1:3000, 1:10 000, and 1:1000, respectively. The antibody against IκB-α (Santa Cruz Biotechnology) was applied at a 1:1000 dilution. Alpha-tubulin (Sigma) were applied to control protein loading (1:10 000 dilution). Primary antibodies were detected with a horseradish peroxidase-linked secondary antibody (Amersham, Munich, Germany).

2.3 Real-time PCR

Total RNA was extracted from HAECs with 1 mL TRIzol Reagent (Invitrogen) as described.[23] Conversion of total cellular RNA to cDNA was carried out with Moloney murine leukaemia virus reverse transcriptase and random hexamer primers (Amersham) in a final volume of 33 μL using 4 μg of RNA. The total cDNA pool obtained served as template for subsequent PCR amplification with primers specific for full-length TF (sense primer: 5′-TCCCCAGAGTTCACACCTTACC-3′, antisense primer: 5′-CCTTTCTCCTGGCCCATACAC-3′; bases 508–529 of *F3* cDNA; NCBI no. NM 001993). Real-time PCR amplification was performed in an MX3000P PCR cycler (Stratagene) using the SYBR Green JumpStart kit (Sigma) in 25 μL final reaction volume containing 2 μL cDNA, 10 pmol of each primer, 0.25 μL of internal reference dye, and 12.5 μL of JumpStart Taq ReadyMix (buffer, dNTP, stabilizers, SYBR Green, Taq polymerase, and JumpStart Taq antibody). A melting curve analysis was performed after amplification to verify the accuracy of the amplicon. Ribosomal L28 RNA in HAECs or S12 RNA in MEFs served as loading control.

2.4 TF activity *in vitro*

TF surface activity in HAECs was analysed using a colorimetric assay (American Diagnostica). Cells were incubated at 37°C with human FVIIa and FX, allowing for the formation of the TF/FVIIa complex at the cell surface. Conversion of FX to FXa was measured by the ability of FXa to cleave a chromogenic substrate. A standard curve was established with lipidated human TF to assure that the results were in the linear range of detection.

2.5 Histone deacetylase activity

Cell-based histone deacetylase activity (HDAC) assay was performed according to the manufacturer's instructions (BIOMOL, Hamburg, Germany). Briefly, HAECs were starved in phenol-red-free media containing 0.5% FCS. After 24 h, cells were incubated with 200 μmol/L Fluor de Lys substrate with or without trichostatin A (TSA; 1 μmol/L, BIOMOL), and with or without splitomicin (100 μmol/L, Sigma). After 2 h, cells were incubated with Fluor de Lys developer, lysed after 30 min, and equal amount of lysates were analysed for enzyme activity using a fluorescence reader (Ex. 360 nm, Em. 460 nm).

2.6 TF promoter activity

An adenoviral vector (Ad5/hTF/Luc) containing the minimal TF promoter (−227 to +121 bp) upstream of the Luciferase cDNA and the SV40 PolyA signal was prepared as described.[26] For viral transfection, the vector was added to HAEC at 100 pfu/cell for 1 h. HAEC were kept in growth medium for 24 h and then serum-starved for 24 h prior to TNF-α stimulation with or without Sirt1 inhibitor pre-treatment. Cells were stimulated with TNF-α for 30 min. Firefly luciferase activity was determined in cell lysates using a luminometer (Bertholg Technologies, Bad Wildbad, Germany).

2.7 NFκB DNA binding assay and NFκB/p65 immunofluorescence

Adhering HAECs were pre-treated with Sirt1 inhibitors for 1 h, followed by stimulation with 10 ng/mL TNF-α for additional 30 min. Nuclear protein was obtained by using a nuclear extraction kit (Active Motif, Rixensart, Belgium). Cells were harvested in hypotonic buffer for 15 min before centrifugation, isolated nuclei were resuspended in a hypertonic buffer, and nuclear protein was extracted by incubation on a rotator for 30 min. The supernatant containing the nuclear protein was collected after centrifugation. The DNA binding reaction was carried out with 5 μg of nuclear protein in a 96-well plate coated with consensus sequences for NFκB (GGGACTTTCC) for 1 h at room temperature. After washing, NFκB/p65 antibody (Active Motif) was added and incubated for 1 h, followed by incubation with a horseradish peroxidase-conjugated secondary antibody. Finally, NFκB/p65 DNA binding was assessed spectrophotometrically at 450 nm.

HAECs were stained with FITC-labelled mouse anti-NFκB/p65 (Santa Cruz Biotechnology). Cytoplasmic NFκB/p65 was analysed using an SP2 confocal microscope (Leica), and quantification performed with the open-source software CellProfiler.[27] Intensity of the green channel was measured in the cytoplasm (nuclear area subtracted from the total cell area) of at least 150 cells per treatment group at the *Z*-section where the nuclei had their largest diameter.

2.8 NFκB/p65 immunoprecipitation

HAECs were treated with 50 μM SIRT1 or scrambled siRNA overnight, followed by stimulation with TNF-α (10 ng/mL) for 20 min. Cells were then harvested and protein extracted in lysis buffer (20 mM HEPES, pH 7.5, 80 mM NaCl, 2.5 mM $MgCl_2$, 1 mM EDTA, 0.5% NP-40, 1 mM phenylmethylsulfonyl fluoride, 10 μg/mL aprotinin, 10 μg/mL leupeptin, and 100 μM splitomicin). One milligram whole-cell lysates were immunoprecipitated with rabbit anti-NFκB/p65 (Santa Cruz) using Protein G agarose (Millipore, Zug, Switzerland). Immunoprecipitated samples were immunoblotted with rabbit anti-$acLys^{310}$ NFκB/p65 (Abcam, Cambridge, UK), the total lysates (5% input) with rabbit anti-SIRT1 and rabbit anti-NFκB/p65 (both from Santa Cruz Biotechnology).

2.9 Carotid artery thrombosis model and TF activity *in vivo*

The investigation conforms to the *Guide for the Care and Use of Laboratory Animals* published by the US National Institutes of Health (NIH Publication no. 85-23, revised 1996). All animal procedures were approved by the local animal committee (Kantonales Veterinäramt Zurich, Switzerland) and performed in accordance with our institutional guidelines. C57BL/6 mice aged 12–14 weeks weighing on average 27 g were anaesthetized by intraperitoneal injection of 87 mg/kg sodium pentobarbital (Butler, Columbus, OH, USA). Rose Bengal (Fisher Scientific, Fair Lawn, NJ, USA) was diluted to 12 mg/mL in phosphate-buffered saline and then injected into the tail vein at a concentration of 63 mg/kg. Mice were secured in a supine position, placed under a dissecting microscope, and the right common carotid artery was exposed following a midline cervical incision. A Doppler flow probe (Model 0.5 VB, Transonic Systems, Ithaca, NY, USA) was applied and connected to a flowmeter (Transonic, Model T106). Six minutes after Rose Bengal injection, a 1.5 mW green light laser (540 nm; Melles Griot, Carlsbad, CA, USA) was applied to the site of injury at a distance of 6 cm for 60 min or until thrombosis occurred. From the onset of injury, blood flow was monitored up to 120 min, at which time the experiment was terminated.[7] Occlusion was defined as flow ≤0.1 mL/min for at least 1 min. Mice were divided into two groups: splitomicin (80 mg/kg with an intraperitoneal injection every 24 h for 5 days), or vehicle control (0.5% methylcellulose).

Right carotid arteries were homogenized in 50 μL of lysis buffer and left to stand on ice for 30 min. TF activity was measured by using the colorimetric assay as described above.

2.10 Statistical analysis

Data are indicated as mean ± SEM. Unpaired Student's *t*-test was used to evaluate differences between two groups. For statistical analysis of data from multiple groups, one-way ANOVA was performed. A P value <0.05 denoted a significant difference. All statistical values are additionally summarized in the Supplementary material online, *Table S1*.

3. Results

3.1 Sirt1 inhibition enhances TF expression and activity

TF protein expression was determined in TNF-α (5 ng/mL for 5 h) stimulated HAECs in the presence or absence of increasing concentrations of splitomicin (25–200 μmol/L) or sirtinol (15–60 μmol/L), respectively. Both inhibitors enhanced TNF-α-induced TF protein expression in a concentration-dependent manner; maximal activation occurred at 100 μmol/L in splitomicin and at 30 μmol/L in sirtinol-treated cells, respectively ($n = 4$; $P < 0.05$; *Figure 1A* and *C*). These effects were paralleled by an increased TF surface activity in cells pretreated with either Sirt1 inhibitor ($n = 4$; $P < 0.01$, *Figure 1B* and *D*). Sirt1 knockdown using specific siRNA enhanced TNF-α-induced TF protein expression ($n = 4$; $P < 0.01$; *Figure 1E*); western blot analysis confirmed reduced Sirt1 expression in cells transfected with Sirt1 siRNA ($n = 4$; $P < 0.01$; *Figure 1F*). Sirt1 inhibition also enhanced TF protein expression in response to stimulation with histamine (10^{-5} mol/L) or thrombin (1 U/mL), respectively ($n = 4$; $P < 0.05$; *Figure 2A*). The expression of TFPI, the physiological antagonist of TF, remained unaffected ($n = 4$; $P =$ NS; *Figure 2B*). TNF-α did not alter endogenous Sirt1 protein expression ($n = 4$; $P =$ NS; *Figure 2C*), and no changes in cell morphology nor LDH release were detected by any of these treatments ($n = 4$ for each; $P =$ NS; Supplementary material online, *Figure S1*).

3.2 TF mRNA expression is induced by Sirt1 inhibition

Real-time rtPCR revealed that TNF-α (5 ng/mL) induced TF mRNA expression within 1 h ($n = 4$; $P < 0.05$; *Figure 3A*). Both splitomicin and sirtinol enhanced TF mRNA expression in stimulated endothelial cells (splitomicin: $n = 4$; $P < 0.05$; *Figure 3A*, sirtinol: $n = 4$; $P < 0.05$; *Figure 3B*). In parallel, Sirt1 knockdown using siRNA enhanced TNF-α-stimulated TF mRNA expression ($n = 4$; $P < 0.01$; *Figure 3C*).

3.3 Sirt1 inhibition reduces HDAC class III activity

A cell-based HDAC assay was performed in HAECs to confirm that the Sirt1 inhibitor splitomicin diminishes intracellular deacetylase activity. Cells were treated with 1 μmol/L TSA to inactivate HDAC classes I and II in the presence or absence of splitomicin (100 μmol/L). Consistent with inhibition of HDAC class III, splitomicin reduced deacetylase activity ($n = 4$; $P < 0.05$; Supplementary material online, *Figure S2A*) as compared with TSA alone. In contrast, splitomicin did not affect TF protein expression in $Sirt1^{-/-}$ MEFs ($n = 4$; $P =$ NS; Supplementary material online, *Figure S2B*).

3.4 Activation of Sirt1 impairs TF expression and activity

Pharmacological activation of Sirt1 by resveratrol, a commonly used, but less specific Sirt1 activator, impaired TNF-α-induced TF protein and mRNA expression ($n = 4$; $P < 0.01$ for TF protein, and $P < 0.05$ for TF mRNA; Supplementary material online, *Figure S3A* and *B*). In parallel, overexpression of Sirt1 in $Sirt1^{-/-}$ MEFs reduced TNF-α-induced TF expression ($n = 4$; $P < 0.01$; Supplementary material online, *Figure S3C* and *D*).

3.5 Sirt1 inhibition enhances TF promoter activity

To assess whether Sirt1 inhibition enhances TF promoter activity, the impact of splitomicin and sirtinol on the TF promoter was analysed. HAECs were transfected with a luciferase plasmid under control of the human minimal TF promoter (−221 up to +121 bp). Splitomicin and sirtinol enhanced stimulated TF promoter activity as compared with TNF-α alone ($n = 5$; $P < 0.01$; *Figure 4A* and *B*).

3.6 MAP kinase activation is not affected by Sirt1 inhibition

To assess whether modulation of Sirt1 activity alters MAP kinase activation, HAECs were examined at different time points after TNF-α stimulation. The MAP kinases p38, ERK, and JNK were transiently

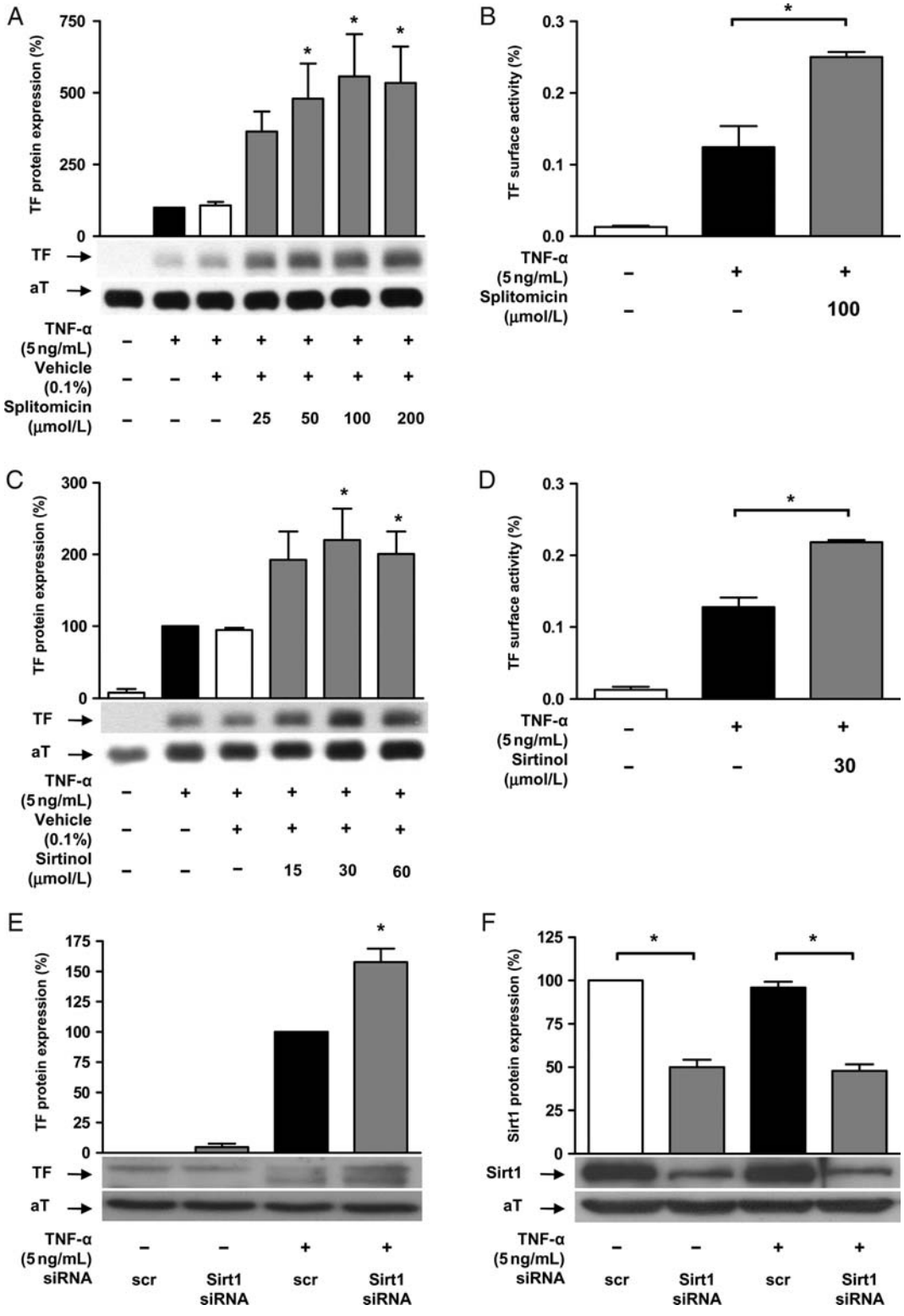

Figure 1 Sirt1 inhibition enhances endothelial TF expression and activity. (*A* and *B*) Splitomicin enhances TNF-α-induced TF protein expression (*$P < 0.05$ vs. TNF-α alone) and surface activity (*$P < 0.01$ vs. TNF-α alone) in human endothelial cells. (*C* and *D*) Sirtinol exerts similar effects on TF protein expression (*$P < 0.05$ vs. TNF-α alone) and activity (*$P < 0.01$ vs. TNF-α alone). (*E* and *F*) Sirt1 siRNA enhances TNF-α-induced TF protein expression (*$P < 0.01$ vs. TNF-α alone).

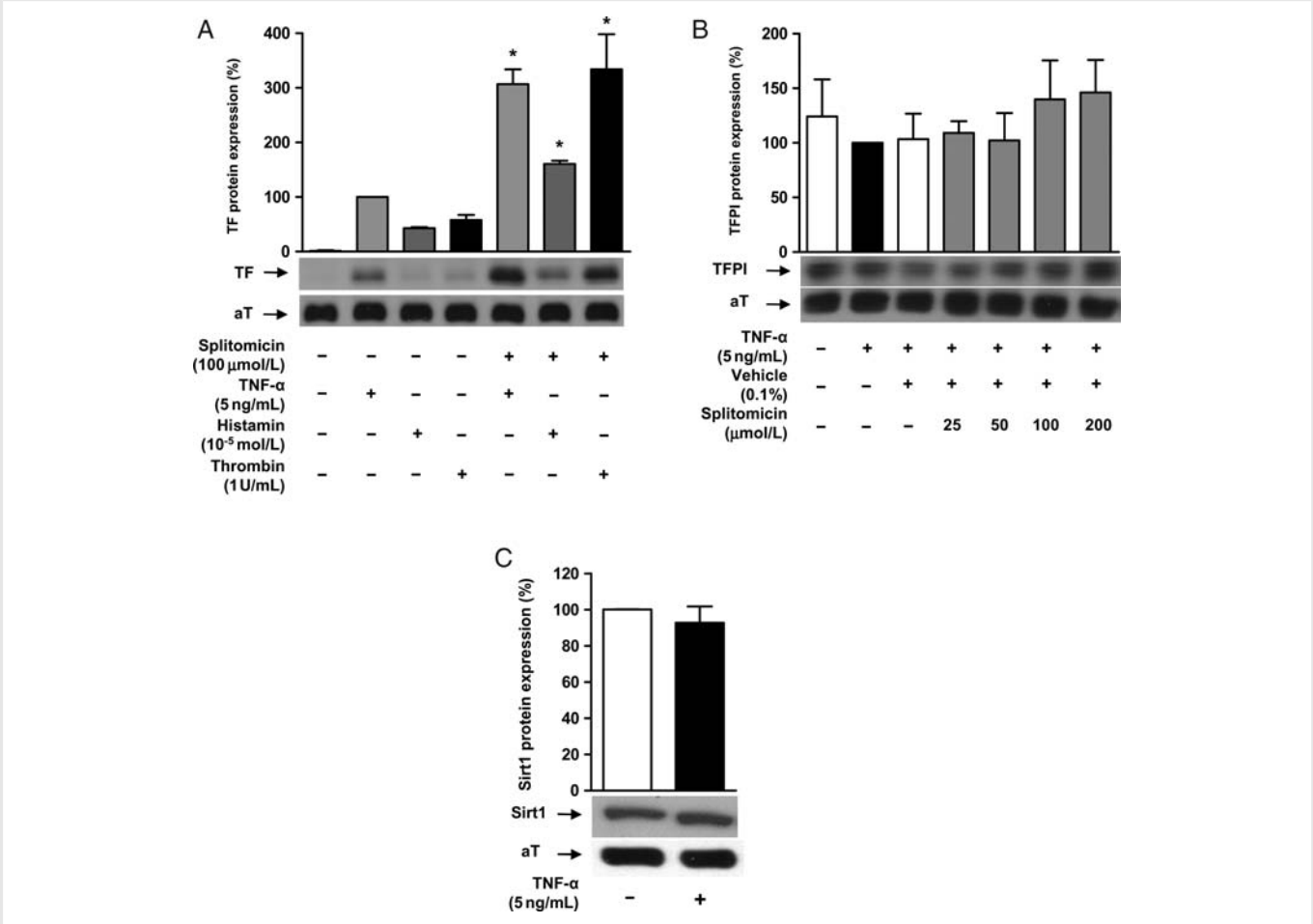

Figure 2 Splitomicin induce TF expression in response to different mediators, but does not alter TFPI expression. TNF-α does not alter Sirt1 expression. (*A*) TNF-α, histamine, and thrombin induce TF protein expression. Splitomicin up-regulates TF expression in response to each stimulus (*$P < 0.05$ vs. each stimulation factor). (*B*) Splitomicin does not alter TFPI expression (P = NS). (*C*) TNF-α stimulation does not change endogenous expression of Sirt1 (P = NS).

activated by TNF-α ($n = 3$; Supplementary material online, *Figures S4 and S5*). Phosphorylation of p38, ERK, and JNK remained unaffected in cells pre-treated with either splitomicin ($n = 3$; P = NS; Supplementary material online, *Figure S4*) or sirtinol, respectively ($n = 3$; P = NS; Supplementary material online, *Figure S5*). Total expression of MAP kinases remained unchanged at any time point with or without Sirt1 inhibitors.

3.7 Sirt1 inhibition enhances NFκB/p65 DNA binding via deacetylation of Lys^{310} of NFκB/p65

NFκB/p65 is a transcription factor that regulates TF expression. Thus, the effect of Sirt1 inhibition on NFκB/p65 activation was investigated. TNF-α (10 ng/mL) induced a significant increase in NFκB/p65 DNA binding as compared with control ($n = 5$; $P < 0.01$; *Figure 5A* and *B*). Sirt1 inhibition with splitomicin (100 µmol/L) or sirtinol (30 µmol/L) enhanced NFκB/p65 DNA binding ($n = 5$; $P < 0.01$; *Figure 5A* and *B*). In line with this, translocation of NFκB/p65 from the cytoplasm to the nucleus was increased after TNF-α stimulation as confirmed by NFκB/p65 immunofluorescence and pre-treatment with splitomicin further enhanced NFκB/p65 nuclear translocation ($n = 5$; $P < 0.01$; Supplementary material online, *Figure S6*).

Since degradation of the inhibitory protein of NFκB, IκB-α, is an early step in activation of NFκB/p65, the effect of Sirt1 inhibition on IκB-α degradation was investigated. TNF-α induced a transient degradation of IκB-α ($n = 3$; Supplementary material online, *Figures S4* and *S5*). Neither splitomicin nor sirtinol altered the degradation pattern of IκB-α as compared with TNF-α alone ($n = 3$; P = NS; Supplementary material online, *Figures S4* and *S5*).

For further analysis, *NFκB/p65*$^{-/-}$ MEFs were used and reconstituted with either wild-type NFκB/p65 or a non-acetylatable Lys^{310}-mutant NFκB/p65. The effect of Sirt1 siRNA on TF expression was less pronounced in MEFs reconstituted with the non-acetylatable Lys^{310}-mutant NFκB/p65 as compared with the wild-type NFκB/p65 ($n = 5$; $P < 0.01$; *Figure 5C*), although both types of reconstituted cells exhibited enhanced TF mRNA expression after TNF-α stimulation when Sirt1 was knocked down by siRNA ($n = 5$; $P < 0.05$; *Figure 5C*). Western blot analysis confirmed reduced Sirt1 expression in all the cells transfected with Sirt1 siRNA ($n = 4$; $P < 0.05$; *Figure 5D*).

Sirt1 was also silenced in HAECs using siRNA. The cells were stimulated with TNF-α (10 ng/mL) and a NFκB/p65

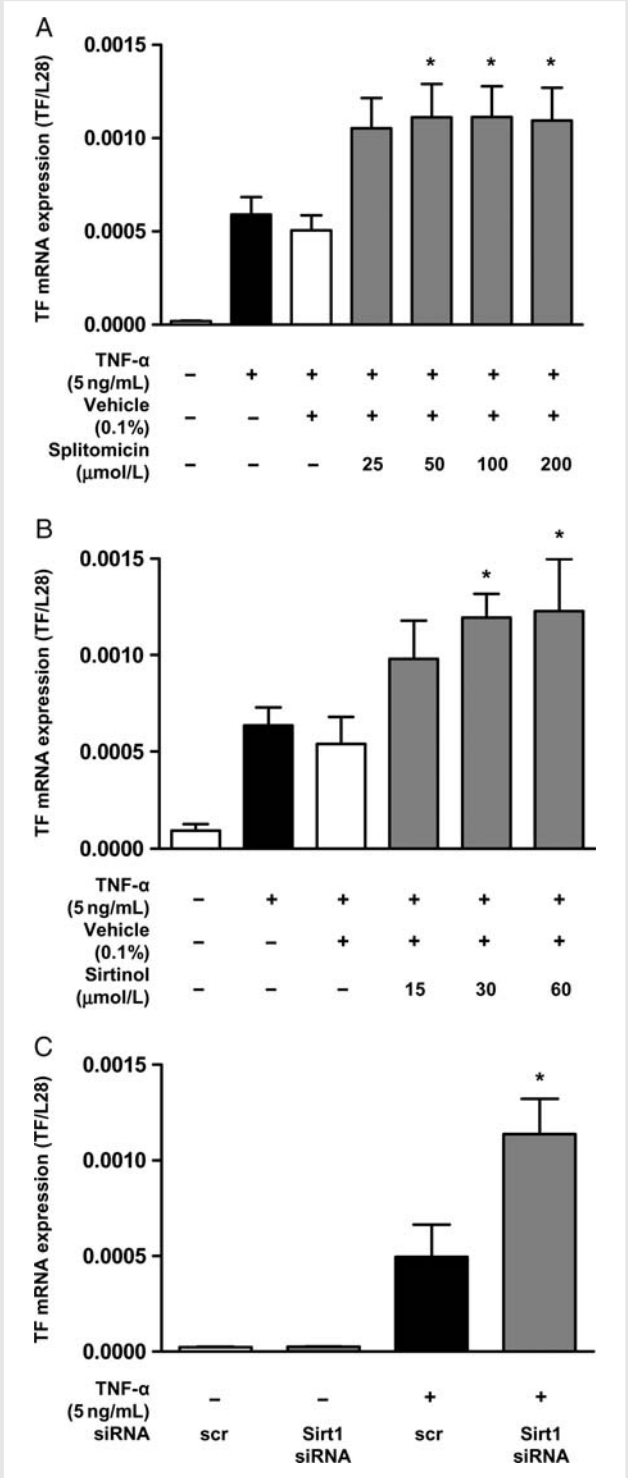

Figure 3 Sirt1 inhibition induces endothelial TF expression at the transcriptional level. (*A* and *B*) Real-time rtPCR reveals that splitomicin and sirtinol enhance TNF-α-induced TF mRNA expression (*$P < 0.05$ vs. TNF-α alone for splitomicin; *$P < 0.05$ vs. TNF-α alone for sirtinol). (*C*) Sirt1 siRNA enhances TNF-α-induced TF mRNA expression (*$P < 0.01$ vs. TNF-α alone).

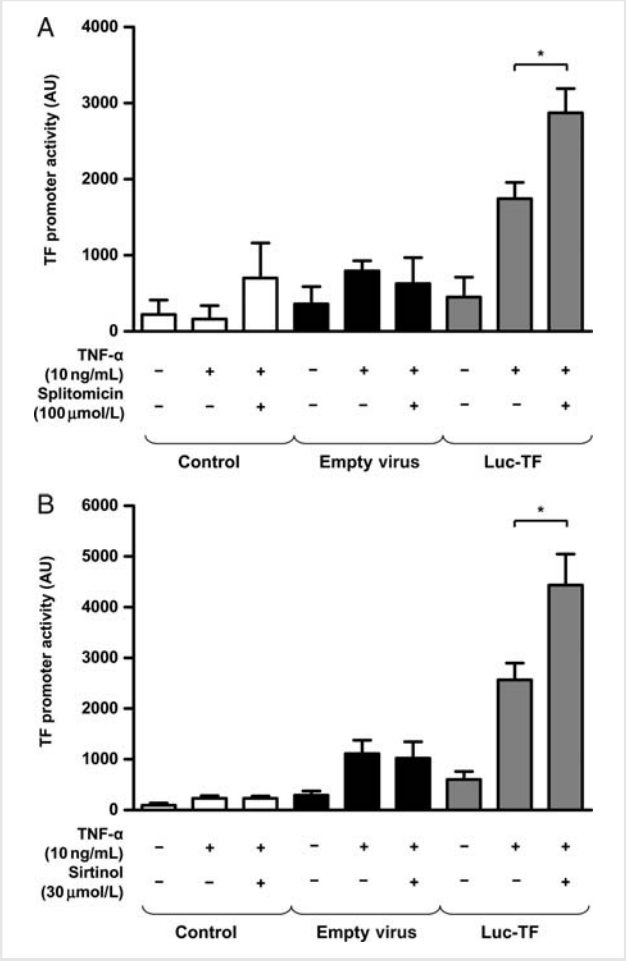

Figure 4 Sirt1 inhibition increases TF promoter activity. (*A* and *B*) TNF-α increases the activity of the minimal TF promoter. Splitomicin (*A*) and sirtinol (*B*) enhance TF promoter activity under cytokine-induced conditions (*$P < 0.01$ vs. TNF-α alone). AU, arbitrary units.

immunoprecipitation was performed. There was a higher extent of Lys^{310} NFκB/p65 acetylation in cells with impaired Sirt1 expression ($n = 3$; *Figure 5E*).

3.8 Sirt1 inhibition induces TF activity and arterial thrombosis *in vivo*

C57Bl/6 mice were treated with splitomicin (80 mg/kg body weight, intraperitoneal injection every 24 h for 5 days) or vehicle (0.5% methylcellulose). Vehicle-treated mice developed carotid artery thrombosis within a mean occlusion time of 57.8. ± 7.5 min, while splitomicin-treated mice occluded within a mean time period of 31.2 ± 5.3 min ($n = 7$; $P < 0.05$; *Figure 6A*). Initial blood flow in carotid artery did not differ between vehicle- and splitomicin-treated mice (0.54 ± 0.05 vs. 0.52 ± 0.05 mL/min; $n = 7$; $P =$ NS; *Figure 6B*). Splitomicin treatment increased TF activity in mouse carotid artery *in vivo* as compared with the controls ($n = 6$; $P < 0.05$; *Figure 6C*).

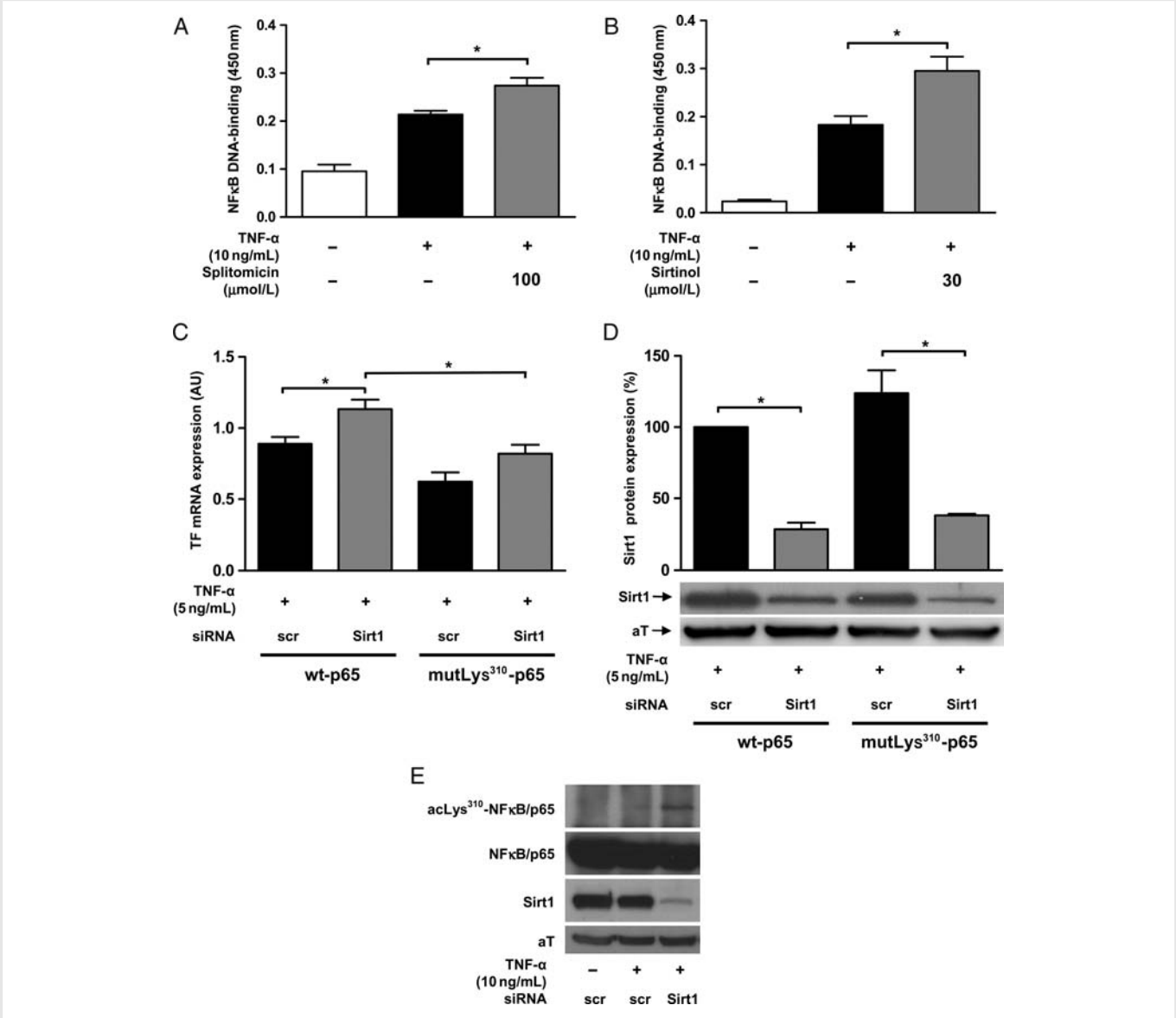

Figure 5 Sirt1 inhibition enhances NFκB/p65 activation via acetylation of Lys^{310} of NFκB/p65. (*A* and *B*) TNF-α stimulates NFκB/p65 DNA binding activity as compared with control conditions. Splitomicin and sirtinol both enhance NFκB/p65 DNA binding (*$P < 0.01$ vs. TNF-α alone). (*C*) Sirt1 siRNA induces TF mRNA up-regulation in the presence of wild-type NFκB/p65, whereas its expression is reduced by a non-acetylatable Lys^{310}-mutant NFκB/p65 (*$P < 0.01$ vs. wild-type NFκB/p65). (*D*) Sirt1 protein down-regulation by specific siRNA is demonstrated. (*E*) NFκB/p65 immunoprecipitation in HAECs reveals more acetylated Lys^{310} NFκB/p65 upon Sirt1 siRNA treatment.

4. Discussion

The present study demonstrates that Sirt1 inhibits TF expression at the transcriptional level via NFκB/p65 in human vascular cells. Furthermore, it shows that inhibition of Sirt1 induces thrombus formation and arterial TF activity *in vivo*.

To inhibit Sirt1 activity in human vascular cells, two different pharmacological agents were applied. Both splitomicin and sirtinol are established inhibitors of Sirt1.[11,28–30] It is still debated to what extent these drugs specifically inhibit Sirt1; indeed, sirtinol may also inhibit Sirt2.[30] Nevertheless, the concentrations of both substances applied in this study are within the established range.[17,19] Moreover, splitomicin did not alter TF expression in *Sirt1*$^{-/-}$ MEFs, and TF was increased when Sirt1 was down-regulated by siRNA. Hence, these data support the conclusion that Sirt1 regulates the expression of TF.

Cytokine-mediated TF expression is mainly regulated at the transcriptional level, where NFκB/p65 is importantly involved.[2] Transcriptionally active NFκB consists of a heterodimeric complex mainly composed of a p65 and a p50 subunit. In quiescent cells, NFκB is retained in the cytoplasm by its inhibitor IκB. Upon cytokine stimulation, IκB becomes degraded allowing NFκB to translocate to the nucleus and to stimulate gene transcription. In this study, both Sirt1 inhibitors enhanced nuclear translocation and DNA binding of NFκB/p65, identifying NFκB/p65 as a downstream target of Sirt1 in the context of TF expression. Since the Sirt1 inhibitors did not affect MAP kinases nor IκB degradation, an involvement of these mediators can be ruled out; thus, a direct effect of Sirt1 on NFκB/p65 seems

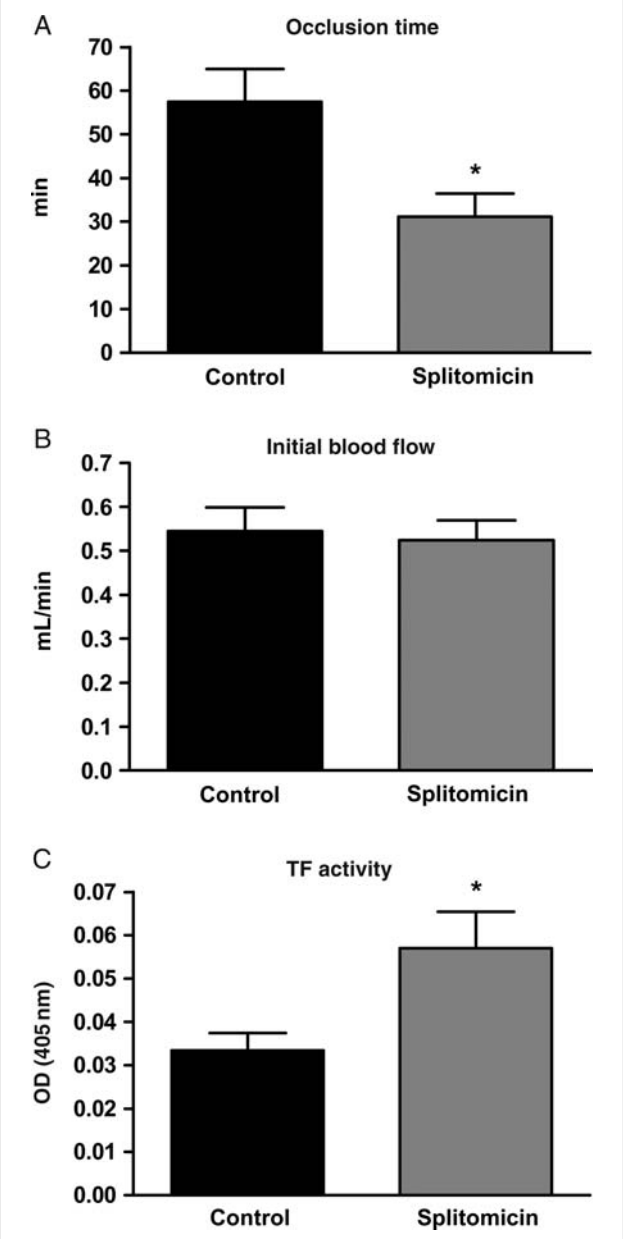

Figure 6 Sirt1 inhibition accelerates arterial thrombus formation. (*A*) Time to thrombotic occlusion after mouse carotid artery photochemical injury *in vivo*. Splitomicin promotes thrombus formation (*$P < 0.05$ vs. vehicle alone). (*B*) Initial blood flow in the carotid artery is unchanged ($P =$ NS). (*C*) Splitomicin increases TF activity in mouse carotid artery *in vivo*. Values are indicated as absorbance at 405 nm (*$P < 0.05$ vs. vehicle).

likely. Acetylation of Lys^{310} and Lys^{221} residues of NFκB/p65 impairs its association with IκB and increases its DNA-binding capacity.[31] Sirt1 deacetylates Lys^{310} of the NFκB/p65 subunit in different cell types and thereby blunts NFκB/p65-mediated gene expression.[17,32] Experiments involving *NFκB/p65*$^{-/-}$ MEFs reconstituted with either wild-type NFκB/p65 or non-acetylatable Lys^{310}-mutant NFκB/p65, respectively, demonstrate that regulation of TF mRNA expression by Sirt1 indeed depends on Lys^{310} acetylation of NFκB/p65. Nevertheless, other downstream targets of Sirt1, such as eNOS or p53, are also known to regulate TF expression,[33,34] and a role of these regulators in Sirt1-mediated TF expression in addition to that of NFκB/p65 cannot be ruled out by the current data.

TF is the key initiator of coagulation and therefore an important trigger of thrombosis.[35] Exposure of TF to the circulating blood results in acute thrombosis and eventually vascular occlusion; in fact, reducing TF expression impairs thrombus formation.[36] To investigate arterial thrombosis *in vivo*, a photochemical vascular injury model was used, since it is an established method to study TF-dependent thrombus formation.[36] Mean occlusion time in splitomicin-treated mice was reduced by nearly 50%, supporting the concept that inhibition of Sirt1 induces arterial thrombosis. The increased TF activity in mouse carotid artery indicates that Sirt1 inhibition regulates thrombosis at least in part via activation of TF *in vivo*. TFPI, the physiological inhibitor of TF, was not affected by splitomicin treatment excluding compensatory effects on TF activity. Given the importance of the balance between TF and TFPI for thrombosis,[37] these findings underscore a role for TF in the modulation of thrombus formation by Sirt1. Hence, Sirt1 activators, which are currently under investigation for the treatment of type 2 diabetes mellitus, may possess additional protective cardiovascular effects by inhibiting arterial thrombus formation.

Sirt1 inhibition resulted in an enhanced TF expression after stimulation with different mediators. Hence, Sirt1 may suppress TF expression especially in the inflammatory environment observed in patients exposed to cardiovascular risk factors and with advanced atherosclerotic lesions.[38] Indeed, elevated levels of soluble TF are observed in patients with atherosclerosis as compared with controls.[39] Furthermore, even higher concentrations are measured in the area around the culprit lesion in patients with unstable angina or acute myocardial infarction as compared with patients with stable angina.[6,40] Taken together, pharmacological or genetic activation of Sirt1 could be a promising therapeutic target in these conditions.

A recent report described that endothelial overexpression of Sirt1 diminishes atherogenesis in *ApoE*-deficient mice, suggesting an anti-atherosclerotic effect of Sirt1.[21] In addition, Sirt1 exerts beneficial effects on cardiovascular risk factors such as type 2 diabetes mellitus and arterial hypertension.[22,41,42] Sirt1 also mediates the effects of caloric restriction on life-span extension,[43] which may in turn improve endothelial function and blood pressure regulation.[44] Since TF expression and activity is increased by cardiovascular risk factors such as type 2 diabetes mellitus[45,46] and arterial hypertension,[47] Sirt1 activators, which are currently under investigation in clinical trials for the treatment of cardiovascular risk factors, could exert a dual beneficial effect preventing arterial thrombosis not only by down-regulating TF expression, but also by interfering with the risk factors inducing it.

In summary, this study demonstrates that Sirt1 inhibition enhances TF *in vitro* as well as *in vivo*, and accelerates arterial thrombus formation. Sirt1 exerts these effects at the transcriptional level by modulating NFκB/p65 DNA binding without affecting MAP kinase activation. These findings reveal a novel action of Sirt1 and suggest that Sirt1 activators may be applied for the prevention of thrombosis.

Acknowledgements

We thank the Center for Microscopy and Image Analysis (University of Zurich, Switzerland) for using their resources.

Conflict of interest: none declared.

Funding

This study was supported by the Swiss National Science Foundation (grant no. 3200B0-113328/1 to F.C.T., grant no. 3100-068118.02/1 to T.F.L., and grant no. 31-114094/1 to C.M.M.; Berne, Switzerland), the Bonizzi-Theler Foundation (Zurich, Switzerland), Velux Foundation (Zurich, Switzerland), Wolfermann Nägeli Foundation (Zurich, Switzerland), MERCATOR Foundation (Essen, Germany), and the Swiss Heart Foundation (Berne, Switzerland).

References

1. Rosamond W, Flegal K, Furie K, Go A, Greenlund K, Haase N *et al.* Heart disease and stroke statistics–2008 update: a report from the American Heart Association Statistics Committee and Stroke Statistics Subcommittee. *Circulation* 2008;**117**:e25–e146.
2. Steffel J, Luscher TF, Tanner FC. Tissue factor in cardiovascular diseases: molecular mechanisms and clinical implications. *Circulation* 2006;**113**:722–731.
3. Tilley R, Mackman N. Tissue factor in hemostasis and thrombosis. *Semin Thromb Hemost* 2006;**32**:5–10.
4. Toschi V, Gallo R, Lettino M, Fallon JT, Gertz SD, Fernandez-Ortiz A *et al.* Tissue factor modulates the thrombogenicity of human atherosclerotic plaques. *Circulation* 1997;**95**:594–599.
5. Wilcox JN, Smith KM, Schwartz SM, Gordon D. Localization of tissue factor in the normal vessel wall and in the atherosclerotic plaque. *Proc Natl Acad Sci USA* 1989;**86**:2839–2843.
6. Ardissino D, Merlini PA, Ariens R, Coppola R, Bramucci E, Mannucci PM. Tissue-factor antigen and activity in human coronary atherosclerotic plaques. *Lancet* 1997;**349**:769–771.
7. Camici GG, Steffel J, Akhmedov A, Schafer N, Baldinger J, Schulz U *et al.* Dimethyl sulfoxide inhibits tissue factor expression, thrombus formation, and vascular smooth muscle cell activation: a potential treatment strategy for drug-eluting stents. *Circulation* 2006;**114**:1512–1521.
8. Steffel J, Akhmedov A, Greutert H, Luscher TF, Tanner FC. Histamine induces tissue factor expression: implications for acute coronary syndromes. *Circulation* 2005;**112**:341–349.
9. Steffel J, Arnet C, Akhmedov A, Iseli SM, Luscher TF, Tanner FC. Histamine differentially interacts with tumor necrosis factor-alpha and thrombin in endothelial tissue factor induction: the role of c-Jun NH_2-terminal kinase. *J Thromb Haemost* 2006;**4**:2452–2460.
10. Gasser SM, Cockell MM. The molecular biology of the SIR proteins. *Gene* 2001;**279**:1–16.
11. Lavu S, Boss O, Elliott PJ, Lambert PD. Sirtuins–novel therapeutic targets to treat age-associated diseases. *Nat Rev Drug Discov* 2008;**7**:841–853.
12. Imai S, Armstrong CM, Kaeberlein M, Guarente L. Transcriptional silencing and longevity protein Sir2 is an NAD-dependent histone deacetylase. *Nature* 2000;**403**:795–800.
13. Motta MC, Divecha N, Lemieux M, Kamel C, Chen D, Gu W *et al.* Mammalian SIRT1 represses forkhead transcription factors. *Cell* 2004;**116**:551–563.
14. Luo J, Nikolaev AY, Imai S, Chen D, Su F, Shiloh A *et al.* Negative control of p53 by Sir2alpha promotes cell survival under stress. *Cell* 2001;**107**:137–148.
15. Picard F, Kurtev M, Chung N, Topark-Ngarm A, Senawong T, Machado De Oliveira R *et al.* Sirt1 promotes fat mobilization in white adipocytes by repressing PPAR-gamma. *Nature* 2004;**429**:771–776.
16. Mattagajasingh I, Kim CS, Naqvi A, Yamamori T, Hoffman TA, Jung SB *et al.* SIRT1 promotes endothelium-dependent vascular relaxation by activating endothelial nitric oxide synthase. *Proc Natl Acad Sci USA* 2007;**104**:14855–14860.
17. Yeung F, Hoberg JE, Ramsey CS, Keller MD, Jones DR, Frye RA *et al.* Modulation of NF-kappaB-dependent transcription and cell survival by the SIRT1 deacetylase. *EMBO J* 2004;**23**:2369–2380.
18. Alcendor RR, Gao S, Zhai P, Zablocki D, Holle E, Yu X *et al.* Sirt1 regulates aging and resistance to oxidative stress in the heart. *Circ Res* 2007;**100**:1512–1521.
19. Ota H, Akishita M, Eto M, Iijima K, Kaneki M, Ouchi Y. Sirt1 modulates premature senescence-like phenotype in human endothelial cells. *J Mol Cell Cardiol* 2007;**43**:571–579.
20. Lagouge M, Argmann C, Gerhart-Hines Z, Meziane H, Lerin C, Daussin F *et al.* Resveratrol improves mitochondrial function and protects against metabolic disease by activating SIRT1 and PGC-1alpha. *Cell* 2006;**127**:1109–1122.
21. Zhang QJ, Wang Z, Chen HZ, Zhou S, Zheng W, Liu G *et al.* Endothelium-specific overexpression of class III deacetylase SIRT1 decreases atherosclerosis in apolipoprotein E-deficient mice. *Cardiovasc Res* 2008;**80**:191–199.
22. Milne JC, Lambert PD, Schenk S, Carney DP, Smith JJ, Gagne DJ *et al.* Small molecule activators of SIRT1 as therapeutics for the treatment of type 2 diabetes. *Nature* 2007;**450**:712–716.
23. Breitenstein A, Stampfli SF, Camici GG, Akhmedov A, Ha HR, Follath F *et al.* Amiodarone inhibits arterial thrombus formation and tissue factor translation. *Arterioscler Thromb Vasc Biol* 2008;**28**:2231–2238.
24. Buerki C, Rothgiesser KM, Valovka T, Owen HR, Rehrauer H, Fey M *et al.* Functional relevance of novel p300-mediated lysine 314 and 315 acetylation of RelA/p65. *Nucleic Acids Res* 2008;**36**:1665–1680.
25. Stein S, Schafer N, Breitenstein A, Besler C, Winnik S, Lohmann C *et al.* SIRT1 reduces endothelial activation without affecting vascular function in ApoE-/-mice. *Aging (Albany NY)* 2010;**2**:353–360.
26. Holy EW, Akhmedov A, Luscher TF, Tanner FC. Berberine, a natural lipid-lowering drug, exerts prothrombotic effects on vascular cells. *J Mol Cell Cardiol* 2009;**46**:234–240.
27. Carpenter AE, Jones TR, Lamprecht MR, Clarke C, Kang IH, Friman O *et al.* CellProfiler: image analysis software for identifying and quantifying cell phenotypes. *Genome Biol* 2006;**7**:R100.
28. Araki T, Sasaki Y, Milbrandt J. Increased nuclear NAD biosynthesis and SIRT1 activation prevent axonal degeneration. *Science* 2004;**305**:1010–1013.
29. Fulco M, Schiltz RL, Iezzi S, King MT, Zhao P, Kashiwaya Y *et al.* Sir2 regulates skeletal muscle differentiation as a potential sensor of the redox state. *Mol Cell* 2003;**12**:51–62.
30. Grubisha O, Smith BC, Denu JM. Small molecule regulation of Sir2 protein deacetylases. *FEBS J* 2005;**272**:4607–4616.
31. Chen LF, Greene WC. Shaping the nuclear action of NF-kappaB. *Nat Rev Mol Cell Biol* 2004;**5**:392–401.
32. Chen J, Zhou Y, Mueller-Steiner S, Chen LF, Kwon H, Yi S *et al.* SIRT1 protects against microglia-dependent amyloid-beta toxicity through inhibiting NF-kappaB signaling. *J Biol Chem* 2005;**280**:40364–40374.
33. Yang Y, Loscalzo J. Regulation of tissue factor expression in human microvascular endothelial cells by nitric oxide. *Circulation* 2000;**101**:2144–2148.
34. Yu JL, May L, Lhotak V, Shahrzad S, Shirasawa S, Weitz JI *et al.* Oncogenic events regulate tissue factor expression in colorectal cancer cells: implications for tumor progression and angiogenesis. *Blood* 2005;**105**:1734–1741.
35. Nemerson Y. Tissue factor and hemostasis. *Blood* 1988;**71**:1–8.
36. Day SM, Reeve JL, Pedersen B, Farris DM, Myers DD, Im M *et al.* Macrovascular thrombosis is driven by tissue factor derived primarily from the blood vessel wall. *Blood* 2005;**105**:192–198.
37. Pedersen B, Holscher T, Sato Y, Pawlinski R, Mackman N. A balance between tissue factor and tissue factor pathway inhibitor is required for embryonic development and hemostasis in adult mice. *Blood* 2005;**105**:2777–2782.
38. Libby P, Ridker PM, Maseri A. Inflammation and atherosclerosis. *Circulation* 2002;**105**:1135–1143.
39. Reilly MP, Rohatgi A, McMahon K, Wolfe ML, Pinto SC, Rhodes T *et al.* Plasma cytokines, metabolic syndrome, and atherosclerosis in humans. *J Investig Med* 2007;**55**:26–35.
40. Annex BH, Denning SM, Channon KM, Sketch MH Jr., Stack RS, Morrissey JH *et al.* Differential expression of tissue factor protein in directional atherectomy specimens from patients with stable and unstable coronary syndromes. *Circulation* 1995;**91**:619–622.
41. Banks AS, Kon N, Knight C, Matsumoto M, Gutierrez-Juarez R, Rossetti L *et al.* SirT1 gain of function increases energy efficiency and prevents diabetes in mice. *Cell Metab* 2008;**8**:333–341.
42. Lee JH, Song MY, Song EK, Kim EK, Sung Moon W, Han MK *et al.* Overexpression of SIRT1 protects pancreatic {beta}-cells against cytokine toxicity through suppressing NF-{kappa}B signaling pathway. *Diabetes* 2009;**58**:344–351.
43. Guarente L, Picard F. Calorie restriction–the SIR2 connection. *Cell* 2005;**120**:473–482.
44. Fontana L, Klein S. Aging, adiposity, and calorie restriction. *JAMA* 2007;**297**:986–994.
45. Diamant M, Nieuwland R, Pablo RF, Sturk A, Smit JW, Radder JK. Elevated numbers of tissue-factor exposing microparticles correlate with components of the metabolic syndrome in uncomplicated type 2 diabetes mellitus. *Circulation* 2002;**106**:2442–2447.
46. Lim HS, Blann AD, Lip GY. Soluble CD40 ligand, soluble P-selectin, interleukin-6, and tissue factor in diabetes mellitus: relationships to cardiovascular disease and risk factor intervention. *Circulation* 2004;**109**:2524–2528.
47. Felmeden DC, Spencer CG, Chung NA, Belgore FM, Blann AD, Beevers DG *et al.* Relation of thrombogenesis in systemic hypertension to angiogenesis and endothelial damage/dysfunction (a substudy of the Anglo-Scandinavian Cardiac Outcomes Trial [ASCOT]). *Am J Cardiol* 2003;**92**:400–405.

Supplementary Material

Figure legends

Supplemental figure 1: Sirt1 inhibitors are not cytotoxic

LDH assay confirms that splitomicin (**A**) and sirtinol (**B**) do not induce cell death (*P*=NS for all concentrations).

Supplemental figure 2: Splitomicin is Sirt1 specific

A. Splitomicin on top of trichostatin A (TSA) reduces HDAC activity in endothelial cells (**P*<0.05 vs TSA alone). AFU: Arbitrary fluorescent units. **B.** Splitomicin does not affect TF protein expression in *Sirt1*$^{-/-}$ MEFs (*P*=NS vs control).

Supplemental figure 3: Sirt1 activation inhibits TF protein and mRNA expression

A and B. Resveratrol decreases TNF-α induced TF mRNA expression (**P*<0.05) and TF protein expression (**P*<0.01). **C.** Sirt1 overexpression in *Sirt1*$^{-/-}$ MEFs decreases cytokine induced TF mRNA expression (**P*<0.01).

Supplemental figure 4: Splitomicin treatment does not alter MAP kinase activation nor IκB-α degradation

TNF-α induces a transient phosphorylation of the MAP kinases p38, JNK, and ERK. Splitomicin does not affect phosphorylation (*P*=NS vs TNF-α alone for each time point) nor TNF-α induced transient IκB-α degradation (*P*=NS vs TNF-α alone for each time point).

Supplemental figure 5: Sirtinol treatment does not alter MAP kinase activation nor IκB-α degradation

TNF-α induces a transient phosphorylation of the MAP kinases p38, JNK, and ERK. Sirtinol does not affect phosphorylation (*P*=NS vs TNF-α alone for each time point) nor TNF-α induced transient IκB-α degradation (*P*=NS vs TNF-α alone for each time point).

Supplemental figure 6: Sirt1 inhibition enhances NFκB/p65 translocation

Immunofluorescence staining for p65 reveals increased nuclear translocation of NFκB/p65 after splitomicin treatment (*P*<0.01).

Supplemental Figure 1

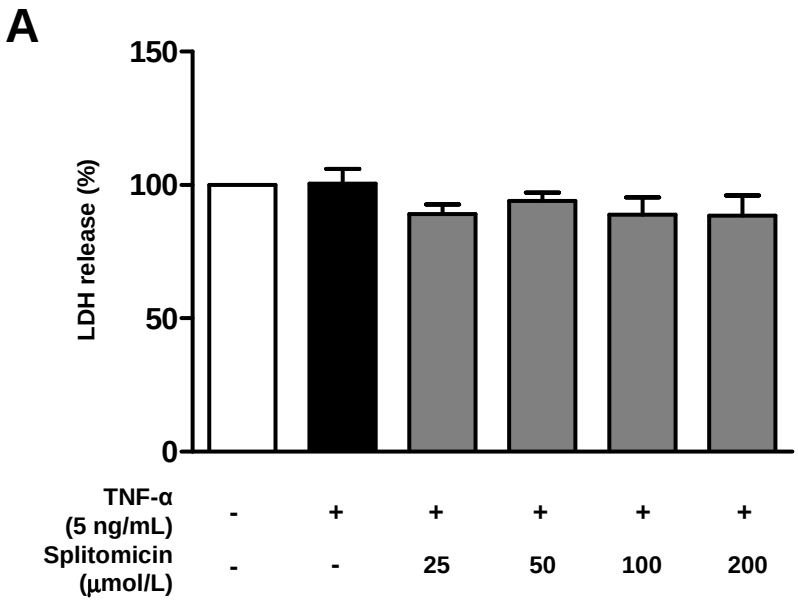

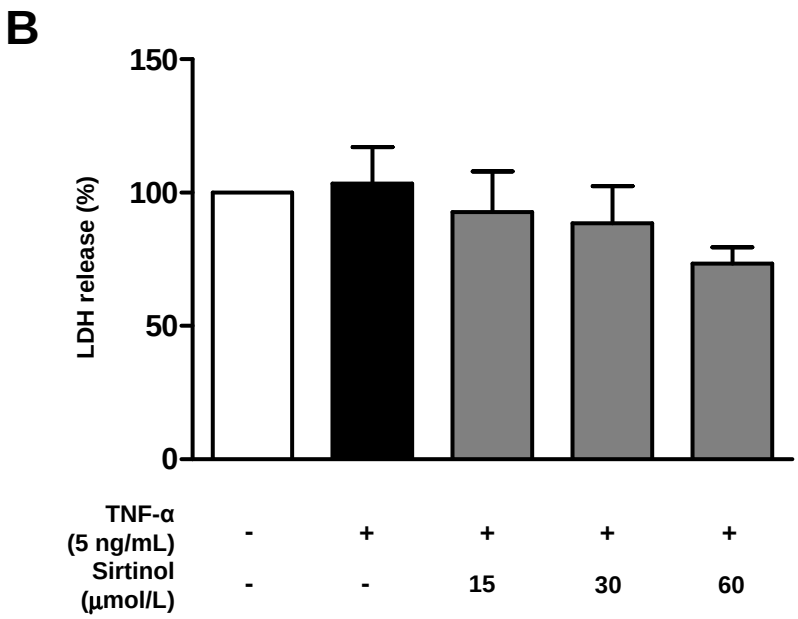

Supplemental Figure 2

A

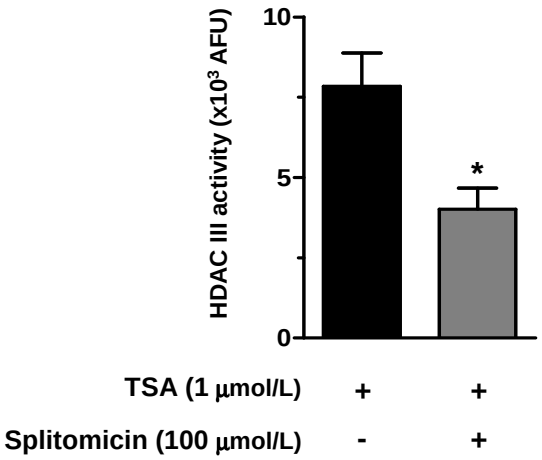

B

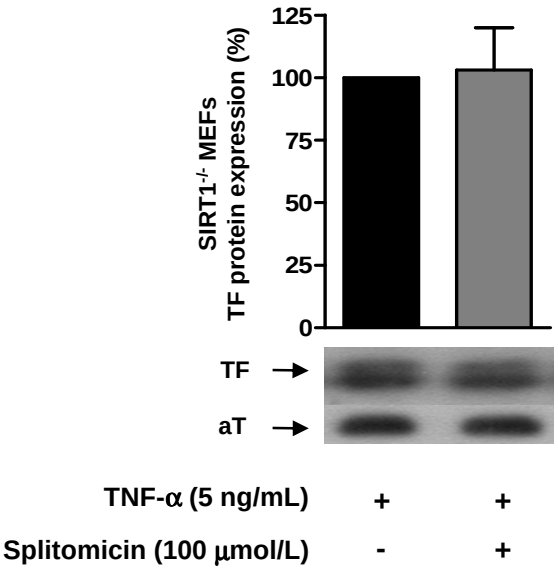

Supplemental Figure 3

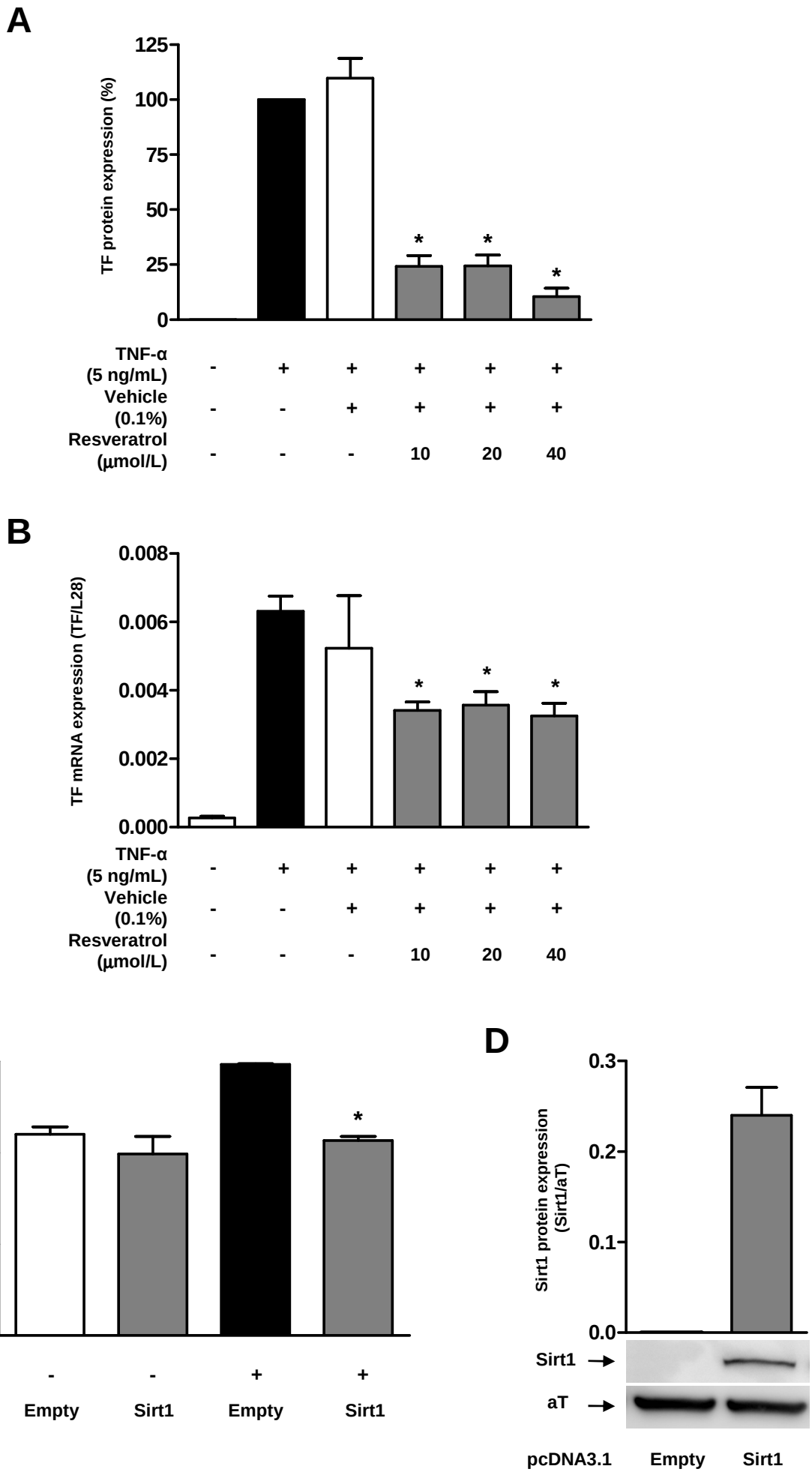

Supplemental Figure 4

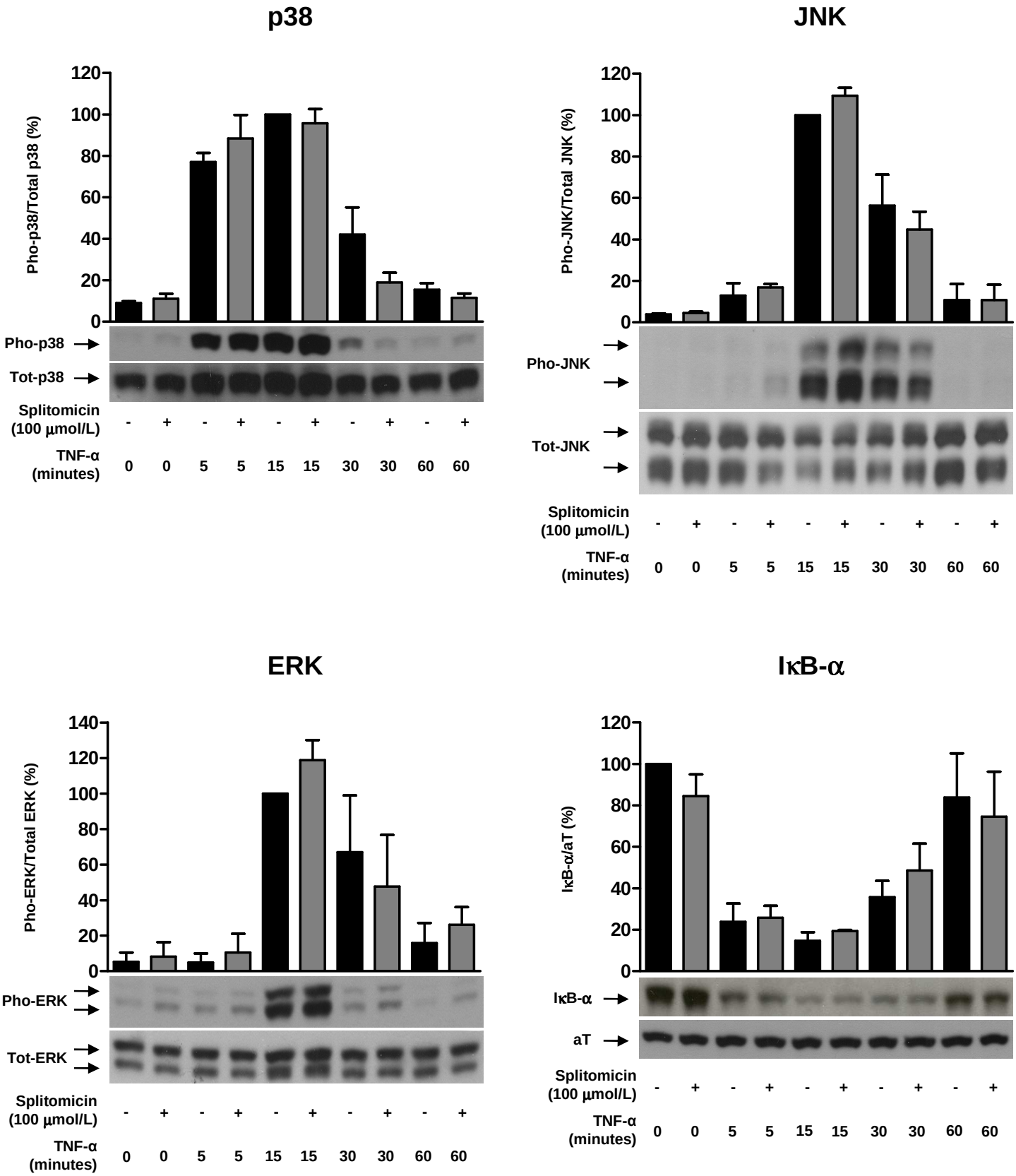

Supplemental Figure 5

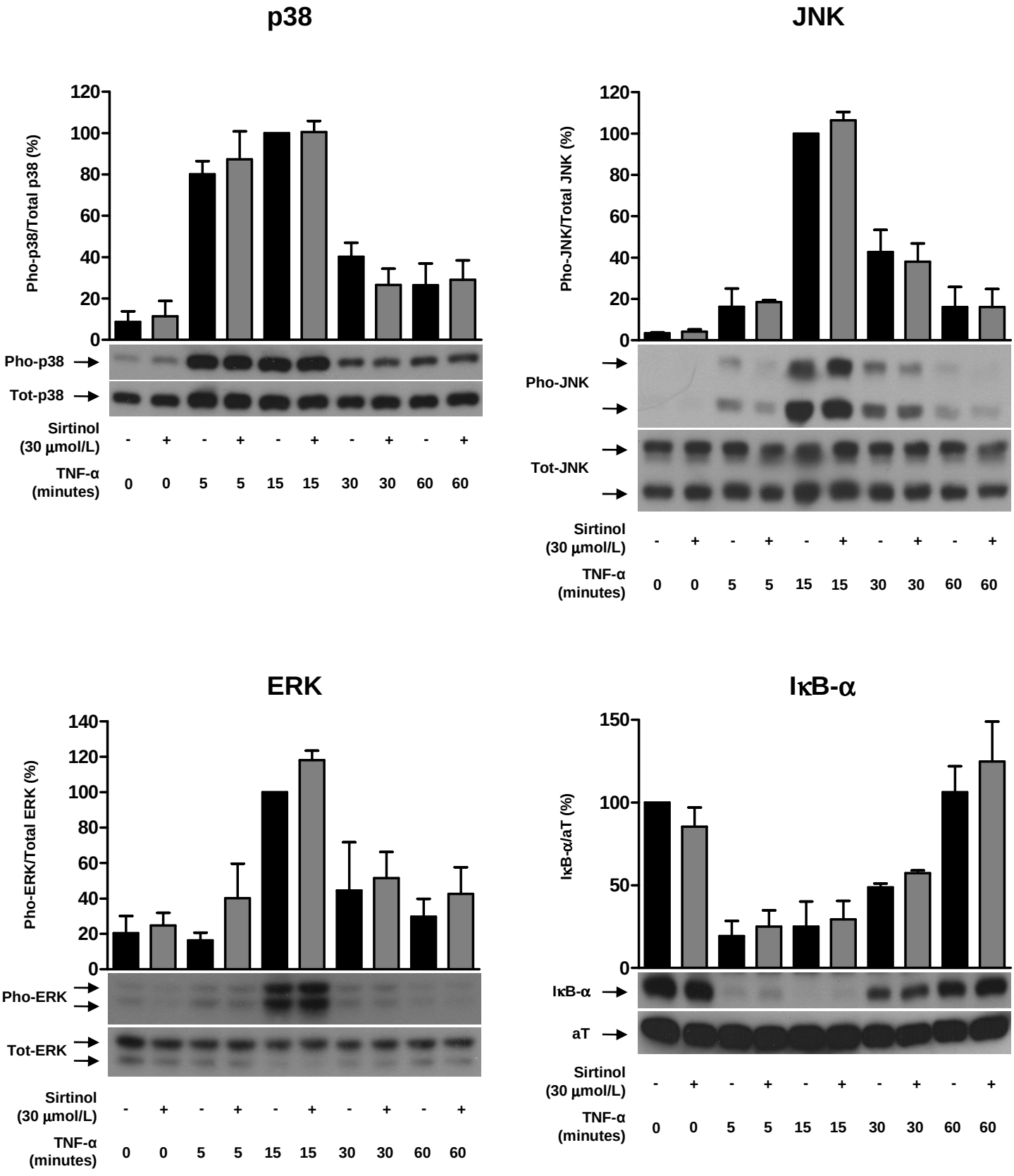

Supplemental Figure 6

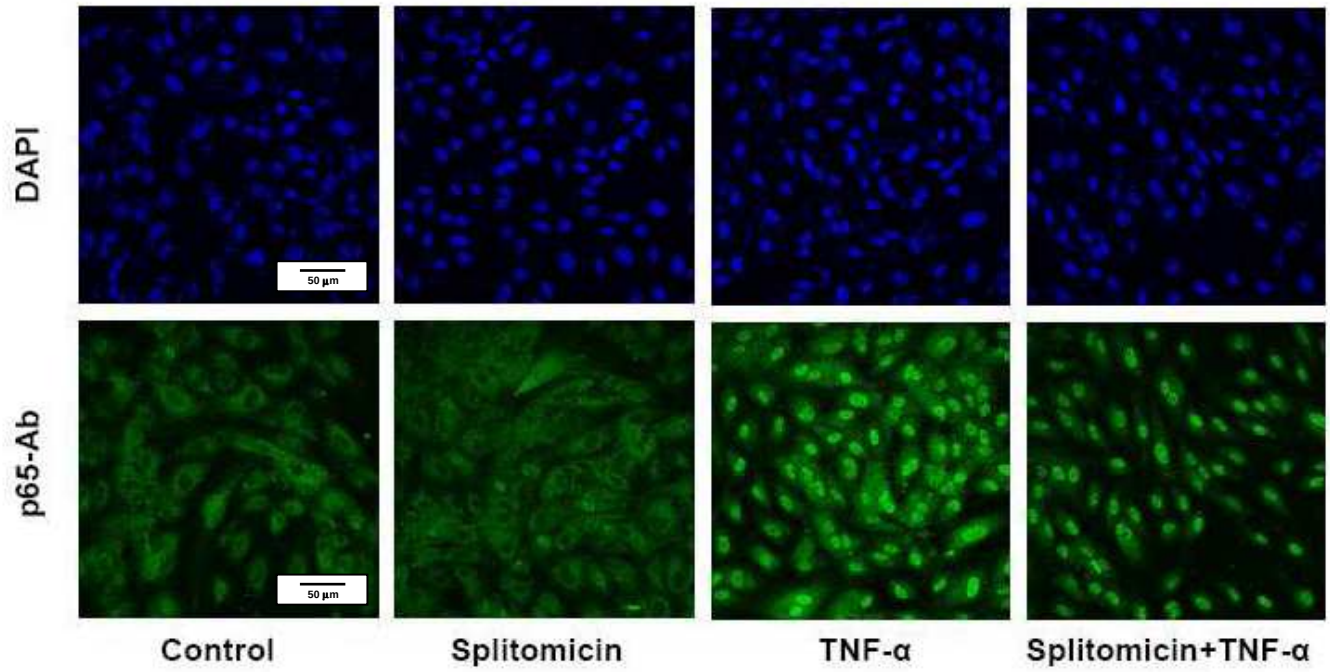

Figure 1A: TF protein expression in splitomicin-treated cells

	Control	TNF-a	DMSO+TNF-a	Splito (25uM)+TNF-a	Splito (50uM)+TNF-a	Splito (100uM)+TNF-a	Splito (200uM)+TNF-a
Mean	0.03	100.00	107.80	365.60	479.60	557.40	534.40
Std. Deviation	0.049	0.00	23.80	138.30	244.60	293.90	254.90
P-value vs TNF-a	<0.05	-	NS	NS	<0.05	<0.01	<0.01
Statistical test	One-way ANOVA						

Figure 1B: TF activity in splitomicin-treated cells

	Control	TNF-a	Splito+TNF-a
Mean	0.0129	0.1243	0.2502
Std. Deviation	0.0039	0.0585	0.0139
P-value vs TNF-a	<0.01	-	<0.01
Statistical test	One-way ANOVA		

Figure 1C: TF protein expression in sirtinol-treated cells

	Control	TNF-a	DMSO+TNF-a	Sirti (15uM)+TNF-a	Sirti (30uM)+TNF-a	Sirti (60uM)+TNF-a
Mean	6.55	100.00	89.03	171.10	201.00	194.00
Std. Deviation	9.14	0.00	13.40	83.47	86.84	56.06
P-value vs TNF-a	<0.05	-	NS	NS	<0.05	<0.05
Statistical test	One-way ANOVA					

Figure 1D: TF activity in sirtinol-treated cells

	Control	TNF-a	Sirti+TNF-a
Mean	0.0130	0.1278	0.2184
Std. Deviation	0.0089	0.0264	0.0052
P-value vs TNF-a	<0.01	-	<0.01
Statistical test	One-way ANOVA		

Figure 1E: TF protein expression in Sirt1 siRNA-treated cells

	Scr	Sirt1 siRNA	Scr+TNF-a	Sirt1 siRNA+TNF-a
Mean	0.01	4.67	100.00	157.70
Std. Deviation	0.01	5.02	0.00	22.31
P-value vs scr+TNF-a	<0.01	<0.01	-	<0.01
Statistical test	One-way ANOVA			

Figure 1F: Sirt1 downregulation by siRNA

	Scr	Sirt1 siRNA	Scr+TNF-a	Sirt1 siRNA+TNF-a
Mean	100.00	56.67	95.92	53.83
Std. Deviation	0.00	10.08	7.71	9.08
P-value vs scr	-	<0.01	-	-
P-value vs scr+TNF-a	-	-	-	<0.01
Statistical test	One-way ANOVA			

Figure 2A: TF protein expression by different stimulations in splitomicin-treated cells

	Control	TNF-a	Hist	Thr	Splito+TNF-a	Splito+Hist	Splito+Thr
Mean	1.343	100.00	43.24	57.88	307.00	161.00	334.10
Std. Deviation	2.685	0.00	3.44	19.48	54.73	10.92	129.10
P-value vs TNF-a	-	-	-	-	<0.01	-	-
P-value vs Hist	-	-	-	-	-	<0.05	-
P-value vs Thr	-	-	-	-	-	-	<0.01
Statistical test	One-way ANOVA						

Figure 2B: TFPI protein expression in splitomicin-treated cells

	Control	TNF-a	DMSO+TNF-a	Splito (25uM)+TNF-a	Splito (50uM)+TNF-a	Splito (100uM)+TNF-a	Splito (200uM)+TNF-a
Mean	124.30	100.00	103.50	109.20	102.20	139.80	146.30
Std. Deviation	68.04	0.00	46.47	21.37	50.43	71.44	59.58
P-value vs TNF-a	NS	-	NS	NS	NS	NS	NS
Statistical test	One-way ANOVA						

Figure 2C: Endogenous Sirt1 expression

	Control	TNF-a
Mean	100.00	92.75
Std. Deviation	0.00	18.03
P-value vs control	-	NS
Statistical test	T-test	

Figure 3A: TF mRNA expression in splitomicin-treated cells

	Control	TNFa	DMSO+TNF-a	Splito (25uM)+TNF-a	Splito (50uM)+TNF-a	Splito (100uM)+TNF-a	Splito (200uM)+TNF-a
Mean	0.0000200	0.0005905	0.0005058	0.0010530	0.0011120	0.0011130	0.0010950
Std. Deviation	0.0000044	0.0001872	0.0001612	0.0003250	0.0003573	0.0003300	0.0003522
P-value vs TNF-a	<0.05	-	NS	NS	<0.05	<0.05	<0.05
Statistical test	One-way ANOVA						

Figure 3B: TF mRNA expression in sirtinol-treated cells

	Control	TNF-a	DMSO+TNF-a	Sirti (15uM)+TNF-a	Sirti (30uM)+TNF-a	Sirti (60uM)+TNF-a
Mean	0.0000940	0.0006356	0.0005390	0.0009813	0.0011940	0.0012280
Std. Deviation	0.0000647	0.0001872	0.0002795	0.0003944	0.0002461	0.0005392
P-value vs TNF-a	<0.05	-	NS	NS	<0.05	<0.05
Statistical test	One-way ANOVA					

Figure 3C: TF mRA expression in Sirt1 siRNA-treated cells

	Scr	Sirt1 siRNA	Scr+TNF-a	Sirt1 siRNA+TNF-a
Mean	0.0000230	0.0000250	0.0004957	0.0011370
Std. Deviation	0.0000078	0.0000056	0.0003381	0.0004513
P-value vs scr+TNF-a	<0.05	<0.05	-	<0.01
Statistical test	One-way ANOVA			

Figure 4A: TF promoter activity in splitomicin-treated cells

	Control	Control+TNF-a	Control+TNF-a+splito	EV	EV+TNF-a	EV+TNF-a+splito	AD	AD+TNF-a	AD+TNF-a+splito
Mean	220.00	160.00	702.50	362.50	795.00	626.70	452.50	1601.00	2871.00
Std. Deviation	382.60	358.20	918.70	449.30	264.30	594.10	521.20	329.10	559.20
P-value vs AD+TNF-a	<0.01	<0.01	NS	<0.01	NS	NS	<0.05	-	<0.01
Statistical test	One-way ANOVA								

Figure 4b: TF promoter activity in sirtinol-treated cells

	Control	Control+TNF-a	Control+TNF-a+sirti	EV	EV+TNF-a	EV+TNF-a+sirti	AD	AD+TNF-a	AD+TNF-a+sirti
Mean	92.00	230.00	234.00	294.00	1112.00	1020.00	602.00	2565.00	4438.00
Std. Deviation	102.60	121.40	100.10	189.00	595.00	735.70	359.80	741.70	1363.00
P-value vs AD+TNF-a	<0.01	<0.01	<0.01	<0.01	<0.01	<0.01	<0.01	-	<0.01
Statistical test	One-way ANOVA								

Figure 5A: NFkB-DNA-binding in splitomicin-treated cells

	Control	TNF-a	Splito+TNFa
Mean	0.0953	0.2134	0.2741
Std. Deviation	0.0278	0.0160	0.0319
P-value vs TNF-a	<0.01	-	<0.01
Statistical test	One-way ANOVA		

Figure 5B: NFkB-DNA-binding in sirtinol-treated cells

	Control	TNF-a	Sirti+TNFa
Mean	0.0239	0.1830	0.2951
Std. Deviation	0.0063	0.0364	0.0593
P-value vs TNF-a	<0.01	-	<0.01
Statistical test	One-way ANOVA		

Figure 5C: Fibroblast TF mRNA expression in Sirt1 siRNA-treated cells

	Scr+TNF-a; wt-p65	Sirt1+TNF-a; wt-p65	Scr+TNF-a; mut-p65	Sirt1+TNF-a; mut-p65
Mean	0.8880	1.1330	0.6215	0.8195
Std. Deviation	0.1199	0.1470	0.1160	0.1400
P-value vs Sirt1 siRNA+TNF-a; wt	<0.05	-	<0.01	<0.01
Statistical test	One-way ANOVA			

Figure 5D: Sirt1 downreglation in MEFs

	Scr+TNF-a; wt-p65	Sirt1+TNF-a; wt-p65	Scr+TNF-a; mut-p65	Sirt1+TNF-a; mut-p65
Mean	100.00	28.86	123.80	38.00
Std. Deviation	0.00	5.93	22.77	1.76
P-value vs scr+TNF-a; wt-p65	-	<0.05	-	-
P-value vs scr+TNF-a; mut-p65	-	-	-	<0.05
Statistical test	One-way ANOVA			

Figure 6A: Time to occlusion

	Vehicle	Splitomicin
Mean	57.8	31.2
Std. Deviation	7.5	5.3
P-value vs vehicle	-	<0.05
Statistical test	T-test	

Figure 6B: Initial blood flow

	Vehicle	Splitomicin
Mean	0.54	0.52
Std. Deviation	0.05	0.05
P-value vs vehicle	-	NS
Statistical test	T-test	

Figure 6C: TF activity

	Vehicle	Splitomicin
Mean	0.03343	0.05701
Std. Deviation	0.00907	0.02061
P-value vs vehicle	-	<0.05
Statistical test	T-test	

Supplemental figure 1A: LDH release in splitomicin-treated cells

	Control	TNF-a (5ng/ml)	Splito (25uM)+TNF-a	Splito (50uM)+TNF-a	Splito (100uM)+TNF-a	Splito (200uM)+TNF-a
Mean	100.00	100.60	89.11	94.00	88.90	88.52
Std. Deviation	0.00	9.35	6.11	5.58	11.07	13.01
P-value vs Control	-	NS	NS	NS	NS	NS
Statistical test	One-way ANOVA					

Supplemental figure 1B: LDH release in sirtinol-treated cells

	Control	TNF-a	Sirti (15uM)+TNF-a	Sirti (30uM)+TNF-a	Sirti (60uM)+TNF-a
Mean	100.00	103.40	88.57	73.47	88.18
Std. Deviation	0.00	23.57	24.10	10.62	10.40
P-value vs Control	-	NS	NS	NS	NS
Statistical test	One-way ANOVA				

Supplemental figure 2A: HDACIII activity

	TSA	TSA+splito
Mean	7841	4026
Std. Deviation	1032	651.8
P-value vs TSA	-	<0.05
Statistical test	T-test	

Supplemental figure 2B: TF protein expression in splitomicin-treated MEFs

	TNF-a	Splito+TNF-a
Mean	100.00	103.10
Std. Deviation	0.00	16.87
P-value vs TNF-a	-	NS
Statistical test	T-test	

Supplemental figure 3A: TF protein expression in resveratrol-treated HAECs

	Control	TNF-a	DMSO+TNF-a	Resv (10uM)+TNF-a	Resv (20uM)+TNF-a	Resv (40uM)+TNF-a
Mean	0.00	100.00	109.70	24.22	24.38	10.42
Std. Deviation	0.00	0.00	18.21	9.71	9.82	7.79
P-value vs TNF-a	<0.01	-	NS	<0.01	<0.01	<0.01
Statistical test	One-way ANOVA					

Supplemental figure 3B: TF mRNA expression in resveratrol-treated HAECs

	Control	TNF-a	DMSO+TNF-a	Resv (10uM)+TNF-a	Resv (20uM)+TNF-a	Resv (40uM)+TNF-a
Mean	0.0002733	0.0063100	0.0052330	0.0034130	0.0035680	0.0032530
Std. Deviation	0.0000856	0.0008782	0.0030610	0.0004893	0.0007942	0.0007421
P-value vs TNF-a	<0.01	-	NS	<0.05	<0.05	<0.05
Statistical test	One-way ANOVA					

Supplemental figure 3C: Sirt1-overexpression inhibits TF expression

	Control	Sirt1	TNF-a	Sirt1+TNF-a
Mean	0.0550600	0.0496500	0.0741500	0.0533400
Std. Deviation	0.0035640	0.0083850	0.0002964	0.0019810
P-value vs TNF-a	<0.01	<0.01	-	<0.01
Statistical test	One-way ANOVA			

Supplemental figure 3D: Confirmation of Sirt1-overexpression

	Control	Sirt1
Mean	0.00	0.24
Std. Deviation	0.00	0.03
P-value vs Sirt1	<0.01	-
Statistical test	T-test	

Supplemental figure 4A: MAP-Kinase activation in splitomicin-treated cells

p38

	TNF-a, 0min	Splito+TNF-a, 0min	TNF-a, 5min	Splito+TNF-a, 5min	TNF-a, 15min	Splito+TNF-a, 15min	TNF-a, 30min	Splito+TNF-a, 30min	TNF-a, 60min	Splito+TNF-a, 60min
Mean	9.03	11.02	77.12	88.40	100.00	95.75	42.05	18.93	15.42	11.56
Std. Deviation	1.22	3.50	6.16	15.98	0.00	9.83	18.59	6.64	4.59	2.85
P-value vs TNF-a	-	NS	-	NS	-	NS	-	NS	-	NS
Statistical test	One-way ANOVA									

JNK

	TNF-a, 0min	Splito+TNF-a, 0min	TNF-a, 5min	Splito+TNF-a, 5min	TNF-a, 15min	Splito+TNF-a, 15min	TNF-a, 30min	Splito+TNF-a, 30min	TNF-a, 60min	Splito+TNF-a, 60min
Mean	3.84	4.52	12.92	16.90	100.00	109.40	56.35	44.89	10.75	10.76
Std. Deviation	0.87	1.05	10.50	2.93	0.00	6.54	25.94	14.82	13.44	12.78
P-value vs TNF-a	-	NS	-	NS	-	NS	-	NS	-	NS
Statistical test	One-way ANOVA									

ERK

	TNF-a, 0min	Splito+TNF-a, 0min	TNF-a, 5min	Splito+TNF-a, 5min	TNF-a, 15min	Splito+TNF-a, 15min	TNF-a, 30min	Splito+TNF-a, 30min	TNF-a, 60min	Splito+TNF-a, 60min
Mean	5.26	8.20	4.98	10.54	100.00	118.80	66.97	47.63	15.85	26.20
Std. Deviation	7.44	11.59	7.05	14.90	0.00	16.06	45.23	41.15	16.01	14.02
P-value vs TNF-a	-	NS	-	NS	-	NS	-	NS	-	NS
Statistical test	One-way ANOVA									

IkB-a

	TNF-a, 0min	Splito+TNF-a, 0min	TNF-a, 5min	Splito+TNF-a, 5min	TNF-a, 15min	Splito+TNF-a, 15min	TNF-a, 30min	Splito+TNF-a, 30min	TNF-a, 60min	Splito+TNF-a, 60min
Mean	100.00	84.55	23.83	25.81	14.66	19.31	35.78	48.61	83.90	74.59
Std. Deviation	0.00	18.22	15.23	9.95	7.33	1.04	13.62	22.62	36.73	37.63
P-value vs TNF-a	-	NS	-	NS	-	NS	-	NS	-	NS
Statistical test	One-way ANOVA									

Supplemental figure 4B: MAP-Kinase activation in sirtinol-treated cells

p38

	TNF-a, 0min	Sirti+TNF-a, 0min	TNF-a, 5min	Sirti+TNF-a, 5min	TNF-a, 15min	Sirti+TNF-a, 15min	TNF-a, 30min	Sirti+TNF-a, 30min	TNF-a, 60min	Sirti+TNF-a, 60min
Mean	8.61	11.33	80.15	87.38	100.00	100.60	40.22	26.53	26.48	29.08
Std. Deviation	8.84	12.96	10.86	23.35	0.00	9.34	11.73	13.73	18.21	16.26
P-value vs TNF-a	-	NS	-	NS	-	NS	-	NS	-	NS
Statistical test	One-way ANOVA									

JNK

	TNF-a, 0min	Sirti+TNF-a, 0min	TNF-a, 5min	Sirti+TNF-a, 5min	TNF-a, 15min	Sirti+TNF-a, 15min	TNF-a, 30min	Sirti+TNF-a, 30min	TNF-a, 60min	Sirti+TNF-a, 60min
Mean	3.41	4.28	16.28	18.52	100.00	106.50	42.73	38.02	16.12	16.14
Std. Deviation	0.63	1.35	12.36	1.19	0.00	5.67	15.22	12.52	13.71	12.37
P-value vs TNF-a	-	NS	-	NS	-	NS	-	NS	-	NS
Statistical test	One-way ANOVA									

ERK

	TNF-a, 0min	Sirti+TNF-a, 0min	TNF-a, 5min	Sirti+TNF-a, 5min	TNF-a, 15min	Sirti+TNF-a, 15min	TNF-a, 30min	Sirti+TNF-a, 30min	TNF-a, 60min	Sirti+TNF-a, 60min
Mean	20.50	24.77	16.41	40.19	100.00	118.20	44.48	51.47	29.67	42.63
Std. Deviation	16.65	12.32	7.52	33.82	0.00	9.31	47.19	25.77	17.68	25.81
P-value vs TNF-a	-	NS	-	NS	-	NS	-	NS	-	NS
Statistical test	One-way ANOVA									

IkB-a

	TNF-a, 0min	Sirti+TNF-a, 0min	TNF-a, 5min	Sirti+TNF-a, 5min	TNF-a, 15min	Sirti+TNF-a, 15min	TNF-a, 30min	Sirti+TNF-a, 30min	TNF-a, 60min	Sirti+TNF-a, 60min
Mean	100.00	85.48	19.26	25.01	25.11	29.39	48.78	57.33	106.40	124.90
Std. Deviation	0.00	20.06	15.98	17.06	26.14	19.42	4.04	2.79	27.25	41.74
P-value vs TNF-a	-	NS	-	NS	-	NS	-	NS	-	NS
Statistical test	One-way ANOVA									

Supplemental figure 6

	TNF-a	Splito+TNF-a
Mean	0.2922	0.2287
Std. Deviation	0.0148	0.0179
P-value vs TNF-a	-	<0.01
Statistical test	T-test	

5.4 ApoE-/- PGC-1a-/- mice display reduced IL-18 levels and do not develop enhanced atherosclerosis

Authors:	Sokrates Stein, Christine Lohmann, Christoph Handschin, Elin Stenfeldt, Jan Borén, Thomas F. Lüscher, and Christian M. Matter
Journal:	PLoS ONE. 2010; 5(10): e13539.
DOI:	10.1371/journal.pone.0013539
PMID:	21042583
Contribution:	Design and analyses of all experiments; performance of most experiments; writing the manuscript.

OPEN ACCESS Freely available online

PLoS one

ApoE−/− PGC-1α−/− Mice Display Reduced IL-18 Levels and Do Not Develop Enhanced Atherosclerosis

Sokrates Stein[1], Christine Lohmann[1], Christoph Handschin[2], Elin Stenfeldt[3], Jan Borén[3], Thomas F. Lüscher[1], Christian M. Matter[1]*

1 Cardiovascular Research, Institute of Physiology, and Zurich Center for Integrative Human Physiology (ZIHP), University of Zurich and Cardiology, Cardiovascular Center, University Hospital Zurich, Zurich, Switzerland, **2** Biozentrum, University of Basel, Basel, Switzerland, **3** Sahlgrenska Center for Cardiovascular and Metabolic Research, University of Goteborg, Goteborg, Sweden

Abstract

Background: Atherosclerosis is a chronic inflammatory disease that evolves from the interaction of activated endothelial cells, macrophages, lymphocytes and modified lipoproteins (LDLs). In the last years many molecules with crucial metabolic functions have been shown to prevent important steps in the progression of atherogenesis, including peroxisome proliferator activated receptors (PPARs) and the class III histone deacetylase (HDAC) SIRT1. The PPARγ coactivator 1 alpha (Ppargc1a or PGC-1α) was identified as an important transcriptional cofactor of PPARγ and is activated by SIRT1. The aim of this study was to analyze total *PGC-1α* deficiency in an atherosclerotic mouse model.

Methodology/Principal Findings: To investigate if total PGC-1α deficiency affects atherosclerosis, we compared *ApoE*$^{-/-}$ *PGC-1α*$^{-/-}$ and *ApoE*$^{-/-}$ *PGC-1α*$^{+/+}$ mice kept on a high cholesterol diet. Despite having more macrophages and a higher ICAM-1 expression in plaques, *ApoE*$^{-/-}$ *PGC-1α*$^{-/-}$ did not display more or larger atherosclerotic plaques than their *ApoE*$^{-/-}$ *PGC-1α*$^{+/+}$ littermates. In line with the previously published phenotype of *PGC-1α*$^{-/-}$ mice, *ApoE*$^{-/-}$ *PGC-1α*$^{-/-}$ mice had marked reduced body, liver and epididymal white adipose tissue (WAT) weight. VLDL/LDL-cholesterol and triglyceride contents were also reduced. Aortic expression of *PPARα* and *PPARγ*, two crucial regulators for adipocyte differentitation and glucose and lipid metabolism, as well as the expression of some PPAR target genes was significantly reduced in *ApoE*$^{-/-}$ *PGC-1α*$^{-/-}$ mice. Importantly, the epididymal WAT and aortic expression of *IL-18* and IL-18 plasma levels, a pro-atherosclerotic cytokine, was markedly reduced in *ApoE*$^{-/-}$ *PGC-1α*$^{-/-}$ mice.

Conclusions/Significance: *ApoE*$^{-/-}$ *PGC-1α*$^{-/-}$ mice, similar as *PGC-1α*$^{-/-}$ mice exhibit markedly reduced total body and visceral fat weight. Since inflammation of visceral fat is a crucial trigger of atherogenesis, decreased visceral fat in *PGC-1α*-deficient mice may explain why these mice do not develop enhanced atherosclerosis.

Citation: Stein S, Lohmann C, Handschin C, Stenfeldt E, Borén J, et al. (2010) ApoE−/− PGC-1α−/− Mice Display Reduced IL-18 Levels and Do Not Develop Enhanced Atherosclerosis. PLoS ONE 5(10): e13539. doi:10.1371/journal.pone.0013539

Editor: Graham Pockley, University of Sheffield, United Kingdom

Received May 16, 2010; **Accepted** September 23, 2010; **Published** October 22, 2010

Funding: This work was funded by the University Research Priority Program 'Integrative Human Physiology' at the University of Zurich and the Swiss National Science Foundation (#31-114094/1, #310030-130626/1, and #3100-068118). The funders had no role in study design, data collection and analysis, decision to publish, or preparation of the manuscript.

Competing Interests: The authors have declared that no competing interests exist.

* E-mail: christian.matter@access.uzh.ch

Introduction

Atherosclerosis is a chronic inflammatory disease that results from interaction between activated endothelial cells, modified low-density lipoproteins (LDL), monocyte-derived macrophages, T cells, and the vessel wall. Activated endothelial cells express adhesion molecules that attract and recruit blood monocytes and lymphocytes. Upon binding to the endothelial layer, these monocytes transmigrate into the subintimal space, and differentiate into macrophages. Plaque macrophages interact with lymphatic cells, mainly T cells, ingest modified LDL via scavenger receptors and become foam cells, thereby promoting plaque formation [1].

PGC-1α was the first described member of the small PGC-1 family of coactivators [2]. Other members of this protein family are PGC-1β and PGC-related coactivator (PRC). PGC-1α is an important cofactor in the transcriptional regulation of genes encoding metabolic enzymes and mitochondrial proteins [3], and it is interacting with many different transcription factors, such as peroxisome proliferator activated receptors (PPARs, including PPARα, PPARβ/δ, and PPARγ), Liver X receptor α and β (LXRα and LXRβ), Glucagon receptor (GR), and Forkhead box O1 (FoxO1) [4,5,6,7,8,9,10].

The phenotype of PGC-1α knock-out mice underlines the central role of this transcription cofactor in homeostatic control of metabolism: they are leaner than wild-type (WT) littermates, have markedly reduced body fat content, and are resistant to diet-induced obesity, hence protected from developing insulin resistance and impaired glucose tolerance [11]. This difference is explained by their CNS-linked hyperactivity and is not a consequence of altered food intake [11].

Overexpression of PGC-1α in human aortic smooth muscle and endothelial cells *in vitro* has been shown to prevent reactive oxygen species (ROS) production and NAD(P)H oxidase activity, with subsequently reduced NF-κB activity and lower expression levels

of MCP-1 and VCAM-1 [12], which are important triggers of inflammation and atherosclerosis. Moreover, PGC-1α overexpression in endothelial cells prevented alpha-linoleic acid-induced ROS formation *in vitro* and improved endothelial dysfunction in aortic rings *ex vivo* [13].

The following studies suggest a link between PGC-1α and atherogenesis at the clinical level: Xie et al. reported a correlation between PGC-1α polymorphism and hypertension [14], and Zhang et al. showed an association between PGC-1α polymorphism and the prevalence of coronary artery disease [15].

Thus, we investigated the effects of *PGC-1α* deficiency on atherogenesis by comparing *ApoE*$^{-/-}$ *PGC-1α*$^{-/-}$ and *ApoE*$^{-/-}$ *PGC-1α*$^{+/+}$ mice.

Results

Total *PGC-1α*$^{-/-}$ deletion does not affect atherogenesis

To study the potential role of PGC-1α in atherogenesis, we crossed *PGC-1α*$^{-/-}$ with *ApoE*$^{-/-}$ mice, and compared 20-week old male *ApoE*$^{-/-}$ *PGC-1α*$^{-/-}$ and *ApoE*$^{-/-}$ *PGC-1α*$^{+/+}$ mice that were kept on a high-cholesterol diet for 12 weeks. Histomorphometry of thoraco-abdominal aortae stained with Oil-Red O (ORO) revealed no difference in atherosclerotic plaque area between *ApoE*$^{-/-}$ *PGC-1α*$^{-/-}$ and *ApoE*$^{-/-}$ *PGC-1α*$^{+/+}$ mice (Fig. 1A). Advanced plaque parameters also revealed a similar total collagen content, plaque diameter or cap thickness in plaques of the aortic sinus that were stained with Elastica van Gieson (Fig. 1B-F).

Increased macrophage and ICAM-1 expression in *ApoE*$^{-/-}$ *PGC-1α*$^{-/-}$ mice

To further analyze cellular and molecular mediators in the progression of atherosclerosis, we quantified the amount of lipids, macrophages, T cells, as well as of the adhesion molecules ICAM-1 and VCAM-1 in plaques from the aortic sinus. No difference in lipid content, CD3-positive T cells, and VCAM-1 expression was observed between *ApoE*$^{-/-}$ *PGC-1α*$^{-/-}$ and *ApoE*$^{-/-}$ *PGC-1α*$^{+/+}$ mice. However, more CD68-positive macrophages and ICAM-1-

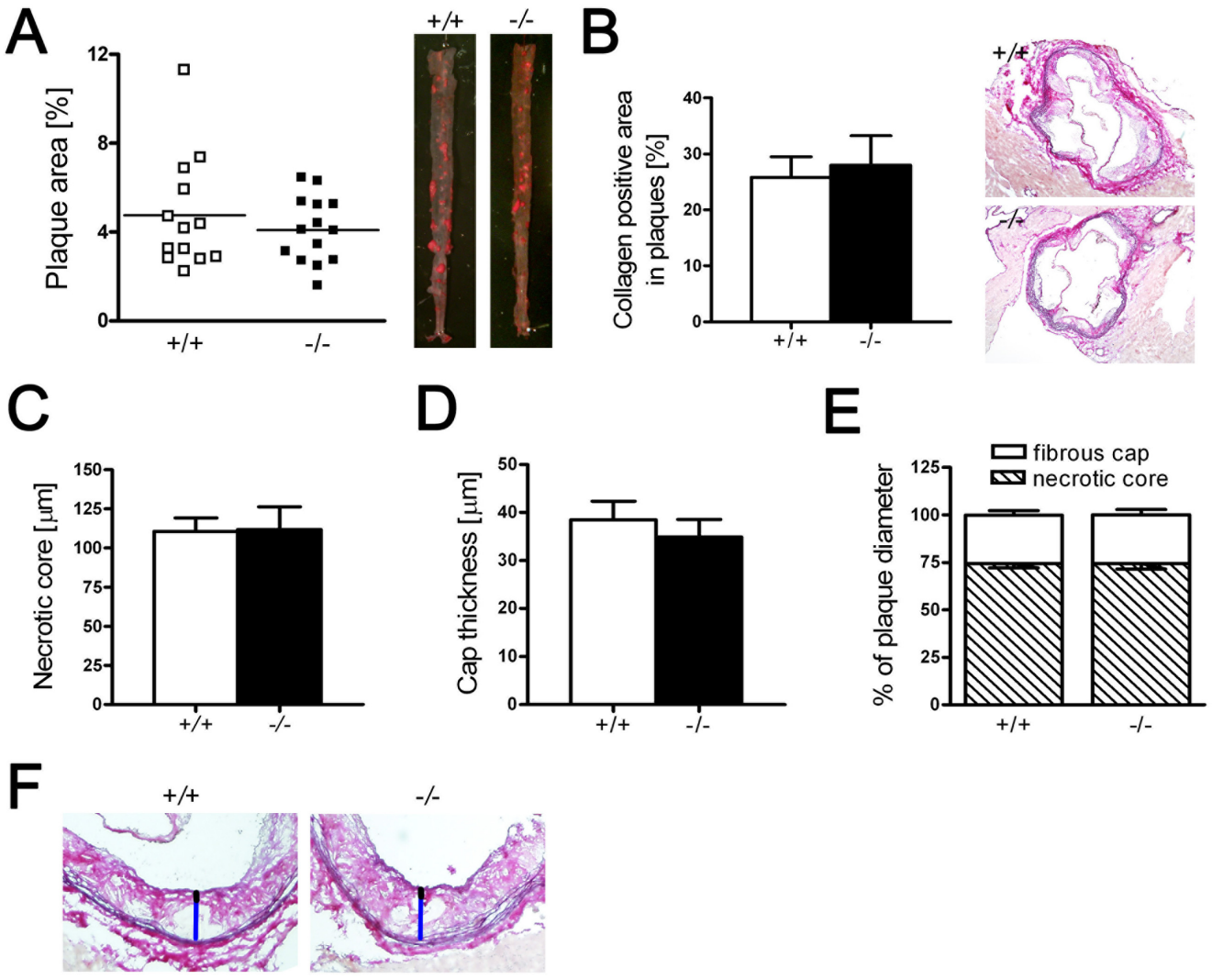

Figure 1. Atherosclerotic lesions and features of plaque vulnerability in *ApoE*$^{-/-}$ *PGC-1α*$^{-/-}$ and *ApoE*$^{-/-}$ *PGC-1α*$^{+/+}$ mice. *En face* plaque quantification of thoraco-abdominal aortae stained with ORO (A). Absolute values of plaque collagen content (B), necrotic core size (C) and cap thickness (D) in plaques from the aortic sinus. Relative values of the necrotic core and fibrous cap size on plaque diameter (E), and representative images to show how the necrotic core (blue line) and fibrous cap (black line) in plaques from the aortic sinus was measured (F). A: *ApoE*$^{-/-}$ *PGC-1α*$^{+/+}$ n = 13 (open circles); *ApoE*$^{-/-}$ *PGC-1α*$^{-/-}$ n = 14 (closed circles). B-E: n = 10. *ApoE*$^{-/-}$ *PGC-1α*$^{-/-}$ (−/−) and *ApoE*$^{-/-}$ *PGC-1α*$^{+/+}$ (+/+).
doi:10.1371/journal.pone.0013539.g001

expressing cells were detected in plaques from *ApoE*$^{-/-}$ *PGC-1α*$^{-/-}$ mice (Fig. 2).

ApoE$^{-/-}$ *PGC-1α*$^{-/-}$ mice exhibit reduced total body weight, epididymal white adipose tissue weight, and VLDL/LDL-cholesterol and VLDL/LDL-triglyceride contents

ApoE$^{-/-}$ *PGC-1α*$^{-/-}$ mice had a lower body, liver, and epididymal fat weight than *ApoE*$^{-/-}$ *PGC-1α*$^{+/+}$ mice (Fig. 3A–D). Spleen weight did not differ between the two groups (Fig. 3E). These data match the published phenotype of *PGC-1α*$^{-/-}$ mice [11]. We next analyzed total cholesterol and triglyceride plasma levels and their distribution in lipoprotein fractions. Both cholesterol and triglyceride contents were lower in VLDL and IDL/LDL particles, whereas their content in HDL particles did not differ (Fig. 4A, B). Total plasma cholesterol showed a clear trend, whereas total triglyceride levels were markedly lower in *ApoE*$^{-/-}$ *PGC-1α*$^{-/-}$ compared to *ApoE*$^{-/-}$ *PGC-1α*$^{+/+}$ mice (Fig. 4C).

Reduced expression of *PPAR* and PPAR target genes

Peroxisome proliferator activated receptors (PPARs) are important regulators of adipocyte differentiation as well as lipid metabolism and inflammation and their transcription is regulated by PGC-1α [6,16,17]. mRNA expression *PPARα* and *PPARγ* was reduced in aortic lysates of *ApoE*$^{-/-}$ *PGC-1α*$^{-/-}$ mice (Fig. 5A), whereas PPARβ/δ levels were not changed (Fig. 5A). To examine if the differential expression of these transcriptional regulators exert functional effects, we quantified the expression of some PPARα and/or PPARγ target genes: *Adipoq (adiponectin)*, *Cebpa (C/EBP-α)*, *Fabp4 (aP2)*, *Fasn (Fatty acid synthase)*, *Fatp1 (Fatty acid transport protein 1)*, *Lipe (Hormone-sensitive lipase)*, *Lpl (Lipoprotein lipase)*,

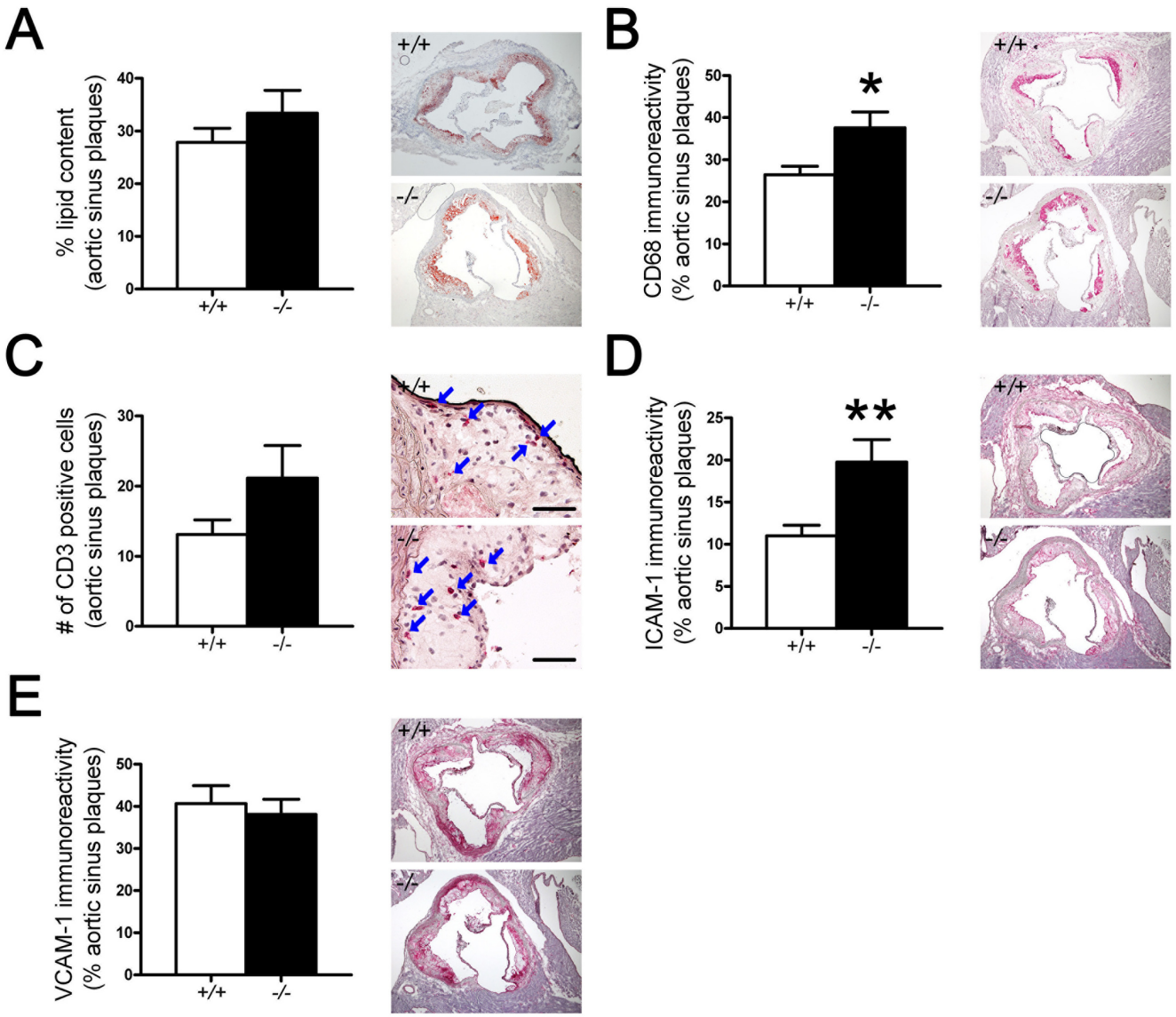

Figure 2. Characterization of plaque inflammation. Quantitative analysis of lipid content in aortic sinus (A; Oil red-O staining), macrophage immunoreactivity (B; CD68-positive cells), T cell number (C; CD3-positive cells; scale bar, 200 μm), VCAM-1 (D) and ICAM-1 (E) immunoreactivity in plaques of the aortic sinus of *ApoE*$^{-/-}$ *PGC-1α*$^{-/-}$ (−/−) and *ApoE*$^{-/-}$ *PGC-1α*$^{+/+}$ (+/+) mice expressed as a proportion of the total plaque areas. n = 10 per genotype. * $p<0.05$. ** $p<0.01$.
doi:10.1371/journal.pone.0013539.g002

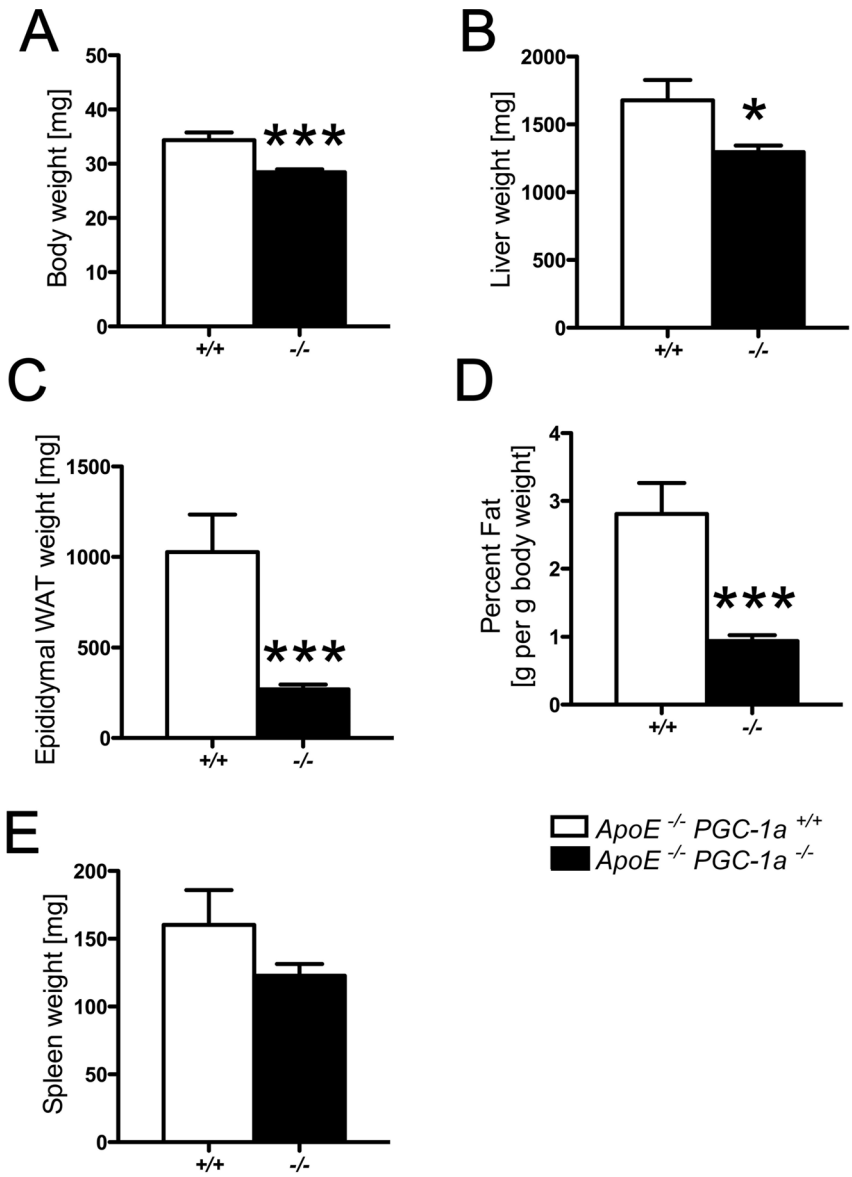

Figure 3. Total body weight and adipose tissue mass. *ApoE*$^{-/-}$ *PGC-1α*$^{-/-}$ exhibit a lower body weight (A), liver weight (B), as well as total epididymal (C) and percent epididymal fat of body weight (D) than *ApoE*$^{-/-}$ *PGC-1α*$^{+/+}$ mice. No difference is observed in spleen weight (E). n≥14 per genotype. * $p<0.05$; *** $p<0.001$.
doi:10.1371/journal.pone.0013539.g003

LXR-α (Liver X receptor α), *Pck1 (Phosphoenolpyruvate carboxykinase 1)*, and *Ucp1 (Uncoupling protein 1)*. Expression of *Cebpa*, *Fabp4*, *Pck1*, and *Ucp1* was significantly lower in *ApoE*$^{-/-}$ *PGC-1α*$^{-/-}$ compared to *ApoE*$^{-/-}$ *PGC-1α*$^{+/+}$ mice, while the expression of *Fasn* showed the same trend and mRNA levels of *Adipoq*, *Fatp1*, *Lipe*, *Lpl*, and *LXR-α* did not differ (Fig. 5B). These data suggest that *PPARα* and *PPARγ* expression and function may at least in part be suppressed in *ApoE*$^{-/-}$ *PGC-1α*$^{-/-}$ mice.

Expression of *IL-18* in epididymal WAT from *ApoE*$^{-/-}$ *PGC-1α*$^{-/-}$ mice is markedly reduced

Mice transplanted with visceral fat develop more atherosclerosis than sham-operated animals [18], supporting the clinical concept that that visceral fat as well as its inflammatory mediators are an important risk factors of atherosclerosis and acute coronary events [19,20]. We therefore analyzed the expression of adipose tissue-derived hormones and cytokines in *ApoE*$^{-/-}$ *PGC-1α*$^{-/-}$ and *ApoE*$^{-/-}$ *PGC-1α*$^{+/+}$ mice. While expression of *Adipoq*, *Nampt (Nicotinamide phosphoribosyltransferase)*, *Retn (Resistin)*, *IL-6*, *IL-10*, *TGF-β*, *MCP-1*, *IFN-γ*, *Agt (Angiotensinogen)*, *11β-HSD1 (11-beta-hydroxysteroid dehydrogenase 1)*, *TNFα*, *and Lpl* was only mildly reduced or unchanged, the expression of *leptin*, *Rarres2 (chemerin)*, *Serpine1 (PAI-1)*, *and IL-18* was lower, and expression of *complement factor D (Cfd* or *adipsin)* higher in *ApoE*$^{-/-}$ *PGC-1α*$^{-/-}$ compared to *ApoE*$^{-/-}$ *PGC-1α*$^{+/+}$ epididymal WAT (Fig. 6).

Reduced expression of IL-18 and CXL16 in aortic lysates from *ApoE*$^{-/-}$ *PGC-1α*$^{-/-}$ mice

The reduced expression of *IL-18* in epididymal WAT is of special interest, since *ApoE*$^{-/-}$ *IL-18*$^{-/-}$ mice develop less atherosclerosis than control *ApoE*$^{-/-}$ mice [21]. Importantly, injection of IL-18 into *SCID/apoE* kockout mice elevated levels of

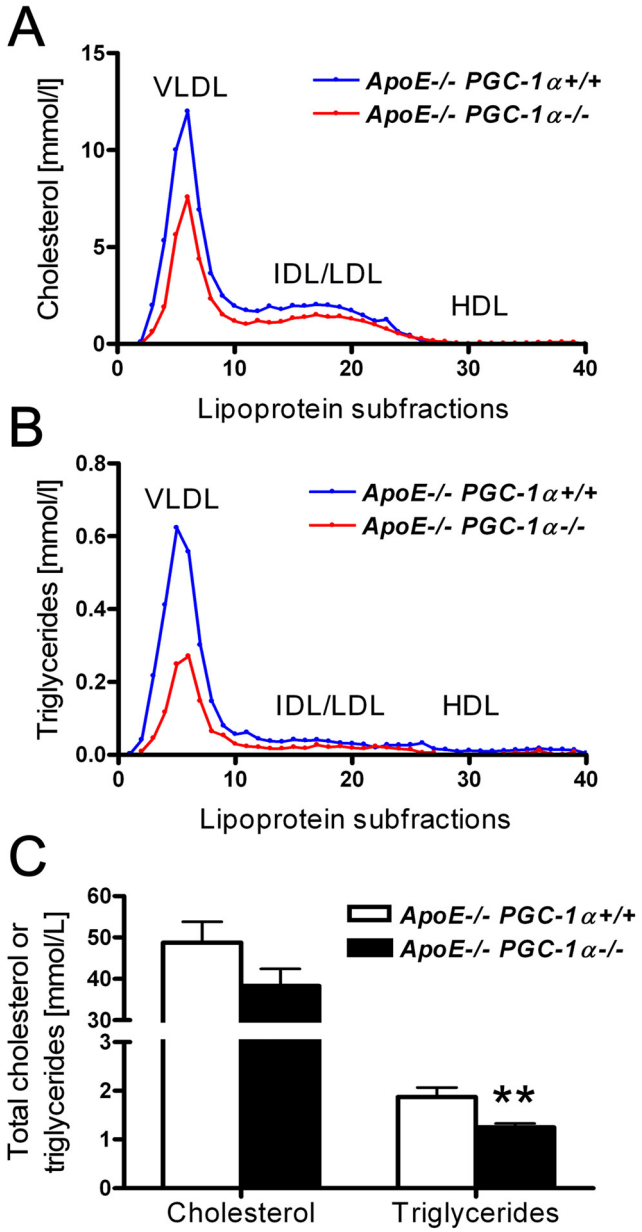

Figure 4. Plasma lipid levels. (A, B) Cholesterol and triglyceride distribution in the plasma lipoprotein fractions of *ApoE*$^{-/-}$ *PGC-1α*$^{-/-}$ and *ApoE*$^{-/-}$ *PGC-1α*$^{+/+}$ mice. Plasma samples were pooled (n = 14 per genotype) and fractionated on a HPLC column. (C) Total cholesterol and triglycerides concentrations were measured with an enzymatic colorimetric assay. n = 14 per genotype. *HPLC*, high pressure liquid chromatography; *HDL*, high-density lipoproteins; *IDL*, intermediate-density lipoproteins; *LDL*, low-density lipoproteins; *VLDL*, very-low-density lipoproteins. ** p<0.01.
doi:10.1371/journal.pone.0013539.g004

IFN-γ and scavenger receptor for phosphatidylserine and oxidized lipoprotein/CXC chemokine ligand 16 (SR-PSOX/CXCL16) in atherosclerotic lesions [22]. Measurement of these factors in aortic tissue, revealed that *IL-18* and SR-PSOX/CXCL16 mRNA levels were reduced in *ApoE*$^{-/-}$ *PGC-1α*$^{-/-}$ mice, while *IFN-γ* expression did not differ between the two genotypes (Fig. 7A). We also quantified the amount of IL-18 and soluble SR-PSOX/CXCL16 in plasma samples. In line with the reduced expression in epididymal WAT and aortae, IL-18 protein level was also reduced in the plasma

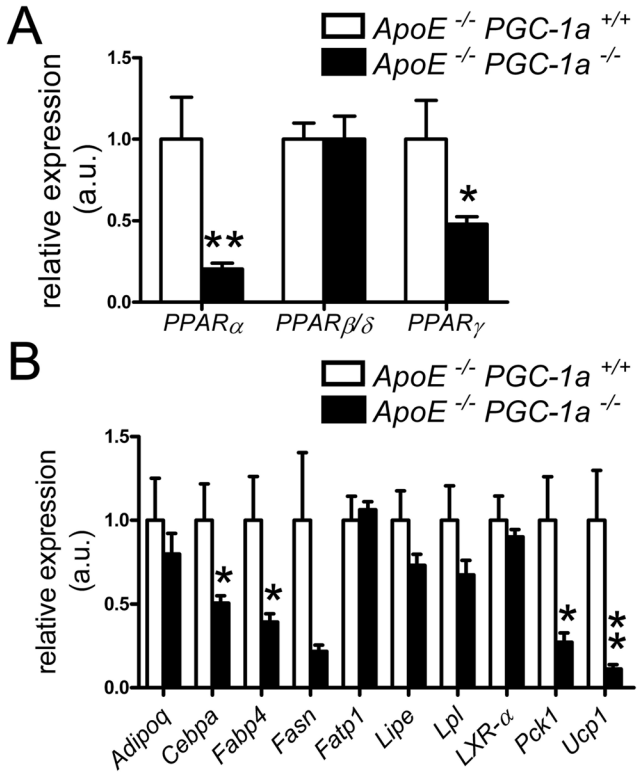

Figure 5. Expression of PPAR and PPAR target genes. (A) Reduced aortic mRNA expression of *PPARα* and *PPARγ*, but unchanged expression of *PPARβ/δ* in *ApoE*$^{-/-}$ *PGC-1α*$^{-/-}$ compared to *ApoE*$^{-/-}$ *PGC-1α*$^{+/+}$ mice. (B) Aortic mRNA expression of *Adipoq, Cebpa, Fabp4, Fasn, Fatp, Lipe, Lpl, LXR-α, Pck1*, and *Ucp1*. n≥9 per genotype. * p<0.05; ** p<0.01.
doi:10.1371/journal.pone.0013539.g005

of *ApoE*$^{-/-}$ *PGC-1α*$^{-/-}$ compared to *ApoE*$^{-/-}$ *PGC-1α*$^{+/+}$ mice (Fig. 7B). In contrast, plasma levels of secreted SR-PSOX/CXCL16 did not differ between the two genotypes (Fig. 7B).

Discussion

Our data show that *ApoE*$^{-/-}$ *PGC-1α*$^{-/-}$ and *ApoE*$^{-/-}$ *PGC-1α*$^{+/+}$ mice do not differ with regard to atherosclerosis, features of plaque vulnerability, expression of VCAM-1, and T cells number. Increased expression of ICAM-1 or CD68-positive cells in plaques of *ApoE*$^{-/-}$ *PGC-1α*$^{-/-}$ do not appear to play a substantial role as they do not affect plaque size. Importantly, the double knockout mice are leaner, have lighter liver and epididymal fat, and less cholesterol and triglycerides in VLDL and LDL subfractions. In addition, aortic expression of *PPARα* and *PPARγ* as well as some of their target genes is reduced in *ApoE*$^{-/-}$ *PGC-1α*$^{-/-}$ mice.

This phenotype is in line with the first study that described the phenotype of *PGC-1α*$^{-/-}$ mice, which also have markedly reduced body fat content [11]. Because visceral (epididymal) WAT inflammation contributes to disease progression [18], it is not astonishing that we observed no difference in plaque lesions between *ApoE*$^{-/-}$ *PGC-1α*$^{-/-}$ and *ApoE*$^{-/-}$ *PGC-1α*$^{+/+}$ mice. Beyond this notion, our data propose that total *PGC-1α* deficiency may rescue an increased atherosclerotic phenotype because of the reduced paracrine effects mediated by the visceral fat.

The lower aortic expression of *PPARα* and *PPARγ* as well as of PPAR target genes proposes that the function of these two PPARs is suppressed in *ApoE*$^{-/-}$ *PGC-1α*$^{-/-}$ mice. Interestingly, both PPARα and PPARγ can exert anti-atherogenic functions in the

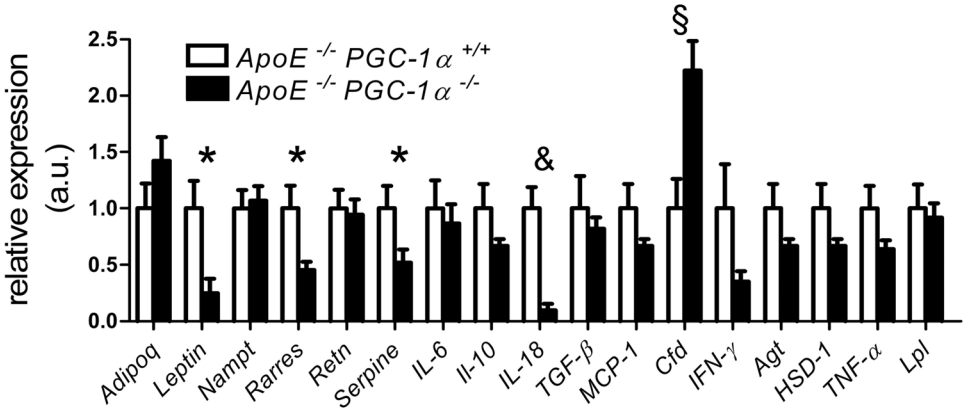

Figure 6. Expression of adipocyte-derived hormones and adipokines. Epididymal WAT mRNA expression in ApoE$^{-/-}$ PGC-1α$^{-/-}$ and ApoE$^{-/-}$ PGC-1α$^{+/+}$ mice: Adipoq, Leptin, Nampt, Rarres2, Retn, Serpine1, IL-6, IL-10, IL-18, TGFβ, MCP-1, Cfd, IFN-γ, Agt, 11β-HSD1, TNFα and Lpl. n = 11 per genotype. * $p<0.05$; § $p<0.01$, & $p<0.001$.
doi:10.1371/journal.pone.0013539.g006

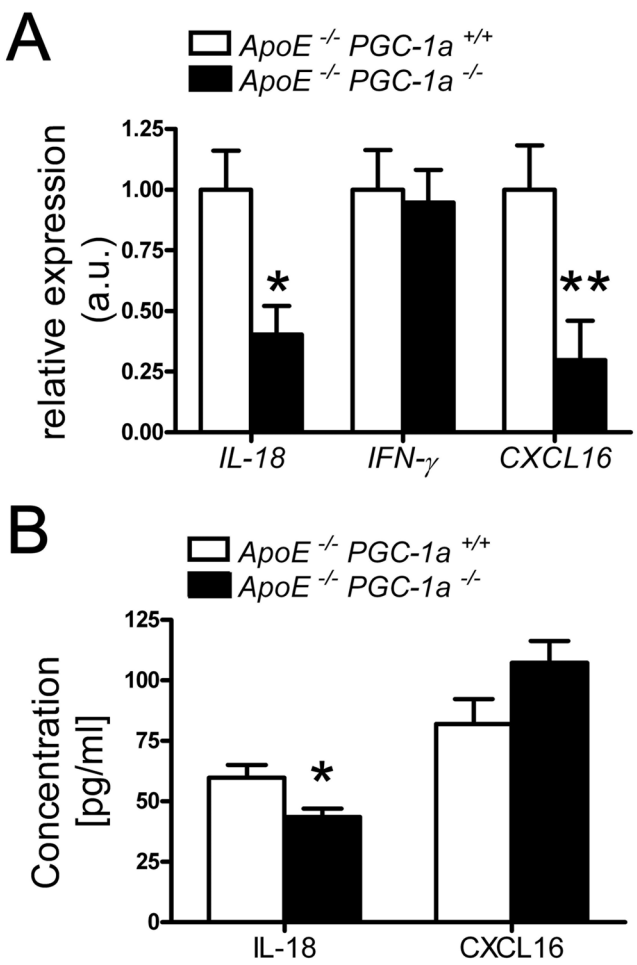

Figure 7. Aortic and plasma expression levels of *IL-18* and *CXCL16*. (A) Reduced aortic mRNA expression of *IL-18* and *CXCL16*, but no change in the expression of *IFN-γ* is observed in *ApoE*$^{-/-}$ *PGC-1α*$^{-/-}$ compared to *ApoE*$^{-/-}$ *PGC-1α*$^{+/+}$ mice. n≥9 per genotype. (B) In plasma samples only IL-18, but not CXCL16 protein levels differed between *ApoE*$^{-/-}$ *PGC-1α*$^{-/-}$ and *ApoE*$^{-/-}$ *PGC-1α*$^{+/+}$ mice. n≥10 per genotype. * $p<0.05$; ** $p<0.01$.
doi:10.1371/journal.pone.0013539.g007

arterial wall. For example, administration of the PPARγ ligand rosiglitazone reduces foam cell formation and atherosclerosis in *LDL-R* knockout mice [23], and transplantation of PPARγ-deficient bone marrow into recipient *LDL-R* knockout mice enhanced atherosclerosis [24]. One of the main atherogenic targets of PPARγ is *LXRα* [24,25], whose expression was not changed between *ApoE*$^{-/-}$ *PGC-1α*$^{-/-}$ and *ApoE*$^{-/-}$ *PGC-1α*$^{+/+}$ aortic lysates.

Reduced expression of *Rarres2 (chemerin), Serpine1 (PAI-1), and IL-18* in visceral adipose tissue could be sufficient to avoid increased atherogenesis. Rarres2 is associated with white adipose tissue inflammation and promotes mobilization and chemotaxis of dendritic cells and macrophages [26,27]. While its expression correlates with inflammatory markers, such as C-reactive protein, it does not predict atherosclerosis in humans [28]. Nevertheless, an atherogenic contribution of Rarres2 cannot be excluded.

PAI-1 is an anti-fibrinolytic enzyme and has beneficial and deleterious effects in atherogenesis. For example, *PAI-1*-deficient mice showed attenuated neointima formation after perivascular cuff-induced injury [29], and local *PAI-1* overexpression prevented the development of abdominal aortic aneurysm [30]. On the other hand, PAI-1 levels are elevated in various cardiovascular diseases and associated with atherothrombosis [31].

The lowest expression of the tested cytokines in the visceral WAT of *ApoE*$^{-/-}$ *PGC-1α*$^{-/-}$ mice was observed for IL-18. IL-18 is a pro-atherogenic cytokine: Overexpression of IL-18 binding protein and direct injection of recombinant IL-18 accelerate atherogenesis, whereas IL-18 deficiency diminishes plaque formation in *ApoE*$^{-/-}$ mice [21,22,32,33]. Furthermore, elevated levels of plasma IL-18 are observed in patients with previous myocardial infarction and are associated with the extent of coronary atherosclerosis [34,35]. We did not only observe a reduced expression of IL-18 in epididymal WAT, but also in aortic tissue and plasma samples of *ApoE*$^{-/-}$ *PGC-1α*$^{-/-}$ mice. It is conceivable that the lower expression of IL-18 alone is sufficient to avoid an acceleration of atherogenesis in our *ApoE*$^{-/-}$ *PGC-1α*$^{-/-}$ mouse model.

Interestingly, IL-18-mediated increase of atherosclerosis is accompanied by elevation of SR-PSOX/CXCL16 expression [22]. SR-PSOX/CXCL16 is a membrane-bound scavenger receptor that binds to the chemokine (C-X-C motif) receptor 6 on lymphocytes [36,37,38,39]. This membrane-anchored chemokine can be further cleaved by specific proteases, hence released in a soluble form [40,41], which has been proposed as a biomarker for acute coronary syndromes [42]. We observed reduced mRNA levels of SR-PSOX/

CXCL16 in epididymal WAT and aortae of *ApoE*$^{-/-}$ *PGC-1α*$^{-/-}$ mice. However, protein levels of the soluble form of SR-PSOX/CXCL16 in plasma did not differ between *ApoE*$^{-/-}$ *PGC-1α*$^{-/-}$ and *ApoE*$^{-/-}$ *PGC-1α*$^{+/+}$ mice, suggesting that the proteolytic cleavage of this chemokine is not affected in *ApoE*$^{-/-}$ *PGC-1α*$^{-/-}$ mice.

Cfd encodes adipsin, the mouse homolog of human complement factor D, which is a serine protease that cleaves factor B in the alternative complement pathway, and it is secreted at high levels in adipose tissue [43,44,45]. While adipsin expression is increased in catabolic conditions such as fasting, it is down-regulated in different models of genetic and acquired obesity [46]. In line with these observations, epididymal WAT expression of *adipsin* was higher in *ApoE*$^{-/-}$ *PGC-1α*$^{-/-}$ compared to *ApoE*$^{-/-}$ *PGC-1α*$^{+/+}$ mice. Expression of adipsin and other components of the alternative complement pathway correlate with atherosclerosis [47], suggesting that the elevation of adipsin in *ApoE*$^{-/-}$ *PGC-1α*$^{-/-}$ provides a pro-atherogenic contribution.

Atherosclerosis is a disease combining the complexity of lipid/lipoprotein and inflammatory/immune disorders [48]. Since PGC-1α is affecting these two important atherogenic systems, it is difficult to dissect the functions of this enzyme in the chosen animal model. For example, the reduced body weight and VLDL/LDL-cholesterol and triglyceride contents as well as the diminished expression of IL-18 are certainly anti-atherogenic, whereas the increased expression of adipsin may play a pro-atherogenic role in *ApoE*$^{-/-}$ *PGC-1α*$^{-/-}$ mice. Further studies using tissue-specific *PGC-1α* knockout or overexpression will be necessary to address these questions in more detail.

Materials and Methods

Animals

ApoE$^{-/-}$ C57BL/6 [49] mice were crossed to *PGC-1α*$^{-/-}$ C57BL/6 [11], to generate *ApoE*$^{-/-}$ *PGC-1α*$^{-/-}$ mice and *ApoE*$^{-/-}$ *PGC-1α*$^{+/+}$ littermates. Of those, male mice were fed a high-cholesterol diet (D12108: 40 kcal% fat, 1.25% cholesterol, Research Diets Inc.) for 12 weeks starting at the age of 8 weeks. Mice were weighted before being sacrificed, and biopsies of aortae, heart, liver, spleen, brown and white adipose tissue, and pancreas frozen in liquid nitrogen or OCT (Optimal Cutting Temperature) for later analyses.

Ethics Statement

All animal procedures were approved by the local animal committee (Kantonales Veterinäramt Zürich, protocol no. 171/2006) and performed in accordance with our institutional guidelines.

Immunohistochemistry

5 mm serial cryosections from the aortic sinus were stained with rat anti-CD68, rat anti-CD3 (Abcam), rat anti-VCAM-1 (BD Biosciences), rat anti-ICAM-1 (Serotec), or oil-red O (ORO). Thoraco-abdominal aortae were fixed with 4% paraformaldehyde and plaques stained with ORO for *en face* analysis. Collagen, fibrous cap thickness, and necrotic core size were analyzed on Elastica van Gieson (EVG)-stained cryosections of the aortic sinus as described [50,51]. Means were taken from n = 10 different mice evaluating 6 serial cryosections/tissue from each mouse.

RNA and protein analysis

Total RNA isolated from proximal aortae was extracted with TRIZOL (Invitrogen), reverse transcribed with Ready-To-Go You-Prime First-Strand Beads (GE Healthcare), and the cDNA (n≥9 per genotype) quantified by qPCR using SYBR Green JumpStart Taq ReadyMix (Sigma-Aldrich). Primer sequences can be found in the supplemental Table S1.

IL-18 and CXCL16 ELISA

Quantification of IL-18 and CXCL16 in plasma of mice where performed with Mouse IL-18 Platinum ELISA kit (Bender MedSystems) and Mouse CXCL16 ELISA kit (RayBiotech) according to the manufacturers instructions. Plasma was diluted 1:2 for the IL-18, and 1:32 for the CXCL16 ELISA assay.

Cholesterol, triglycerides, and lipoprotein subfractioning

Total plasma cholesterol and triglycerides were quantified using Infinity Cholesterol TR13421 and Infinity Triglycerides TR22421 (Thermo Electron Cooperation), respectively. The lipid distribution in plasma lipoprotein fractions was assessed by fast-performance liquid chromatography gel filtration with a Tricorn Superose 6 10/300 GL column (GE Healthcare) [52].

Statistical analyses

Data are presented as mean ± SEM. The *en face* ORO quantification was analyzed using a non-parametric Mann-Whitney U *t*-test. Statistical significance of differences of all other experiments was calculated using an unpaired Student's *t*-test. Significance was accepted at the level of $p<0.05$.

Supporting Information

Table S1 Primer sequences.
Found at: doi:10.1371/journal.pone.0013539.s001 (0.08 MB PDF)

Acknowledgments

We thank S. Winnik for help with the statistical analysis.

Author Contributions

Conceived and designed the experiments: SS CH CMM. Performed the experiments: SS CL ES. Analyzed the data: SS CH CMM. Contributed reagents/materials/analysis tools: JB TL. Wrote the paper: SS CMM.

References

1. Hansson GK (2005) Inflammation, atherosclerosis, and coronary artery disease. N Engl J Med 352: 1685–1695.
2. Puigserver P, Wu Z, Park CW, Graves R, Wright M, et al. (1998) A cold-inducible coactivator of nuclear receptors linked to adaptive thermogenesis. Cell 92: 829–839.
3. Lin J, Handschin C, Spiegelman BM (2005) Metabolic control through the PGC-1 family of transcription coactivators. Cell Metab 1: 361–370.
4. Vega RB, Huss JM, Kelly DP (2000) The coactivator PGC-1 cooperates with peroxisome proliferator-activated receptor alpha in transcriptional control of nuclear genes encoding mitochondrial fatty acid oxidation enzymes. Mol Cell Biol 20: 1868–1876.
5. Wang YX, Lee CH, Tiep S, Yu RT, Ham J, et al. (2003) Peroxisome-proliferator-activated receptor delta activates fat metabolism to prevent obesity. Cell 113: 159–170.
6. Puigserver P, Spiegelman BM (2003) Peroxisome proliferator-activated receptor-gamma coactivator 1 alpha (PGC-1 alpha): transcriptional coactivator and metabolic regulator. Endocr Rev 24: 78–90.
7. Oberkofler H, Schraml E, Krempler F, Patsch W (2003) Potentiation of liver X receptor transcriptional activity by peroxisome-proliferator-activated receptor gamma co-activator 1 alpha. Biochem J 371: 89–96.
8. Kressler D, Schreiber SN, Knutti D, Kralli A (2002) The PGC-1-related protein PERC is a selective coactivator of estrogen receptor alpha. J Biol Chem 277: 13918–13925.
9. Yoon JC, Puigserver P, Chen G, Donovan J, Wu Z, et al. (2001) Control of hepatic gluconeogenesis through the transcriptional coactivator PGC-1. Nature 413: 131–138.
10. Puigserver P, Rhee J, Donovan J, Walkey CJ, Yoon JC, et al. (2003) Insulin-regulated hepatic gluconeogenesis through FOXO1-PGC-1alpha interaction. Nature 423: 550–555.

11. Lin J, Wu PH, Tarr PT, Lindenberg KS, St-Pierre J, et al. (2004) Defects in adaptive energy metabolism with CNS-linked hyperactivity in PGC-1alpha null mice. Cell 119: 121–135.
12. Kim HJ, Park KG, Yoo EK, Kim YH, Kim YN, et al. (2007) Effects of PGC-1alpha on TNF-alpha-induced MCP-1 and VCAM-1 expression and NF-kappaB activation in human aortic smooth muscle and endothelial cells. Antioxid Redox Signal 9: 301–307.
13. Won JC, Park JY, Kim YM, Koh EH, Seol S, et al. (2010) Peroxisome proliferator-activated receptor-gamma coactivator 1-alpha overexpression prevents endothelial apoptosis by increasing ATP/ADP translocase activity. Arterioscler Thromb Vasc Biol 30: 290–297.
14. Xie G, Guo D, Li Y, Liang S, Wu Y (2007) The impact of severity of hypertension on association of PGC-1alpha gene with blood pressure and risk of hypertension. BMC Cardiovasc Disord 7: 33.
15. Zhang Y, Xu W, Li X, Tang Y, Xie P, et al. (2008) Association between Ppargc1a Gene Polymorphisms and Coronary Artery Disease in a Chinese Population. Clin Exp Pharmacol Physiol.
16. Tontonoz P, Spiegelman BM (2008) Fat and Beyond: The Diverse Biology of PPARgamma. Annu Rev Biochem 77: 289–312.
17. Desvergne B, Wahli W (1999) Peroxisome proliferator-activated receptors: nuclear control of metabolism. Endocr Rev 20: 649–688.
18. Ohman MK, Shen Y, Obimba CI, Wright AP, Warnock M, et al. (2008) Visceral adipose tissue inflammation accelerates atherosclerosis in apolipoprotein E-deficient mice. Circulation 117: 798–805.
19. See R, Abdullah SM, McGuire DK, Khera A, Patel MJ, et al. (2007) The association of differing measures of overweight and obesity with prevalent atherosclerosis: the Dallas Heart Study. J Am Coll Cardiol 50: 752–759.
20. Lakka HM, Lakka TA, Tuomilehto J, Salonen JT (2002) Abdominal obesity is associated with increased risk of acute coronary events in men. Eur Heart J 23: 706–713.
21. Elhage R, Jawien J, Rudling M, Ljunggren HG, Takeda K, et al. (2003) Reduced atherosclerosis in interleukin-18 deficient apolipoprotein E-knockout mice. Cardiovasc Res 59: 234–240.
22. Tenger C, Sundborger A, Jawien J, Zhou X (2005) IL-18 accelerates atherosclerosis accompanied by elevation of IFN-gamma and CXCL16 expression independently of T cells. Arterioscler Thromb Vasc Biol 25: 791–796.
23. Li AC, Brown KK, Silvestre MJ, Willson TM, Palinski W, et al. (2000) Peroxisome proliferator-activated receptor gamma ligands inhibit development of atherosclerosis in LDL receptor-deficient mice. J Clin Invest 106: 523–531.
24. Chawla A, Boisvert WA, Lee CH, Laffitte BA, Barak Y, et al. (2001) A PPAR gamma-LXR-ABCA1 pathway in macrophages is involved in cholesterol efflux and atherogenesis. Mol Cell 7: 161–171.
25. Akiyama TE, Sakai S, Lambert G, Nicol CJ, Matsusue K, et al. (2002) Conditional disruption of the peroxisome proliferator-activated receptor gamma gene in mice results in lowered expression of ABCA1, ABCG1, and apoE in macrophages and reduced cholesterol efflux. Mol Cell Biol 22: 2607–2619.
26. Mussig K, Staiger H, Machicao F, Thamer C, Machann J, et al. (2009) RARRES2, encoding the novel adipokine chemerin, is a genetic determinant of disproportionate regional body fat distribution: a comparative magnetic resonance imaging study. Metabolism 58: 519–524.
27. Wittamer V, Franssen JD, Vulcano M, Mirjolet JF, Le Poul E, et al. (2003) Specific recruitment of antigen-presenting cells by chemerin, a novel processed ligand from human inflammatory fluids. J Exp Med 198: 977–985.
28. Lehrke M, Becker A, Greif M, Stark R, Laubender RP, et al. (2009) Chemerin is associated with markers of inflammation and components of the metabolic syndrome but does not predict coronary atherosclerosis. Eur J Endocrinol 161: 339–344.
29. Ploplis VA, Castellino FJ (2001) Attenuation of neointima formation following arterial injury in PAI-1 deficient mice. Ann N Y Acad Sci 936: 466–468.
30. Qian HS, Gu JM, Liu P, Kauser K, Halks-Miller M, et al. (2008) Overexpression of PAI-1 prevents the development of abdominal aortic aneurysm in mice. Gene Ther 15: 224–232.
31. Vaughan DE (2005) PAI-1 and atherothrombosis. J Thromb Haemost 3: 1879–1883.
32. Mallat Z, Corbaz A, Scoazec A, Graber P, Alouani S, et al. (2001) Interleukin-18/interleukin-18 binding protein signaling modulates atherosclerotic lesion development and stability. Circ Res 89: E41–45.
33. Whitman SC, Ravisankar P, Daugherty A (2002) Interleukin-18 enhances atherosclerosis in apolipoprotein E(−/−) mice through release of interferon-gamma. Circ Res 90: E34–38.
34. Hulthe J, McPheat W, Samnegard A, Tornvall P, Hamsten A, et al. (2006) Plasma interleukin (IL)-18 concentrations is elevated in patients with previous myocardial infarction and related to severity of coronary atherosclerosis independently of C-reactive protein and IL-6. Atherosclerosis 188: 450–454.
35. Suchanek H, Mysliwska J, Siebert J, Wieckiewicz J, Hak L, et al. (2005) High serum interleukin-18 concentrations in patients with coronary artery disease and type 2 diabetes mellitus. Eur Cytokine Netw 16: 177–185.
36. Matloubian M, David A, Engel S, Ryan JE, Cyster JG (2000) A transmembrane CXC chemokine is a ligand for HIV-coreceptor Bonzo. Nat Immunol 1: 298–304.
37. Shimaoka T, Kume N, Minami M, Hayashida K, Kataoka H, et al. (2000) Molecular cloning of a novel scavenger receptor for oxidized low density lipoprotein, SR-PSOX, on macrophages. J Biol Chem 275: 40663–40666.
38. Shimaoka T, Nakayama T, Fukumoto N, Kume N, Takahashi S, et al. (2004) Cell surface-anchored SR-PSOX/CXC chemokine ligand 16 mediates firm adhesion of CXC chemokine receptor 6-expressing cells. J Leukoc Biol 75: 267–274.
39. Shimaoka T, Nakayama T, Hieshima K, Kume N, Fukumoto N, et al. (2004) Chemokines generally exhibit scavenger receptor activity through their receptor-binding domain. J Biol Chem 279: 26807–26810.
40. Gough PJ, Garton KJ, Wille PT, Rychlewski M, Dempsey PJ, et al. (2004) A disintegrin and metalloproteinase 10-mediated cleavage and shedding regulates the cell surface expression of CXC chemokine ligand 16. J Immunol 172: 3678–3685.
41. Abel S, Hundhausen C, Mentlein R, Schulte A, Berkhout TA, et al. (2004) The transmembrane CXC-chemokine ligand 16 is induced by IFN-gamma and TNF-alpha and shed by the activity of the disintegrin-like metalloproteinase ADAM10. J Immunol 172: 6362–6372.
42. Mitsuoka H, Toyohara M, Kume N, Hayashida K, Jinnai T, et al. (2009) Circulating soluble SR-PSOX/CXCL16 as a biomarker for acute coronary syndrome -comparison with high-sensitivity C-reactive protein. J Atheroscler Thromb 16: 586–593.
43. Cook KS, Min HY, Johnson D, Chaplinsky RJ, Flier JS, et al. (1987) Adipsin: a circulating serine protease homolog secreted by adipose tissue and sciatic nerve. Science 237: 402–405.
44. Min HY, Spiegelman BM (1986) Adipsin, the adipocyte serine protease: gene structure and control of expression by tumor necrosis factor. Nucleic Acids Res 14: 8879–8892.
45. White RT, Damm D, Hancock N, Rosen BS, Lowell BB, et al. (1992) Human adipsin is identical to complement factor D and is expressed at high levels in adipose tissue. J Biol Chem 267: 9210–9213.
46. Flier JS, Cook KS, Usher P, Spiegelman BM (1987) Severely impaired adipsin expression in genetic and acquired obesity. Science 237: 405–408.
47. Recinos A 3rd, Carr BK, Bartos DB, Boldogh I, Carmical JR, et al. (2004) Liver gene expression associated with diet and lesion development in atherosclerosis-prone mice: induction of components of alternative complement pathway. Physiol Genomics 19: 131–142.
48. Glass CK, Witztum JL (2001) Atherosclerosis. the road ahead. Cell 104: 503–516.
49. Plump AS, Smith JD, Hayek T, Aalto-Setala K, Walsh A, et al. (1992) Severe hypercholesterolemia and atherosclerosis in apolipoprotein E-deficient mice created by homologous recombination in ES cells. Cell 71: 343–353.
50. Lutgens E, Gorelik L, Daemen MJ, de Muinck ED, Grewal IS, et al. (1999) Requirement for CD154 in the progression of atherosclerosis. Nat Med 5: 1313–1316.
51. Stein S, Lohmann C, Schäfer N, Hofmann J, Rohrer L, et al. (2010) SIRT1 decreases Lox-1-mediated foam cell formation in atherogenesis. Eur Heart J 31(18): 2301–2309.
52. Purcell-Huynh DA, Farese RV, Jr., Johnson DF, Flynn LM, Pierotti V, et al. (1995) Transgenic mice expressing high levels of human apolipoprotein B develop severe atherosclerotic lesions in response to a high-fat diet. J Clin Invest 95: 2246–2257.

Table S1 - Primer sequences

Mouse gene name	anti/sense	Sequence (5' to 3')
11β-HSD1	S	CACTTATCTGAAGCCTCAAGGGCG
11β-HSD1	A	CCAATCCCTTTGCTGGCCCC
Adiponectin (Adipoq)	S	AATCCTGCCCAGTCATGCCG
Adiponectin (Adipoq)	A	CTTTCCTGCCAGGGGTTCCG
Angiotensinogen (Agt)	S	TGCCCCAGCTGGAAATCCGA
Angiotensinogen (Agt)	A	ATGGCGAACAGGAAGGGGCT
Cebpa (C/EBP-α)	S	GTCACTGGTCAACTCCAGCA
Cebpa (C/EBP-α)	A	TGGACAAGAACAGCAACGAG
Cfd (Adipsin)	S	GCCCTACATGGCTTCCGTGC
Cfd (Adipsin)	A	TGGGGACCCAACGAGGCATT
Cxcl16	S	GGGACAGAAGGCGCCACCAC
Cxcl16	A	CCCTGGTTGCCATCGCCTGG
IFN-γ	S	ATCTGGAGGAACTGGCAAAA
IFN-γ	A	TGAGCTCATTGAATGCTTGG
IL-10	S	CCAAGCCTTATCGGAAATGA
IL-10	A	TTTTCACAGGGGAGAAATCG
IL-18	S	ACAACTTTGGCCGACTTCAC
IL-18	A	TGGATCCATTTCCTCAAAGG
IL-6	S	CCTCTCTGCAAGAGACTTCCATCCA
IL-6	A	AGCCTCCGACTTGTGAAGTGGT
Lep (leptin)	S	CAGCAGCTGCAAGGTGCAAG
Lep (leptin)	A	GCCAGTGACCCTCTGCTTGG
Lipe (Hormone-sensitive lipase)	S	GGGCCTGGCAGTGGTGTGTAAC
Lipe (Hormone-sensitive lipase)	A	TGAGAACGCTGAGGCTTTGATCTTG
Lpl	S	TTTGGCTCCAGAGTTTGACCGC
Lpl	A	CGAAGGTCTTGCTGCTGTGGTT
MCP-1	S	ACTGAAGCCAGCTCTCTCTTCCTC
MCP-1	A	TTCCTTCTTGGGGTCAGCACAGAC
Nampt (visfatin)	S	TCCCGAGGGCTCTGTCATCC
Nampt (visfatin)	A	GCCCCTATGCCAGCAGTCTCT
PAI-1 (Serpine 1)	S	CAGAGGGCCCCTGGAGAAGT
PAI-1 (Serpine 1)	A	ATTGTCTCTGTCGGGTTGTGCC
Pck1 (Pepck)	S	CCAACGTGGCCGAGACTAGCG
Pck1 (Pepck)	A	GGCACATGGTTCCGCGTCCT
PPARα	S	ATGCCAGTACTGCCGTTTTC
PPARα	A	GGCCTTGACCTTGTTCATGT
PPARβ/δ	S	TGGAGCTCGATGACATGTAC
PPARβ/δ	A	GTACTGGCTGTCAGGGTGGT
PPARγ	S	TCCGAAGAACCATCCGATTGAA
PPARγ	A	CATACAAATGCTTTGCCAGGGC
Rarres2 (chemerin)	S	ACCTGTGCAGTTGGCCTTCC
Rarres2 (chemerin)	A	GAGGATCCTGAGGCCCTTGCT
Retn (resistin)	S	CAGCATGCCACTGTGTCCCA
Retn (resistin)	A	CACGAATGTCCCACGAGCCA
TGF-β	S	GGACCGCAACAACGCCATCT
TGF-β	A	CCTTGGTTCAGCCACTGCCG
TNF-α	S	CCCTCACACTCAGATCATCTTCT
TNF-α	A	GCTACGACGTGGGCTACAG
Ucp1 (Uncoupling protein 1)	S	TCAGCTGTTCAAAGCACACA
Ucp1 (Uncoupling protein 1)	A	GTACCAAGCTGTGCGATGTC

6 Discussion

6.1 Brief summary of the results

The data obtained in this PhD thesis shed light into the role of SIRT1 in atherosclerosis. In contrast to a published observation, endogenous SIRT1 seems to suppress inflammatory events rather than affecting vascular function in atherosclerotic *ApoE*$^{-/-}$ mice. In this regard, suppression of the NF-κB signaling pathway by SIRT1 is of crucial importance. The studies with *ApoE*$^{-/-}$ *PGC-1α* $^{+/+}$ and *ApoE*$^{-/-}$ *PGC-1α* $^{-/-}$ mice did not clarify the exact role of PGC-1α in atherosclerosis, but propose that a balance between pro- and anti-atherogenic events governs the atherosclerotic phenotype of *ApoE*$^{-/-}$ *PGC-1α* $^{-/-}$ mice.

6.2 Discussion of the individual projects

SIRT1 in atherosclerosis

Figure 8 summarizes the main findings regarding the role of SIRT1 in atherosclerosis. These findings are summarized based on the results obtained from experiments done with *ApoE*$^{-/-}$ *SIRT1*$^{+/+}$ and *ApoE*$^{-/-}$ *SIRT1*$^{+/-}$ mice in vivo, with primary cells obtained from these mice ex vivo, with wild-type (WT) C57BL/6 mice treated with a SIRT1 inhibitor in vivo, and with genetic and pharmacological modulation of SIRT1 expression or activity in primary and/or established cancer lines from murine or human origin.

SIRT1 in vascular function

Some reports proposed that SIRT1 influences endothelium-dependent vascular function. SIRT1 deacetylates and activates eNOS in vitro and improves vascular function in aortic rings ex vivo (Mattagajasingh et al., 2007). During the course of this PhD thesis it has been further shown that endothelial overexpression of SIRT1 (SIRT1-Tg) prevents atherosclerosis by improving vascular function in atherosclerosis-prone *ApoE*$^{-/-}$ mice kept on a high-fat diet (Zhang et al., 2008a). This was very surprising since I have been doing similar organ chamber experiments using aortic rings of *ApoE*$^{-/-}$ *SIRT1*$^{+/+}$ and *ApoE*$^{-/-}$ *SIRT1*$^{+/-}$ mice, and in contrast to Zhang et al., I did not observe any difference in endothelium-dependent vascular function (Stein et al., 2010c). Several reasons may explain this discrepancy: (1) In Zhang's study not only did the WT and SIRT1-Tg mice fed a high-fat diet display endothelial dysfunction, but also the control WT and SIRT1-Tg mice fed a normal chow. Thus, the methodology and

reproducibility of the results by Zhang et al. is not convincing. (2) Zhang et al. overexpressed the human SIRT1 gene in mouse endothelial cells. Even though SIRT1 is conserved from bacteria to humans, the possibility that the mouse and human enzymes may differently affect eNOS activity cannot be excluded. (3) *ApoE*$^{-/-}$ *SIRT1*$^{+/-}$ mice are haploinsufficient, meaning that the intact allele cannot compensate the lack of transcript from the deficient allele. If SIRT1 is essential for proper endothelium-dependent vascular function, haploinsufficient *ApoE*$^{-/-}$ *SIRT1*$^{+/-}$ mice should display a dysfunction. Nevertheless, we cannot exclude the possibility that the single allele produces sufficient protein to regulate eNOS. (4) Furthermore, the diets and treatment periods differ between the two studies. This discrepancy was also point of discussion in a commentary from Zhihong Yang and Xiu-Fen Ming on our study (Yang and Ming, 2010).

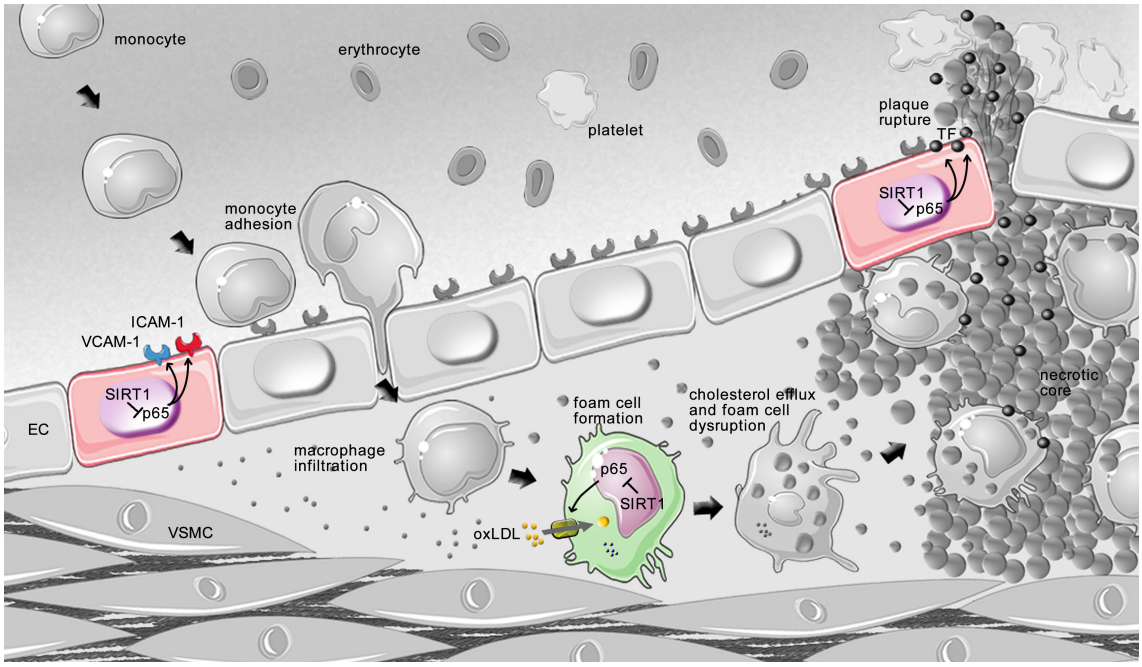

Figure 8 Role of SIRT1 in atherosclerosis

SIRT1-mediated suppression of NF-κB signaling hinders the development of atherosclerosis at different stages (from left to right): In early stages it reduces the endothelial expression of adhesion molecules that attract monocytes and T cells to atheromatous lesions. In advanced stages SIRT1 suppresses the expression of Lox-1 and reduces uptake of oxLDL, thereby preventing macrophage foam cell formation. In the latest stage, during plaque rupture, SIRT1 may prevent atherothrombosis by downregulating the endothelial expression of tissue factor.

SIRT1 in endothelial activation

The role of SIRT1 in endothelial activation is less controversial. Studies form our lab as well as others suggest that SIRT1 exerts anti-inflammatory effects in vascular endothelial cells (Csiszar et al., 2009; Csiszar et al., 2008; Gracia-Sancho et al., 2010). Our in vitro data showed that SIRT1 deacetylates RelA/p65 at K310 and suppresses its binding to naked DNA, therefore interfering with a crucial step in NF-κB signaling activation and reducing the expression of endothelial adhesion molecules (Stein et al., 2010c). These findings are in line with previous reports showing that SIRT1 deacetylates RelA/p65 at the lysine residue K310 in human epithelial lung cells (Yeung et al., 2004). In agreement with these reports, we demonstrated that this mechanism of RelA/p65 signaling suppression is present in HAECs.

More importantly, we provided evidence that suppression of NF-κB signaling by SIRT1 also plays a role in vivo: Upon injection of lipopolysaccharide (LPS) to boost NF-κB signaling, endothelial expression of ICAM-1 and VCAM-1 was increased in non-atherosclerotic aortae of *ApoE*$^{-/-}$ *SIRT1*$^{+/-}$ compared to *ApoE*$^{-/-}$ *SIRT1*$^{+/+}$ mice (Stein et al., 2010c).

SIRT1 in macrophage function and foam cell formation

In macrophages we demonstrated that SIRT1 suppresses the expression of Lox-1, reduces the uptake of oxLDL, and prevents macrophage foam cell formation (Stein et al., 2010b). While we focused our attention on oxLDL uptake and macrophage foam cell formation, other groups studied the roles of macrophage SIRT1 in inflammation, where SIRT1 prevents fatty acid-induced inflammation (Yang et al., 2010), reduces the expression of many pro-inflammatory molecules such as TNF-α, MCP-1 and interleukins (Schug et al., 2010; Shen et al., 2009), modulates insulin sensitivity (Yoshizaki et al., 2010), and diminishes Cyclooxygenase 2 (COX-2) expression and Prostaglandin E_2 (PGE_2) secretion (Zhang et al., 2010). The study from Schug et al. (2010), which appeared shortly after the publication of our respective results, is of special interest because they showed that SIRT1-deficient macrophages display NF-κB hyperacetylation that results in enhanced expression of various pro-inflammatory genes as well as increased accumulation of activated macrophages in the liver and adipose tissue in mice fed a high-fat diet (Schug et al., 2010). Other interesting studies show that macrophage SIRT1 regulates the expression of matrix metalloproteinases (MMP) and the MMP-regulator Tissue Inhibitor of MMP3 (TIMP3) under pathological conditions (Cardellini et al., 2009; Nakamaru et al., 2009). These findings suggest that SIRT1 does not only regulate the expression of scavenger receptors and cholesterol metabolism, but also has beneficial anti-

inflammatory effects in macrophages and regulates the expression of MMPs, which promote plaque vulnerability.

Our bone marrow (BM) transplantation (BMT) experiments confirmed that macrophage SIRT1 is crucial to prevent atherosclerosis (Stein et al., 2010b). However, an important control is missing in our study: The reverse experiment in which BM-derived cells from *ApoE*$^{-/-}$ mice would be transferred into irradiated *ApoE*$^{-/-}$ *SIRT1*$^{+/+}$ and *ApoE*$^{-/-}$ *SIRT1*$^{+/-}$ mice. The reason why we did not perform the reverse experiment is that the *ApoE*$^{-/-}$ *SIRT1*$^{+/-}$ genotype was on a mixed genetic background whereas the *ApoE*$^{-/-}$ donors would have been on a pure C57BL/6 background. We confirmed that the transfer of 129/B6 BM into B6 recipients is well tolerated without graft-versus-host (GvH) disease. In contrast, the reverse transfer of pure B6 BM into 129/B6 recipients could potentially lead to adverse GvH reactions: Mature T cells present in the BM would be alloreactive towards the 129-MHC. After having backcrossed the *ApoE*$^{-/-}$ *SIRT1*$^{+/-}$ mice with mixed genetic background to pure C57BL/6 background, this reverse BMT experiment could be performed without any limitation.

SIRT1 in reverse cholesterol transport

So far only one study shows that SIRT1 regulates cholesterol efflux: Li et al. demonstrated that SIRT1 directly deacetylates and thereby regulates the transcriptional activity of LXRα, an important regulator of lipid homeostasis and inflammation (Li et al., 2007). Activation of LXRα leads to expression of the ATP-binding cassette (ABC) transporter A1 (ABCA1) that regulates the efflux of cholesterol into pre-βHDL particles. Indeed, Li et al. show that cholesterol efflux from primary SIRT1+/+ is higher than from SIRT1-/- macrophages. Furthermore, the authors claim that the SIRT1 inhibitor NAM inhibits cholesterol efflux in the human monocytic cell line THP-1 (Li et al., 2007). In contrast, we did not observe any change in cholesterol efflux in the mouse macrophage cell line RAW 246.7 upon treatment with the SIRT1 inhibitor splitomicin (Stein et al., 2010b). The different inhibitors or cell types that have been used may explain the controversial results. Neither NAM nor splitomicin are solely specific for SIRT1. NAM is an end product inhibitor of the deacetylation reaction mediated by the NAD^+-dependent sirtuins (Bitterman et al., 2002), and therefore an inhibitor of all NAD^+-dependent enzymes. Splitomicin was identified as an inhibitor of the *Saccharomyces cerevisiae* Sir2p (Bedalov et al., 2001). Although splitomicin shows weak inhibitory potential towards human SIRT1 (Hirao et al., 2003; Posakony et al., 2004), it has been successfully used by different groups to inhibit human or mouse SIRT1 (Biacsi et al., 2008; Hou et al., 2008; Kim et al., 2007a; Prozorovski et al., 2008). Future studies using

different specific SIRT1 inhibitors and activators as well as genetic approaches are necessary to confirm a role of SIRT1 in cholesterol efflux regulation in vivo.

SIRT1 in atherothrombosis

In the latest stage of atherogenesis, during plaque rupture, SIRT1 may prevent atherothrombosis by downregulating the endothelial expression of tissue factor. Indeed, treatment of wild-type mice with the SIRT1 inhibitor splitomicin in vivo enhanced tissue factor activity and markedly reduced the time upon coagulation in a photochemical vascular injury model (occlusion was defined as a flow of ≤0.1 ml/min for at least 1 minute) (Breitenstein et al., 2010). In vitro, we could show that SIRT1 diminishes tissue factor expression by deacetylating RelA/p65 and suppressing NF-κB signaling in HAECs. Inhibition or siRNA-mediated SIRT1 silencing in HAECs stimulated with inflammatory mediators lead to increased tissue factor expression (Breitenstein et al., 2010). Patients with atherosclerosis have elevated levels of tissue factor (Reilly et al., 2007) and even higher concentrations are measured in the area around the culprit lesion in patients with unstable angina or acute myocardial infarction compared to patients with stable angina (Annex et al., 1995; Ardissino et al., 1997). Our studies showing that SIRT1 reduces atherosclerosis and arterial thrombosis suggest SIRT1 activation as a promising therapeutic strategy in these patients.

PGC-1α in atherosclerosis

In order to test the role of PGC-1a in atherosclerosis, a genetic approach was used: We observed no difference in atherosclerosis between *ApoE*$^{-/-}$ *PGC-1α*$^{-/-}$ and *ApoE*$^{-/-}$ *PGC-1α*$^{+/+}$ mice. However, *ApoE*$^{-/-}$ *PGC-1α*$^{-/-}$ mice were leaner, had lighter liver and epididymal WAT, and less cholesterol and triglycerides in VLDL and LDL subfractions than *ApoE*$^{-/-}$ *PGC-1α*$^{+/+}$ mice (Stein et al., 2010a). This phenotype is in line with the first study that described the phenotype of *PGC-1α*$^{-/-}$ mice, which also have markedly reduced body fat content (Lin et al., 2004a). Thus, the effects of PGC-1a on atherosclerosis may be attributed to these confounding factors, under which a clear cause-effect relationship could not be established.

Several of our findings suggest that less atherosclerosis should be exprected in *ApoE*$^{-/-}$ *PGC-1α*$^{-/-}$ compared to *ApoE*$^{-/-}$ *PGC-1α*$^{+/+}$ mice: (1) reduced body and fat weight (Stevens et al., 1998), (2) less visceral WAT inflammation (Ohman et al., 2008), (3) diminished aortic and plasma levels of *IL-18* (Elhage et al., 2003; Mallat et al., 2001; Tenger et al., 2005; Whitman et al., 2002), and (4) lower cholesterol and TG content in VLDL and IDL/LDL particles (Drexel et al., 1994; Goldstein et al., 1983). Since we do not observe any difference in atherosclerosis between *ApoE*$^{-/-}$ *PGC-1α*$^{-/-}$ and *ApoE*$^{-/-}$ *PGC-1α*$^{+/+}$ mice (Stein et al., 2010a), there have to be pro-atherogenic contributions that resemble the anti-atherogenic functions of PGC-1α that are lacking in these mice (Figure 9).

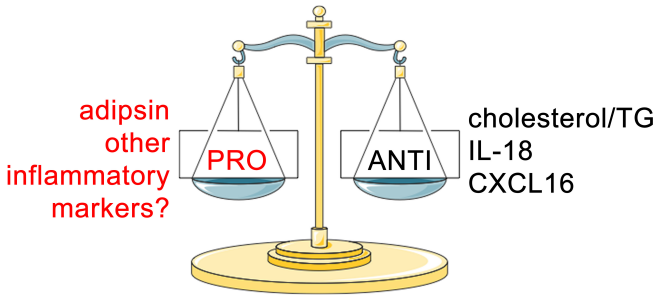

Figure 9 Atherosclerotic balance model of *ApoE*$^{-/-}$ *PGC-1α*$^{-/-}$ mice

***ApoE*$^{-/-}$ *PGC-1α*$^{-/-}$ mice do not develop more atherosclerosis than *ApoE*$^{-/-}$ *PGC-1α*$^{+/+}$ mice. Our data suggests that the contribution of pro and anti-atherogenic functions mediated by PGC-1α is balanced. For example, a pro-atherogenic contribution is the enhanced *adipsin* expression in WAT, and an anti-atherogenic contribution the reduced expression of *IL-18* in WAT and aortae.**

Our data proposes two possible pro-atherogenic contributions in *ApoE*$^{-/-}$ *PGC-1α*$^{-/-}$ mice. First, the reduced aortic expression of *PPARα* and *PPARγ* as well as of PPAR target genes proposes that the function of these two PPARs is suppressed in *ApoE*$^{-/-}$ *PGC-1α*$^{-/-}$ mice (Stein et al., 2010a). Importantly, both PPARα and PPARγ can exert anti-atherogenic functions in the arterial wall. For example, administration of the PPARγ ligand rosiglitazone reduces foam cell formation and atherosclerosis in *LDL-R* knockout mice (Li et al., 2000), and transplantation of PPARγ-deficient bone marrow into recipient *LDL-R* knockout mice enhanced atherosclerosis (Chawla et al., 2001).

The second pro-atherogenic contribution is the increased expression of *adipsin* in WAT (Stein et al., 2010a). Adipsin is a serine protease that cleaves factor B in the alternative complement pathway, and it is secreted at high levels in adipose tissue (Cook et al., 1987; Min and Spiegelman, 1986; White et al., 1992). Notably, expression of adipsin and other components of the alternative complement pathway correlate with atherosclerosis (Recinos et al., 2004).

The main limitation of our study is the complex phenotype of the *ApoE*$^{-/-}$ *PGC-1α*$^{-/-}$ mice. The interplay of direct or indirect endocrine, paracrine and autocrine PGC-1α-driven effects is to complex to distinguish between the single specific effects that PGC-1α may exert in different tissues. Therefore, future studies using tissue-specific PGC-1α knock-in or knock-out mice will be necessary to study these effects.

6.3 Perspectives

SIRT1 - a potent anti-inflammatory molecule

Many studies, including our own, demonstrate that SIRT1 exhibits anti-inflammatory properties both in vitro (e.g. fatty acid-induced inflammation), and in vivo (e.g. myeloid deletion, atherosclerosis, sustainment of normal immune function in knock-out mice) as well as in clinical studies (e.g. COPD patients) (Breitenstein et al., 2010; Rajendrasozhan et al., 2008; Schug et al., 2010; Sequeira et al., 2008; Stein et al., 2010b; Stein et al., 2010c; Yang et al., 2010). These studies propose that SIRT1 activation may be a promising strategy for treating chronic inflammatory diseases, such as atherosclerosis and atherothrombosis (Figure 10).

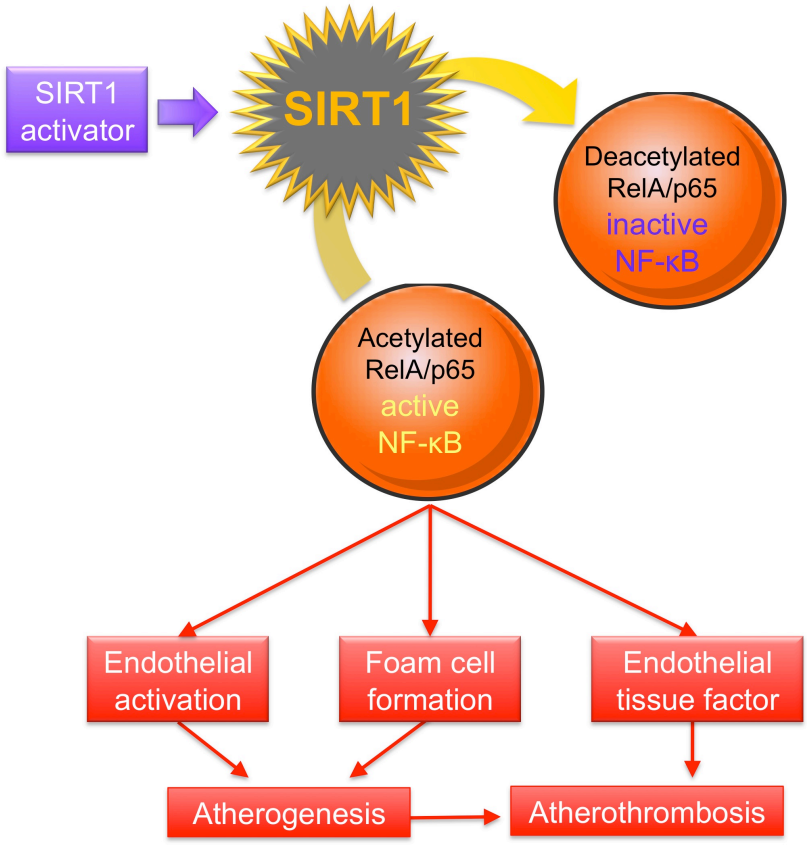

Figure 10 SIRT1 as therapeutic target for patients with atherosclerosis

Pharmacological activation of SIRT1 diminishes atherogenesis by suppressing NF-kB signaling-mediated pro-inflammatory events. Therefore SIRT1 may be a promising therapeutical target for patients with atherosclerosis or atherothrombosis.

Indeed, several SIRT1 activators have been developed by Sirtris™ Pharmaceuticals (Milne et al., 2007). While some studies claim that these Sirtris™ activators are specific (Dai et al., 2010; Funk et al., 2010; Yamazaki et al., 2009), others demonstrated that these compounds do not act via direct SIRT1 activation (Pacholec et al., 2010). According to Sirtris™ Pharmaceuticals new SIRT1-activating drugs are being developed and tested in phase IIa clinical trials in patients with type 2 diabetes, inflammation and cardiovascular disease (www.sirtrispharma.com). Future studies will be necessary to better understand the SIRT1 specificity, clinical effects and side effects of these promising activators.

Preventing NF-κB signaling pathway activation to treat atherosclerosis

The NF-κB pathway plays an important role in atherosclerosis. Numerous studies show a link between NF-κB pathway activation and disease development and/or progression. Of note, different stimuli/regulators, different cell types and time points have different anti- or pro-atherogenic effects (Collins and Cybulsky, 2001; Kutuk and Basaga, 2003; Xanthoulea et al., 2005), suggesting that the particular tissue milieu determines the final outcome related to NF-κB pathway activation.

Several studies suggest a direct correlation between the activation of the NF-κB signaling pathway and atherosclerosis. The pro-inflammatory NF-κB-dependent response in human atherosclerotic lesions is mediated by the canonical NF-κB pathway, including the p65, p50 and c-Rel subunits of NF-κB as well as the IKK2 kinase (Monaco et al., 2004). Endothelial cell-specific disruption of the NF-κB pathway prevents the expression of pro-inflammatory adhesion molecules and protects *ApoE-/-* mice from atherosclerosis (Gareus et al., 2008). Furthermore, several pharmacological agents, including statins, angiotensin-converting enzyme (ACE) inhibitors or the phytohormone genistein, prevent atherosclerosis at least in part by suppressing the NF-κB pathway (Choi et al., 2003; Hernandez-Presa et al., 1997; Hernandez-Presa et al., 1998; Lopez-Franco et al., 2006; Wang et al., 2008; Yang et al., 2006). Finally, clinical studies propose that the activation of the NF-κB signaling pathway is enhanced in patients with advanced atherosclerosis (Martin-Ventura et al., 2004; Zhang et al., 2009).

On the other hand, the function of macrophage NF-κB signaling in foam cell formation and atherosclerosis remains controversial. Macrophage-restricted deletion of IκB kinase (*IKK2*) to disrupt NF-κB signaling increases atherosclerosis in *LDL-R* knockout mice (Kanters et al., 2003). Conversely, studies using macrophage-specific *p50* deletion or a dominant-negative

IκBα mutant to disrupt NF-κB signaling resulted in diminished uptake of lipoproteins and less atherosclerosis (Ferreira et al., 2007; Kanters et al., 2004). NF-κB terminates its own activation by inducing the expression of IκBα and A20. While haploinsufficient *ApoE-/- A20+/-* mice develop more atherosclerosis than control *ApoE-/- A20+/+* mice, overexpression of A20 decreases atherosclerosis, suggesting that A20 diminishes atherosclerosis by decreasing NF-κB activity (Wolfrum et al., 2007).

It may therefore be more promising to modulate the function of regulators (Ahn et al., 2007). For example, inhibition of HATs that acetylate RelA/p65 or activation of HDACs that deacetylate RelA/p65 may block NF-κB pathway activation and, therefore exert anti-atherogenic properties.

To test whether acetylation/deacetylation of RelA/p65 affects atherosclerosis in vivo, it would be interesting to compare mice with a mutation affecting acetylatable lysines of RelA/p65, such as K310R as non-acetylatable and K310Q as acetylation mimic mutants. For example, crossing *K310R-RelA/p65* mice into an *ApoE-/- SIRT1+/-* background would demonstrate which of the observed effects of this thesis are really mediated by SIRT1-dependent acK310-RelA/p65 deacetylation.

Understanding the effect of posttranscriptional modifications of components of the NF-κB signaling pathway on the transcriptional regulation of its target genes is crucial for future pharmacological approaches. Therefore, further investigations will be needed to precisely understand the effect of these modifications and to translate these approaches to the clinical arena.

7 References

Ahn, K.S., Sethi, G., and Aggarwal, B.B. (2007). Nuclear factor-kappa B: from clone to clinic. Curr Mol Med *7*, 619-637.

Ait-Oufella, H., Herbin, O., Bouaziz, J.D., Binder, C.J., Uyttenhove, C., Laurans, L., Taleb, S., Van Vre, E., Esposito, B., Vilar, J.*, et al.* (2010). B cell depletion reduces the development of atherosclerosis in mice. J Exp Med *207*, 1579-1587.

Anitschkow, N., and Chalatow, S. (1912). Über experimentelle Cholesterinsteatose und ihre Bedeutung für die Entstehung einiger pathologischer Prozesse. Zentralbl allg Pathol pathol Anat *24*, 1-9.

Annex, B.H., Denning, S.M., Channon, K.M., Sketch, M.H., Jr., Stack, R.S., Morrissey, J.H., and Peters, K.G. (1995). Differential expression of tissue factor protein in directional atherectomy specimens from patients with stable and unstable coronary syndromes. Circulation *91*, 619-622.

Ardissino, D., Merlini, P.A., Ariens, R., Coppola, R., Bramucci, E., and Mannucci, P.M. (1997). Tissue-factor antigen and activity in human coronary atherosclerotic plaques. Lancet *349*, 769-771.

Avalos, J.L., Bever, K.M., and Wolberger, C. (2005). Mechanism of sirtuin inhibition by nicotinamide: altering the NAD(+) cosubstrate specificity of a Sir2 enzyme. Mol Cell *17*, 855-868.

Baur, J.A., Chen, D., Chini, E.N., Chua, K., Cohen, H.Y., de Cabo, R., Deng, C., Dimmeler, S., Gius, D., Guarente, L.P.*, et al.* (2010). Dietary restriction: standing up for sirtuins. Science *329*, 1012-1013; author reply 1013-1014.

Bedalov, A., Gatbonton, T., Irvine, W.P., Gottschling, D.E., and Simon, J.A. (2001). Identification of a small molecule inhibitor of Sir2p. Proc Natl Acad Sci U S A *98*, 15113-15118.

Biacsi, R., Kumari, D., and Usdin, K. (2008). SIRT1 inhibition alleviates gene silencing in Fragile X mental retardation syndrome. PLoS Genet *4*, e1000017.

Bitterman, K.J., Anderson, R.M., Cohen, H.Y., Latorre-Esteves, M., and Sinclair, D.A. (2002). Inhibition of silencing and accelerated aging by nicotinamide, a putative negative regulator of yeast sir2 and human SIRT1. J Biol Chem *277*, 45099-45107.

Blander, G., and Guarente, L. (2004). The Sir2 family of protein deacetylases. Annu Rev Biochem *73*, 417-435.

Brachmann, C.B., Sherman, J.M., Devine, S.E., Cameron, E.E., Pillus, L., and Boeke, J.D. (1995). The SIR2 gene family, conserved from bacteria to humans, functions in silencing, cell cycle progression, and chromosome stability. Genes Dev *9*, 2888-2902.

Breitenstein, A., Stein, S., Holy, E.W., Camici, G.G., Lohmann, C., Akhmedov, A., Spescha, R., Elliott, P.J., Westphal, C.H., Matter, C.M.*, et al.* (2010). Sirt1 inhibition promotes in vivo arterial thrombosis and tissue factor expression in stimulated cells. Cardiovasc Res. 2010 Nov 21. Epub ahead of print. doi: 10.1093/cvr/cvq339

Breslow, J.L. (1996). Mouse models of atherosclerosis. Science *272*, 685-688.

Caligiuri, G., Nicoletti, A., Poirier, B., and Hansson, G.K. (2002). Protective immunity against atherosclerosis carried by B cells of hypercholesterolemic mice. J Clin Invest *109*, 745-753.

Canto, C., and Auwerx, J. (2009). PGC-1alpha, SIRT1 and AMPK, an energy sensing network that controls energy expenditure. Curr Opin Lipidol *20*, 98-105.

Canto, C., Gerhart-Hines, Z., Feige, J.N., Lagouge, M., Noriega, L., Milne, J.C., Elliott, P.J., Puigserver, P., and Auwerx, J. (2009). AMPK regulates energy expenditure by modulating NAD+ metabolism and SIRT1 activity. Nature *458*, 1056-1060.

Canto, C., Jiang, L.Q., Deshmukh, A.S., Mataki, C., Coste, A., Lagouge, M., Zierath, J.R., and Auwerx, J. (2010). Interdependence of AMPK and SIRT1 for metabolic adaptation to fasting and exercise in skeletal muscle. Cell Metab *11*, 213-219.

Cardellini, M., Menghini, R., Martelli, E., Casagrande, V., Marino, A., Rizza, S., Porzio, O., Mauriello, A., Solini, A., Ippoliti, A.*, et al.* (2009). TIMP3 is reduced in atherosclerotic plaques from subjects with type 2 diabetes and increased by SirT1. Diabetes *58*, 2396-2401.

Chawla, A., Boisvert, W.A., Lee, C.H., Laffitte, B.A., Barak, Y., Joseph, S.B., Liao, D., Nagy, L., Edwards, P.A., Curtiss, L.K.*, et al.* (2001). A PPAR gamma-LXR-ABCA1 pathway in macrophages is involved in cholesterol efflux and atherogenesis. Mol Cell *7*, 161-171.

Choi, J.H., Jeong, T.S., Kim, D.Y., Kim, Y.M., Na, H.J., Nam, K.H., Lee, S.B., Kim, H.C., Oh, S.R., Choi, Y.K.*, et al.* (2003). Hematein inhibits atherosclerosis by inhibition of reactive oxygen generation and NF-kappaB-dependent inflammatory mediators in hyperlipidemic mice. J Cardiovasc Pharmacol *42*, 287-295.

Collins, T., and Cybulsky, M.I. (2001). NF-kappaB: pivotal mediator or innocent bystander in atherogenesis? J Clin Invest *107*, 255-264.

Collins, T., Read, M.A., Neish, A.S., Whitley, M.Z., Thanos, D., and Maniatis, T. (1995). Transcriptional regulation of endothelial cell adhesion molecules: NF-kappa B and cytokine-inducible enhancers. FASEB J *9*, 899-909.

Colman, R.J., Anderson, R.M., Johnson, S.C., Kastman, E.K., Kosmatka, K.J., Beasley, T.M., Allison, D.B., Cruzen, C., Simmons, H.A., Kemnitz, J.W.*, et al.* (2009). Caloric restriction delays disease onset and mortality in rhesus monkeys. Science *325*, 201-204.

Cook, K.S., Min, H.Y., Johnson, D., Chaplinsky, R.J., Flier, J.S., Hunt, C.R., and Spiegelman, B.M. (1987). Adipsin: a circulating serine protease homolog secreted by adipose tissue and sciatic nerve. Science *237*, 402-405.

Csiszar, A., Labinskyy, N., Jimenez, R., Pinto, J.T., Ballabh, P., Losonczy, G., Pearson, K.J., de Cabo, R., and Ungvari, Z. (2009). Anti-oxidative and anti-inflammatory vasoprotective effects of caloric restriction in aging: role of circulating factors and SIRT1. Mech Ageing Dev *130*, 518-527.

Csiszar, A., Labinskyy, N., Podlutsky, A., Kaminski, P.M., Wolin, M.S., Zhang, C., Mukhopadhyay, P., Pacher, P., Hu, F., de Cabo, R.*, et al.* (2008). Vasoprotective effects of resveratrol and SIRT1: attenuation of cigarette smoke-induced oxidative stress and proinflammatory phenotypic alterations. Am J Physiol Heart Circ Physiol *294*, H2721-2735.

Dai, H., Kustigian, L., Carney, D., Case, A., Considine, T., Hubbard, B.P., Perni, R.B., Riera, T.V., Szczepankiewicz, B., Vlasuk, G.P.*, et al.* (2010). SIRT1 activation by small molecules - kinetic and biophysical evidence for direct interaction of enzyme and activator. J Biol Chem.

Deanfield, J.E., Halcox, J.P., and Rabelink, T.J. (2007). Endothelial function and dysfunction: testing and clinical relevance. Circulation *115*, 1285-1295.

Denu, J.M. (2005). The Sir 2 family of protein deacetylases. Curr Opin Chem Biol *9*, 431-440.

Drexel, H., Amann, F.W., Beran, J., Rentsch, K., Candinas, R., Muntwyler, J., Luethy, A., Gasser, T., and Follath, F. (1994). Plasma triglycerides and three lipoprotein cholesterol fractions are independent predictors of the extent of coronary atherosclerosis. Circulation *90*, 2230-2235.

Elhage, R., Jawien, J., Rudling, M., Ljunggren, H.G., Takeda, K., Akira, S., Bayard, F., and Hansson, G.K. (2003). Reduced atherosclerosis in interleukin-18 deficient apolipoprotein E-knockout mice. Cardiovasc Res *59*, 234-240.

Endemann, G., Stanton, L.W., Madden, K.S., Bryant, C.M., White, R.T., and Protter, A.A. (1993). CD36 is a receptor for oxidized low density lipoprotein. J Biol Chem *268*, 11811-11816.

Esterbauer, H., Gebicki, J., Puhl, H., and Jurgens, G. (1992). The role of lipid peroxidation and antioxidants in oxidative modification of LDL. Free Radic Biol Med *13*, 341-390.

Faggiotto, A., Ross, R., and Harker, L. (1984). Studies of hypercholesterolemia in the nonhuman primate. I. Changes that lead to fatty streak formation. Arteriosclerosis *4*, 323-340.

Ferreira, V., van Dijk, K.W., Groen, A.K., Vos, R.M., van der Kaa, J., Gijbels, M.J., Havekes, L.M., and Pannekoek, H. (2007). Macrophage-specific inhibition of NF-kappaB activation reduces foam-cell formation. Atherosclerosis *192*, 283-290.

Finkel, T., Deng, C.X., and Mostoslavsky, R. (2009). Recent progress in the biology and physiology of sirtuins. Nature *460*, 587-591.

Fontana, L., Partridge, L., and Longo, V.D. (2010). Extending healthy life span--from yeast to humans. Science *328*, 321-326.

Forstermann, U. (2010). Nitric oxide and oxidative stress in vascular disease. Pflugers Arch *459*, 923-939.

Frye, R.A. (1999). Characterization of five human cDNAs with homology to the yeast SIR2 gene: Sir2-like proteins (sirtuins) metabolize NAD and may have protein ADP-ribosyltransferase activity. Biochem Biophys Res Commun *260*, 273-279.

Funk, J.A., Odejinmi, S., and Schnellmann, R.G. (2010). SRT1720 induces mitochondrial biogenesis and rescues mitochondrial function after oxidant injury in renal proximal tubule cells. J Pharmacol Exp Ther *333*, 593-601.

Gareus, R., Kotsaki, E., Xanthoulea, S., van der Made, I., Gijbels, M.J., Kardakaris, R., Polykratis, A., Kollias, G., de Winther, M.P., and Pasparakis, M. (2008). Endothelial cell-specific NF-kappaB inhibition protects mice from atherosclerosis. Cell Metab *8*, 372-383.

Goldstein, J.L., Ho, Y.K., Basu, S.K., and Brown, M.S. (1979). Binding site on macrophages that mediates uptake and degradation of acetylated low density lipoprotein, producing massive cholesterol deposition. Proc Natl Acad Sci U S A *76*, 333-337.

Goldstein, J.L., Kita, T., and Brown, M.S. (1983). Defective lipoprotein receptors and atherosclerosis. Lessons from an animal counterpart of familial hypercholesterolemia. N Engl J Med *309*, 288-296.

Gottlieb, S., and Esposito, R.E. (1989). A new role for a yeast transcriptional silencer gene, SIR2, in regulation of recombination in ribosomal DNA. Cell *56*, 771-776.

Gracia-Sancho, J., Villarreal, G., Jr., Zhang, Y., and Garcia-Cardena, G. (2010). Activation of SIRT1 by resveratrol induces KLF2 expression conferring an endothelial vasoprotective phenotype. Cardiovasc Res *85*, 514-519.

Haigis, M.C., and Guarente, L.P. (2006). Mammalian sirtuins--emerging roles in physiology, aging, and calorie restriction. Genes Dev *20*, 2913-2921.

Hansson, G.K. (2005). Inflammation, atherosclerosis, and coronary artery disease. N Engl J Med *352*, 1685-1695.

Hardie, D.G. (2007). AMP-activated/SNF1 protein kinases: conserved guardians of cellular energy. Nat Rev Mol Cell Biol *8*, 774-785.

Henriksen, T., Mahoney, E.M., and Steinberg, D. (1981). Enhanced macrophage degradation of low density lipoprotein previously incubated with cultured endothelial cells: recognition by receptors for acetylated low density lipoproteins. Proc Natl Acad Sci U S A *78*, 6499-6503.

Hernandez-Presa, M., Bustos, C., Ortego, M., Tunon, J., Renedo, G., Ruiz-Ortega, M., and Egido, J. (1997). Angiotensin-converting enzyme inhibition prevents arterial nuclear factor-kappa B activation, monocyte chemoattractant protein-1 expression, and macrophage infiltration in a rabbit model of early accelerated atherosclerosis. Circulation *95*, 1532-1541.

Hernandez-Presa, M.A., Bustos, C., Ortego, M., Tunon, J., Ortega, L., and Egido, J. (1998). ACE inhibitor quinapril reduces the arterial expression of NF-kappaB-dependent proinflammatory factors but not of collagen I in a rabbit model of atherosclerosis. Am J Pathol *153*, 1825-1837.

Hirao, M., Posakony, J., Nelson, M., Hruby, H., Jung, M., Simon, J.A., and Bedalov, A. (2003). Identification of selective inhibitors of NAD+-dependent deacetylases using phenotypic screens in yeast. J Biol Chem *278*, 52773-52782.

Horkko, S., Bird, D.A., Miller, E., Itabe, H., Leitinger, N., Subbanagounder, G., Berliner, J.A., Friedman, P., Dennis, E.A., Curtiss, L.K.*, et al.* (1999). Monoclonal autoantibodies specific for oxidized phospholipids or oxidized phospholipid-protein adducts inhibit macrophage uptake of oxidized low-density lipoproteins. J Clin Invest *103*, 117-128.

Horkko, S., Miller, E., Dudl, E., Reaven, P., Curtiss, L.K., Zvaifler, N.J., Terkeltaub, R., Pierangeli, S.S., Branch, D.W., Palinski, W.*, et al.* (1996). Antiphospholipid antibodies are directed against epitopes of oxidized phospholipids. Recognition of cardiolipin by monoclonal antibodies to epitopes of oxidized low density lipoprotein. J Clin Invest *98*, 815-825.

Hou, X., Xu, S., Maitland-Toolan, K.A., Sato, K., Jiang, B., Ido, Y., Lan, F., Walsh, K., Wierzbicki, M., Verbeuren, T.J.*, et al.* (2008). SIRT1 regulates hepatocyte lipid metabolism through activating AMP-activated protein kinase. J Biol Chem *283*, 20015-20026.

Houtkooper, R.H., Canto, C., Wanders, R.J., and Auwerx, J. (2010). The secret life of NAD+: an old metabolite controlling new metabolic signaling pathways. Endocr Rev *31*, 194-223.

Imai, S., Armstrong, C.M., Kaeberlein, M., and Guarente, L. (2000). Transcriptional silencing and longevity protein Sir2 is an NAD-dependent histone deacetylase. Nature *403*, 795-800.

Ishibashi, S., Brown, M.S., Goldstein, J.L., Gerard, R.D., Hammer, R.E., and Herz, J. (1993). Hypercholesterolemia in low density lipoprotein receptor knockout mice and its reversal by adenovirus-mediated gene delivery. J Clin Invest *92*, 883-893.

Kaeberlein, M. (2010). Lessons on longevity from budding yeast. Nature *464*, 513-519.

Kaeberlein, M., McVey, M., and Guarente, L. (1999). The SIR2/3/4 complex and SIR2 alone promote longevity in Saccharomyces cerevisiae by two different mechanisms. Genes Dev *13*, 2570-2580.

Kaeberlein, M., and Powers, R.W., 3rd (2007). Sir2 and calorie restriction in yeast: a skeptical perspective. Ageing Res Rev *6*, 128-140.

Kanters, E., Gijbels, M.J., van der Made, I., Vergouwe, M.N., Heeringa, P., Kraal, G., Hofker, M.H., and de Winther, M.P. (2004). Hematopoietic NF-kappaB1 deficiency results in small atherosclerotic lesions with an inflammatory phenotype. Blood *103*, 934-940.

Kanters, E., Pasparakis, M., Gijbels, M.J., Vergouwe, M.N., Partouns-Hendriks, I., Fijneman, R.J., Clausen, B.E., Forster, I., Kockx, M.M., Rajewsky, K.*, et al.* (2003). Inhibition of NF-kappaB activation in macrophages increases atherosclerosis in LDL receptor-deficient mice. J Clin Invest *112*, 1176-1185.

Kawashima, S., and Yokoyama, M. (2004). Dysfunction of endothelial nitric oxide synthase and atherosclerosis. Arterioscler Thromb Vasc Biol *24*, 998-1005.

Kim, E.J., Kho, J.H., Kang, M.R., and Um, S.J. (2007a). Active regulator of SIRT1 cooperates with SIRT1 and facilitates suppression of p53 activity. Mol Cell *28*, 277-290.

Kim, H.J., Park, K.G., Yoo, E.K., Kim, Y.H., Kim, Y.N., Kim, H.S., Kim, H.T., Park, J.Y., Lee, K.U., Jang, W.G.*, et al.* (2007b). Effects of PGC-1alpha on TNF-alpha-induced MCP-1 and VCAM-1 expression and NF-kappaB activation in human aortic smooth muscle and endothelial cells. Antioxid Redox Signal *9*, 301-307.

Knowles, J.W., Reddick, R.L., Jennette, J.C., Shesely, E.G., Smithies, O., and Maeda, N. (2000). Enhanced atherosclerosis and kidney dysfunction in eNOS(-/-)Apoe(-/-) mice are ameliorated by enalapril treatment. J Clin Invest *105*, 451-458.

Kodama, T., Freeman, M., Rohrer, L., Zabrecky, J., Matsudaira, P., and Krieger, M. (1990). Type I macrophage scavenger receptor contains alpha-helical and collagen-like coiled coils. Nature *343*, 531-535.

Kressler, D., Schreiber, S.N., Knutti, D., and Kralli, A. (2002). The PGC-1-related protein PERC is a selective coactivator of estrogen receptor alpha. J Biol Chem *277*, 13918-13925.

Kuo, M.H., and Allis, C.D. (1998). Roles of histone acetyltransferases and deacetylases in gene regulation. Bioessays *20*, 615-626.

Kutuk, O., and Basaga, H. (2003). Inflammation meets oxidation: NF-kappaB as a mediator of initial lesion development in atherosclerosis. Trends Mol Med *9*, 549-557.

Lagouge, M., Argmann, C., Gerhart-Hines, Z., Meziane, H., Lerin, C., Daussin, F., Messadeq, N., Milne, J., Lambert, P., Elliott, P.*, et al.* (2006). Resveratrol improves mitochondrial function and protects against metabolic disease by activating SIRT1 and PGC-1alpha. Cell *127*, 1109-1122.

Laursen, J.B., Somers, M., Kurz, S., McCann, L., Warnholtz, A., Freeman, B.A., Tarpey, M., Fukai, T., and Harrison, D.G. (2001). Endothelial regulation of vasomotion in apoE-deficient mice: implications for interactions between peroxynitrite and tetrahydrobiopterin. Circulation *103*, 1282-1288.

Lavu, S., Boss, O., Elliott, P.J., and Lambert, P.D. (2008). Sirtuins--novel therapeutic targets to treat age-associated diseases. Nat Rev Drug Discov *7*, 841-853.

Li, A.C., Brown, K.K., Silvestre, M.J., Willson, T.M., Palinski, W., and Glass, C.K. (2000). Peroxisome proliferator-activated receptor gamma ligands inhibit development of atherosclerosis in LDL receptor-deficient mice. J Clin Invest *106*, 523-531.

Li, A.C., and Glass, C.K. (2002). The macrophage foam cell as a target for therapeutic intervention. Nat Med *8*, 1235-1242.

Li, X., Zhang, S., Blander, G., Tse, J.G., Krieger, M., and Guarente, L. (2007). SIRT1 deacetylates and positively regulates the nuclear receptor LXR. Mol Cell *28*, 91-106.

Lin, J., Handschin, C., and Spiegelman, B.M. (2005). Metabolic control through the PGC-1 family of transcription coactivators. Cell Metab *1*, 361-370.

Lin, J., Wu, P.H., Tarr, P.T., Lindenberg, K.S., St-Pierre, J., Zhang, C.Y., Mootha, V.K., Jager, S., Vianna, C.R., Reznick, R.M.*, et al.* (2004a). Defects in adaptive energy metabolism with CNS-linked hyperactivity in PGC-1alpha null mice. Cell *119*, 121-135.

Lin, S.J., Defossez, P.A., and Guarente, L. (2000). Requirement of NAD and SIR2 for life-span extension by calorie restriction in Saccharomyces cerevisiae. Science *289*, 2126-2128.

Lin, S.J., Ford, E., Haigis, M., Liszt, G., and Guarente, L. (2004b). Calorie restriction extends yeast life span by lowering the level of NADH. Genes Dev *18*, 12-16.

Lin, S.J., Kaeberlein, M., Andalis, A.A., Sturtz, L.A., Defossez, P.A., Culotta, V.C., Fink, G.R., and Guarente, L. (2002). Calorie restriction extends Saccharomyces cerevisiae lifespan by increasing respiration. Nature *418*, 344-348.

Lopez-Franco, O., Hernandez-Vargas, P., Ortiz-Munoz, G., Sanjuan, G., Suzuki, Y., Ortega, L., Blanco, J., Egido, J., and Gomez-Guerrero, C. (2006). Parthenolide modulates the NF-kappaB-mediated inflammatory responses in experimental atherosclerosis. Arterioscler Thromb Vasc Biol *26*, 1864-1870.

Mackman, N. (2008). Triggers, targets and treatments for thrombosis. Nature *451*, 914-918.

Maillet, L., Boscheron, C., Gotta, M., Marcand, S., Gilson, E., and Gasser, S.M. (1996). Evidence for silencing compartments within the yeast nucleus: a role for telomere proximity and Sir protein concentration in silencer-mediated repression. Genes Dev *10*, 1796-1811.

Major, A.S., Fazio, S., and Linton, M.F. (2002). B-lymphocyte deficiency increases atherosclerosis in LDL receptor-null mice. Arterioscler Thromb Vasc Biol *22*, 1892-1898.

Mallat, Z., Corbaz, A., Scoazec, A., Graber, P., Alouani, S., Esposito, B., Humbert, Y., Chvatchko, Y., and Tedgui, A. (2001). Interleukin-18/interleukin-18 binding protein signaling modulates atherosclerotic lesion development and stability. Circ Res *89*, E41-45.

Martin-Ventura, J.L., Blanco-Colio, L.M., Munoz-Garcia, B., Gomez-Hernandez, A., Arribas, A., Ortega, L., Tunon, J., and Egido, J. (2004). NF-kappaB activation and Fas ligand overexpression in blood and plaques of patients with carotid atherosclerosis: potential implication in plaque instability. Stroke *35*, 458-463.

Matloubian, M., David, A., Engel, S., Ryan, J.E., and Cyster, J.G. (2000). A transmembrane CXC chemokine is a ligand for HIV-coreceptor Bonzo. Nat Immunol *1*, 298-304.

Mattagajasingh, I., Kim, C.S., Naqvi, A., Yamamori, T., Hoffman, T.A., Jung, S.B., DeRicco, J., Kasuno, K., and Irani, K. (2007). SIRT1 promotes endothelium-dependent vascular relaxation by activating endothelial nitric oxide synthase. Proc Natl Acad Sci U S A *104*, 14855-14860.

Michan, S., and Sinclair, D. (2007). Sirtuins in mammals: insights into their biological function. Biochem J *404*, 1-13.

Milne, J.C., Lambert, P.D., Schenk, S., Carney, D.P., Smith, J.J., Gagne, D.J., Jin, L., Boss, O., Perni, R.B., Vu, C.B., *et al.* (2007). Small molecule activators of SIRT1 as therapeutics for the treatment of type 2 diabetes. Nature *450*, 712-716.

Min, H.Y., and Spiegelman, B.M. (1986). Adipsin, the adipocyte serine protease: gene structure and control of expression by tumor necrosis factor. Nucleic Acids Res *14*, 8879-8892.

Monaco, C., Andreakos, E., Kiriakidis, S., Mauri, C., Bicknell, C., Foxwell, B., Cheshire, N., Paleolog, E., and Feldmann, M. (2004). Canonical pathway of nuclear factor kappa B activation selectively regulates proinflammatory and prothrombotic responses in human atherosclerosis. Proc Natl Acad Sci U S A *101*, 5634-5639.

Mueller, C.F., Laude, K., McNally, J.S., and Harrison, D.G. (2005). ATVB in focus: redox mechanisms in blood vessels. Arterioscler Thromb Vasc Biol *25*, 274-278.

Murad, F. (2006). Shattuck Lecture. Nitric oxide and cyclic GMP in cell signaling and drug development. N Engl J Med *355*, 2003-2011.

Nakamaru, Y., Vuppusetty, C., Wada, H., Milne, J.C., Ito, M., Rossios, C., Elliot, M., Hogg, J., Kharitonov, S., Goto, H., *et al.* (2009). A protein deacetylase SIRT1 is a negative regulator of metalloproteinase-9. FASEB J.

Napoli, C., D'Armiento, F.P., Mancini, F.P., Postiglione, A., Witztum, J.L., Palumbo, G., and Palinski, W. (1997). Fatty streak formation occurs in human fetal aortas and is greatly enhanced by maternal hypercholesterolemia. Intimal accumulation of low density lipoprotein and its oxidation precede monocyte recruitment into early atherosclerotic lesions. J Clin Invest *100*, 2680-2690.

Oberkofler, H., Schraml, E., Krempler, F., and Patsch, W. (2003). Potentiation of liver X receptor transcriptional activity by peroxisome-proliferator-activated receptor gamma co-activator 1 alpha. Biochem J *371*, 89-96.

Ohman, M.K., Shen, Y., Obimba, C.I., Wright, A.P., Warnock, M., Lawrence, D.A., and Eitzman, D.T. (2008). Visceral adipose tissue inflammation accelerates atherosclerosis in apolipoprotein E-deficient mice. Circulation *117*, 798-805.

Olsson, A.G., and Yuan, X.M. (1996). Antioxidants in the prevention of atherosclerosis. Curr Opin Lipidol *7*, 374-380.

Oorni, K., Pentikainen, M.O., Ala-Korpela, M., and Kovanen, P.T. (2000). Aggregation, fusion, and vesicle formation of modified low density lipoprotein particles: molecular mechanisms and effects on matrix interactions. J Lipid Res *41*, 1703-1714.

Pacholec, M., Bleasdale, J.E., Chrunyk, B., Cunningham, D., Flynn, D., Garofalo, R.S., Griffith, D., Griffor, M., Loulakis, P., Pabst, B., *et al.* (2010). SRT1720, SRT2183, SRT1460, and resveratrol are not direct activators of SIRT1. J Biol Chem *285*, 8340-8351.

Packard, R.R., Lichtman, A.H., and Libby, P. (2009). Innate and adaptive immunity in atherosclerosis. Semin Immunopathol *31*, 5-22.

Paigen, B., Holmes, P.A., Mitchell, D., and Albee, D. (1987). Comparison of atherosclerotic lesions and HDL-lipid levels in male, female, and testosterone-treated female mice from strains C57BL/6, BALB/c, and C3H. Atherosclerosis *64*, 215-221.

Palinski, W., Horkko, S., Miller, E., Steinbrecher, U.P., Powell, H.C., Curtiss, L.K., and Witztum, J.L. (1996). Cloning of monoclonal autoantibodies to epitopes of oxidized lipoproteins from apolipoprotein E-deficient mice. Demonstration of epitopes of oxidized low density lipoprotein in human plasma. J Clin Invest *98*, 800-814.

Palinski, W., and Napoli, C. (2002). The fetal origins of atherosclerosis: maternal hypercholesterolemia, and cholesterol-lowering or antioxidant treatment during pregnancy influence in utero programming and postnatal susceptibility to atherogenesis. FASEB J *16*, 1348-1360.

Picard, F., Kurtev, M., Chung, N., Topark-Ngarm, A., Senawong, T., Machado De Oliveira, R., Leid, M., McBurney, M.W., and Guarente, L. (2004). Sirt1 promotes fat mobilization in white adipocytes by repressing PPAR-gamma. Nature *429*, 771-776.

Plump, A.S., Smith, J.D., Hayek, T., Aalto-Setala, K., Walsh, A., Verstuyft, J.G., Rubin, E.M., and Breslow, J.L. (1992). Severe hypercholesterolemia and atherosclerosis in apolipoprotein E-deficient mice created by homologous recombination in ES cells. Cell *71*, 343-353.

Poole, J.C., and Florey, H.W. (1958). Changes in the endothelium of the aorta and the behaviour of macrophages in experimental atheroma of rabbits. J Pathol Bacteriol *75*, 245-251.

Posakony, J., Hirao, M., Stevens, S., Simon, J.A., and Bedalov, A. (2004). Inhibitors of Sir2: evaluation of splitomicin analogues. J Med Chem *47*, 2635-2644.

Potente, M., Ghaeni, L., Baldessari, D., Mostoslavsky, R., Rossig, L., Dequiedt, F., Haendeler, J., Mione, M., Dejana, E., Alt, F.W*., et al.* (2007). SIRT1 controls endothelial angiogenic functions during vascular growth. Genes Dev *21*, 2644-2658.

Prozorovski, T., Schulze-Topphoff, U., Glumm, R., Baumgart, J., Schroter, F., Ninnemann, O., Siegert, E., Bendix, I., Brustle, O., Nitsch, R*., et al.* (2008). Sirt1 contributes critically to the redox-dependent fate of neural progenitors. Nat Cell Biol *10*, 385-394.

Puigserver, P., Rhee, J., Donovan, J., Walkey, C.J., Yoon, J.C., Oriente, F., Kitamura, Y., Altomonte, J., Dong, H., Accili, D*., et al.* (2003). Insulin-regulated hepatic gluconeogenesis through FOXO1-PGC-1alpha interaction. Nature *423*, 550-555.

Puigserver, P., and Spiegelman, B.M. (2003). Peroxisome proliferator-activated receptor-gamma coactivator 1 alpha (PGC-1 alpha): transcriptional coactivator and metabolic regulator. Endocr Rev *24*, 78-90.

Puigserver, P., Wu, Z., Park, C.W., Graves, R., Wright, M., and Spiegelman, B.M. (1998). A cold-inducible coactivator of nuclear receptors linked to adaptive thermogenesis. Cell *92*, 829-839.

Rajendrasozhan, S., Yang, S.R., Kinnula, V.L., and Rahman, I. (2008). SIRT1, an antiinflammatory and antiaging protein, is decreased in lungs of patients with chronic obstructive pulmonary disease. Am J Respir Crit Care Med *177*, 861-870.

Recinos, A., 3rd, Carr, B.K., Bartos, D.B., Boldogh, I., Carmical, J.R., Belalcazar, L.M., and Brasier, A.R. (2004). Liver gene expression associated with diet and lesion development in atherosclerosis-prone mice: induction of components of alternative complement pathway. Physiol Genomics *19*, 131-142.

Reilly, M.P., Rohatgi, A., McMahon, K., Wolfe, M.L., Pinto, S.C., Rhodes, T., Girman, C., and Rader, D.J. (2007). Plasma cytokines, metabolic syndrome, and atherosclerosis in humans. J Investig Med *55*, 26-35.

Rine, J., and Herskowitz, I. (1987). Four genes responsible for a position effect on expression from HML and HMR in Saccharomyces cerevisiae. Genetics *116*, 9-22.

Rodgers, J.T., Lerin, C., Haas, W., Gygi, S.P., Spiegelman, B.M., and Puigserver, P. (2005). Nutrient control of glucose homeostasis through a complex of PGC-1alpha and SIRT1. Nature *434*, 113-118.

Rogina, B., and Helfand, S.L. (2004). Sir2 mediates longevity in the fly through a pathway related to calorie restriction. Proc Natl Acad Sci U S A *101*, 15998-16003.

Rohrer, L., Freeman, M., Kodama, T., Penman, M., and Krieger, M. (1990). Coiled-coil fibrous domains mediate ligand binding by macrophage scavenger receptor type II. Nature *343*, 570-572.

Sawamura, T., Kume, N., Aoyama, T., Moriwaki, H., Hoshikawa, H., Aiba, Y., Tanaka, T., Miwa, S., Katsura, Y., Kita, T.*, et al.* (1997). An endothelial receptor for oxidized low-density lipoprotein. Nature *386*, 73-77.

Schug, T.T., Xu, Q., Gao, H., Peres-da-Silva, A., Draper, D.W., Fessler, M.B., Purushotham, A., and Li, X. (2010). Myeloid deletion of SIRT1 induces inflammatory signaling in response to environmental stress. Mol Cell Biol.

Schulte, S., Sukhova, G.K., and Libby, P. (2008). Genetically programmed biases in Th1 and Th2 immune responses modulate atherogenesis. Am J Pathol *172*, 1500-1508.

Sequeira, J., Boily, G., Bazinet, S., Saliba, S., He, X., Jardine, K., Kennedy, C., Staines, W., Rousseaux, C., Mueller, R.*, et al.* (2008). sirt1-null mice develop an autoimmune-like condition. Exp Cell Res *314*, 3069-3074.

Shen, Z., Ajmo, J.M., Rogers, C.Q., Liang, X., Le, L., Murr, M.M., Peng, Y., and You, M. (2009). Role of SIRT1 in regulation of LPS- or two ethanol metabolites-induced TNF-alpha production in cultured macrophage cell lines. Am J Physiol Gastrointest Liver Physiol *296*, G1047-1053.

Shimaoka, T., Kume, N., Minami, M., Hayashida, K., Kataoka, H., Kita, T., and Yonehara, S. (2000). Molecular cloning of a novel scavenger receptor for oxidized low density lipoprotein, SR-PSOX, on macrophages. J Biol Chem *275*, 40663-40666.

Silverstein, R.L., and Febbraio, M. (2009). CD36, a scavenger receptor involved in immunity, metabolism, angiogenesis, and behavior. Sci Signal *2*, re3.

Song, L., Leung, C., and Schindler, C. (2001). Lymphocytes are important in early atherosclerosis. J Clin Invest *108*, 251-259.

Stein, S., Lohmann, C., Handschin, C., Stenfeldt, E., Boren, J., Luscher, T.F., and Matter, C.M. (2010a). ApoE-/- PGC-1alpha-/- mice display reduced IL-18 levels and do not develop enhanced atherosclerosis. PLoS ONE *5*, e13539.

Stein, S., Lohmann, C., Schäfer, N., Hofmann, J., Rohrer, L., Besler, C., Rothgiesser, K.M., Becher, B., Hottiger, M.O., Borén, J.*, et al.* (2010b). SIRT1 decreases Lox-1-mediated foam cell formation in atherogenesis. Eur Heart J *Apr 23. [Epub ahead of print], doi: 10.1093/eurheartj/ehq107*.

Stein, S., Schafer, N., Breitenstein, A., Besler, C., Winnik, S., Lohmann, C., Heinrich, K., Brokopp, C.E., Handschin, C., Landmesser, U.*, et al.* (2010c). SIRT1 reduces endothelial activation without affecting vascular function in ApoE-/- mice. Aging (Albany NY) *2*, 353-360.

Steinberg, D. (1989). The cholesterol controversy is over. Why did it take so long? Circulation *80*, 1070-1078.

Steinberg, D. (2002). Atherogenesis in perspective: hypercholesterolemia and inflammation as partners in crime. Nat Med *8*, 1211-1217.

Steinberg, D. (2009). The LDL modification hypothesis of atherogenesis: an update. J Lipid Res *50 Suppl*, S376-381.

Steinbrecher, U.P., Parthasarathy, S., Leake, D.S., Witztum, J.L., and Steinberg, D. (1984). Modification of low density lipoprotein by endothelial cells involves lipid peroxidation and degradation of low density lipoprotein phospholipids. Proc Natl Acad Sci U S A *81*, 3883-3887.

Stevens, J., Tyroler, H.A., Cai, J., Paton, C.C., Folsom, A.R., Tell, G.S., Schreiner, P.J., and Chambless, L.E. (1998). Body weight change and carotid artery wall thickness. The Atherosclerosis Risk in Communities (ARIC) Study. Am J Epidemiol *147*, 563-573.

Stokes, K.Y., Clanton, E.C., Russell, J.M., Ross, C.R., and Granger, D.N. (2001). NAD(P)H oxidase-derived superoxide mediates hypercholesterolemia-induced leukocyte-endothelial cell adhesion. Circ Res *88*, 499-505.

Tabas, I. (2010). Macrophage death and defective inflammation resolution in atherosclerosis. Nat Rev Immunol *10*, 36-46.

Tanner, K.G., Landry, J., Sternglanz, R., and Denu, J.M. (2000). Silent information regulator 2 family of NAD- dependent histone/protein deacetylases generates a unique product, 1-O-acetyl-ADP-ribose. Proc Natl Acad Sci U S A *97*, 14178-14182.

Taylor, D.M., Maxwell, M.M., Luthi-Carter, R., and Kazantsev, A.G. (2008). Biological and potential therapeutic roles of sirtuin deacetylases. Cell Mol Life Sci *65*, 4000-4018.

Tenger, C., Sundborger, A., Jawien, J., and Zhou, X. (2005). IL-18 accelerates atherosclerosis accompanied by elevation of IFN-gamma and CXCL16 expression independently of T cells. Arterioscler Thromb Vasc Biol *25*, 791-796.

Thurberg, B.L., and Collins, T. (1998). The nuclear factor-kappa B/inhibitor of kappa B autoregulatory system and atherosclerosis. Curr Opin Lipidol *9*, 387-396.

Tissenbaum, H.A., and Guarente, L. (2001). Increased dosage of a sir-2 gene extends lifespan in Caenorhabditis elegans. Nature *410*, 227-230.

Tontonoz, P., and Spiegelman, B.M. (2008). Fat and Beyond: The Diverse Biology of PPARgamma. Annu Rev Biochem *77*, 289-312.

Tsang, A.W., and Escalante-Semerena, J.C. (1998). CobB, a new member of the SIR2 family of eucaryotic regulatory proteins, is required to compensate for the lack of nicotinate mononucleotide:5,6-dimethylbenzimidazole phosphoribosyltransferase activity in cobT mutants during cobalamin biosynthesis in Salmonella typhimurium LT2. J Biol Chem *273*, 31788-31794.

Vega, R.B., Huss, J.M., and Kelly, D.P. (2000). The coactivator PGC-1 cooperates with peroxisome proliferator-activated receptor alpha in transcriptional control of nuclear genes encoding mitochondrial fatty acid oxidation enzymes. Mol Cell Biol *20*, 1868-1876.

Wang, J., Zhang, R., Xu, Y., Zhou, H., Wang, B., and Li, S. (2008). Genistein inhibits the development of atherosclerosis via inhibiting NF-kappaB and VCAM-1 expression in LDLR knockout mice. Can J Physiol Pharmacol *86*, 777-784.

Wang, Y.X., Lee, C.H., Tiep, S., Yu, R.T., Ham, J., Kang, H., and Evans, R.M. (2003). Peroxisome-proliferator-activated receptor delta activates fat metabolism to prevent obesity. Cell *113*, 159-170.

White, R.T., Damm, D., Hancock, N., Rosen, B.S., Lowell, B.B., Usher, P., Flier, J.S., and Spiegelman, B.M. (1992). Human adipsin is identical to complement factor D and is expressed at high levels in adipose tissue. J Biol Chem *267*, 9210-9213.

Whitman, S.C., Ravisankar, P., and Daugherty, A. (2002). Interleukin-18 enhances atherosclerosis in apolipoprotein E(-/-) mice through release of interferon-gamma. Circ Res *90*, E34-38.

Wolfrum, S., Teupser, D., Tan, M., Chen, K.Y., and Breslow, J.L. (2007). The protective effect of A20 on atherosclerosis in apolipoprotein E-deficient mice is associated with reduced expression of NF-kappaB target genes. Proc Natl Acad Sci U S A *104*, 18601-18606.

Wood, J.G., Rogina, B., Lavu, S., Howitz, K., Helfand, S.L., Tatar, M., and Sinclair, D. (2004). Sirtuin activators mimic caloric restriction and delay ageing in metazoans. Nature *430*, 686-689.

Wood, K.M., Cadogan, M.D., Ramshaw, A.L., and Parums, D.V. (1993). The distribution of adhesion molecules in human atherosclerosis. Histopathology *22*, 437-444.

Xanthoulea, S., Curfs, D.M., Hofker, M.H., and de Winther, M.P. (2005). Nuclear factor kappa B signaling in macrophage function and atherogenesis. Curr Opin Lipidol *16*, 536-542.

Xie, G., Guo, D., Li, Y., Liang, S., and Wu, Y. (2007). The impact of severity of hypertension on association of PGC-1alpha gene with blood pressure and risk of hypertension. BMC Cardiovasc Disord *7*, 33.

Yamazaki, Y., Usui, I., Kanatani, Y., Matsuya, Y., Tsuneyama, K., Fujisaka, S., Bukhari, A., Suzuki, H., Senda, S., Imanishi, S.*, et al.* (2009). Treatment with SRT1720, a SIRT1 Activator, Ameliorates Fatty Liver with Reduced Expression of Lipogenic Enzymes in MSG Mice. Am J Physiol Endocrinol Metab.

Yang, X., Wang, L., Zeng, H., Dubey, L., Zhou, N., and Pu, J. (2006). Effects of simvastatin on NF-kappaB-DNA binding activity and monocyte chemoattractant protein-1 expression in a rabbit model of atherosclerosis. J Huazhong Univ Sci Technolog Med Sci *26*, 194-198.

Yang, Z., Kahn, B.B., Shi, H., and Xue, B.Z. (2010). Macrophage alpha1 AMP-activated protein kinase (alpha1AMPK) antagonizes fatty acid-induced inflammation through SIRT1. J Biol Chem *285*, 19051-19059.

Yang, Z., and Ming, X.F. (2010). The vascular SIRTainty. Aging (Albany NY) *2*, 331-332.

Yeung, F., Hoberg, J.E., Ramsey, C.S., Keller, M.D., Jones, D.R., Frye, R.A., and Mayo, M.W. (2004). Modulation of NF-kappaB-dependent transcription and cell survival by the SIRT1 deacetylase. Embo J *23*, 2369-2380.

Yoon, J.C., Puigserver, P., Chen, G., Donovan, J., Wu, Z., Rhee, J., Adelmant, G., Stafford, J., Kahn, C.R., Granner, D.K.*, et al.* (2001). Control of hepatic gluconeogenesis through the transcriptional coactivator PGC-1. Nature *413*, 131-138.

Yoshizaki, T., Schenk, S., Imamura, T., Babendure, J.L., Sonoda, N., Bae, E.J., Oh, D.Y., Lu, M., Milne, J.C., Westphal, C.*, et al.* (2010). SIRT1 inhibits inflammatory pathways in macrophages and modulates insulin sensitivity. Am J Physiol Endocrinol Metab *298*, E419-428.

Zernecke, A., Shagdarsuren, E., and Weber, C. (2008). Chemokines in atherosclerosis: an update. Arterioscler Thromb Vasc Biol *28*, 1897-1908.

Zhang, Q.J., Wang, Z., Chen, H.Z., Zhou, S., Zheng, W., Liu, G., Wei, Y.S., Cai, H., Liu, D.P., and Liang, C.C. (2008a). Endothelium-specific overexpression of class III deacetylase

SIRT1 decreases atherosclerosis in apolipoprotein E-deficient mice. Cardiovasc Res *80*, 191-199.

Zhang, R., Chen, H.Z., Liu, J.J., Jia, Y.Y., Zhang, Z.Q., Yang, R.F., Zhang, Y., Xu, J., Wei, Y.S., Liu, D.P.*, et al.* (2010). SIRT1 suppresses activator protein-1 transcriptional activity and cyclooxygenase-2 expression in macrophages. J Biol Chem *285*, 7097-7110.

Zhang, S.H., Reddick, R.L., Piedrahita, J.A., and Maeda, N. (1992). Spontaneous hypercholesterolemia and arterial lesions in mice lacking apolipoprotein E. Science *258*, 468-471.

Zhang, W., Xing, S.S., Sun, X.L., and Xing, Q.C. (2009). Overexpression of activated nuclear factor-kappa B in aorta of patients with coronary atherosclerosis. Clin Cardiol *32*, E42-47.

Zhang, Y., Xu, W., Li, X., Tang, Y., Xie, P., Ji, Y., Fan, L., and Chen, Q. (2008b). Association between PPARGC1A gene polymorphisms and coronary artery disease in a Chinese population. Clin Exp Pharmacol Physiol *35*, 1172-1177.

Zhou, X., Nicoletti, A., Elhage, R., and Hansson, G.K. (2000). Transfer of CD4(+) T cells aggravates atherosclerosis in immunodeficient apolipoprotein E knockout mice. Circulation *102*, 2919-2922.

8 Acknowledgement

I want to thank the following people for their support during my PhD study:

Burkhard Becher, Marc Donath, Christian Matter, and Walter Wahli for their valuable input as members of my PhD committee.

Christian Matter, the Zurich Center for Integrative Human Physiology (ZIHP), and the Foundation for Cardiovascular Research for providing finances for the research projects and my PhD salary.

Christian Besler, Stephan Winnik, Stefanie Nusser, Gabriela Kania, Przemyslaw Blyszczuk, Susanna Sluka, Nicola Schäfer, and Michael Hottiger for scientific discussions and help.

Nicola Schäfer, Janin Hofman, Karin Rothgiesser, Stefanie Nusser, Christian Besler, Christine Lohmann, Stephan Winnik, Kathrin Heinrich, Susanna Sluka, Alexander Breitenstein, Pavani Mocharla, Carola Dörries, Helen Greutert, Stephan Keller, and Elin Stenfeldt for experimental advices and help.

Heidi Preisig and Annemarie-Brennwald for their kind help with administrative issues and organizing the PhD retreats.

Stefanie Nusser, Philipp Schläfli, Susanna Sluka, Nicola Schäfer, Christopher Lott, Stephan Winnik, Fred Owala, Juan Escobar, Matthias Morf, Sarfarazhussain Farooqui, Ivo Rimann, Magdalene Adamczyk, Erik Holy, Branko Simic, Christian Besler, Kathrin Heinrich, Christian Seelandt, Rafael Studiger, Remo Spescha, Francesco Paneni, Christine Lohmann, Maya Müller, Yi Shi, Stephan Keller, Meliana Riwanto and others for the enjoyable after-work beers at Neubühl, barbeques, Aare-trips, skiing-trips, climbing-trips (best thing to forget the daily stress!), ‘chupacabra’ SOLA team 2010 (we were not the last!), Feldschlösschen ‘chupacabra’ world cup 2010 bet team (we got the third place ;-), parties, etc.

Stefanie Nusser and my family for their lovely support.

9 Curriculum Vitae

Surname: STEIN

Given names: Matthias Alexander Sokrates

Date of birth: June 22 1982

Citizenship: Brazilian and German

Studies

Mar. 2008 – date	PhD study in Integrative Molecular Medicine, Institute of Physiology, University of Zurich, in Zurich, Switzerland (supervisors: Christian M. Matter, Burkhard Becher, Marc Donath and Walter Wahli)
Aug. – Dec. 2007	Research assistant (Predoc) at the Max Planck Institute for Developmental Biology, Department of Molecular Biology, in Tübingen, Germany (supervisor: Ingrid Lohmann)
Jul. 2007	Certified biologist (A-level)
Oct. 2006 – Jul. 2007	Diploma thesis at the Max Planck Institute for Developmental Biology, Department of Molecular Biology, in Tübingen, Germany Title: Involvement of the transcription factors Apt, Brk, Disco, Doc1, Ems, En, Gcm & Slp1 in the Deformed-dependent regulation of the apoptosis gene reaper (supervisors: Ingrid Lohmann and Detlef Weigel)
Oct. 2005 – Aug. 2007	Biology, University of Tübingen, Germany
Jan. – Jul. 2005	Molecular Biology, University of Oslo, Norway
Oct. 2002 to Dec. 2004	Biology, University of Tübingen, Germany
May 2001	Certificate: Abitur
1999 – 2001	Max-Beckmann-Schule, Frankfurt am Main, Deutschland
1988 – 1999	Colégio Humboldt – Deutsche Schule, São Paulo, Brasilien

International Experience & Meetings

Oct. 2010	16th Cardiovascular Biology & Clinical Implications Meeting, in Muntelier, Switzerland
	Poster: ApoE-/- PGC-1α-/- mice display reduced IL-18 levels and do not develop enhanced atherosclerosis
Nov. 2009	American Heart Association (AHA) Scientific Sessions 2009, in Orlando, USA
	Oral presentation: SIRT1 Decreases Lox-1 Mediated Foam Cell Formation In Atherogenesis
Nov. 2009	ATVB Early career networking reception, Orange County Convention Center, in Orlando, USA - Nov 17, 2007
	Invited poster: SIRT1 Decreases Lox-1 Mediated Foam Cell Formation In Atherogenesis
Sep. 2009	15th Cardiovascular Biology & Clinical Implications Meeting, in Muntelier, Switzerland
	Oral presentation: SIRT1 Prevents Atherosclerosis by Diminishing Macrophage Foam Cell Formation
Aug. 2009	European Society of Cardiology (ESC) Congress 2009, in Barcelona, Spain
	Oral presentation: Endogenous SIRT1 Protects Against Atherosclerosis by Decreasing Macrophage Infiltration and Foam Cell Formation
Aug. 2009	5th Symposium of the Zurich Center for Integrative Human Physiology (ZIHP), in Zurich, Switzerland
	Oral presentation: SIRT1 Decreases Macrophage Infiltration and Foam Cell Formation in Atherogenesis
Oct. 2008	14th Cardiovascular Biology & Clinical Implications Meeting, in Muntelier, Switzerland
Aug. 2008	4th Symposium of the Zurich Center for Integrative Human Physiology (ZIHP), in Zurich, Switzerland
Nov. 2006	12th Regional *Drosophila* Meeting, in Vienna, Austria
Aug. 2004	Symbiose 2004: Symposium of European biology students, in Zagreb and Zadar, Croatia
May 2004	Ecology and sustainable development, students meeting, in Sofia, Balchik and Varna, Bulgaria
Aug. 2003	Symbiose 2003: Symposium of European biology students, in Oslo, Norway

Scholarship funds and research grants

Nov. 2009	Travel grant for the AHA Congress 2009, in Orlando, USA
Aug. 2009	Travel grant for the ESC Congress 2009, in Barcelona, Spain
Jan. 2005 to Oct. 2007	Scholarship awarded by the 'Friedrich-Ebert-Stiftung' (www.fes.de)

Original research articles

ApoE-/- PGC-1α-/- mice display reduced IL-18 levels and do not develop enhanced atherosclerosis

Sokrates Stein, Christine Lohmann, Christoph Handschin, Elin Stenfeldt, Jan Borén, Thomas F. Lüscher, and Christian M. Matter

PLoS ONE. 2010; 5(10): e13539.

SIRT1 Inhibits Endothelial Tissue Factor Expression

Alexander Breitenstein,* Sokrates Stein,* Giovanni G. Camici, Alexander Akhmedov, Christine Lohmann, Peter J. Elliott, Christoph H. Westphal, Christian M. Matter, Thomas F. Lüscher, Felix C. Tanner (*equal contribution)

Cardiovasc Res. 2010 Nov 21. Epub ahead of print. (doi:10.1093/cvr/cvq339)

SIRT1 reduces endothelial activation without affecting vascular function in ApoE-/- mice

Sokrates Stein, Nicola Schäfer, Alexander Breitenstein, Christian Besler, Christine Lohmann, Kathrin Heinrich, Chad E. Brokopp, Christoph Handschin, Ulf Landmesser, Felix C. Tanner, Thomas F. Lüscher, and Christian M. Matter

Aging (Albany NY). 2010; 2(6):353-360.

SIRT1 decreases Lox-1-mediated foam cell formation in atherogenesis

Sokrates Stein, Christine Lohmann, Nicola Schäfer, Janin Hofmann, Lucia Rohrer, Christian Besler, Karin M. Rothgiesser, Burkhard Becher, Michael O. Hottiger, Jan Borén, Michael W. McBurney, Ulf Landmesser, Thomas F. Lüscher and Christian M. Matter

Eur Heart J. 2010 Apr 23., Epub ahead of print. (doi:10.1093/eurheartj/ehq107)

Heart-infiltrating prominin-1+/CD133+ progenitor cells represent the cellular source of TGF-beta-mediated cardiac fibrosis in experimental autoimmune myocarditis

Gabriela Kania, Przemyslaw Blyszczuk, Sokrates Stein, Alan Valaperti, Davide Germano, Stephan Dirnhofer, Lukas Hunziker, Christian Matter, Urs Eriksson

Circ Res. 2009; 105(5):462-70.

Atherosclerotic Mice Exhibit Systemic Inflammation in Periadventitial and Visceral Adipose Tissue, Liver, and Pancreatic Islets

Christine Lohmann, Nicola Schäfer, Tobias von Lukowicz, M. A. Sokrates Stein, Jan Borén, Sabine Rütti, Walter Wahli, Marc Y. Donath, Thomas F. Lüscher, Christian M. Matter

Atherosclerosis. 2009; 207(2):360-7.

Multifactorial Regulation of a Hox Target Gene

Petra Stöbe, M. A. Sokrates Stein, Anette Habring-Müller, Daniela Bezdan, Aurelia L. Fuchs, Stefanie D. Hueber, Haijia Wu, Ingrid Lohmann

PLoS Genet. 2009; 5(3): e1000412 - (doi:10.1371/journal.pgen.1000412)

Expression of the apoptosis gene reaper in homeotic, segmentation and other mutants in *Drosophila*

Zhai, Z., Stein, M.A.S., Lohmann, I.

Gene Expr Patterns. 2009; 9(5):357-63.

Editorial/Research communication

A dual role of $CD4^+$ T cells in adipose tissue?

Christian M. Matter & M. A. Sokrates Stein

Circ Res. 2009;104(8):928-30.